



COPYRIGHT AND USE OF THIS THESIS

This thesis must be used in accordance with the provisions of the Copyright Act 1968.

Reproduction of material protected by copyright may be an infringement of copyright and copyright owners may be entitled to take legal action against persons who infringe their copyright.

Section 51 (2) of the Copyright Act permits an authorized officer of a university library or archives to provide a copy (by communication or otherwise) of an unpublished thesis kept in the library or archives, to a person who satisfies the authorized officer that he or she requires the reproduction for the purposes of research or study.

The Copyright Act grants the creator of a work a number of moral rights, specifically the right of attribution, the right against false attribution and the right of integrity.

You may infringe the author's moral rights if you:

- fail to acknowledge the author of this thesis if you quote sections from the work
- attribute this thesis to another author
- subject this thesis to derogatory treatment which may prejudice the author's reputation

For further information contact the University's Copyright Service.

sydney.edu.au/copyright

Tryptophan-catabolising enzymes in animal models



Felicita Fedelis Jusof

A thesis submitted for the requirements of the degree

Doctor of Philosophy

Discipline of Pathology, School of Medical Sciences

Faculty of Medicine

University of Sydney, 2015

1.3.3.4	IDO2 inhibitors	31
1.3.3.5	IDO2 in autoimmune diseases	32
1.3.3.6	IDO2 plays an essential role in inflammation	33
1.3.4	Tryptophan-independent signalling of GCN2/mTOR	34
1.4	Organ development	38
1.4.1	Tryptophan-degrading activity in placenta	38
1.4.2	Tryptophan-catabolising activity in yolk sac	41
1.4.3	Tryptophan-catabolic activity in embryonic and neonatal liver	42
1.5	Zebrafish as an experimental model in biomedicine	43
1.5.1	<i>D. rerio</i> embryonic development stages	46
1.5.2	Tryptophan-catabolising enzymes in <i>D. rerio</i>	48
1.6	Scope of thesis	51

Chapter 2: Human IFN γ bioassay **53-62**

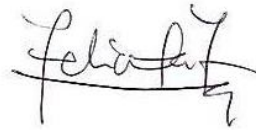
2.1	Introduction	54
2.2	Statement of contributions	56
2.3	Manuscript	57

Chapter 5: Expression of <i>Ido2</i> in various adult and embryonic murine tissues	168- 233
5.1 Introduction	169
5.2 Methods	172
5.3 Results	176
5.4 Discussion	207
5.5 Summary	232
Chapter 6: General Discussions and Future Directions	234-259
6.1 General discussion	235
6.2 Future directions	248
6.3 Final Conclusion	253
References	260

DECLARATION

This thesis is submitted to the University of Sydney in fulfilment of the requirement for the Doctor of Philosophy.

I, Felicity Fedelis Jusof, declare this thesis and its contents to be my original work. It has not been previously submitted for the application of a degree. Credit for any assistance received has been acknowledged within the text and all source material has been appropriately referenced.



Signed:

Date: 25.03.2015

ABSTRACT

Research on indoleamine 2,3-dioxygenase (IDO) 2 has become an area of interest in the domain of tryptophan (Trp) metabolism. Discovered less than a decade ago, this isoenzyme of IDO1 catalyses the same reaction as its isoform and tryptophan 2,3-dioxygenase (TDO2), namely the degradation of tryptophan to N-formylkynurenine in the kynurenine (Kyn) pathway. Despite IDO2 possessing the ability to catabolise Trp, this activity is relatively low compared to TDO2 and IDO1, suggesting that this protein may possess alternative roles. While most mammals, including humans and mice, possess two homologues of IDO, lower vertebrates such as chicken and fish only possess one, and that enzyme is more similar to IDO2 than IDO1. Constitutive expression of IDO2 mRNA and protein in the mouse has been reported to be highest in the liver and the kidney, with the distribution apparently cytoplasmic in hepatocytes and tubules respectively. However, the detection of a cross-reacting protein of a similar molecular weight in the kidney lysates of *Ido2*^{-/-} mice cast doubt upon the veracity of this observation. Over the last five years, possible roles for IDO2 in cancer, inflammation and autoimmunity have been suggested, but more research is needed before its functions in physiology and pathophysiology can be fully understood.

We began this project by developing a human interferon gamma (IFN γ) bioassay based on the induction of IDO1 activity in human brain endothelial cells (HBECs). The focus then shifted to studying the distribution of IDO2 in adult mouse tissues and in developmental series from mouse and zebrafish. At the cellular level, we found IDO2 localised perinuclearly in hepatocytes, while its presence in other tissues (kidney, brain, colon, testis and epididymis) could not be confirmed. Its cellular localisation in the liver differed

to its distribution in transfected human embryonic kidney (HEK) cells, which appeared cytoplasmic. The distribution of *ido* mRNA in developing zebrafish embryos, where it was found localised only in the intestine, was different to that in both embryonic and adult mouse tissues. *Ido2* mRNA was detectable in placenta and yolk sac in the mouse developmental series as well as in adult liver, kidney, brain, epididymis and colon (although IDO2 protein was found only in the liver). In zebrafish embryos, *tdo2a* and *tdo2b* mRNAs were detected in the liver and the intestine, while in the murine developmental series *Tdo2* was detectable in the placenta and yolk sac but not in the liver. *Ido1* also was detected in the yolk sac and placenta of mouse developmental tissues.

Mice deficient for two Trp-catabolic enzymes were generated to complement those deficient in IDO1, IDO2 or TDO2 that the laboratory previously had acquired. These gene knockout mice were used to examine at the molecular level the relationship between the three enzymes. In the absence of IDO1, *Ido2* mRNA was downregulated in the brain, kidney and epididymis. However, the expression of neither *Tdo2* nor *Ido1* was affected in the absence of one or two of the other Trp-degrading enzymes.

Global gene expression in liver lysates deficient for IDO2 and/or TDO2 relative to their equivalent wild-types (WT) was analysed by microarray analysis. The expression of some genes subsequently was validated by RT-qPCR. By microarray analysis a total of 63 genes was up- or down-regulated in the liver in the absence of IDO2. The expression of 20 of these was further assessed by RT-qPCR, and that of *Xdh*, *Cyp4a14*, *Acot1*, *Gdf15*, *Moxd1*, *Igfbp1*, *Fam25c* and *Ehd3* was found significantly dysregulated ($p < 0.05$). In liver lysates of *Tdo2*^{-/-} mice relative to *Tdo2*^{+/+}, the expression of only two genes was validated, with

Cyp4a14 and *Moxd1* found to be differentially regulated by RT-qPCR. In mice deficient in both IDO2 and TDO2, expression of four genes was found dysregulated in the liver, relative to *Ido2*^{+/+}*Tdo2*^{+/+} animals, upon RT-qPCR analysis, namely *Saa1*, *Lcn2*, *Nrep* and *Acot4*. A number of the genes found differentially expressed in the absence of IDO2 and/or TDO2 previously have been implicated in inflammation, obesity and diabetes. These observations led us to propose a possible role for IDO2 in averting inflammation, which if unchecked may lead to obesity and/or diabetes. We suggest that the absence of IDO2 might lead to the dysregulation of T cell proliferation and/or inflammatory mediators, which may contribute to an inflammatory onset in the liver.

This is the first report demonstrating the cellular localisation of IDO2 in adult mouse liver with *Ido2*^{-/-} mice as the negative control, as well as the mRNA expression of Trp-catabolising enzymes in embryonic developmental series of zebrafish (*tdo2a*, *tdo2b* and *ido*) and mouse (*Tdo2*, *Ido1* and *Ido2*). Both *tdo2a* and *tdo2b* were detected in zebrafish embryonic liver, whereas all three genes coding for Trp-catabolic enzymes were found in the intestine. In murine developmental tissues, *Tdo2*, *Ido1* and *Ido2* were all detectable in the yolk sac and placenta, with the expression of *Tdo2* being the highest. Finally, we are the first to postulate a possible role for IDO2 in averting inflammation and metabolic dysregulation in the liver.

ACKNOWLEDGEMENTS

Three years and eight months and we are finally here. Despite the challenges, it has been an enriching process, through which I have acquired many virtues and skills that will be essential in every day work and life. Undoubtedly, this learning process would not have been possible without some pivotal persons to whom I owe this page.

First and foremost, I'd like to thank my main supervisor, Prof Nicholas Hunt, through whom I learnt the art of being a good researcher. Thank you for being a supervisor, who not only taught but also cared (even after you have retired). Thank you for the constructive feedbacks and patience these past four odd years. Secondly, I am extremely grateful to my co-supervisor, Dr Helen Ball, without whom I could not have completed this project. Thank you for your training, assistance, patience, ideas and encouragement especially when things were challenging. I have learnt so much from you and I do not think I can thank you enough. I will miss you both and remain immensely indebted. My labmates, Belinda, Jin, Lay Khoon, Supun, and Tim, thank you for your friendships, kindness and support all these years, especially for the times you endured listening to me rant about everything under the sky. Thank you so very much!

This project had a number of experts from different fields collaborating. I am grateful for the friendship and directions of Dr Nicholas Cole, Dr Andrew Badrock and Dr Emily Don, for their invaluable guidance in the area of zebrafish research. I also thank the zebrafish lab managers, Claire Winnick and Dasha Syal for helping me with the fish husbandry. The work on murine developmental series was the fruit of collaboration with Dr Stuart Fraser whose inputs, training and teaching are very much appreciated. The IHC work seen in this thesis comprised of two long years of troubleshooting. I especially thank Dr Sanaz Maleki

and Shanna Trollip, from the histopathology lab of the University of Sydney as well as Dr Jennifer Huch, whose assistance was instrumental in this work.

I also must thank The University of Malaya, especially Datuk Ghauth Jasmon, the then-vice chancellor of the university and the Ministry of Higher Education of Malaysia.

Without your generosity, this would have remained merely a dream and an ambition.

Thank you for the scholarship.

To my family, mom, dad, Justina and Basil, thank you for your love. Thank you for giving me the freedom to pursue my dreams. Thank you for all your prayers, cares, concerns and support. I thank also Bernadette, Marian, Anna, David, Paulynn, Yani, Kathlin, Claudia, Victor, Su Jin, Abigail and Danica for always being available for that chat, cup of coffee (or meal), encouragement and challenge when necessary. Thank YOU!

Next, I cannot but thank my beloved best friend, driver, confidante and fiancé. I could not have managed this while maintaining my sanity if it wasn't for you. I couldn't have pulled off running between Uni of Sydney and Macquarie over the weekends and finishing up experiments at odd hours without your support and encouragement. You inspire me. Thank you for always making sure I am fed, well rested and for providing a comfortable space for me to write my thesis in. Thank you!

Last but definitely not least, I thank God for inspiring me to Work out of Love. Thank You for providing always in more than one way. Thank you for the consolation and inner strength that kept me going while still managing a smile on my face. Thank You for the opportunity to be here in Sydney, to learn, to grow and to become better. Thank You.

Publications and abstracts arising from this thesis

JUSOF, F. F., KHAW, L. T., BALL, H. J. & HUNT, N. H. 2013. Improved spectrophotometric human interferon-gamma bioassay. *J Immunol Methods*, 394, 115-20.

JUSOF, F. F., BALL, H. J., FRASER, S. T. & HUNT, N. H. 2014. Tryptophan-metabolising enzymes in murine tissues. Australian Health and Medical Research Congress, Melbourne, Australia.

JUSOF, F. F., BALL, H. J., FRASER, S. T. & HUNT, N. H. 2014. Tryptophan-metabolising enzymes in murine tissues. Bosch Institute XIV Young Investigators Symposium, Sydney, Australia.

JUSOF, F. F., BALL, H. J. & HUNT, N. H. 2012. Improved spectrophotometry IFN γ bioassay. Bosch Institute XII Young Investigators Symposium, Sydney, Australia.

ABBREVIATIONS

1-MT	1-methyl tryptophan
3-HAA	3-Hydroxyanthranilic acid
5-HIA	5-Hydroxyindole acetaldehyde
5-HIAA	5-Hydroxyindole acetic acid
5-HT	5-Hydroxytryptamine
5-HTP	5-Hydroxytryptophan
ACOT1	Acyl coenzyme A thioesterase 1
ACOT4	Acyl coenzyme A thioesterase 1
AhR	Aryl hydrocarbon receptor
ANOVA	Analysis of variance
APC	Antigen-presenting cells
BBB	Blood-brain barrier
BCA	Bicinchoninic acid
CCL	Chemokine (C-C motif) ligand 2
CHS	Contact hypersensitivity
CMV	Cytomegalovirus
CNS	Central nervous system
CRISPR	Clustered, regularly interspaced, short palindromic repeats
CRISPR-Cas	CRISPR-associated caspase system
CXCL10	Chemokine (C-X-C motif) ligand 1
CYP4A14	Cytochrome P450, family 4, subfamily a, polypeptide 14

D-1-MT	D-isomer of 1-methyl tryptophan
DAB	Diaminobenzidine
DIG	Digoxigenin
DMEM	Dulbecco's Modified Eagle's Medium
DNP	Dinitrophenyl
DPX	Dibutylphthalate in xylene
Dpc	Days-post-coitus
Dpf	Days-post-fertilisation
EDTA	Ethylenediaminetetraacetic acid
EHD3	EH domain-containing 3
eIF2α	Eukaryotic initiation factor 2
Fam25c	Fam25c (family with sequence similarity 25, member C)
GCN2	General control nonderepressible 2
G-CSF	Granulocyte colony-stimulating factor
GM-CSF	Granulocyte macrophage colony-stimulating factor
GDF15	Growth differentiation factor 15
HEK	Human embryonic kidney
HIV	Human immunodeficiency virus
Hpf	Hours-post-fertilisation
IDO1	Indoleamine 2,3-dioxygenase 1
IDO2	Indoleamine 2,3-dioxygenase 2
IFN	Interferon
IFNα	Interferon alpha

IFNβ	Interferon beta
IFNγ	Interferon gamma
IFNτ	Interferon tau
IFNω	Interferon omega
IGFBP1	Insulin-like growth factor binding protein 1
IHC	Immunohistochemistry
IL-1	Interleukin 1
IL-1β	Interleukin 1 beta
IL-4	Interleukin 4
IL-6	Interleukin 6
IL-12	Interleukin 12
IL-18	Interleukin 18
ISH	<i>In situ</i> hybridisation
ISRE	IFN γ -stimulated response element
JAK-STAT	Janus kinase - Signal Transducer and Activator of Transcription
KA	Kynurenic acid
K_m	Michaelis Menten constant; substrate concentration at which the reaction rate is half of <i>V_{max}</i>
Kyn	Kynurenine
L-1-MT	L-isomer of 1-methyl tryptophan
LCN2	Lipocalin 2
LIP	Liver inhibitory protein

LPS	Lipopolysaccharide
L-Trp	L-isoform of Tryptophan
MCP-1	Monocyte chemoattractant protein -1
MHC	Major histocompatibility complexes
MOXD1	Monoxygenase, DBH like 1
mTOR	Mammalian target of rapamycin
M.O.M	Mouse-on-mouse
MyD88	Myeloid differentiation primary response 88
NaCl	Sodium chloride
NAD⁺	Nicotinamide adenine dinucleotide +
NADH	Reduced NAD
NEFA	Non-esterified fatty acids
NHS	Normal horse serum
NK	Natural killer
NREP	Neuronal regeneration-related protein
pDC	Plasmacytoid dendritic cell
PbA	<i>Plasmodium berghei</i> ANKA
PBST	Phosphate buffered saline with Tween 20
PMA	Phorbol myristate acetate
PNS	Peripheral nervous system
PAGE	Polyacrylamide gel electrophoresis
PPAR	Peroxisome proliferator-activated receptor
Rcf	Relative centrifugal force

RIPA	Radioimmunoprecipitation assay
RT-PCR	Reverse transcriptase polymerase chain reaction
RT-qPCR	Quantitative RT-PCR
SAA1	Serum amyloid A 1
SDS	Sodium dodecyl sulphate
SEM	Standard error of mean
SNP	Single nucleotide polymorphism
TALENs	Transcription activator-like effector nucleases
TDLN	Tumour-draining lymph nodes
TDO/TDO2	Tryptophan 2,3-dioxygenase
TGC	Trophoblast giant cells
TLR	Toll-like receptor
TNF	Tumour necrosis factor
T_H	Helper T
TPH	Tryptophan hydroxylase
TPH2	Brain-specific TPH
T_{reg}	Regulatory T cells
Trp	Tryptophan
VYS	Visceral yolk sac
WT	Wild-type (mice)
XDH	Xanthine dehydrogenase
XO	Xanthine oxidase
XOR	Xanthine oxidoreductase

ZFIN

Zebrafish information network

ZFN

Zinc finger nucleases

LIST OF FIGURES

- Figure 1.1** Tryptophan metabolism by tryptophan hydroxylase in serotonergic neurons
- Figure 1.2** Tryptophan metabolism through the kynurenine pathway
- Figure 1.3** Phylogenetic tree of known IDOs and IDO-related proteins
- Figure 1.4** Possible mechanisms of immune suppression through IDO1-induced tryptophan deficiency.
- Figure 1.5** Sketches of embryo at selected stages of development. In the earlier stages, the animal pole is to the top while in the later stages, the anterior is to the top
- Figure 3.1** Morpholino injection protocol on one-cell stage *D. rerio* embryos
- Figure 3.2** An alignment of *D. rerio* Tdo2a (NP_001096086.1) and Tdo2b (NP_956150.1) proteins using T-Coffee using their FASTA sequences
- Figure 3.3** Phylogenetic tree of known TDOs in different species
- Figure 3.4** Enzymatic activity and sequence homology of zebrafish Ido and Tdo2 proteins
- Figure 3.5** The expression of all three genes coding for tryptophan-catabolising enzymes in zebrafish embryonic development
- Figure 3.6** The expression of genes coding tryptophan-catabolising enzymes in the intestine and liver of zebrafish embryo

- Figure 3.7** Knock down of *ido* gene expression using morpholinos and the expression of *tdo2a* gene in *ido* morphants
- Figure 3.8** Knockdown of *ido* gene expression increases the mortality rate in zebrafish embryos
- Figure 3.9** Morphology of surviving *ido* exon 1 morphants
- Figure 3.10 Zebrafish embryos injected with *ido* exon 9 morpholino only (A) as well as *ido* morpholino and *ido* RNA transcript (B) at 3 dpf showed cardiac oedema
- Figure 3.11** Efficiency of *tdo2a* exon 6, *tdo2a* exon 3 and *tdo2b* exon 6 knockdown in morphants
- Figure 3.12** Morphology of *tdo2a* ex 6 and ex 3 morphants
- Figure 4.1** Flow chart of the protocol of Western Blot detection using immunoprecipitated protein lysates
- Figure 4.2** Protocol flow of IDO2 protein localisation in tissues by IHC using the Vector M.O.M. ImmPRESS kit
- Figure 4.3** Detection of IDO2 protein in liver of *Ido2*^{+/+} mice using 5 different anti-IDO2 antibodies
- Figure 4.4** Expression of IDO2 protein in kidney lysates of *Ido2*^{+/+} (wild-type) and *Ido2*^{-/-} mouse
- Figure 4.5** Localisation of IDO2 protein in mouse liver

- Figure 4.6** Representative image of kidney sections stained with anti-IDO2 mouse monoclonal antibody
- Figure 4.7** Representative image of brain sections stained with anti-IDO2 antibody
- Figure 4.8** Representative image of colon sections stained with anti-IDO2 antibody
- Figure 4.9** Representative image of testis sections stained with anti-IDO2 antibody
- Figure 4.10** Representative image of epididymis sections stained with anti-IDO2 antibody
- Figure 4.11** Representative images of HEK cells transfected with plasmid carrying mouse *Ido1* cDNA
- Figure 4.12** Representative images of HEK cells transfected with mouse *Ido2* cDNA plasmid
- Figure 4.13** Trp-catabolising genes *Ido1*, *Ido2* and *Tdo2* mRNA expression in placenta of developing QS strain embryos at different time points
- Figure 4.14** Ratio of expression of Trp-catabolising genes *Ido1*, *Ido2* and *Tdo2* mRNA expression in placenta of developing QS strain embryos relative to the reference gene *Rpl13a*
- Figure 4.15** Trp-catabolising genes *Ido1*, *Ido2* and *Tdo2* mRNA expression in yolk sac of developing QS strain embryos
- Figure 4.16** Ratio of Trp-catabolising genes *Ido1*, *Ido2* and *Tdo2* expression in yolk sac of developing embryos relative to the reference gene *Rpl13a*

- Figure 4.17** Trp-catabolising genes *Ido2* and *Tdo2* mRNA expression in liver of embryos, neonates and adults of outbred QS mice strain and inbred Cre transgenic mice strain relative to the expression of the respective genes in 8-week-old adult mouse liver
- Figure 4.18** The relative mRNA expression of *Ido2* and *Tdo2* in the liver tissue of nine different transgenic mouse strains
- Figure 4.19** The relative mRNA expression of *Ido2* in kidney tissues of nine different transgenic mouse strains
- Figure 4.20** The relative mRNA expression of *Ido2* and *Tdo2* in brain tissues of nine different transgenic mouse strains
- Figure 4.21** The relative mRNA expression of *Ido1* and *Tdo2* in testes tissues of nine different transgenic mouse strains
- Figure 4.22** The relative mRNA expression of *Ido1* (A) and *Ido2* (B) in epididymis of nine different transgenic mouse strains
- Figure 5.1** Genes that were significantly differentially regulated in *Ido2*^{-/-} relative to *Ido2*^{+/+} as assessed by RT-qPCR
- Figure 5.2** *Cyp4a14* and *Moxd1* were significantly differentially regulated in *Tdo2*^{-/-} liver lysates relative to *Tdo2*^{+/+}, where p<0.05, as assessed by RT-qPCR
- Figure 5.3** *Saa1* and *Lcn2* were significantly upregulated while *Acot4* and *Nrep* were significantly downregulated in *Ido2*^{-/-}*Tdo2*^{-/-} liver lysates relative to *Ido2*^{+/+}*Tdo2*^{+/+} as determined by RT-qPCR

- Figure 5.4** *Cyp4a14* was upregulated in both *Ido2*^{-/-} and *Tdo2*^{-/-} single knockouts (n_≥5 each group) as determined by RT-qPCR
- Figure 5.5** *Moxd1* was downregulated in both *Ido2*^{-/-} and *Tdo2*^{-/-} single knockouts (n_≥5 each group) as determined by RT-qPCR
- Figure 5.6** Venn diagram depicting differentially-regulated genes in liver lysates of *Ido2*^{-/-} and *Tdo2*^{-/-} as well as *Ido2*^{-/-}*Tdo2*^{-/-} mice strains based on RT-qPCR
- Figure 5.7** Possible mechanism through which IDO2 deficiency leads to *Xdh* upregulation, and its implications.
- Figure 5.8** Possible mechanism through which *Acot1* is upregulated in the liver of IDO2-deficient mice, and its implications.
- Figure 5.9** Diagram summarising the validated differentially regulated genes in *Ido2*^{-/-}, *Tdo2*^{-/-} and *Ido2*^{-/-}*Tdo2*^{-/-} relative to their respective wild-types and their roles
- Figure 6.1** Diagrammatic summary of thesis findings involving the expression of genes coding Trp-catabolising enzymes in zebrafish and murine model

LIST OF TABLES

- Table 3.1** Primers used to amplify zebrafish *tdo2a*, *tdo2b* and *ido* mRNA and cDNA from zebrafish genome
- Table 3.2** Morpholino sequences targeting splice sites to knock-down gene expression
- Table 3.3** Percentage of mortality in *ido* Exon 1 morphants, *ido* morphants rescued with *ido* mRNA, embryos injected with *ido* mRNA alone, and uninjected wild-type controls.
- Table 4.1** Summary of tissue and cellular distribution of Trp-catabolising enzymes in different tissues
- Table 4.2** List of knockout strains with their wild-type equivalents used for mRNA assessment of Trp-catabolising gene expression
- Table 4.3** Primer sequences of genes coding Trp-catabolising enzymes and reference genes
- Table 4.4** Stained nuclei count and average surface area in livers of *Ido2*^{+/+} and *Ido2*^{-/-} mice
- Table 5.1** List of primer sequences of genes differentially regulated according to microarray analysis for validation by RT-qPCR and reference genes
- Table 5.2** Genes upregulated in liver lysates of *Ido2*^{-/-} relative to *Ido2*^{+/+}
- Table 5.3** Genes downregulated in liver lysates of *Ido2*^{-/-} relative to *Ido2*^{+/+}

- Table 5.4** List generated by Partek Pathway of top 30 pathways implicated by genes differentially-regulated in liver lysates of *Ido2*^{-/-} relative to *Ido2*^{+/+} mice
- Table 5.5** Gene expression in liver lysates of *Ido2*^{-/-} relative to *Ido2*^{+/+} mice, evaluated by RT-qPCR from the list of genes differentially regulated according to microarray analysis
- Table 5.6** Genes upregulated in liver lysates of *Tdo2*^{-/-} relative to *Tdo2*^{+/+}
- Table 5.7** Genes downregulated in liver lysates of *Tdo2*^{-/-} relative to *Tdo2*^{+/+}
- Table 5.8** List of top 30 pathways implicated by genes differentially-regulated in liver lysates of *Tdo2*^{-/-} relative to *Tdo2*^{+/+} mice
- Table 5.9** Gene expression in liver lysates of *Tdo2*^{-/-} relative to *Tdo2*^{+/+} mice, analysed by RT-qPCR from the list of genes differentially regulated according to microarray analysis
- Table 5.10** Genes upregulated in liver lysates of *Ido2*^{-/-}*Tdo2*^{-/-} relative to its equivalent wild type, *Ido2*^{+/+}*Tdo2*^{+/+} mice
- Table 5.11** Genes downregulated in liver lysates of *Ido2*^{-/-}*Tdo2*^{-/-} relative to *Ido2*^{+/+}*Tdo2*^{+/+} mice
- Table 5.12** List of top 30 pathways implicated by genes differentially regulated in liver lysates of *Ido2*^{-/-}*Tdo2*^{-/-} relative to *Ido2*^{+/+}*Tdo2*^{+/+} mice
- Table 5.13** Gene expression in liver lysates of *Ido2*^{-/-}*Tdo2*^{-/-} relative to *Ido2*^{+/+}*Tdo2*^{+/+} mice

Table 5.14 Percentage of genes differentially regulated according to microarray analysis that were assessed and validated by RT-qPCR

Table 6.1 Summary of the findings of the thesis

CHAPTER 1

INTRODUCTION

CHAPTER 1 LITERATURE REVIEW

1.1 Tryptophan

Tryptophan (Trp) is an important amino acid that makes up only about (2%) of the total amino acids in the body (Connick et al., 1989). As it cannot be synthesised *de novo*, it is obtained primarily through diet where Trp is present in most foods. A striking attribute of this amino acid is that it is one of the few that binds to plasma albumin and its presence in the plasma is an interplay of balance between its bound and free forms (McMenamy, 1965). Most of the circulating Trp exists in its albumin-bound form (90%) in the resting state whereas the rest circulates in the free form (Madras et al., 1974).

Dysregulation of Trp metabolism has been implicated in the pathogenesis of a number of central nervous system (CNS)-related diseases such as Alzheimer's disease (Wu et al., 2013), Huntington's disease (Connick et al., 1989) and schizophrenia (Linderholm et al., 2012), as well as in infectious diseases such as microbial and human immunodeficiency viral (HIV) infections (Favre et al., 2010). Its role in autoimmune-related conditions such as allergy (Kawasaki et al., 2014) and cancer also has been discussed (Platten et al., 2005; Opitz et al., 2011; Liu et al., 2010).

Non-esterified fatty acids (NEFA) are pivotal in the balance of free to albumin-bound Trp ratio. NEFA binds to albumin competitively with Trp and is therefore able to displace the amino acid from albumin, increasing the levels of free Trp in the plasma (Curzon et al., 1973). Conditions such as sustained exercise (Fernstrom and Fernstrom, 2006) and β -adrenoceptor-mediated lipolysis (Cleroux et al., 1989) can result in the elevation of NEFA levels in the plasma. This increase in NEFA displaces Trp from albumin, increasing the

pool of its free form in plasma. Some drugs are capable of eliciting similar effects, even at their pharmacological doses (Muller and Wollert, 1975; Spano et al., 1974). It is this elevation in plasma Trp levels that is believed to consequently influence brain Trp uptake and levels (Tagliamonte et al., 1973). However, it was demonstrated that an increase in brain Trp level was still evident even when the rise in plasma NEFA during exercise was completely blocked by nicotinic acid pretreatment (Fernstrom and Fernstrom, 1993), suggesting an alternative mechanism for Trp increase in the brain. The activation of the sympathetic nervous system, was later shown, to have a greater influence in the regulation of Trp availability in the brain than the displacement of Trp from albumin by NEFA (Fernstrom and Fernstrom, 2006; Ruddick et al., 2006). Trp homeostasis in the brain also may be affected by other NEFA-independent factors, including various stress stimuli, carbohydrate intake, cytokines as well as some drugs (Lenard and Dunn, 2005; Curzon et al., 1972; Dunn, 1992; Wang and Dunn, 1998).

Once Trp has crossed the blood-brain barrier (BBB), it can then be taken into the cells of the CNS system and distributed to different metabolic pathways according to the needs of the system. It is the regulation of Trp uptake across the BBB that ultimately controls serotonin synthesis (Grahame-Smith, 1971; Tagliamonte et al., 1973).

Apart from being incorporated into proteins, Trp plays a significant role in a number of pathophysiological and physiological conditions as it generates neuroactive metabolites such as serotonin, 3-hydroxykynurenine, quinolinic acid and kynurenic acid, among others. Trp can be metabolised either through the serotonin or kynurenine pathways, with the latter catabolising the majority of Trp obtained from the plasma. As Trp is an essential amino acid, its depletion acts as a strategic approach for the host to eliminate

pathogens by promoting nutritional competition between host cells and pathogens (Pfefferkorn and Guyre, 1984). This depletion of Trp in the cells invaded by pathogens and neighbouring cells inhibits the proliferation of the pathogen, efficiently retarding further pathogen growth. This mechanism has been shown to help control microbial infections in salmonellosis, listeriosis and toxoplasmosis (Adams et al., 2004; Durr and Kindler, 2013; Knubel et al., 2010; Konen-Waisman and Howard, 2007; Popov et al., 2006).

Evidence suggests that the depletion of Trp also modulates immune tolerance to non-self as in seen in the cases of transplants and allogeneic pregnancies (Munn et al., 1998; Uyttenhove et al., 2003; Alexander et al., 2002). More recently, it was shown that tolerance to non-self was not the only role of Trp catabolism as degradation of Trp also facilitated tolerance towards tumours (Uyttenhove et al., 2003). The depletion of Trp was found to modulate these effects by suppression of T cell proliferation (Munn et al., 1999; Lee et al., 2002) through either the activation of the GCN2 (General control nonderepressible 2) stress-kinase pathway (Munn et al., 2005; Zhang et al., 2002) or inhibition of mTOR (mammalian target of rapamycin) (Gao et al., 2002; Rohde et al., 2001). The generation of toxic Trp metabolites through the kynurenine pathway is an alternative mechanism through which the immunosuppressive effects of Trp metabolism have been suggested to be exerted (Fallarino et al., 2002; Frumento et al., 2002; Terness et al., 2002).

1.2 Serotonin pathway

In this pathway, Trp is hydrolysed by tryptophan hydroxylase (TPH) to 5-hydroxytryptophan (5-HTP) (Stoll and Goldman, 1991; Grahame-Smith, 1964). 5-HTP then is quickly metabolised to 5-hydroxytryptamine (5-HT), also known as serotonin, by aromatic amino acid decarboxylase (Fig. 1.1). Serotonin, an aminergic neurotransmitter, then can be either packed in synaptic vesicles and stored until use or metabolised first to 5-hydroxyindole acetaldehyde (5-HIA) and then to 5-hydroxyindoleacetic acid (5-HIAA). It also can be converted eventually to melatonin, a neurohormone (Ruddick et al., 2006). The availability of Trp itself can also, to a lesser degree, exert rate limiting effects on serotonin synthesis (Fernstrom and Wurtman, 1971; Richard et al., 2009). It was initially thought that the catabolism of Trp to serotonin in the CNS as well as the peripheral nervous system (PNS) was catalysed by the same enzyme, TPH. However, it was discovered recently that mice ablated for TPH function only had 5-hydroxytryptamine (5-HT) deficiency in the periphery and pineal gland (Walther et al., 2003). The levels of 5-HT remained normal in the brain despite *Tph* gene ablation. This led to the discovery of a new, brain-specific *Tph* gene, now known as *Tph2*, which was responsible for the catabolism of Trp to serotonin in the brain (Walther et al., 2003). It also has been demonstrated that TPH2 has higher affinity for Trp than TPH1 (McKinney et al., 2005). Even within TPH itself, there is a difference between TPH of neural and non-neural origin (Hasegawa et al., 1987). Serotonin has been shown to play a role in a number of major organ systems as well as the CNS, with its dysregulation implicated in psychiatric and neurological disorders such as anxiety, depression, schizophrenia, suicidal behaviour and

alcohol abuse as well as in physiological activities such as arousal and sleep (Roth et al., 2004; Berger et al., 2009; Morrissette and Stahl, 2014) .

In peripheral tissues, only about 1% of Trp is converted to serotonin, while more than 95% of dietary tryptophan is catabolised to kynurenines (Botting, 1995; Stone, 1993; Wolf, 1974). Due to the discovery of serotonin as an important neurotransmitter, the research focus on Trp catabolism shifted from the kynurenine pathway to the serotonin pathway instead. However, there has been resurgence in interest in the kynurenine pathway following findings on the neurological activities of kynurenine metabolites such as quinolinic acid and kynurenic acid.

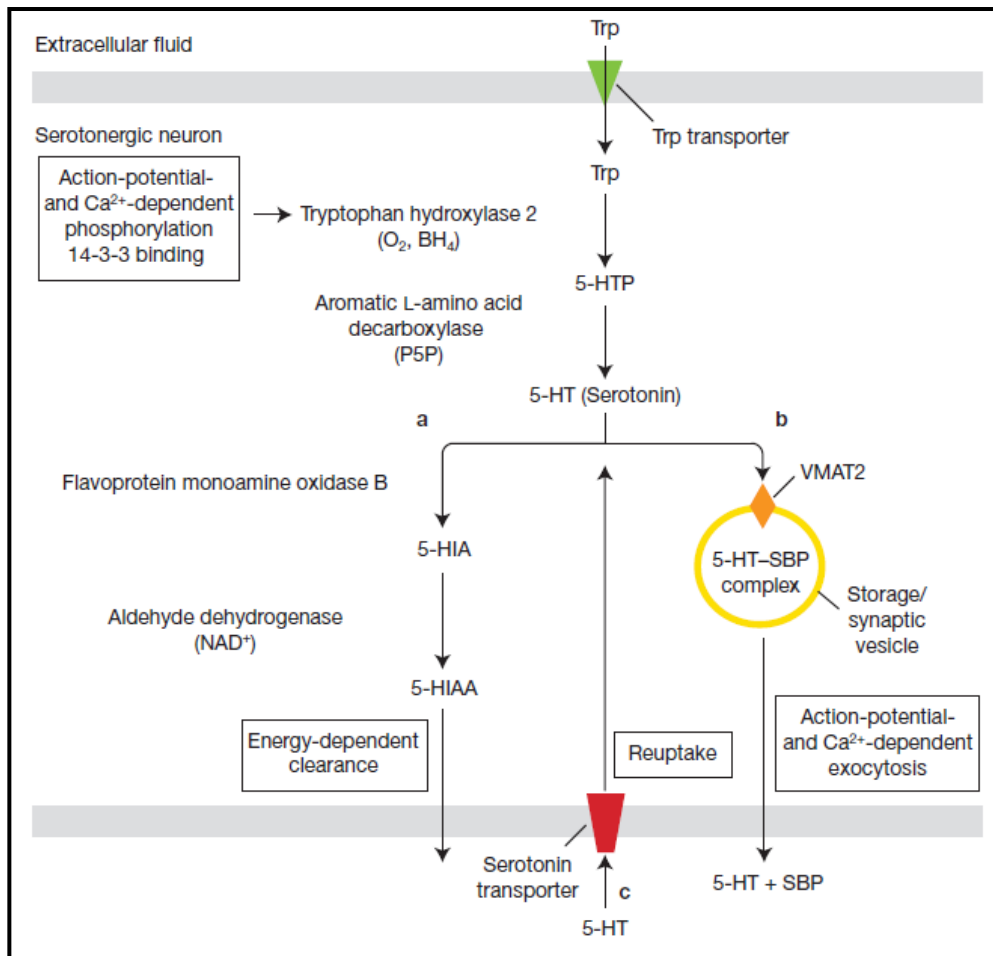


Fig. 1.1 Tryptophan metabolism by tryptophan hydroxylase in serotonergic neurons

Abbreviations: 5-HTP, 5-Hydroxytryptophan; 5-HT, 5-Hydroxytryptamine; 5-HIA, 5-Hydroxyindole acetaldehyde; 5-HIAA, 5-Hydroxyindole acetic acid; VMAT2, Vesicular monoamine transporter 2; SBP, Serotonin-binding protein; BH4, cofactor tetrahydrobiopterin.

Reproduced from (Ruddick et al., 2006)

1.3 Kynurenine Pathway

This pathway begins with oxidative cleavage of Trp, by either indoleamine 2,3-dioxygenase 1 (IDO1), IDO2 or tryptophan 2,3-dioxygenase (TDO2), all of which are haem-dependent enzymes (Knox and Auerbach, 1955; Higuchi and Hayaishi, 1967; Ball et al., 2007). The product of this step, N-formylkynurenine, is then broken down to kynurenine by a formamidase (Fig. 1.2). Kynurenine can then undergo different fates. It can either be broken down to (i) anthranilic acid by kynureninase, (ii) kynurenic acid (KA) by kynurenine aminotransferase or (iii) 3-hydroxykynurenine by kynurenine-3-monooxygenase (Botting, 1995). In the case that kynurenine undergoes the first option, it may be used subsequently for the biosynthesis of aromatic amino acids. On the other hand, kynurenic acid is a rather stable compound, which can be further catalysed to quinolines. In the case where kynurenine follows the third route, the pathway continues on to contribute to the formation of NADH as the final product.

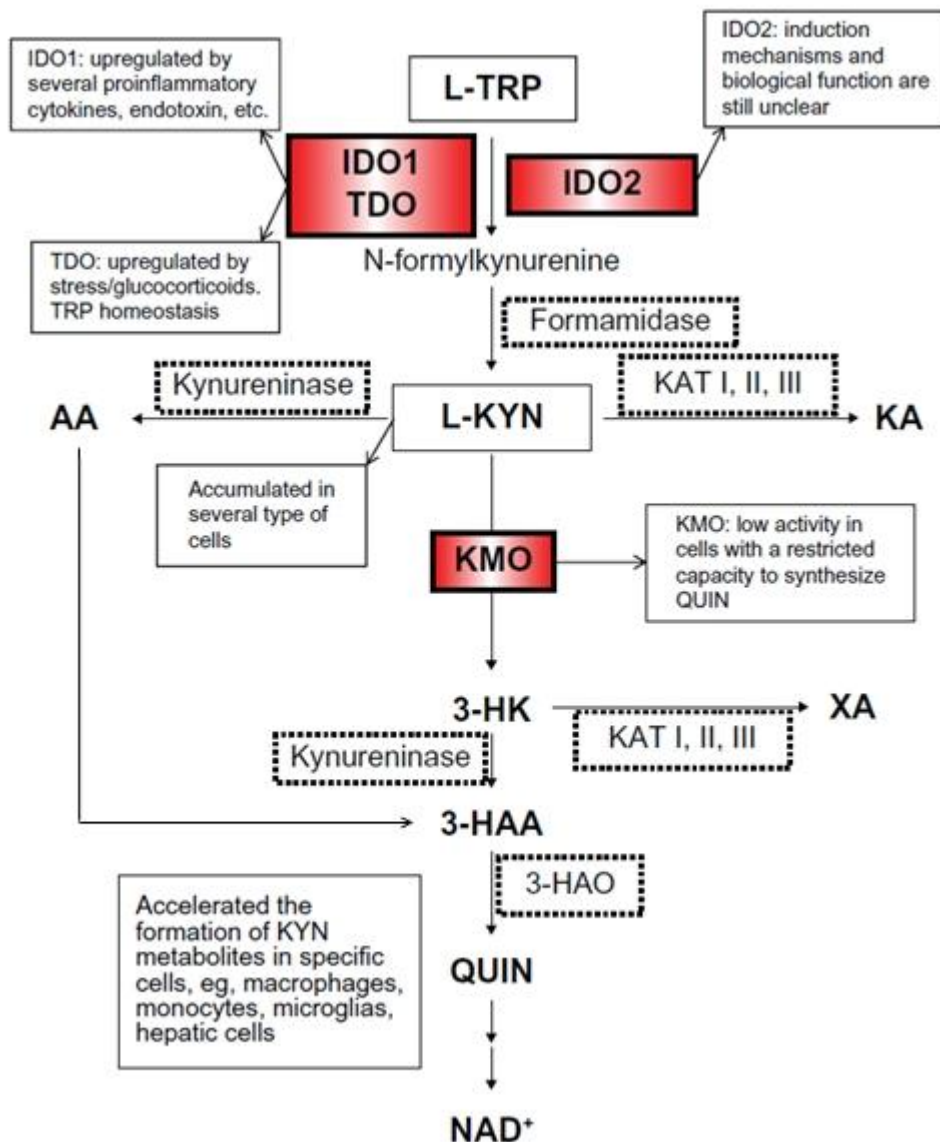


Figure 1.2 Schematic overview of the kynurenine pathway.

Abbreviations: L-TRP, L-Tryptophan; L-KYN, IDO, Indoleamine 2,3 dioxygenase; TDO, Tryptophan 2,3 dioxygenase; L-Kynurenine; KAT I, II, III, Kynurenine aminotransferase; KA, kynurenic acid; KMO, kynurenine 3-monoxygenase; AA, anthranilic acid; 3-HK, 3-hydroxykynurenine; XA, xanthurenic acid; 3-HAA, 3-hydroxyanthranilic acid; 3-HAO, 3-hydroxyanthranic acid oxidase; NAD⁺, nicotinamide adenine dinucleotide+.

Reproduced from (Murakami and Saito, 2013) and (Stone, 1993).

Furthermore, the consequence or fate of Trp in the kynurenine pathway differs according to tissue type, as not all cells are capable of catabolising the substrates downstream in the pathway (Heyes et al., 1997; Owe-Young et al., 2008). This difference is caused by the absence or low expression of the enzymes downstream in the pathway. For example, in endothelial cells, Trp is catabolised to KA constitutively, whereas in cells primed with Interferon gamma (IFN γ), high levels of both kynurenine and kynurenic acid was detected (Owe-Young et al., 2008; Wang et al., 2010). Another key observation of the pathway in endothelial cells was that there was little or very low quinolinic acid detected. Even in conditions where BBB endothelial cells were incubated with an excess of 3-hydroxyanthranilic acid, quinolinic acid was undetectable, indicating that 3-hydroxyanthranilic acid (3-HAA) was not a substrate for the kynurenine pathway in BBB endothelial cells. Exogenous quinolinic acid added to these cells did not alter in levels, which showed that it is not metabolised further in the endothelial cells. The inability of endothelial cells to metabolise 3-hydroxyanthranilic acid, and the absence of quinolinic acid in these cells, suggests that it is most likely that the enzymes downstream in the pathway are either inactive, absent or expressed at levels too low to cause any functional effect (Owe-Young et al., 2008). This observation is consolidated further by the inability of BBB endothelial cells to metabolise exogenous quinolinic acid. Similar observations were reported in human foetal brain cultures and lung cells, where kynurenine 3-monooxygenase (sometimes known as kynurenine 3-hydroxylase) activity was low and the production of quinolinic acid was little to none, despite stimulation with IFN γ (Heyes et al., 1996; Heyes et al., 1997). In some cells types, the enzyme downstream in the pathway is expressed and active, and therefore downstream products are detectable. Quinolinic acid was detected at high levels in monocytes, microglial and liver cells, with

the highest accumulation observed in monocytes, indicating the capacity of these cell types to metabolise substrates downstream of the pathway (Heyes et al., 1992; Heyes et al., 1997). In the presence of IFN γ there was an even more marked production of quinolinic acid in these cells (Heyes et al., 1997).

The involvement of the kynurenine pathway has been reported in some physiological processes, such as pregnancy, as well as pathophysiological processes such as cancer, dementia, schizophrenia and malaria (Munn et al., 1998; Sanni et al., 1998; Heyes et al., 1991; Platten et al., 2012; Linderholm et al., 2012; Pfefferkorn and Guyre, 1984). This pathway also has been identified as the major route for NAD⁺ supply in rat hepatocytes (Bender and Olufunwa, 1988).

The first step of this pathway is rate-limiting. Although there are three enzymes that catalyse this reaction, these enzymes differ in their distribution and roles. TDO2, the enzyme first discovered to catalyse this reaction, is a hepatic protein responsible mainly for the regulation of dietary Trp (Knox and Auerbach, 1955). IDO1 was first isolated from rabbit ileum in 1967 (Higuchi and Hayaishi, 1967). Its expression, however, was induced more in inflammatory conditions than constitutively (Yoshida et al., 1979; Pfefferkorn et al., 1986b). The third and most recently discovered enzyme that catalyses the first step of the kynurenine pathway is IDO2, an isoform of IDO1 (Ball et al., 2007; Metz et al., 2007; Yuasa et al., 2007). Although it has been implicated in inflammation and adaptive immunity, little is known about its role in physiological and pathological circumstances (Merlo et al., 2014; Metz et al., 2014). The possibility that the expression and role of IDO2 may be influenced by, or is dependent on, the expression IDO1 also has been discussed recently (Metz et al., 2014) and will be further explored in Chapter 4 of this thesis.

1.3.1 TRYPTOPHAN 2,3-DIOXYGENASE

Tryptophan 2,3-dioxygenase (TDO/TDO2), also known previously as tryptophan oxygenase, tryptophan peroxidase or tryptophan pyrrolase, is coded for by the *Tdo2* gene, which is located on chromosome 3 and 4 in mice and humans, respectively. It was first described by Kotake and Masayama (1936) who observed the conversion of L-Trp to L-kynurenine in crude extracts of rabbit liver (Knox and Mehler, 1950; Mehler and Knox, 1950). Apart from the liver, *Tdo2* mRNA is expressed constitutively in low levels in the epididymis, testis, pancreas, heart, brain, maternal-foetal interface and early stage embryos (Britan et al., 2006; Suzuki et al., 2001). However, the exact role of the enzyme in these tissues is not very well understood. Despite catalysing the same reaction as IDO1 and IDO2, TDO2 shares very little sequence identity with the two, especially around the area pivotal for catalytic activity (Zhang et al., 2007b; Forouhar et al., 2007; Metz et al., 2007). This difference in sequence identity also could be suggesting distinct roles for the three enzymes depending on the physiological or pathological condition.

TDO2 is enantiomer-specific, cleaving highly specifically the L-isomer of Trp, a contrasting feature to IDO1 which has a wider substrate range (Hayaishi, 1976; Forouhar et al., 2007; Capece et al., 2010). The indole ring of Trp is cleaved oxidatively by TDO2, which has a short half-life of 2 hours in mammals (Stone, 1993). When exogenous Trp was administered to WT mice, the rapid degradation of TDO2 is inhibited, thereby facilitating the catabolism of Trp by the enzyme (Schimke et al., 1965a; Schimke et al., 1965b). Concurrent with this observation is the finding that the activity of TDO2 is induced mainly by dietary Trp or its related compounds such as α -methyl tryptophan (Knox and Auerbach, 1955; Schimke et al., 1965b). Glucocorticoids also seem to induce

this enzyme, by a mechanism that results in production of more TDO2 mRNA and protein. Although TDO2 is known to be unresponsive to immunological signals, a striking difference to IDO1, a substantial inhibition of liver TDO2 activity in infectious or inflammatory states has been reported (Takikawa et al., 1986; Saito et al., 1993; Moreau et al., 2005). However, when human TDO2-transfected HeLa cells, capable of degrading Trp and producing kynurenine upon stimulation with tetracycline, were infected with *Toxoplasma gondii*, *Staphylococcus aureus* or *Herpes Simplex* virus, the growth of these pathogens was inhibited (Schmidt et al., 2009). This suggested that TDO2 may possess antimicrobial properties, exerted through the depletion of Trp in the microenvironment. In the light of the earlier finding that TDO2 activity is suppressed during infection and inflammation, the antimicrobial effects seen could be a feature of extrahepatic TDO2 and not liver TDO2. The same publication also found that TDO2-positive cells were capable of suppressing T cell proliferation and IFN γ production driven by alloantigen, an immunoinhibitory effect that can be reversed by supplementation with Trp. This implicated TDO2 in a possible immunoregulatory role, especially in liver transplantation.

Another condition in which TDO2 is suggested to play a role is cancer, as *TDO2* mRNA was detected in a wide range of human tumour samples as well as in cancer cell lines (Pilotte et al., 2012; Opitz et al., 2011). In addition, when human and murine cancer cell lines were treated with a TDO2-selective inhibitor, a reduction in kynurenine production was observed, which was not seen with cells treated with the IDO1-selective inhibitor the L isomer of methyl-Trp (L-1-MT). In mice injected with TDO2-expressing tumour cells, a more rapid progression of the tumour was seen (Pilotte et al., 2012). Opitz et al. (2011) also showed that kynurenine constitutively generated by TDO2 of human tumour cell line

origin was an endogenous ligand of aryl hydrocarbon receptor (AhR). AhR is involved in a number of cellular processes, tumourigenesis being one of them. Both these findings are consistent with the suggestion that TDO2 might be mediating immunotolerance in certain cancer types.

Low levels of *Tdo2* have been reported in the brain (Gal, 1974). As the kynurenine pathway has been implicated in a number of psychiatric disorders, it has been suggested that TDO2 is the Trp-catabolic enzyme that plays a role in the pathology of these disorders. Elevated levels of kynurenic acid and kynurenine were found in postmortem brain samples of schizophrenic patients (Schwarcz et al., 2001), and these were later attributed to TDO2 (Miller et al., 2004; Miller et al., 2006). A similar upregulation of TDO2 in post-mortem brain samples of bipolar patients with psychosis also was reported, although the difference was less marked than that seen in schizophrenic patients (Miller et al., 2006). Interestingly, the absence of TDO2 resulted in reduced anxiety in *Tdo2*^{-/-} mice (Kanai et al., 2009). As plasma levels of Trp and 5-hydroxyindoleacetic acid were elevated in these mice, it was postulated that the absence of TDO2 increased plasma levels of Trp, resulting in upregulation of serotonin synthesis in the brain, which could cause the anxiolytic symptoms detected in the *Tdo2*^{-/-} mice. Collectively, the presence of TDO2 in the brain, as well as the ability of TDO2 to modulate the expression of serotonin in its absence, suggests a possible role for TDO2 in neurological or psychiatric disorders. One of the outcomes of the kynurenine pathway is the generation of NAD⁺. Of the three Trp-catabolising enzymes, it is TDO2 that was proposed to be the primary enzyme driving this process (Badawy, 1981). This view was consolidated with more recent reports that TDO enzymes were able to salvage the NA-auxotrophic yeast strain, but not IDO2 (Ball et

al., 2014; Yuasa and Ball, 2013). Surprisingly, no difference was found in liver NAD⁺ levels between WT and TDO2-deficient mice (Terakata et al., 2013). Terakata and colleagues, therefore, speculated that in TDO2-deficient mice, IDO1 is essential to synthesise the minimum required amount of nicotinamide, suggesting extrahepatic IDO1 compensates for the role of TDO2 in generating niacin in these mice.

1.3.2 INDOLEAMINE 2,3-DIOXYGENASE 1

IDO has been well conserved throughout evolution (Sedlmayr et al., 2014) and widely distributed from bacteria to metazoans. It is even found in fungi, in which TDO is absent (Ball et al., 2014). In some animals, IDO homologues are found. Both *Ascomycota* and *Basidiomycota* fungi possess multiple IDO homologues (Yuasa and Ball, 2011). In mammals such as mice and humans, two IDO gene homologues have been reported (Ball et al., 2007; Metz et al., 2007; Yuasa et al., 2007). A phylogenetic tree showing the distribution of IDO in different organisms is depicted in Fig 1.3.

The first IDO gene discovered in mammals was re-classified as IDO1, following the discovery of the second homologue, IDO2. IDO1 is the second enzyme reported to catalyse the same reaction as TDO2, namely the catabolism of Trp to N-formylkynurenine, by cleaving the 2,3-double bond of its indole ring (Higuchi and Hayaishi, 1967). Unlike the tetrameric TDO2, IDO1 is monomeric, despite both proteins containing haem molecules. IDO1 is active in its reduced form (Fe^{2+}) but inactive in its oxidised form (Fe^{3+}) (Shimizu et al., 1978). Initially, it was proposed that IDO1 is reduced from the Fe^{3+} to Fe^{2+} form by superoxide anion (Taniguchi et al., 1977). More recently, this was refuted and cytochrome b_5 ($\text{cy}b_5$) working with cytochrome P450 reductase and NADPH was reported to be the major physiological reductant of oxidised human IDO1 (Maghzal et al., 2008).

IDO1 can catalyse a greater number of indole-containing substrates than TDO2, including D-Trp, L-Trp, tryptamine, 5-hydroxytryptophan and 5-hydroxytryptamine catabolism (Shimizu et al., 1978; Thomas and Stocker, 1999). Its affinity for L-Trp also was significantly higher than IDO2 with a K_m of about 30 μM .

The most well-known inhibitor of IDO1 is 1-methyltryptophan (1-MT), which has been used in various studies to inhibit the enzyme's activity (Munn et al., 1998; Uyttenhove et al., 2003). More recently, it was reported that the L-isomer of 1-MT was more efficient in blocking mouse IDO1 activity than the D-isomer (Austin et al., 2010; Lob et al., 2009). However, in clinical studies, the D-isomer has been reported to be more effective in increasing survival and reducing tumour growth in mice models of cancer (Hou et al., 2007). However, the earlier studies were reported before the discovery of IDO2 and did not take into account the potential targets of this inhibitor on the second isoform of IDO. The effects of 1-MT on IDO2 will be discussed in Section 1.3.3.4.

In mice, IDO1 mRNA and protein are expressed constitutively at relatively low levels in the epididymis, gut, brain, lymph nodes, spleen, thymus, lung, and placenta, despite being absent from the liver (Munn et al., 1998; Yoshida et al., 1979). IDO1 protein localisation has been reported in the apical and principal cells of the caput epididymis (Britan et al., 2006; Dai and Zhu, 2010). Certain cell types such as endothelial cells, dendritic cells, fibroblasts and monocyte-derived macrophages also possess an inducible form of IDO1 (Daubener et al., 2001; Hwu et al., 2000; Munn et al., 1999; Pfefferkorn et al., 1986b).

The observation that IDO1 does not catabolise excess dietary Trp led to the question of why IDO1 was conserved in mammals. It was only recently that IDO1 was suggested to play an immunomodulatory role through Trp depletion and T cell suppression (Mellor and Munn, 1999; Mellor and Munn, 2004).

The role of the kynurenine pathway in antimicrobial responses is well documented (Byrne et al., 1986a; Pfefferkorn and Guyre, 1984; Yoshida et al., 1979). Its expression also is

markedly higher during inflammatory states such as cancer and cerebral malaria as well as neurological conditions like Alzheimer's disease, schizophrenia and AIDS dementia complex (Pfefferkorn et al., 1986b; Sanni et al., 1998; Knubel et al., 2010; Gupta et al., 1994; Yamada et al., 2009; Uyttenhove et al., 2003). Apart from cancer, IDO1 was reported to play a role in other autoimmune diseases, such as arthritis, colitis, encephalomyelitis and asthma (Criado et al., 2009; Hayashi et al., 2004; Gurtner et al., 2003; Sakurai et al., 2002; Szanto et al., 2007). The involvement of IDO1 in pregnancy is a relatively new development (Munn, 1998), where the enzyme in the placenta was shown to prevent rejection of allogeneic foetuses.

Its induction in inflammatory conditions is driven by a few immunological signals, namely lipopolysaccharide (LPS), tumour necrosis factor (TNF) and IFN γ (Higuchi and Hayaishi, 1967; Pfefferkorn et al., 1986b; Yoshida et al., 1979). Of the three most well-known inducers of IDO1, IFN γ is the most potent. Type I interferons, IFN α and IFN β were reported to possess stimulatory effects on IDO1 expression too, although to a lesser degree (Carlin et al., 1987).

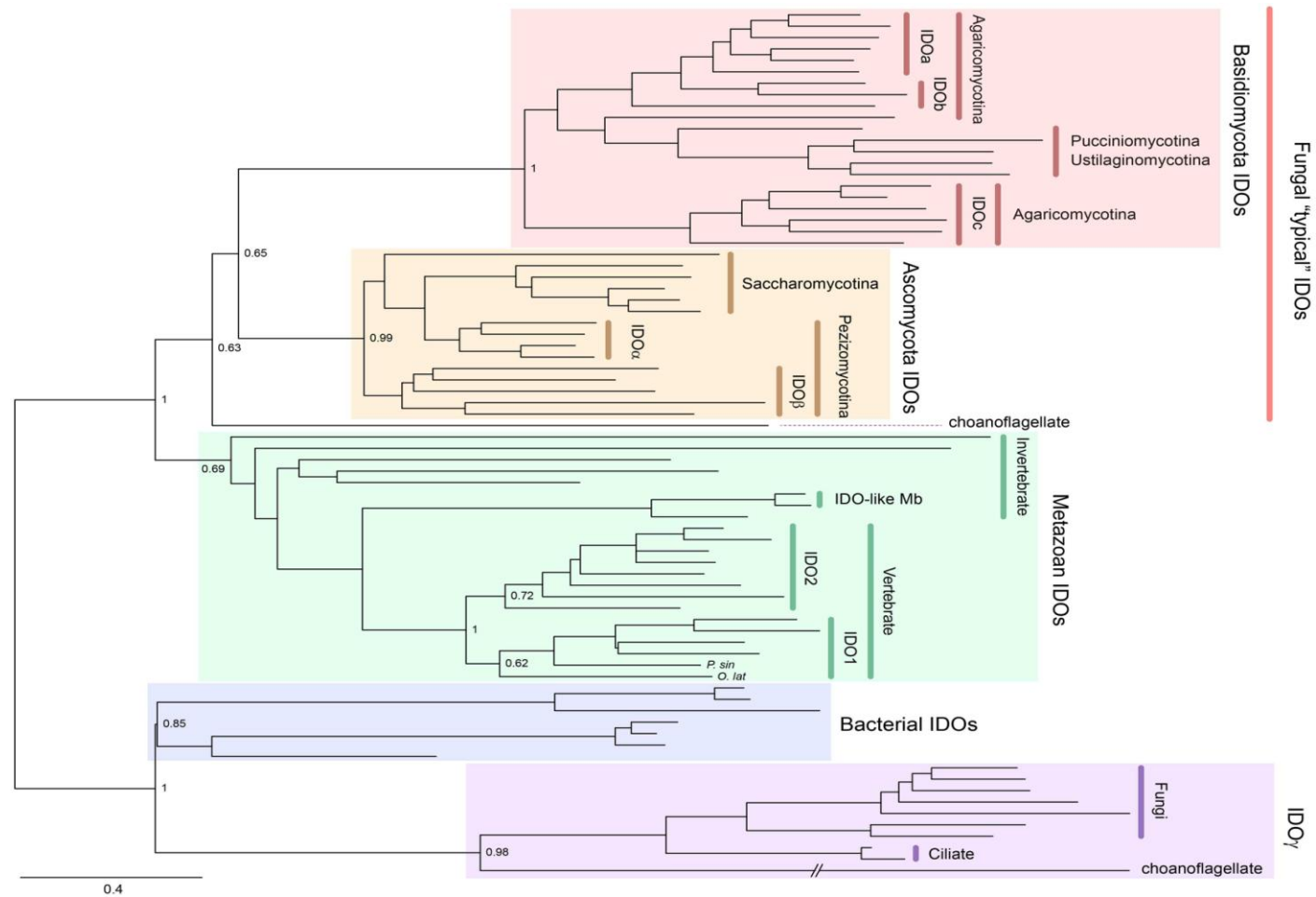


Fig 1.3 Phylogenetic tree of known IDOs and IDO-related proteins. Reproduced from (Ball et al., 2014). The Medaka-fish, *Oryzias latipes* (*O. lat*) and a soft-shelled turtle, *Pelodiscus sinensis* (*P. sin*) have a putative IDO1. The tree shows that the gene duplication, generating IDO1 and IDO2, occurred before the divergence of vertebrates. The internal branch labels are bootstrap values with 100 replications. The scale bar corresponds to 0.4 substitutions per site.

1.3.2.1 Interferons

Interferons (IFN), first reported in 1957, derive their name from the word interfere due to their ability to induce virus interference, which essentially refers to the protection of host cells from a virus (Isaacs and Lindenmann, 1957). This family of proteins, classified as cytokines, have been shown to possess various cellular functions. The viral interference functions of IFNs were demonstrated by Isaacs and colleagues where they showed that chorio-allantoic membrane released IFNs with antiviral properties when challenged with heat-inactivated, non-infective influenza virus (Isaacs and Lindenmann, 1957; Isaacs et al., 1957). This observation was consolidated when mice injected with anti-IFN antibodies exhibited greater susceptibility to viral diseases (Gresser, 1990). IFNs also were shown to exert immunoregulatory roles (Boehm et al., 1997; Carnaud et al., 1999; Young and Hardy, 1995).

IFNs have been classified into two main groups, Type I and Type II. Type I IFNs possess structural similarity to each other and consist of IFN α , IFN β , IFN ω and IFN τ . Type II IFN, on the other hand, refers to IFN γ , which has no structural similarity to Type I IFNs. While IFN β is mainly synthesised by fibroblasts, haematopoietic cells are responsible for most IFN α and IFN τ production. It is Type I IFNs that are often induced in the case of a viral infection, with IFN α and IFN β being the more commonly expressed cytokines in the group (Bach et al., 1997; Jonasch and Haluska, 2001).

IFN γ , the interferon that plays a greater role in immunomodulation, is mainly secreted by CD4⁺ Helper T (T_H) cells, CD8⁺ cytotoxic lymphocytes, natural killer (NK) cells, B cells and antigen-presenting cells (APCs) such as monocytes, macrophages and dendritic cells under the influence of immune or inflammatory stimuli (Frucht et al., 2001; Gessani and

Belardelli, 1998; Yoshimoto et al., 1998; Flaishon et al., 2000; Harris et al., 2000; Bach et al., 1997). Two proinflammatory cytokines, IL-12 and IL-18, have been shown to induce the expression of IFN γ in APCs (Munder et al., 1998; Yoshimoto et al., 1998). IFN γ acts on IFN γ receptors, which are distinctly different from IFN α and IFN β receptors (Branca and Baglioni, 1981; Aguet et al., 1988), and is able to induce transcription of a number of cellular genes, leading to the translation of proteins such as major histocompatibility complexes (MHCs), IL-12, CXCL10, TNF and IDO1 (Akbar et al., 1996; Mosca et al., 2000; Luster et al., 1985; Billiau and Matthys, 2009; Collart et al., 1986; Pfefferkorn et al., 1986a).

The immunomodulatory effects of IFN γ include coordinating leukocyte attraction, as well as influencing the growth, maturation and differentiation of various cell types such as human myeloid cells, B cells and NK cells (Boehm et al., 1997; Perussia et al., 1983; Young and Hardy, 1995). In addition, its ability to induce NK cell activity and regulate immunoglobulin production by influencing B cells has been documented (Boehm et al., 1997; Carnaud et al., 1999; Finkelman et al., 1988).

IFN γ exerts some of its immunoregulatory effects through the activation of IDO1, which results in Trp depletion and suppression of T cell proliferation (Pfefferkorn et al., 1986a; Pfefferkorn et al., 1986b; Tashiro et al., 1961). IFN γ induction of IDO1 expression was found to be through the IFN γ -stimulated response element (ISRE), which flanks the gene (Hassanain et al., 1993; Dai and Gupta, 1990). This response element makes IDO1 inducible by IFN γ but not IFN α or IFN β .

1.3.2.2 IDO1 in infections

In infections such as *T. gondii*, *Chlamydia pneumoniae*, *S. aureus*, group B streptococci and mycobacteria, IDO1 plays a role in the innate host immune response (Byrne et al., 1986b; Pfefferkorn et al., 1986a; MacKenzie et al., 1998; Hayashi et al., 2001; Schroten et al., 2001). In these infections, IFN γ -mediated induction of IDO1 resulted in Trp catabolism, which led to the deprivation of this essential amino acid in the local microenvironment. The depletion of Trp then retarded pathogen growth, an effect that was reversible when the growth medium was replenished with Trp. Replication of viruses such as cytomegalovirus and herpes simplex virus also was inhibited upon induction of IDO1 *in vitro* in infected cell lines, through a similar mechanism (Bodaghi et al., 1999; Adams et al., 2004).

1.3.2.3 IDO1 in cancer

IDO1 has been implicated in a number of cancer types and an upregulation of the gene was seen in some cancer cell lines when primed with IFN γ (Taylor and Feng, 1991; Uyttenhove et al., 2003; Yoshida et al., 1988). An increase in IDO1 levels resulted in worse prognosis in some cancer types, while in some others an improved prognosis was seen (Ozaki et al., 1988; Ino et al., 2006; Okamoto et al., 2005; Godin-Ethier et al., 2011). In cancer cell lines such as oral carcinoma and colon adenocarcinoma cell lines, an inhibition of tumour growth was seen as a result of the Trp deprivation triggered by IDO1 activation (Ozaki et al., 1988). However, the general consensus is that IDO1 activation in cancer cells resulted in immune tolerance and prevented tumour rejection, while increasing the metastasis risk. An upregulation of IDO1 seen in endometrial, ovarian, colorectal and

various other carcinomas resulted in poor clinical outcomes and reduced patient survival (Ino et al., 2006; Okamoto et al., 2005; Uyttenhove et al., 2003; Brandacher et al., 2006; Inaba et al., 2009; Yoshida et al., 2008).

There are two mechanisms through which IDO1 is suggested to contribute to the progression of cancer. The first is through the suppression of effector T cells in the tumour local microenvironment whereas the second mechanism involves the expression of IDO1 in the antigen-presenting cells (APCs) of tumour-draining lymph nodes (TDLN). In the former, suppression of CD3⁺ / CD8⁺ T cells has been observed at the site of IDO1-expressing tumour cells (Brandacher et al., 2006; Uyttenhove et al., 2003; Inaba et al., 2009). This led to reduced immune infiltration and antitumour response to the malignant cells. IDO1-expressing APCs such plasmacytoid dendritic cells (pDCs) and eosinophils in TDLN are proposed to be the key players in the second proposed mechanism of IDO1's tolerogenic action in tumours (Munn, 2006; Sharma et al., 2007; Prendergast et al., 2010; Munn et al., 2004; Astigiano et al., 2005). When phorbol myristate acetate (PMA), a chemical that induces chronic local inflammation and thus promotes growth of premalignant lesions upon exposure to carcinogen, is applied topically on the skin, an immune stimulatory response is elicited (Muller et al., 2008). In this immune response, pDCs of local TDLN are activated to synthesise IDO1. As mentioned previously, IDO1 exerts T cell suppressor activity on these pDCs, resulting in the suppression of T cell stimulatory activity of other DCs. Immunological signals such as IFN α , IFN β , IFN γ receptors, TLR/IL-1 signalling adaptor MyD88 and GCN2 stress response kinase were reported to be some of the key activators of IDO1 production in pDCs. The suppression of T cells by IDO1 promotes tumour growth while IDO1 deficiency resulted in an aggressive

antitumour response in the same skin cancer model (Muller et al., 2008). Additionally, IDO1-positive pDCs are also reported to act by activating regulatory T cells (T_{regs}), which are generally immunosuppressive, either by converting them from naive T cells or by recruiting them from existing cells (Fallarino et al., 2006; Sharma et al., 2007). The sustained presence of regulatory T cells inhibits immune infiltration by cytotoxic T cells, promoting self-tolerance (Wood and Sakaguchi, 2003).

1.3.2.4 IDO1 in pregnancy

As the foetus contains both maternal and paternal genetic material, it can be considered partially foreign, and the maternal immune system may attack the foetus, recognising it as non-self. However, in a successful pregnancy, this immune response is suppressed. This indicates the establishment of immune tolerance to the 'foreign' foetus. IDO1 was found to contribute to this tolerance. During pregnancy, IDO1 is expressed at the foetal-maternal interface in a human-term placenta, suggesting a possible role for this protein in pregnancy (Munn et al., 1998; Shayda et al., 2009; Sedlmayr and Blaschitz, 2012). Coinciding with this observation was the progressive decline of serum Trp seen in the first to the third trimester of human pregnancy (Schrocksadel et al., 1996). Initially, this finding was rather contradictory to the physiology of foetal growth as IDO1 seem to be catabolising and causing the depletion of an essential amino acid that would be necessary for foetal growth. However, it was eventually shown that the activation of IDO1 in the microenvironment resulted in T cell suppression in the foetal-maternal interface, pivotal to preventing the rejection of allogeneic concepti (Munn et al., 1998). As maternal T lymphocytes encounter the Trp-deficient microenvironment, suppression of T cell

activation and proliferation occurs, preventing immune infiltration that could lead to the rejection of the foetus. Surprisingly, in the light of this observation, no significant difference was seen in the pregnancy outcome of *Ido1*^{-/-} relative to wild-type mice (Baban et al., 2004). It was postulated that this difference in outcomes in pregnant mice when either IDO1 activity is inhibited in mice naturally expressing IDO1 or IDO1 activity is ablated through permanent genetic alteration (*Ido1*^{-/-}) mice suggests that there may be an alternative compensatory mechanism in genetically IDO1-deficient pregnant mice that induces immunosuppression to prevent pregnancy failures (Baban et al., 2004).

1.3.3 INDOLEAMINE 2,3-DIOXYGENASE 2 (IDO2)

IDO2 is an enzyme of the kynurenine pathway that was identified only recently (Ball et al., 2007; Metz et al., 2007). It is structurally and phylogenetically very similar to IDO1 and catalyses the first and rate-limiting step of the kynurenine pathway, as do the two other Trp-catabolising enzymes, IDO1 and TDO2, as previously discussed. Phylogenetic analysis showed that both IDO1 and IDO2 are present in *Homo sapiens* (humans), *Pan troglodytes* (chimpanzees), *Macaca mulatta* (rhesus macaque/Nuzari monkeys), *Mus musculus* (mice), *Rattus norvegicus* (rats), *Canis familiaris* (domestic dog) and *Bos Taurus* (cattle). In chicken and fish genomes, only one IDO was detected, which bore more similarities to IDO2 than to IDO1 (Yuasa et al., 2007).

Most haem enzymes have more than one isoenzyme catalysing the same reaction. This was the case for the IDO enzymes as well. However, unlike other haem enzymes such as haem oxygenase, cyclooxygenase and nitric oxide synthase, whose isoenzymes are located on different chromosomes although they had a common ancestral gene, both IDO1 and IDO2 are located on chromosome 8, adjacent to each other (Ball et al., 2007). This strongly supports the theory that one of the IDO enzymes arose from genetic duplication. Phylogenetic analysis also suggested that it is more likely that this gene duplication occurred before the tetrapods emerged at the end of Devonian cycle more than 300 million years ago (Ball et al., 2007). As only a single IDO gene was found in lower vertebrates such as chicken and fish, which resembled IDO2 more than IDO1, it was postulated that IDO2 was the ancestral gene from which IDO1 arose by a gene duplication occurring in mammals (Yuasa et al., 2007). However, more recently, IDO homologues were detected in several species of fish and (at least two species of) turtle,

which possessed higher homology to mammalian IDO1 than IDO2 (Ball et al., 2014). This latest finding suggests that the duplication occurred early in vertebrate evolution and IDO1 has been lost in a number of lower vertebrate lineages.

1.3.3.1 Low tryptophan-catabolic activity of IDO2

Both IDO1 and IDO2 share striking genomic structural similarities, with only slight differences in their first and last exons (Ball et al., 2007). IDO1 and IDO2 shared about 43% amino acid identity in both mice and humans (Ball et al., 2007; Metz et al., 2007). Despite structural similarity, the substrate specificity and biochemical characteristics of the two differ. IDO2 has a low Trp-catalytic activity with a high K_m value (Austin et al., 2010; Yuasa et al., 2007). This was demonstrated by the lower levels of Kyn produced by mammalian cells transfected with mouse IDO2 compared to IDO1 (Ball et al., 2007; Metz et al., 2007). Through similar experiments, it also was shown that the Trp-catabolic activity of mouse IDO2 was higher than human IDO2 (Metz et al., 2007; Qian et al., 2012). *Cyb₅* which was established to be a physiological IDO-reductant, also was capable of reducing mouse IDO2 from its oxidised form in a cell-free system (Maghzal et al., 2008; Austin et al., 2010). In addition to this, *cyb₅* was shown to also increase the Trp-catabolic activity of this second isoform of mouse IDO in the presence of human CPR, a physiological electron donor of *cyb₅*, and an NADPH regenerating system, compared to the standard in vitro containing methylene blue as an electron donor (Austin et al., 2010). Both *cyb₅* and CPR needed to be present in order to activate recombinant mouse IDO2 – either component alone was insufficient. An increase in substrate specificity of IDO2 for L-Trp as well as turnover rate was observed in the presence of *cyb₅* (Austin et al., 2010).

The Trp-catabolic activity of IDO2 was too low to contribute to the generation of NAD⁺ as neither human nor mouse IDO2 was able to rescue NA-auxotrophic yeast strain in the same way as IDO1 (Yuasa and Ball, 2013). Despite the low enzymatic activity of IDO2, it is proposed that the level of activity is still capable of eliciting biological effects. This was suggested by knocking down human IDO2 in dendritic cells, which resulted in decreased Kyn levels and fewer regulatory T cells (Trabanelli et al., 2014).

1.3.3.2 IDO2 Distribution in tissues and cell populations

There have been contradictory findings regarding the distribution of IDO2 within tissues. When full length mRNA transcripts were assessed by reverse transcriptase polymerase chain reaction (RT-PCR) in human tissues, *IDO2* was detected only in the brain and placenta (Metz et al., 2007). However, when RT-PCR was performed targeting a shorter *IDO2* mRNA transcript, exon 10 specifically, it was detected in the liver, skeletal muscle, small intestine, thymus, lung, brain and placenta, suggesting that there may be other transcription start sites in the gene (Metz et al., 2007). Another study reported *Ido2* mRNA distribution in mouse tissues, where *Ido2* mRNA was detected in the liver, kidney, testis and epididymis, with its expression being very low or almost undetectable in tissues such as brain, lung, spleen and heart (Ball et al., 2007). Fukunaga et al. (2012), on the other hand, observed *Ido2* mRNA in the brain (cerebral cortex and cerebellum), liver, kidney and epididymis of mice.

In the epididymis, IDO2 was detected in the spermatozoan tail, but not in the epididymal cells themselves, a different distribution pattern to IDO1, which was localised in the principal and apical cells of the caput epididymis. Interestingly, a compensatory role for

IDO2 in the absence of IDO1 in the epididymis has been proposed as an upregulation of IDO2 was reported in *Ido1*^{-/-} epididymis (Fukunaga et al., 2012). In the testis, where IDO1 expression was undetectable, IDO2 was localised in the spermatozoan tail, similar to its localisation in the epididymis (Ball et al., 2007).

Another tissue in which both IDO1 and IDO2 was detected is the kidney. IDO1 was detected in the blood vessels, whereas IDO2 expression was seen in the tubules (Ball et al., 2007). This highlighted a difference in the protein localisation of IDO1 and IDO2 in the same tissues, indicating that each isoform may be playing a different, specialised role, despite catalysing the same reaction in these tissues. Investigation of cellular and subcellular localisation of both IDO1 and IDO2 could shed more light on the differential roles of each enzyme.

In cell populations, IFN γ -inducible IDO2 was present in antigen-presenting dendritic cells, macrophages, astrocytes and mesenchymal stem cells (Croitoru-Lamoury et al., 2011; Lob et al., 2009; Metz et al., 2007). However, *in vivo*, no *Ido2* induction was seen the kidney or liver of mice infected with malaria, which are known to have high levels of circulating IFN γ (Ball et al., 2007). Even in IFN γ ^{-/-} mice, there was no significant differences in the *Ido2* mRNA levels compared to wild-type mice, suggesting that IDO2 was not significantly inducible by IFN γ (Ball et al., 2007). It is worth considering that IDO2 may be IFN γ -inducible in specific cell types but not necessarily throughout the system.

Similarly, an upregulation of *Ido2* mRNA in macrophages from *Ido1*^{-/-} mice was detected when populations of macrophages were studied (Metz et al., 2007). However, when *Ido2* mRNA in *Ido1*^{-/-} kidney and liver was assessed, a significant downregulation was detected. This difference at the mRNA level did not translate into protein as there was no

significant differences detected between the *Ido1*^{-/-} tissues relative to the wild-type (Ball et al., 2007). *Ido2* mRNA regulation in different cell and tissue types may warrant deeper study of IDO2. It could be indicative of the presence of an additional, undiscovered factor within tissues that regulates the expression of IDO2.

Despite relatively higher levels of *Ido2* mRNA in the kidneys of *Plasmodium berghei* ANKA (PbA)-infected C57BL/6 mice than in the same tissue in uninfected mice, this difference was not significant relative to uninfected animals (Ball et al., 2007). However, a significant reduction of *Ido2* mRNA was seen in liver of PbA-infected mice compared to uninfected C57BL/6. There was also a down-regulation of *Ido2* mRNA in kidneys from *Ido1*^{-/-} mice compared to kidney tissues of uninfected C57BL/6 mice. In *Ifny*^{-/-} mice, *Ido2* mRNA was sustained at levels similar to those in wild-types (Ball et al., 2007).

With contradictory results in the three main publications, a need to assess the expression levels of *Ido2* mRNA in *Ido2*^{-/-} mice relative to wild type animals became pertinent.

1.3.3.3 Genetic polymorphism of IDO2 and splice forms of IDO2

Two single nucleotide polymorphisms (SNPs) that ablate the enzymatic activity of human IDO2 also have been reported (Metz et al., 2007). In addition to these, both human and mouse IDO2 have been shown to possess various splice forms (Metz et al., 2007). Even more recently, it was shown that in macrophages ablated for *Ido1* gene expression, the alternatively spliced form of *Ido2* is upregulated (Metz et al., 2014). This splice form gave rise to a truncated IDO2 protein, with diminished Trp-catabolising properties. Therefore, despite what seemed to be a compensatory mechanism in *Ido1*^{-/-} macrophages that gives rise to higher levels of total *Ido2* mRNA production, this compensation did not translate

into higher IDO2 protein activity. Indeed, the contrary was true, as IDO2 enzymatic activity was diminished in *Ido1*^{-/-} macrophages. Whether this truncated form of IDO2 possesses other biological catalytic properties remains to be uncovered.

In the liver, however, *Ido1* expression did not seem to be affected by the ablation of *Ido2* gene function in *Ido2*^{-/-} mice (Metz et al., 2014). The converse was also true, in that *Ido2* expression was not significantly different between murine wild-type and *Ido1*^{-/-} liver tissues. The differences in observations between whole tissues such as liver and cell populations such as macrophages indicate that any regulatory or compensatory role *Ido2* plays seems to be restricted to specific cell or tissue types. As the differential regulation of *Ido2* was seen mostly in macrophages and kidney tissue, IDO2 may play a specific role in the haematopoietic cells of the innate and/or adaptive immune systems.

1.3.3.4 IDO2 inhibitors

As mentioned previously in Section 1.3.2, 1-MT is a commonly used inhibitor of IDO1. D-1-MT was reported to be the more efficient inhibitor of IDO1 clinically (Hou et al., 2007). However, the biochemical activity of D-1-MT as an IDO1 inhibitor was lower than that of L-1-MT (Hou et al., 2007). This led to the speculation that either D-1-MT targeted an IDO1 isoform or a completely different target. It has been demonstrated that 1-MT, more specifically the D-isomer of 1-MT, is also capable of inhibiting IDO2 (Metz et al., 2007). Subsequently, this report was challenged as some studies found L-1-MT to be a more potent inhibitor of IDO2 (Yuasa et al., 2010; Austin et al., 2010). Interestingly, D-1-MT did not only inhibit IDO2, it also was demonstrated to restore mTOR activity, which was

inhibited by Trp deficiency, mimicking Trp-sufficient conditions (Metz et al., 2012). This Trp-mimetic character of D-1-MT also was seen in L-1-MT.

A number of selective mouse IDO2 inhibitors have been reported (Bakmiwewa et al., 2012). Proton-pump inhibitors such as tenatoprazole, lansoprazole and pantoprazole are a group of inhibitors that potently and selectively inhibited IDO2. Other IDO2-selective inhibitors reported were retinoic acid, sildenafil, nifedipine, and troglitazone, with sildenafil possessing the highest IDO2-selectivity.

1.3.3.5 IDO2 in autoimmune diseases

After its discovery, there was interest in elucidating whether IDO2 could be playing a similar role to IDO1 in autoimmune diseases. IDO2 mRNA and protein were reported in a number of pancreatic cancer cell lines, which were also IFN γ -inducible (Witkiewicz et al., 2009). Some primary human colon, gastric and renal tumours also expressed *Ido2* mRNA (Lob et al., 2009). However, the enzyme did not seem to contribute to Trp degradation in these tumours, which seemed to be completely driven by IDO1.

IDO2 was reported to be involved in the pathogenesis of arthritis, an autoimmune disorder in which IDO1 also has been implicated (Merlo et al., 2014; Criado et al., 2009). Using the KRN pre-clinical model of rheumatoid arthritis, IDO2 was demonstrated to play a key role in the progression of the disease (Merlo et al., 2014). Joint inflammation was significantly alleviated in mice deficient for *Ido2* relative to wild-type. Kynurenine levels in the *Ido2*^{-/-} mice were however unaltered compared to the levels in wild-types. The reductions in autoantibody production and antibody-secreting cells were attributed to the mitigation of the inflammatory symptoms of rheumatoid arthritis seen in joints of

Ido2^{-/-} mice (Merlo et al., 2014). IDO2 was shown to be crucial for the activation of CD4⁺ helper T cells. In addition, the absence of IDO2 also resulted in lower autoantibody levels in the mice, although B cells from *Ido2*^{-/-} themselves proliferated and produced Ig at similar levels to B cells from WT mice, suggesting that IDO2 is involved in B cell responses to autoantigens, B cell antibody responses to model antigens.

1.3.3.6 IDO2 plays an essential role in inflammation

An immunomodulatory role of IDO2 in inflammation and IDO1-dependent T cell regulation was discussed recently (Metz et al., 2014). IDO1-dependent T cell regulation was found to require activation of IDO2. The ability of T_{regs} to inhibit T cell proliferation was greatly diminished in the absence of IDO2 relative to the wild-type, as was also seen in the absence of IDO1 (Sharma et al., 2007). This implied that IDO2 was essential for IDO1-mediated T cell regulation. This evidence also pointed to possible interaction between IDO1 and IDO2 in regulating T cells. However, when the role of IDO2 was studied in another pathophysiology in which IDO1 has been implicated previously, namely inflammatory skin cancer (Muller et al., 2008), the outcome differed. IDO2 deficiency did not result in the alleviated inflammatory symptoms and impedance of tumour progression like that seen in IDO1-deficient experimental models. The difference in the outcome suggested distinct biological functions for IDO1 and IDO2. Although IDO2 did not seem to play a role in inflammatory carcinogenesis, it was proposed to play a role in contact hypersensitivity (CHS) (Metz et al., 2014). The susceptibility of wild-type, *Ido1*^{-/-} and *Ido2*^{-/-} mice to hapten-induced contact hypersensitivity was compared. Inflammation observed in the ears of *Ido2*^{-/-} mice challenged with oxazolone, a contact sensitiser, was

reduced by about 40% compared to that in the wild-type counterparts. A similar reduction in inflammation was not seen in *Ido2*^{-/-} mice challenged with an inflammatory agent that triggers an innate immunity response only. These observations implied a possible role for *Ido2*^{-/-} in the adaptive immune system. The inflammatory response in *Ido1*^{-/-} mouse ears also was reduced, although only by about 20%. When levels of cytokine expression in the CHS model of *Ido2*^{-/-} and *Ido1*^{-/-} were compared to wild-type, a clear difference was evident in the cytokine expression patterns and levels (Metz et al., 2014). Significantly lower levels of IFN γ , TNF, IL-6, MCP-1/CCL2, GM-CSF and G-CSF were found in the ears of *Ido2*^{-/-} mice treated with oxazolone relative to the similarly-treated wild-type. Increased expressions of the same cytokines were observed in the ears of treated *Ido1*^{-/-} mice relative to wild-type animals. These differences point to a difference in the mechanism of actions of both IDO1 and IDO2, despite apparently contributing to similar outcomes in the pathophysiology of CHS.

1.3.4 Tryptophan-independent signalling of GCN2/mTOR

The depletion of Trp modulated by the kynurenine pathway leads to the suppression of T cells. It has been proposed that the mechanism through which Trp depletion leads to suppression of T cell proliferation is either by (i) the mTOR kinase pathway or (ii) the GCN2 stress kinase pathway.

mTOR, is the mammalian homologue of TOR, which possesses kinase activities, that can be inhibited by rapamycin (Sabatini et al., 1994) Inhibition of this complex arrests cell cycle progression of activated T cells, which inhibits T cell proliferation, reducing the number of T cells (Terada et al., 1993). While amino acid availability drives the mTOR

pathway (Gingras et al., 2001), amino acid starvation inhibits mTOR in a similar fashion to rapamycin (Hannan et al., 2003). Therefore it was proposed that the depletion of Trp by IDO suppresses T cells by repressing its proliferation through the inhibition of the mTOR complex. Although earlier reports suggested that the mTOR signalling pathway is unlikely to be the main cause of T cell suppression since mTOR inhibitors such as rapamycin did not restore the proliferative arrest seen in IDO1-mediated suppression (Fox et al., 2005; Munn et al., 2005), a more recent publication showed that in an inflammatory carcinogenesis mouse model, IDO1-mediated Trp depletion inhibited mTOR kinase (Metz et al., 2012). This inhibition was reversible with the addition of Trp or 1-MT (IDO1 and IDO2 inhibitor), an observation that further consolidates the suggestion that IDO1-catalysed Trp catabolism inhibits the mTOR pathway.

The alternative pathway that could be driving T cell suppression by Trp depletion is the integrated stress response kinase GCN2 signalling pathway. GCN2 kinase is activated in amino acid deprivation (Zhang et al., 2002). Tryptophan catabolism initiated by IDO1 activates GCN2, which phosphorylates eIF2 α . During this process, LIP (liver inhibitory protein), an inhibitory isoform of the immune regulatory transcription factor NF-IL6, is also activated (Metz et al., 2007). GCN2 was found necessary for the suppression of T cell proliferation (Munn et al., 2005). In the absence of GCN2, T cell proliferation proceeded normally both *in vitro* and *in vivo*. It has been shown that GCN2 activation by IDO1 led to cell cycle arrest and anergy in CD8⁺ T cells, while suppressing the differentiation of T helper 17 (T_H17) and promoting maturation of T_{regs} suppressor activity in CD4⁺ T cells (Fallarino et al., 2006; Munn et al., 2005; Sharma et al., 2007; Sundrud et al., 2009). Upon supplementation of the culture medium with Trp, the immunosuppressive effect of IDO1

was reversed. The mechanism through which IDO1 activates GCN2 has not yet been ascertained. An increase in uncharged tRNA is an established stimulus of GCN2 (Dong et al., 2000). Tryptophanyl-tRNA synthetase, an enzyme responsible for ligating Trp to its specific tRNA, has been shown to be induced by IFN γ , as is IDO1 (Bange et al., 1992). In the absence of Trp, an increase in uncharged tRNA would naturally result. It has been proposed that IDO1 could be activating the GCN2 kinase signalling pathway through the increase in uncharged tRNA (Mellor and Munn, 2004; Munn et al., 2005).

Although IDO2 was found to similarly activate this pathway, its effect could not be rescued by supplementation of tryptophan. This suggests that IDO2 may produce a tryptophan-independent signal, distinct from that which is elicited by IDO1 (Metz et al., 2007).

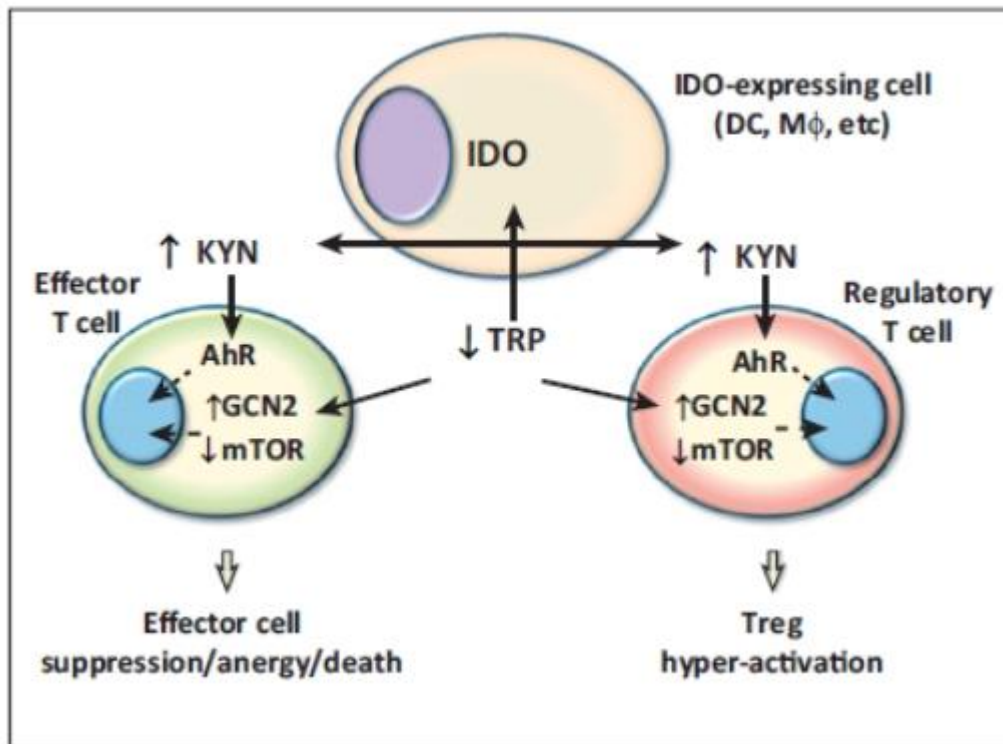


Fig. 1.4 Possible mechanisms of immune suppression through IDO1-induced tryptophan deficiency. IDO, indoleamine 2,3-dioxygenase; DC, dendritic cell; M Φ , macrophage; KYN, Kynurenine; TRP, Tryptophan; AhR, aryl hydrocarbon receptor; T_{reg}, regulatory T cells; GCN2, General control nonderepressible 2; mTOR, mammalian homologue of target of rapamycin

Reproduced from (Munn and Mellor, 2013)

1.4 Organ development

1.4.1 Trp-degrading activity in placenta

Placenta is an important tissue in embryonic development, upon which the growth and survival of a foetus depend. By forming the foetal-maternal interface, it plays a pivotal role in metabolite and gas exchange as well as foetal waste disposal. In addition, the placenta secretes hormones that prepare maternal physiology for pregnancy while forming an immunity barrier between the mother and foetus.

Both human and rodent placenta are comprised of three layers: the outer maternal layer, the middle junctional region and an inner layer (Watson and Cross, 2005). The outer layer is made up of decidual cells of the uterus and maternal vasculature that transports blood between the implantation site and the maternal circulation. The middle junctional region, on the other hand, is comprised of the trophoblast cells of foetal-placental origin, permeating the uterine wall and maternal vessels. It is also this layer which adheres the placenta to the uterus. The third layer, the inner layer, facilitates efficacious nutrient exchange through its highly branched villous layer. In mice, placental development begins as early as embryonic day (E) 3.5 in the blastocyst, during which the trophectoderm separates from the inner cell mass. When implantation takes place on E4.5, the mural trophectoderm differentiates to become trophoblast giant cells (TGC). These cells become polyploid as their DNA continues replicating, although the cells themselves have stopped dividing. TGCs facilitate the physical attachment of the embryo to the uterus, a step essential to the development of the embryo (Cross et al., 1994). During this process, TGCs stimulate uterine lining to develop and evolve functionally (Hu and Cross, 2010). TGCs also increase in number in the uterine stroma (Hu and Cross, 2010; Bevilacqua and

Abrahamsohn, 1989). Together with underlying parietal endoderm cells, they also form the parietal yolk sac, a transitory structure that facilitates nutrient and endocrine signal interchange in the early stages of pregnancy (Hu and Cross, 2010) Welsh and Enders 1987. The parietal yolk sac permeates the uterine epithelium and connects them to maternal blood spaces, to mediate this exchange (Bevilacqua and Abrahamsohn, 1989). Following implantation, TGCs adapt a more endocrine role, synthesising hormones, growth factors and cytokines that are pivotal for the adaptation of maternal physiology to support pregnancy as well as growth of the foetus (Hu and Cross, 2010; Cross et al., 1994). An example of such hormones is prolactin, whereby genes from the prolactin/placental lactogen/prolactin-like protein family, except pituitary prolactin, are secreted only by the placenta (Hu and Cross, 2010; Simmons et al., 2008). A remarkable change in the pool of uterine immune cells is also evident during pregnancy (Hu and Cross, 2010). This modification is pivotal to avert the immune system of the mother from rejecting allogeneic concepti. However, the exact mechanism that modulates this immune tolerance was not fully understood. It was proposed that perhaps progesterone, which is highly expressed during pregnancy may contribute to this tolerance, as it was found to activate Type II helper T cells (T_H2) (Szekeres-Bartho and Wegmann, 1996; Hu and Cross, 2010).

High Trp-catabolising activity has been ascribed to human placental tissue, and this was attributed to IDO1 (Yamazaki et al., 1985). IDO1 in murine placental tissues was shown to facilitate immune tolerance, which prevented allogeneic foetal rejection (Munn et al., 1998). IDO1 expression in various foetal-maternal tissues has been described previously (Blaschitz et al., 2011; Yamazaki et al., 1985; Sedlmayr et al., 2002; Ligam et al., 2005). In

humans, IDO1 was not detected in placental villi in the first trimester, albeit being observed in subtrophoblastic capillaries and glandular epithelium of the decidua (Sedlmayr et al., 2002; Sedlmayr et al., 2014; Blaschitz et al., 2011). During mid-gestation, the expression of IDO1 was restricted to foetal TGC (Baban et al., 2004). In a term human placenta, expression of IDO1 was found in the mesenchymal core and syncytiotrophoblasts (Sedlmayr et al., 2002). While IDO1 remains undetectable in the umbilical cord of term placenta, endothelium in the tissues closest to the foetal-maternal interface in humans, such as the large vessels in stem villi as well as arteries and veins of the chorionic plate, have been reported to be IDO1-positive (Blaschitz et al., 2011; Sedlmayr et al., 2002).

Although initially IDO1 expression also was reported in trophoblast cells (Kudo et al., 2004; Sedlmayr et al., 2002; Honig et al., 2004), contradictory reports that followed subsequently challenged this observation (Blaschitz et al., 2011; Wang et al., 2011). Wang et al. (2011) showed that IDO1 expression is induced in trophoblasts only upon viral infection and is not constitutively expressed in these cells (Kudo et al., 2004; Ligam et al., 2005).

Also, the kynurenine-to-Trp ratio in the blood of term placenta at delivery was found to be significantly higher than that of peripheral blood of healthy adults, suggesting that IDO1-mediated Trp-catabolic activity remains high even after the arrest of placental blood circulation (Blaschitz et al., 2011). Blaschitz and colleagues assumed that the Trp-catabolic activity seen in term placenta is mediated by IDO1 as an earlier report found that the expression of TDO2 in murine placenta decreased as the embryo grew (Suzuki et al., 2001) as will be discussed in the next paragraph.

TDO2 has been detected in both murine and human placenta (Suzuki et al., 2001; Dharane Nee Ligam et al., 2010). Suzuki and colleagues also demonstrated that the high Trp-degrading activity in early murine gestation (from E6.5 dpc) was attributable to TDO2 and not IDO1, as the latter was not detected at such an early stage. The expression of IDO1 during the developmental period was shown to be transient as it was absent in the early developmental stages and detected only between two to three days from E8.5 to 12.5 dpc, whereas TDO2 was detected from E6.5 to E18.5 dpc although the levels were lower in the older embryos (Suzuki et al., 2001). This observation led some to suggest that TDO2 also may be involved in immune tolerance to prevent rejection of allogeneic foetuses during pregnancy, to a greater extent than IDO1 (Suzuki, 2001; Britan, 2006).

IDO2 RNA and protein have been reported in human placenta (Lob et al., 2008; Metz et al., 2007). However, its localisation and possible role in pregnancy has not been explored previously.

1.4.2 Trp catabolising activity in the yolk sac

Another important extraembryonic tissue during pregnancy is the yolk sac, which is responsible for the transport of various substances in mammals, such as vitamins, immunoglobulins, and plasma proteins (Jollie, 1986). While being the primary membrane for placental exchange in lower vertebrates, the role of the yolk sac in mammals may not necessarily be placental (Jollie, 1986). In some eutherian mammals, placental function is played by the choriovitelline placenta in early stages of development and is eventually taken over by the chorioallantois. It forms the choriovitelline placenta by fusing with the inner surface of the chorion. In rodents and insectivores, the placental function is

performed by a more intricate mammalian yolk sac-placenta (Jollie, 1986). In these organisms, the parietal yolk sac comprises of the non-vascularised wall of the membrane, the chorion to which it is apposed and the decidua capsularis to which these membranes are attached. This structure eventually breaks down, exposing the vascularised membrane, known as visceral yolk sac (VYS), to uterine substances. While the parietal yolk sac is transitory, visceral yolk sacs remain until term. The VYS is central in supplying amino acids and nucleotides for embryonic protein synthesis to the growing foetus by driving protein degradation and absorption at the membrane (Freeman and Lloyd, 1983; Beckman et al., 1990; Beckman et al., 1991; Rowe and Kalaizis, 1985).

The role of yolk sac in providing or catabolising the essential amino acid Trp to the growing murine embryo and the expression or role of any of the three Trp-degrading enzyme in the yolk has not been discussed previously. Whether Trp-catabolic activity is present in the yolk sac, which Trp-degrading enzyme drives this activity and the possible roles of Trp catabolism in this tissue remain to be elucidated.

1.4.3 Trp-catabolic activity in embryonic and neonatal liver

Despite being expressed in high levels in adult liver, neither TDO2 RNA nor protein was detected in embryonic liver (Franz and Knox, 1967; Nakamura et al., 1987). Constitutive Trp-catabolic activity was reported in neonatal liver as young as 2 weeks old, which was initially attributed to TDO2 (Franz and Knox, 1967). However, with the recent discovery of another liver Trp-catabolising enzyme, IDO2, the expression and role of this enzyme in Trp catabolism in the liver during development need to be further investigated.

1.5 Zebrafish as an experimental model in biomedicine

The zebrafish (*Danio rerio*) is becoming a popular study model organism in the field of biomedicine, with it being used in the fields of developmental genetics, neurophysiology, organogenesis and disease processes, and more recently in drug screening (Kinth et al., 2013; Meeker and Trede, 2008; Renshaw and Trede, 2012; Schlegel and Gut, 2015; Tavares and Santos Lopes, 2013). This tropical fresh water fish species was first reported in the Ganges region in eastern India, by a surgeon with the British East India company stationed in West Bengal (Spence et al., 2008). Zebrafishes are relatively small with the adults rarely exceeding 40mm in length. Domesticated zebrafishes have an average life span of 42 months. Fertilisation occurs outside the mother's body, where female fishes can spawn every couple of days, and contain several hundreds of eggs per clutch (Spence et al., 2008). The embryos continue to develop *ex utero* and can be observed from their earliest developmental stages. Zebrafish embryos are relatively large compared to other fishes with a diameter of 0.7mm at fertilisation. (Kimmel et al., 1995). Their rapid development, with precursors to all major organs developing within 36 hours, can be followed easily due to the optical transparency of the embryos (Kimmel et al., 1995).

One of the earliest studies using zebrafish as a model research organism was by Streisinger and colleagues who paved the way for the use of zebrafish for the study of molecular genetics in vertebrate embryology (Streisinger et al., 1981). To date, the zebrafish has been used as a human disease model for cancer (Stanton, 1965; Taylor and Zon, 2009; Spitsbergen et al., 2000), diabetes (Gleeson et al., 2007; Andersson et al., 2012; Moss et al., 2009), cardiovascular disease (Holden et al., 2011; Sabeh et al., 2012; Dahme et al., 2009), neurodegeneration (Xi et al., 2011) and drug screenings (Rubinstein,

2003) (Tavares and Santos Lopes, 2013). Physiology of lipid metabolism in the digestive system also has been studied, where phospholipid processing in the digestive system was investigated using fluorescently-tagged lipid (Farber et al., 2001). Some of these will be discussed more thoroughly in the following paragraphs.

Fishman described the zebrafish as the canonical vertebrate due to its similarities to mammalian biology (Fishman, 2001). Due to the optical transparency of the zebrafish embryo, phenotypical changes that take place in mutants are identifiable at the level of individual cells (Fishman, 2001). One is able to discover the role of a protein before the gene coding the protein is deciphered as phenotypes of randomly induced mutations are recognised first in genetic screens before the gene sequence is decoded.

Zebrafish have been used as a human disease model in cancer. Innately, they possess a low frequency of inherent tumour growth, with only 10% of the fish developing cancer over their lifetime (Tavares and Santos Lopes, 2013). However, they develop malignant tumours when exposed to carcinogens, although the responsiveness to carcinogenic stimulus was most evident among embryos and fry while older zebrafishes appeared resistant to such treatment (Spitsbergen et al., 2000). An exciting aspect in cancer research in zebrafish is the potential to follow tumour cell fate within the system, after transplanting human tumour cells into zebrafish embryos (Taylor and Zon, 2009).

Zebrafish models for diabetes and lipid-related disorders also have been reported. Destruction of pancreatic β cells led to hyperglycaemia in zebrafish, a condition that reversed with time and normoglycaemia returned without the administration of exogenous insulin (Andersson et al., 2012; Moss et al., 2009). This restoration of normoglycaemia was attributed to the regeneration of insulin-positive β cells. The

simplicity of organ structures within the zebrafish enabled investigators to follow the development of the pancreas and study signalling pathways that may be involved in the regeneration process (Andersson et al., 2012). In addition, the zebrafish experimental model also allowed for the screening of about 7000 compounds that could support or stimulate pancreatic regeneration in the hope of finding new therapeutic approaches for treatment of, in particular, Type I diabetes (Andersson et al., 2012).

The optical transparency of the embryo also has enabled the investigation of various vascular processes. The assessment of cardiovascular pacemaking, rhythm and contractility is one example (Baker et al., 1997). Molecular control of vascular development also has been studied extensively using this model as the developing heart and blood vessels can be observed across timepoints (Holden et al., 2011). The use of fluorescent markers further intensifies the visualisation of vasculatures in these studies. As oxygen is delivered to zebrafish embryos by surface diffusion in the first week of development, embryos with cardiovascular defects can still develop through embryogenesis and into the larval stages. This allowed for the comprehensive phenotyping of blood flow velocity, electrocardiograms and determination of cardiac atrial and ventricular shortening fraction (Dahme et al., 2009).

To put it succinctly, zebrafish embryos are optically transparent animals that develop *ex utero*. They are genetically amenable and breed in high numbers while taking a shorter period to develop to maturity. These features make it a highly desirable experimental model that has been used in the study of various pathological and physiological processes.

1.5.1 *D. rerio* embryonic developmental stages

There are seven broad periods in zebrafish embryogenesis that occur from the point of the unfertilised egg to its hatching (Kimmel, 1995). The first period is the formation of the zygote, which involves the fertilisation of the egg by the sperms of male fish (Fig. 1.4) (Kimmel et al., 1995). At the one-cell stage, cytoplasmic streaming occurs towards the animal pole from the yolk (also known as the vegetal pole), to form the blastodisc. At this stage, the formed embryos are in the one-cell stage for about 0.75 hours, before cleavage occurs, marking the second period of embryogenesis.

During this second period, cell cycles occur rapidly resulting in a 64-cell stage embryo, just prior to the growth of the egg to form a blastula (128-cell stage embryo). During the blastula (third) period, epiboly commences and asynchronous, lengthened cell cycles occur at the midblastula region (Kimmel et al., 1995). The achievement of 50% epiboly marks the beginning of the fourth period, the gastrula period. During this period, the thickness of the blastoderm is maintained and the germ ring begins to form from the animal pole. The shield begins to appear from about six hours-post-fertilisation (hpf), and the gastrula period ends with the formation of the tail bud and 100% epiboly occurring.

The fifth period, the segmentation period, begins after the tenth hour, during which the polster becomes noticeable while the optic and Kupffer's vesicle begins to form. It is during this period when primary organogenesis occurs, the tail begins to appear and early movements can be detected in the embryos.

The body axis begins to unbend and the development of fins, circulation and pigmentations can be seen during the pharyngula (sixth) period (24 to 42 hpf),

Morphogenesis of the primary organs is completed during the seventh and final period, accompanied by the cartilage formation in the head and pectoral fin.

It should be noted that *D. rerio* embryos of a single clutch can develop at different rates (Kimmel et al., 1995). Hence, the final stage, which is the hatching, also occurs asynchronously. During the early larval stage (72 hpf onwards), the swim bladder inflates and the embryos exhibit distinct behaviours including food-seeking and active avoidance. The development of the embryo is depicted in Fig. 1.4.

Liver and intestinal development during zebrafish embryogenesis has been studied previously (Field et al., 2003; Ng et al., 2005). The budding phase begins after the aggregation of hepatocytes around 24 hpf, during which the liver buds off the intestinal rod (Field et al., 2003). The formation of the hepatic duct at 50 hpf marks the end of this phase. The second phase is marked by a voluminous modification of liver shape and size. A reasonable increase in liver size is seen by 72 hpf, although no change in shape is seen. Following this growth is the medial expansion of the liver.

The zebrafish gut, on the other hand, is segmented into pharynx, oesophagus, intestinal bulb, mid-intestine and posterior intestine (Field et al., 2003; Ng et al., 2005). In zebrafish, the intestine is joined directly to the oesophagus as zebrafish does not have a stomach. The characterisation of the endoderm cells takes place between 26 to 126 hpf, after the primitive gut is formed by the convergence of the endoderm precursor. During the first half of this process, the whole intestinal endoderm is rapidly dividing. Stage I of zebrafish gut development involves lumen formation, which occurs between 26 to 52 hpf and, by the end of this stage, cell masses related to the developing gut are evident (Ng et al., 2005). By about 74 hpf, the second stage of gut development, characterised by epithelial

cell polarisation, is noticeable. The third and final stage of gut development involves the most complex and elaborate processes where remodelling and differentiation of intestinal epithelium take place. This stage is characterised by the compartmentalisation of the intestinal tract into intestinal bulb, mid-intestine and posterior intestine. While the epithelial cells in the posterior intestine remain highly proliferative, diminished proliferation was documented in the mid-intestinal region. This diminished proliferation, however, is accompanied by increased differentiation in this region. Distinct folds begin to form in the intestinal bulb and mid intestine at this stage. Proliferation and differentiation of goblet and enteroendocrine cells that are restricted to mid-intestine also can be seen. By 5 dpf, a digestive system made up of mouth, pharynx, oesophagus, intestinal bulb, mid-intestine, posterior intestine and anal opening is distinct. The yolk also is completely resorbed by this stage.

Studying the development of zebrafish shows that its embryogenesis occurs rapidly, with hatching occurring by the third dpf. The development of the organs can be observed and imaged live during embryogenesis, rendering it a highly favourable model organism to study disease and physiological processes. As TDO2 and IDO2 have been reported in murine liver whereas IDO1 has been detected in murine intestine, the zebrafish embryo can be an excellent model to study the role these enzymes may play in zebrafish embryonic development.

1.5.2 Tryptophan-catabolising enzymes in *Danio rerio* (zebrafish)

As mentioned previously (Section 1.3.3), in mammals and most vertebrates two homologues of *IDO* genes were found. However, in lower vertebrates such as chicken and fish, only a single *IDO* gene was found (Ball et al., 2007; Yuasa et al., 2007). This gene shared greater genomic similarity with the *IDO2* gene in mammals than with *IDO1*. Due to this characteristic of the *IDO* gene in fish and chicken, studying the expression patterns and role of the *IDO* gene in fish may shed light on the possible roles that *IDO2* may play in more complex mammalian systems.

In the zebrafish, there are three Trp-catabolising proteins, namely tryptophan 2,3-dioxygenase 2a (*Tdo2a*), tryptophan 2,3-dioxygenase 2b (*Tdo2b*) and indoleamine 2,3-dioxygenase (*Ido*). Despite the similarity in the nomenclature of the first two enzymes, they are located on different chromosomes, *tdo2a* on Chromosome 14 and *tdo2b* on chromosome 11.

To date, there are only sparse data on the RNA expression of *tdo2b* in zebrafish embryos (> 5 dpf), a direct data submission to ZFIN, which showed *tdo2b* RNA expression in the liver and posterior intestine (Thisse and Thisse, 2004).

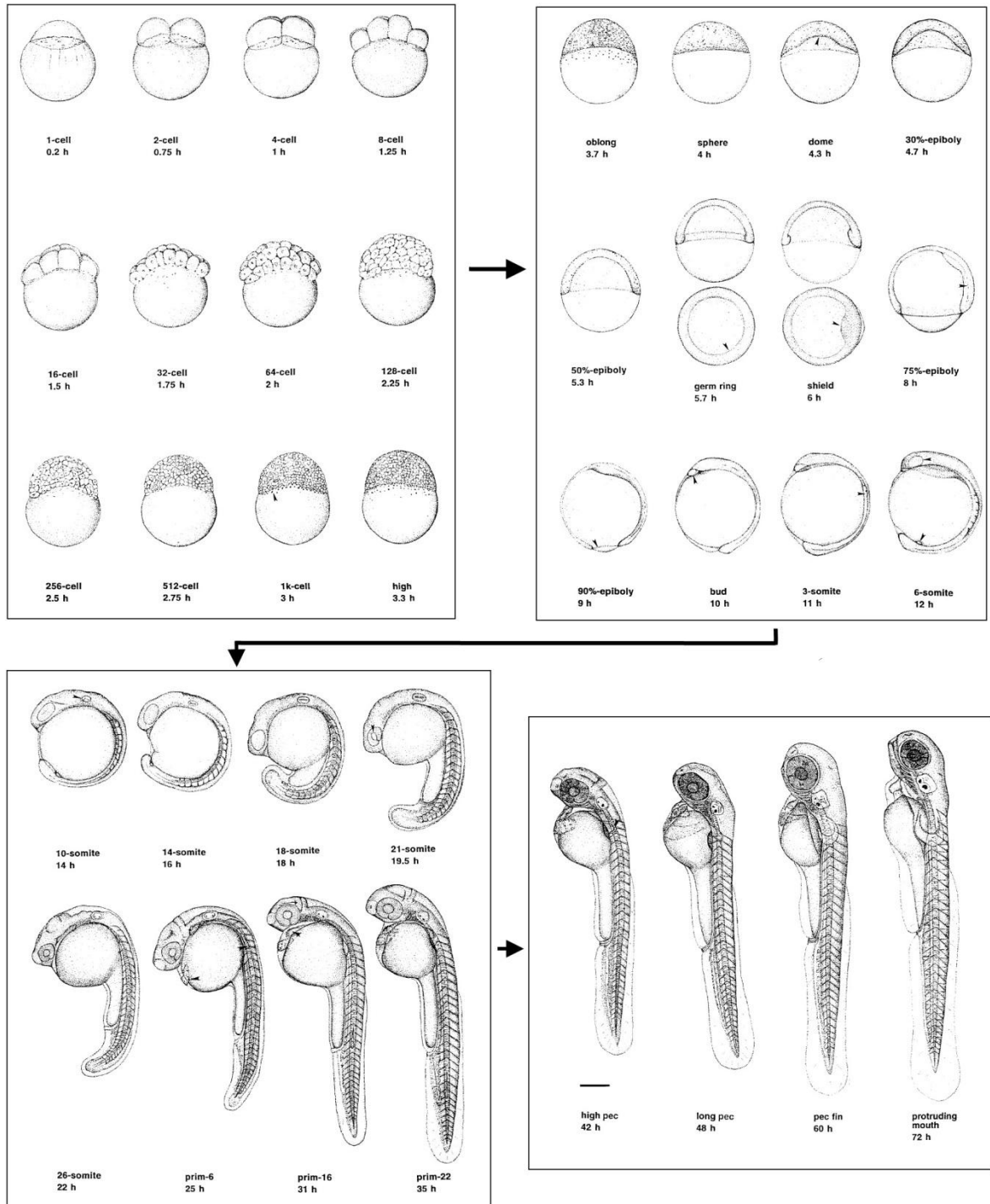


Fig. 1.5. Sketches of zebrafish embryos at selected stages of development. In the earlier stages, the animal pole is to the top while, in the later stages, the anterior is to the top. Diagram taken from Kimmel et al. (1995).

1.6 Scope of the thesis

The general aim of this thesis is to investigate the distribution of IDO2 and its possible role in mouse and fish physiology. Three Trp-catabolising enzymes have been found in zebrafish, namely *Tdo2a*, *Tdo2b* and *Ido*. Unlike mammalian systems, only one IDO homologue is known in zebrafish, which is more similar to IDO2 than IDO1. Therefore, we aimed to investigate the distribution of *tdo2a*, *tdo2b* and *ido* expression as well as the possible roles these enzymes, especially *Ido*, may play in zebrafish. We also were interested to elucidate possible interactions or interdependency between the three Trp-catabolising enzymes present in the mouse. The downregulation of IDO2 activity in the absence of IDO1 in macrophages (Metz et al., 2014) as well as the upregulation of *Ido2* mRNA in the epididymis of mice deficient for IDO1 has been reported previously (Fukunaga et al., 2012). At the functional level, the absence of IDO2 affected IDO1-dependent T cell regulation (Metz et al., 2014). These were the first pieces of evidence for a non-redundant role of IDO2 as well as a possible interaction between two Trp-catabolic enzymes in mammals, namely IDO1 and IDO2. In some tissues, the expression of two enzymes that catalyse the metabolism of Trp through the kynurenine pathway has been reported. Despite catalysing the same reaction, it was speculated that the role of the two may differ and be specialised.

In the beginning of the project, we aimed to develop a simpler, easier IFN γ spectrophotometric bioassay based on the observation that endothelial cells express inducible-IDO1. Due to the unavailability of the downstream enzymes of the kynurenine pathway in this cell type, the pathway is retarded at the level of kynurenine production. As spectrophotometric detection of kynurenine is relatively easy using Ehrlich's reagent,

we aimed to develop an IFN γ bioassay based on the ability of the enzyme to induce IDO1 expression and activity, thereby increasing kynurenine formation.

Therefore, in this thesis, we aimed to:

1. Develop an improved human IFN γ spectrophotometric bioassay utilising endothelial cells.
2. Investigate the expression of the three Trp-catabolising enzymes present in zebrafish by *in situ* hybridisation as well as elucidate possible roles they may play in zebrafish embryonic development using the morpholino knockdown approach.
3. Identify the cellular distribution of IDO2 in various murine tissues as well as the intracellular distribution of IDO1 and IDO2 in transfected cells.
4. Examine possible interactions between the three Trp-catabolising enzymes in various murine tissues by examining mRNA expression of *Ido1*, *Ido2* and *Tdo2* in these tissues. We developed mutant mice deficient in two of the three Trp-degrading enzymes alongside their equivalent wild-types (*Ido1*^{-/-}*Tdo2*^{-/-}, *Ido2*^{-/-}*Tdo2*^{-/-} and *Ido1*^{+/+}*Ido2*^{+/+}*Tdo2*^{+/+}) to complement the mutant mice deficient in one Trp-catabolic enzyme that we already had in our laboratory (*Ido1*^{-/-}, *Ido2*^{-/-} and *Tdo2*^{-/-}).
5. Determine global gene expression in the liver of mice deficient in one or both the Trp-catabolic enzymes (*Ido2*^{-/-}, *Tdo2*^{-/-} and *Ido2*^{-/-}*Tdo2*^{-/-}) relative to their equivalent wild-types.

CHAPTER 2

AN IMPROVED

HUMAN INTERFERON GAMMA (IFN γ)

BIOASSAY

CHAPTER 2 HUMAN INTERFERON GAMMA (IFN γ) BIOASSAY

2.1 INTRODUCTION

The major mechanism through which tryptophan is catabolised is via the kynurenine pathway. The conversion of tryptophan into N-formylkynurenine is the first and rate-limiting step in this pathway and is catalysed by the enzymes IDO1, IDO2 or TDO2.

Structurally, TDO2 and IDO1 differ significantly, as TDO2 is a homotetrameric haem B-containing protein whereas IDO1 is a monomeric protein with a single haem B protein.

The second isoform of IDO1, now known as IDO2, has similar genomic structures to IDO1 but possesses different tissue distribution patterns and substrate specificity (Ball et al., 2007; Ball et al., 2009). Despite possessing tryptophan-catabolising properties, IDO2 has a much lower affinity for tryptophan than IDO1 with a K_m more than 400 times higher than IDO1 (Austin et al., 2010). Due to the low enzymatic activity of IDO2, it is uncertain whether IDO2 performs a tryptophan-catabolic role physiologically or if it possesses an alternative role, independent of its tryptophan-catabolising capacity (Section 1.3.3.1).

While TDO2, which is expressed constitutively at high levels in the liver, is induced by glucocorticoids and is involved more with the regulation of dietary tryptophan, the expression of IDO2 has been reported in the liver (Ball et al., 2007) and is known to be moderately induced by IFN γ in certain cell types (Metz et al., 2007; Lob et al., 2009; Croitoru-Lamoury et al., 2011; Witkiewicz et al., 2009).

IDO1, on the other hand, is stimulated in inflammatory conditions such as viral or bacterial infections, schizophrenia, dementia and cancer, with low constitutive expression only in the epididymis, intestine and lung. High expression of IDO1 was detected in the

placenta, which led to the discovery of the role of IDO1 in preventing allogeneic foetal rejection (Munn et al., 1998). Inflammatory cytokines such as IFN γ (Taylor and Feng, 1991), TNF (Babcock and Carlin, 2000) and LPS (Fujigaki et al., 2001) are established to be potent inducers of IDO1.

IFN γ , one of the most potent inducers of IDO1, belongs to a family of interferons, which act as immunomodulators as well as antivirals (Bach et al., 1997; Schroder et al., 2004). Previously, human IFN γ has been assayed by anti-viral assays (Green et al., 1981; Sato et al., 1984), enzyme-linked immunosorbent assay (ELISA) (Gibson and Kramer, 1989; Mazurek et al., 2001) and high performance liquid chromatography (HPLC) (Byrne et al., 1986a; Mailankot and Nagaraj, 2010). While antiviral assays were technically demanding, ELISAs did not reflect the actual activity of the protein in its measurement. HPLC, the more commonly used method in the recent years, is laborious. In the work reported in this chapter in the form of a published manuscript, we demonstrate an improved spectrophotometric approach to assaying human IFN γ using the Ehrlich's reagent assay of kynurenine as a measure of IDO1 activity in a human brain endothelial cell line (HBEC).

2.2 STATEMENT OF CONTRIBUTIONS

Note: This chapter consists of published work




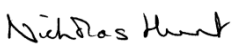
Contributions to the work described in the manuscript “Improved spectrophotometric human interferon-gamma bioassay”, published in the Journal of Immunological Methods, 2013, 394: 115-120.

Tasks	FFJ*	LKT	HJB	NHH
Planned study	50	0	30	20
Performed experiments	95	5	0	0
Analysed data	90	10	0	0
Interpreted data	60	0	20	20
Wrote first draft	100	0	0	0
Commented on manuscript	0	0	50	50
Answered reviewer’s comments, revised manuscript	30	0	20	50

*FFJ is the first author

I confirm that the contributions of authors are as listed above:

Signature and date

Felicita F. Jusof		<u>10/03/2015</u>
Loke Khaw Tim		<u>05/02/2015</u>
Helen J. Ball		<u>09/02/2015</u>
Nicholas H. Hunt		<u>16/03/2015</u>



ELSEVIER

Contents lists available at SciVerse ScienceDirect

Journal of Immunological Methods

journal homepage: www.elsevier.com/locate/jim

Research paper

Improved spectrophotometric human interferon-gamma bioassay

Felicitia Fedelis Jusof^{a,b}, Loke Tim Khaw^c, Helen J. Ball^a, Nicholas H. Hunt^{a,*}^a School of Medical Sciences (Pathology) and Bosch Institute, Faculty of Medicine, University of Sydney, NSW 2006, Australia^b Department of Physiology, Faculty of Medicine, University of Malaya, 50603 Kuala Lumpur, Malaysia^c Department of Parasitology, Faculty of Medicine, University of Malaya, 50603 Kuala Lumpur, Malaysia

ARTICLE INFO

Article history:

Received 3 May 2013

Accepted 24 May 2013

Available online 31 May 2013

Keywords:

Bioassay

Interferon gamma

Indoleamine 2,3-dioxygenase 1 (IDO1)

ABSTRACT

Interferon gamma (IFN γ) is a cytokine involved in many anti-viral and immunoregulatory processes. One of the major mechanisms through which IFN γ exerts these effects is by inducing expression of indoleamine 2,3 dioxygenase-1 (IDO1), an enzyme that catalyses the first, rate-limiting step of the kynurenine pathway. In this pathway, tryptophan can be catabolised to many products, including picolinic acid and nicotinamide adenine dinucleotide. However, in endothelial cells, the pathway ends at the production of kynurenine. This is due to little or no expression of enzymes that metabolise kynurenine. Production of kynurenine has been used as an indicator of human IDO1 activity, and hence as an hIDO1 bioassay. Due to IFN γ 's ability to induce IDO1 expression, kynurenine production can also be a measure of human IFN γ (hIFN γ) bioactivity. Previously, the levels of hIFN γ have been commonly determined by anti-viral assays, high performance liquid chromatography and ELISA. Apart from their technical complexity, these assays are costly and only the anti-viral assay measures bioactive IFN γ . Here, we report the development of an improved IFN γ spectrophotometric bioassay using a human brain endothelial cell line (HBEC 5i). The method is sensitive, easy to perform and cost efficient.

© 2013 Elsevier B.V. All rights reserved.

1. Introduction

Interferons are a family of proteins known for their antiviral and antiproliferative effects. In humans, three distinct forms of interferon have been identified: interferon alpha, beta and gamma, respectively abbreviated IFN α , IFN β and IFN γ (Lengyel, 1982). All have antiviral and immunoregulatory properties, but Type 1 interferons (IFN α , IFN β) are more involved in the former whereas Type 2 interferon (IFN γ) has a predominantly immunoregulatory role (Bach et al., 1997; Schroder et al., 2004).

Bioactive IFN γ has been measured by an interferon anti-viral assay known as the cytopathic protection effect (CPE) assay (Green et al., 1981; Sato et al., 1984; Svedersky et al., 1984). Enzyme-linked immunosorbent assay (ELISA) for IFN γ is also commercially available and often used for its measurement

(Gibson and Kramer, 1989; Mazurek et al., 2001). However, a limitation of ELISA is that it detects only the protein itself without reflecting its activity.

One of the major mechanisms through which IFN γ exerts its antiviral, antiproliferative and immunomodulatory effects is via the induction of tryptophan catabolism along the kynurenine pathway (Tashiro et al., 1961; Pfefferkorn, 1984; Yoshida et al., 1988; Munn et al., 1999). This is a pivotal pathway involved in numerous physiological and pathophysiological processes, which at the first step is catalysed by three enzymes (Tryptophan 2,3 dioxygenase, TDO; Indoleamine 2,3-dioxygenase 1, IDO1; Indoleamine 2,3-dioxygenase 2, IDO2) that differ in their tissue distribution and expression (Ball et al., 2009). Of these, only IDO1 is reportedly inducible by IFN γ , with its activity being highly increased in pathophysiological or pathological conditions such as cancer, malaria, microbial infection, Alzheimer disease, schizophrenia and organ transplantation (Munn et al., 1998; Sanni et al., 1998; Hansen et al., 2000, 2004; Okamoto et al., 2005; Ino et al., 2006; Takao et al., 2007; Lin et al., 2008; Wang et al., 2010; Weng et al., 2011). The induction of IDO1 is through

* Corresponding author at: Molecular Immunopathology Unit, Room 114, Level 1, Medical Foundation Building (K25), University of Sydney, NSW 2006, Australia.
E-mail address: nicholas.hunt@sydney.edu.au (N.H. Hunt).

an IFN γ -stimulated response element (ISRE) flanking the gene (Caplen and Gupta, 1988; Sen and Lengyel, 1992). Upon the induction of IDO1 activity, tryptophan is metabolised to N-formyl-kynurenine, which can then be converted to kynurenine and other metabolites by enzymes present in the tissue (Owe-Young et al., 2008; Ball et al., 2009). Based on this, IFN γ bioactivity has been assessed indirectly by high performance liquid chromatography (HPLC) through measurement of the substrate, tryptophan, and indirect product, kynurenine (Byrne et al., 1986; Mailankot and Nagaraj, 2010). Despite being commonly used, HPLC is a laborious method. Colorimetric measurement of kynurenine with Ehrlich's reagent also has been described (Daubener et al., 1994).

It was recently reported that kynurenine in endothelial cells cannot be converted to subsequent products of the pathway due to the absence or low expression of the necessary enzymes (Hunt et al., 2006; Owe-Young et al., 2008). This fundamental characteristic of endothelial cells suggested that they would be ideal candidates for a human IFN γ bioassay, since they are known to upregulate IDO1 expression in response to the cytokine both *in vivo* (Hansen et al., 2000) and *in vitro* (Weiser, 2007; Wang et al., 2010).

In this study, we report an optimised and improved spectrophotometric human IFN γ bioassay using an endothelial cell line, human brain endothelial cell (HBEC) 5i. The assay is more sensitive than IDO1 RT-qPCR and simpler to perform than HPLC, ELISA or viral proliferation assays.

2. Materials and methods

2.1. Cell culture and treatments

The HBEC 5i cell line was cultured in phenol red-free DMEM-F12, supplemented with 10% (v/v) foetal bovine serum (FBS), 100 μ g/mL streptomycin and 100 U/mL of penicillin (15070-063, GIBCO, Life Technologies). Primary human brain microvascular endothelial cells (HBMEC) (Angio Proteomie, cAP-0002) were grown in 100 μ L endothelial basal medium EBM-2 (Clonetics CC3156, LONZA) supplemented with 5% (v/v) FBS, ascorbic acid (5 μ g/mL), hydrocortisone (1.4 μ mol/L), chemically defined lipid concentrate (CDLC) (1/100 dilution), HEPES (10 mmol/L) and β -FGF (1 ng/mL). Cells were plated at a density of 2×10^4 per well in 96-well flat bottom plates (Corning® Costar® 3599). The following day, the medium was replaced with 100 μ L of fresh medium supplemented with 400 μ mol/L L-Tryptophan with or without recombinant human IFN γ (AbD Serotec PHP0501) or peripheral blood mononuclear cells (PBMC, Australian Red Cross Blood Service, Sydney) supernatant. For the neutralising experiments, 1 μ g/mL of human IFN γ antibody (monoclonal mouse IgG2A Clone 25718, R&D Systems) was mixed with the supplemented medium containing recombinant IFN γ or PBMC supernates, before addition to the plated cells. The cells were further incubated for 48 h before supernates were harvested for the kynurenine assay and cells lysed for RNA extraction.

2.2. Stimulating IFN γ expression in peripheral blood mononuclear cells (PBMC)

Each well of a 24-well plate (Corning® Costar® 3524) was coated with 220 μ L of 1 μ g/mL of anti-human CD-3 functional

grade purified monoclonal antibody (Clone HIT3a, Catalog no. 16-0039-85, eBioscience) overnight prior to the addition of 2×10^6 PBMC in DMEM. The cells were incubated at 37 °C for 72 h, medium collected thereafter and frozen at –80 °C until further use. To examine whether products of the kynurenine pathway, potentially produced by activated PBMC, might interfere with measurements of kynurenine produced by endothelial cells, a known concentration of kynurenine (200 μ mol/L) was added to anti-CD3 activated PBMC supernatant and phenol red-free, 10% FBS-supplemented DMEM. The two samples were further diluted in cell medium and assayed using the spectrophotometric method.

2.3. Kynurenine assay

Protein was precipitated from the supernates (80 μ L) by the addition of trichloroacetic acid (final concentration 4% w/v) and centrifugation at 16,100 rcf for 10 min at 4 °C. After centrifugation, 90 μ L of the supernate was added to an equal volume of 2% w/v Ehrlich's reagent, namely 4-(Dimethylamino) benzaldehyde (SIGMA-156477) in glacial acetic acid (AnalaR, BDH 100015 N). The absorbance was read on a spectrophotometer (SPECTRAmax 190, Molecular Devices) at a wavelength of 485 nm.

2.4. Reverse transcription quantitative polymerase chain reaction (RT-qPCR)

RNA extraction was performed using the RNeasy QIAGEN kit, according to the manufacturer's protocol, and one-quarter of the eluted RNA was used to synthesise cDNA. Briefly, RNA was heat-denatured (70 °C, 5 min) and primed with random hexamers (0.5 μ g; 1 μ L). Then, 2 μ L of 20 mmol/L dNTPs, 50 U/ μ L U Bioscript and its supplied $1 \times$ FS reaction buffer (Bioline) were added and the 20 μ L reaction incubated for 45 min at 37 °C. Following heat denaturation (95 °C for 2 min) the cDNA was diluted 10-fold with water and used for RT-qPCR. The RT-qPCR reaction (20 μ L) contained 9 μ L cDNA, 0.1 μ mol/L of each primer in $1 \times$ KAPA SYBR Fast Universal qPCR Master Mix (KP-KK4602). Amplification was performed in a Rotorgene 3000 (Corbett Research) with 40 cycles of 95 °C for 15 s followed by 60 °C for 45 s. Expression of *IDO1* was calculated with the $\Delta\Delta C_t$ method, with normalisation to the *HPRT1* reference gene. These genes have similar amplification efficiencies, as assessed using serial dilutions of cDNA, and the purity of the PCR products was assessed by melting curve analysis. The primer sequences were: 5' GGA GCT ACC ATCTG C AAA TCGT 3' and 5' TGG CTT GCA GGA ATC AGG AT 3' for human *IDO1* and 5' CGT CTT GCT CGA GAT GTG ATG 3' and 5' GGG CTA CAA TGT GAT GGC CT 3' for human *HPRT*.

2.5. Cytometric bead array (CBA)

Human IFN γ levels in the PBMC supernatants were analysed using an optimised CBA using the CBA human soluble protein master buffer kit (Becton Dickinson Biosciences, Catalog no: 558264) and A Human Soluble IFN γ Flex Set (Bd Biosciences, Cat. no: 560111). Using the principles of CBA, the fluorescence intensity of hIFN γ was measured on a flow cytometer (Cytomics FC500; Beckman Coulter, Fullerton,

CA) and the data subsequently analysed using FlowJo (Flow Cytometry analysis software, Tree Star Inc.).

2.6. High performance liquid chromatography

Tryptophan and kynurenine in HBEC supernatants were analysed by HPLC as described (Christen et al., 1990), where 30 μ L of 20% (v/v) TCA was added to 120 μ L of supernatants harvested from the culture. Following a quick vortex and centrifugation for 10 min at 8 $^{\circ}$ C, 1600 rcf in a microfuge (Eppendorf, Germany), 100 μ L of the supernate was added to an equal amount of 1 mol/L phosphate buffer pH 7.3. The solution was vortexed and centrifuged again before 160 μ L of the supernate was added to HPLC glass vials (Agilent, USA) for HPLC analysis (Agilent 1100 HPLC System) under the supervision of Drs Ghassan Maghzal and Cacang Suarna (Centre for Vascular Research, University of Sydney). The HPLC was equipped with a Luna C18 (2) reverse phase column (250 \times 4.6 mm, 5 μ m particle size) (Phenomenex, USA). Elution of the samples was performed over 15 min at 0.8 mL/min using a gradient 0–40% mobile phase B (80% v/v acetonitrile). HPLC grade water was used as mobile phase A. Tryptophan was detected via fluorescence (excitation and emission at 285 nm and 365 nm respectively), whereas kynurenine was detected by ultraviolet absorption at 364 nm.

Concentrations of tryptophan and kynurenine were calculated from pre-made standards that were analysed concurrently.

3. Results

In preliminary experiments, we optimised HBEC 5i cell density (20,000 cells/well) and incubation time (48 h) (data not shown). The bioassay was performed, using the optimised conditions, with a range of recombinant hIFN γ concentrations. A linear relationship between the hIFN γ concentration and absorbance (kynurenine production) was observed (Fig. 1A). The sensitivity of the bioassay was evaluated by determining the concentration of the dose that gave half of the maximal response, EC_{50} , and comparing it to that based on IDO1 mRNA measurement by RT-qPCR (Fig. 1B), as well as a bioassay performed using a primary human endothelial cell line (Fig. 1C). The EC_{50} in the spectrophotometric bioassay (Fig. 1A) was slightly lower than that derived from RT-qPCR. The sensitivity of the spectrophotometric bioassay (EC_{50} = 173.8 U/mL) was markedly superior when performed using a primary human microvascular endothelial cell line (MVEC) which gave an EC_{50} of 9.5 U/mL. Assessment by HPLC of tryptophan consumption and kynurenine production in supernates of HBEC treated with 250 U/mL IFN γ is shown in Fig. 1D.

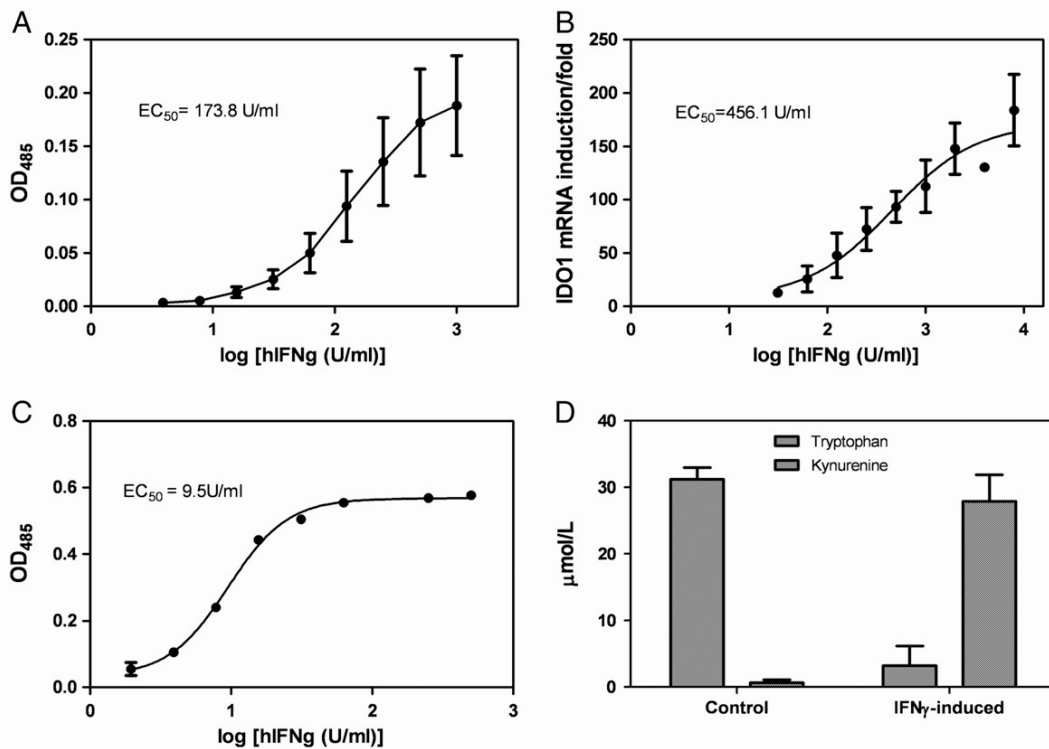


Fig. 1. A. Kynurenine levels in medium of HBEC 5i treated with increasing concentrations of recombinant hIFN γ . $N = 3$, $r^2 = 0.7305$. B. IDO1 mRNA fold induction at different concentrations of hIFN γ as detected by RT-qPCR in two experiments performed in triplicate. $N = 2$, $r^2 = 0.8408$. C. Kynurenine levels in medium of MVEC treated with increasing concentrations of hIFN γ in a single experiment performed in triplicate. $r^2 = 0.9915$. D. Tryptophan and kynurenine assayed by HPLC in supernates of HBEC 5i treated with 250 U/mL IFN γ in a single experiment. Error bars represent standard error of mean (SEM). EC_{50} is the concentration of hIFN γ that induces half of the maximal response.

To ensure that the kynurenine detected through Ehrlich's reagent by spectrophotometry was indeed derived from IDO1 activation by hIFN γ , a neutralising experiment was performed with hIFN γ antibody. Initially, a constant hIFN γ concentration was neutralised using different concentrations of anti-hIFN γ before the optimal anti-hIFN γ concentration was determined (data not shown). Once the optimal anti-hIFN γ concentration for neutralisation was established, the assay was repeated using an increasing concentration of recombinant hIFN γ treated with 1 μ g/ml of anti-hIFN γ . In the presence of the anti-hIFN γ neutralising antibody, hIFN γ failed to induce significant kynurenine production (Fig. 2A).

Next, the bioassay was assessed on biological samples, using a supernate from activated PBMC, containing an unknown level of hIFN γ , as the test sample. Recombinant hIFN γ was used as standard alongside the PBMC supernate. The level of hIFN γ in the supernate was determined by interpolating the unknowns on the recombinant hIFN γ standard curve. The concentration of hIFN γ detected by the bioassay (Fig. 2B) was compared to the level of hIFN γ detected in the supernate by CBA (Fig. 2C). hIFN γ concentration detected by CBA was 46,881 U/mL whereas the value from the bioassay was 25,215 U/mL. To ensure that the kynurenine detected by the bioassay was indeed specifically due to the action of hIFN γ , a neutralising experiment with

anti-hIFN γ was also performed on the PBMC supernate. The antibody eliminated any detectable kynurenine (Fig. 2D), demonstrating that the bioassay is selective for IFN γ in complex biological samples.

Other products of the kynurenine pathway, notably 3-hydroxyanthranilic acid (3HAA) and 3-hydroxykynurenine (3OHKyn), have been shown to interfere with kynurenine measurement using the spectrophotometric assay (Alegre et al., 2005). Activation of PBMC may lead to the formation of these products. So, we investigated whether kynurenine measurements may be affected by the activated PBMC supernatants. Firstly we used the spectrophotometric assay to measure kynurenine in the PBMC supernatants diluted in cell medium at the lower range of dilution factors used in the IFN γ bioassay (Fig. 3). No increase in kynurenine, as a result of PBMC activation, was detected at these dilutions. In addition, we investigated whether activation of the PBMC might produce factors that interfere with the detection of kynurenine. Known concentrations of kynurenine were added to cell medium and activated PBMC supernatant and then both were diluted in cell medium (Fig. 3). The dilution curves generated by these samples were not significantly different, indicating that the activation of the PBMCs did not produce products that interfered with kynurenine measurement using the spectrophotometric assay.

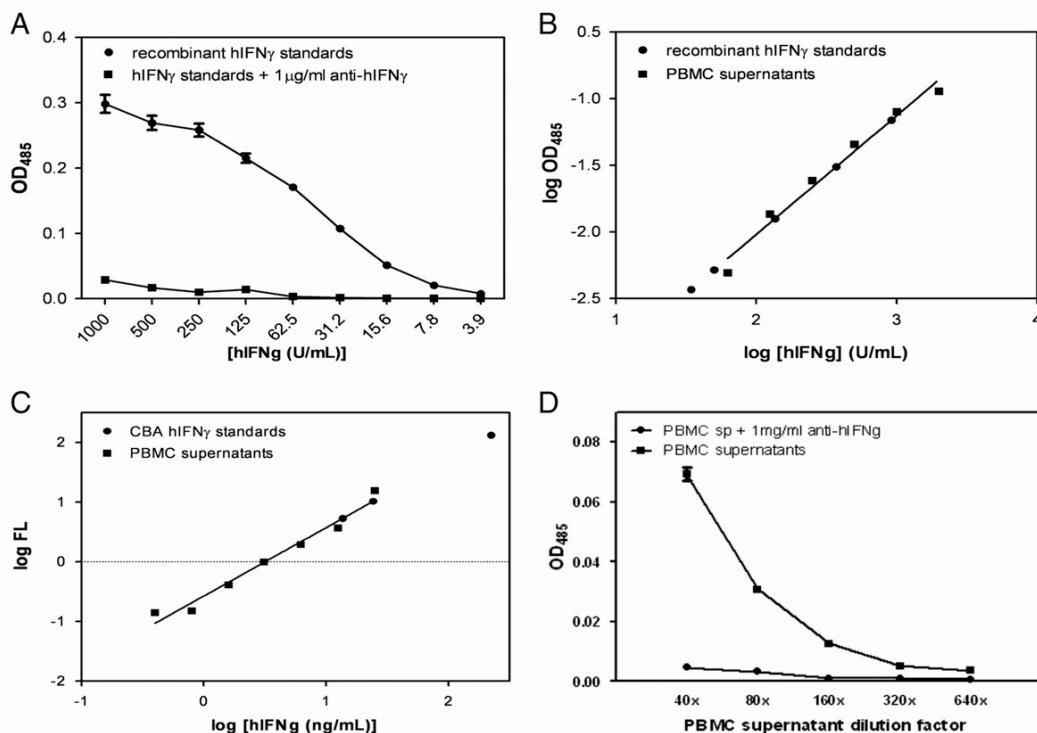


Fig. 2. A. Kynurenine levels in medium of HBEC treated with increasing concentrations of hIFN γ and 1 μ g/ml anti-hIFN γ in a single experiment performed in triplicate. B. Kynurenine levels in medium of HBEC treated with increasing concentrations of recombinant hIFN γ in a single experiment performed in triplicate and in PBMC supernates serially diluted 20 \times to 640 \times . $R^2 = 0.9363$. C. Fluorescence levels of CBA recombinant hIFN γ standards and PBMC supernates diluted 20 \times , 100 \times and 200 \times in a single experiment. $R^2 = 0.9719$. D. Kynurenine levels in medium of HBEC treated with serially diluted PBMC supernates and 1000 ng/ml anti-hIFN γ in a single experiment performed in triplicate. Error bars represent standard error of mean (SEM).

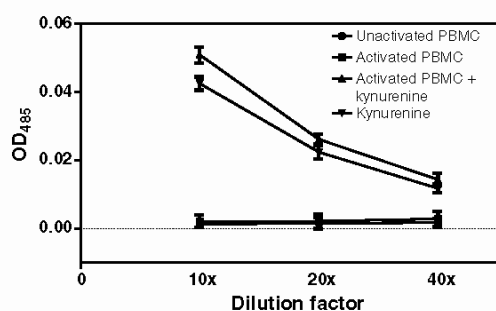


Fig. 3. Kynurenine pathway products generated by activated PBMC supernatants as detected by the spectrophotometric assay. Unactivated and anti-CD3 activated PBMC supernatants were diluted in cell medium, at the lowest dilutions used in the interferon gamma activity assays (10 \times , 20 \times , 40 \times dilution factors respectively), then assayed for kynurenine production. Kynurenine (200 μ mol/L) was added to cell medium and activated PBMC supernatant which were then further diluted in cell medium and assayed (10 \times , 20 \times and 40 \times dilution factors respectively, corresponding to final added kynurenine concentration 20 μ mol/L, 10 μ mol/L and 5 μ mol/L), N = 3. Error bars represent standard error of mean (SEM).

4. Discussion

This spectrophotometric IFN γ bioassay, which principally utilises the detection of kynurenine by Ehrlich's reagent, shows greater sensitivity than the molecular bioassay (RT-qPCR). In addition, the bioassay is cheaper and easier to perform than HPLC.

When a PBMC supernate of unknown hIFN γ concentration was assessed using the bioassay, the level determined was lower than that detected by the CBA. This may be reflective of the characteristics of the kynurenine bioassay, which specifically measures hIFN γ biological activity whereas the CBA measures the total amount of immunoreactive protein, without taking into account its biological activity. The bioassay, therefore, gives a more accurate representation of the biological activity of IFN γ in samples than does CBA.

In the past, a viral propagation technique has been commonly used to assay IFN γ . However, this method is not readily accessible to many laboratories. Despite the availability of IFN γ ELISA as a reliable assay, as for the CBA, ELISA does not provide information on the bioactivity of the detected IFN γ . Daubener et al. (1994) proposed a similar colorimetric-based bioassay using a human glioblastoma cell line. However, recent findings on the inability of endothelial cells to further metabolise kynurenine to its downstream products suggested that they would be a more efficient alternative cell line for this assay.

Using endothelial cells as our candidate cell line for the assay effectively counters the possibility of interference by the kynurenine metabolites 3HAA and 3OHKyn of the Ehrlich's method (Alegre et al., 2005), as kynurenine is not further broken down to its downstream metabolites in endothelial cells (Hunt et al., 2006; Owe-Young et al., 2008). Although activating the PBMC did not result in the formation of metabolites that interfered with our kynurenine measurements (Fig. 3), it is possible that other biological samples may contain more significant concentrations of such products. Therefore, the method should always include assaying the sample, diluted in endothelial cell medium, both before and

after incubation with the endothelial cells to obtain a baseline absorbance measurement. A further recommended control is to spike an aliquot of the sample with kynurenine to verify that interfering substances are not present.

The transformed human brain endothelial cell line HBEC 5i showed a linear correlation between IFN γ concentrations and kynurenine production. Although the bioassay was more sensitive when performed using a primary cell line (MVEC) than with the transformed cell line (HBEC 5i), primary cell lines are expensive to culture and not as readily available as transformed cell lines.

Taking into account all these factors, hIFN γ bioassay using spectrophotometric kynurenine detection and an endothelial cell line has obvious advantages over the currently available assays.

5. Conclusion

Kynurenine assay using a transformed endothelial cell line is an efficient method for determining IFN γ activity. The bioassay is simple, easy to perform and cost-efficient.

Acknowledgements

Julie Wheway, Vascular Immunology Unit, The University of Sydney, for providing the primary MVEC cell line and monoclonal anti-CD3; Ghassan Maghzal and Cacang Suarna for running the HPLC. Funding from the Australian National Health and Medical Research Council to Nicholas Hunt and Helen Ball. Felicita Jusof was supported by an SLAI scholarship from the Ministry of Higher Education and The University of Malaya, Malaysia.

References

- Alegre, E., Lopez, A.S., Gonzalez, A., 2005. Tryptophan metabolites interfere with the Ehrlich reaction used for the measurement of kynurenine. *Anal. Biochem.* 339, 188.
- Bach, E.A., Aguet, M., Schreiber, R.D., 1997. The IFN gamma receptor: a paradigm for cytokine receptor signaling. *Annu. Rev. Immunol.* 15, 563.
- Ball, H.J., Yuasa, H.J., Austin, C.J., Weiser, S., Hunt, N.H., 2009. Indoleamine 2,3-dioxygenase-2; a new enzyme in the kynurenine pathway. *Int. J. Biochem. Cell Biol.* 41, 467.
- Byrne, G.I., Lehmann, L.K., Kirschbaum, J.G., Borden, E.C., Lee, C.M., Brown, R.R., 1986. Induction of tryptophan degradation in vitro and in vivo: a gamma-interferon-stimulated activity. *J. Interf. Res.* 6, 389.
- Caplen, H.S., Gupta, S.L., 1988. Differential regulation of a cellular gene by human interferon-gamma and interferon-alpha. *J. Biol. Chem.* 263, 332.
- Christen, S., Peterhans, E., Stocker, R., 1990. Antioxidant activities of some tryptophan metabolites: possible implication for inflammatory diseases. *Proc. Natl. Acad. Sci. U. S. A.* 87, 2506.
- Daubener, W., Wanagat, N., Pilz, K., Seghrouchni, S., Fischer, H.G., Hadding, U., 1994. A new, simple, bioassay for human IFN-gamma. *J. Immunol. Methods* 168, 39.
- Gibson, U.E., Kramer, S.M., 1989. Enzyme-linked bio-immunoassay for IFN-gamma by HLA-DR induction. *J. Immunol. Methods* 125, 105.
- Green, J.A., Yeh, T.J., Overall Jr., J.C., 1981. Sequential production of IFN-alpha and immune-specific IFN-gamma by human mononuclear leukocytes exposed to herpes simplex virus. *J. Immunol.* 127, 1192.
- Hansen, A.M., Driussi, C., Turner, V., Takikawa, O., Hunt, N.H., 2000. Tissue distribution of indoleamine 2,3-dioxygenase in normal and malaria-infected tissue. *Redox Rep.* 5, 112.
- Hansen, A.M., Ball, H.J., Mitchell, A.J., Miu, J., Takikawa, O., Hunt, N.H., 2004. Increased expression of indoleamine 2,3-dioxygenase in murine malaria infection is predominantly localised to the vascular endothelium. *Int. J. Parasitol.* 34, 1309.
- Hunt, N.H., Golenser, J., Chan-Ling, T., Parekh, S., Rae, C., Potter, S., Medana, I.M., Miu, J., Ball, H.J., 2006. Immunopathogenesis of cerebral malaria. *Int. J. Parasitol.* 36, 569.

- Ino, K., Yoshida, N., Kajiyama, H., Shibata, K., Yamamoto, E., Kidokoro, K., Takahashi, N., Terauchi, M., Nawa, A., Nomura, S., Nagasaka, T., Takikawa, O., Kikkawa, F., 2006. Indoleamine 2,3-dioxygenase is a novel prognostic indicator for endometrial cancer. *Br. J. Cancer* 95, 1555.
- Lengyel, P., 1982. Biochemistry of interferons and their actions. *Annu. Rev. Biochem.* 51, 251.
- Lin, Y.C., Goto, S., Tateno, C., Nakano, T., Cheng, Y.F., Jawan, B., Kao, Y.H., Hsu, L.W., Lai, C.Y., Yoshizato, K., Chen, C.L., 2008. Induction of indoleamine 2,3-dioxygenase in livers following hepatectomy prolongs survival of allogeneic hepatocytes after transplantation. *Transplant. Proc.* 40, 2706.
- Mailankot, M., Nagaraj, R.H., 2010. Induction of indoleamine 2,3-dioxygenase by interferon-gamma in human lens epithelial cells: apoptosis through the formation of 3-hydroxykynurenine. *Int. J. Biochem. Cell Biol.* 42, 1446.
- Mazurek, G.H., LoBue, P.A., Daley, C.L., Bernardo, J., Lardizabal, A.A., Bishai, W.R., Iademarco, M.F., Rothel, J.S., 2001. Comparison of a whole-blood interferon gamma assay with tuberculin skin testing for detecting latent *Mycobacterium tuberculosis* infection. *JAMA* 286, 1740.
- Munn, D.H., Zhou, M., Attwood, J.T., Bondarev, I., Conway, S.J., Marshall, B., Brown, C., Mellor, A.L., 1998. Prevention of allogeneic fetal rejection by tryptophan catabolism. *Science* 281, 1191.
- Munn, D.H., Shafizadeh, E., Attwood, J.T., Bondarev, I., Pashine, A., Mellor, A.L., 1999. Inhibition of T cell proliferation by macrophage tryptophan catabolism. *J. Exp. Med.* 189, 1363.
- Okamoto, A., Nikaido, T., Ochiai, K., Takakura, S., Saito, M., Aoki, Y., Ishii, N., Yanaiharu, N., Yamada, K., Takikawa, O., Kawaguchi, R., Isonishi, S., Tanaka, T., Urashima, M., 2005. Indoleamine 2,3-dioxygenase serves as a marker of poor prognosis in gene expression profiles of serous ovarian cancer cells. *Clin. Cancer Res.* 11, 6030.
- Owe-Young, R., Webster, N.L., Mukhtar, M., Pomerantz, R.J., Smythe, G., Walker, D., Armati, P.J., Crowe, S.M., Brew, B.J., 2008. Kynurenine pathway metabolism in human blood-brain-barrier cells: implications for immune tolerance and neurotoxicity. *J. Neurochem.* 105, 1346.
- Pfefferkorn, E.R., 1984. Interferon gamma blocks the growth of *Toxoplasma gondii* in human fibroblasts by inducing the host cells to degrade tryptophan. *Proc. Natl. Acad. Sci. U. S. A.* 81, 908.
- Sanni, L.A., Thomas, S.R., Tattam, B.N., Moore, D.E., Chaudhri, G., Stocker, R., Hunt, N.H., 1998. Dramatic changes in oxidative tryptophan metabolism along the kynurenine pathway in experimental cerebral and noncerebral malaria. *Am. J. Pathol.* 152, 611.
- Sato, M., Yoshida, H., Yanagawa, T., Yura, Y., Urata, M., Atsumi, M., Furumoto, N., Hayashi, Y., Takegawa, Y., 1984. Interferon activity and its characterization in the sera of patients with head and neck cancer. *Cancer* 54, 1239.
- Schroder, K., Hertzog, P.J., Ravasi, T., Hume, D.A., 2004. Interferon-gamma: an overview of signals, mechanisms and functions. *J. Leukoc. Biol.* 75, 163.
- Sen, G.C., Lengyel, P., 1992. The interferon system. A bird's eye view of its biochemistry. *J. Biol. Chem.* 267, 5017.
- Svedersky, L.P., Benton, C.V., Berger, W.H., Rinderknecht, E., Harkins, R.N., Palladino, M.A., 1984. Biological and antigenic similarities of murine interferon-gamma and macrophage-activating factor. *J. Exp. Med.* 159, 812.
- Takao, M., Okamoto, A., Nikaido, T., Urashima, M., Takakura, S., Saito, M., Okamoto, S., Takikawa, O., Sasaki, H., Yasuda, M., Ochiai, K., Tanaka, T., 2007. Increased synthesis of indoleamine-2,3-dioxygenase protein is positively associated with impaired survival in patients with serous-type, but not with other types of, ovarian cancer. *Oncol. Rep.* 17, 1333.
- Tashiro, M., Tsukada, K., Kobayashi, S., Hayashi, O., 1961. A new pathway of D-tryptophan metabolism: enzymic formation of kynurenic acid via D-kynurenine. *Biochem. Biophys. Res. Commun.* 6, 155.
- Wang, Y., Liu, H., McKenzie, G., Witting, P.K., Stasch, J.P., Hahn, M., Changsirivathanathamrong, D., Wu, B.J., Ball, H.J., Thomas, S.R., Kapoor, V., Celermajer, D.S., Mellor, A.L., Keaney Jr., J.F., Hunt, N.H., Stocker, R., 2010. Kynurenine is an endothelium-derived relaxing factor produced during inflammation. *Nat. Med.* 16, 279.
- Weiser, S., 2007. In vitro studies on the pathogenesis of cerebral malaria. *Discipline of Pathology, Vol. Doctor of Philosophy. The University of Sydney, Sydney, Australia*, p. 350.
- Weng, M.Z., Xu, Y.G., Zhang, Y., Zhang, J.Y., Quan, Z.W., Xu, J.M., Peng, Z.H., 2011. Indoleamine 2,3-dioxygenase as a predictor of acute rejection after orthotopic liver transplantation in rat model. *Transplant. Proc.* 43, 3969.
- Yoshida, R., Park, S.W., Yasui, H., Takikawa, O., 1988. Tryptophan degradation in transplanted tumor cells undergoing rejection. *J. Immunol.* 141, 2819.

CHAPTER 3

GENES CODING

TRYPTOPHAN-CATABOLISING ENZYMES

IN ZEBRAFISH

CHAPTER 3: GENES CODING FOR TRYPTOPHAN-CATABOLISING ENZYMES IN ZEBRAFISH DURING DEVELOPMENT

3.1 INTRODUCTION

Tryptophan (Trp) is an essential amino acid that can be metabolised through either the serotonin or kynurenine (Kyn) pathways. Most dietary Trp is catabolised through the Kyn pathway, which can exert biological effects through depletion of Trp and/or generation of biologically-active metabolites (Opitz et al., 2007). The Kyn pathway has been implicated in a number of pathological conditions such as cerebral malaria, cancer, microbial infections, dementia and schizophrenia, as well as the physiological process of pregnancy (Romani et al., 2008; Sanni et al., 1998; Chang et al., 2011; Okamoto et al., 2005; Ino et al., 2006; Muller and Schwarz, 2007; O'Connor et al., 2009; Linderholm et al., 2012; Munn et al., 1998).

The first step in the Kyn pathway is the catabolism of Trp to N-formylkynurenine. This step can be catalysed by either tryptophan 2,3-dioxygenase (TDO) or indoleamine 2,3-dioxygenase (IDO) enzymes (Higuchi and Hayaishi, 1967; Knox and Auerbach, 1955). TDO is found in most metazoan species and some bacteria, but not in fungi, and its enzymatic activity is well conserved (Ball et al., 2014). In humans and mice, TDO is highly expressed in the liver, can be stimulated by dietary Trp and is involved in regulating plasma Trp levels (Kanai et al., 2009; Knox and Auerbach, 1955).

IDO is present in some bacteria, fungi, invertebrates and all vertebrates. The evolution of IDO enzymes is complex, with multiple gene duplication events giving rise to species possessing two or more IDO enzymes with distinct enzymatic activities and expression

patterns (Ball et al., 2014; Ball et al., 2009). For example, the first IDO enzyme to be described in mammals, now known as IDO1, has high efficiency for Trp catabolism and is expressed constitutively in the intestine, epididymis and placenta (Britan et al., 2006; Hayaishi, 1996; Munn et al., 1998). IDO1 expression is induced in inflammatory conditions by cytokines such as IFN γ , TNF and LPS (Taylor and Feng, 1991; Yoshida et al., 1981). IDO1 activity has been implicated in microbial infections and CNS-related disorders such as depression and schizophrenia. More recently a second IDO enzyme, IDO2, was described (Ball et al., 2007; Metz et al., 2007; Yuasa et al., 2007) that has a lower efficiency for Trp metabolism and is expressed in mouse liver and dendritic cells (Austin et al., 2010; Ball et al., 2007). Certain cytokines trigger its expression in specific cell types and studies employing *Ido2*^{-/-} mice suggest a role in autoimmunity (Merlo et al., 2014; Metz et al., 2007).

IDO2 is found in all vertebrates while IDO1 is present in mammals and several species of fish and turtles. This suggests that IDO1 and IDO2 arose via gene duplication in an ancestor of the vertebrates. IDO1 has been lost in many lower vertebrate lineages while IDO2 is well conserved (Yuasa *et al.* manuscript submitted). An IDO2 orthologue, but not IDO1, is present in the model organism, zebrafish (*Danio rerio*). The optical transparency of zebrafish embryos enables the study of gene expression in whole embryos as well as the progression of organogenesis in embryos. Therefore the zebrafish represents a model organism where the function and expression of *Ido2* can be examined in the absence of *Ido1*. In addition, gene duplication has generated two *Tdo2* enzymes in zebrafish, with the genes having been named as *tdo2a* and *tdo2b*. To date, only the expression of *tdo2b* in 5 days-post-fertilisation (dpf) old embryos has been reported (Thisse and Thisse, 2004),

being detected in the liver and posterior intestine. That work was a preliminary screen of *tdo2b* expression, and an in-depth analysis of the expression of Trp-catabolising enzymes remains lacking in zebrafish. In the light of IDO2 and TDO being highly conserved, understanding the role of Trp-catabolising enzymes in the biology of lower vertebrates may also shed light on their function in mammals. Thus, in the present study we aimed to determine the expression patterns of the three Trp-catabolising genes (*tdo2a*, *tdo2b* and *ido*) in a zebrafish developmental series and to examine the effects of suppressing the gene expression of these three enzymes.

3.2 METHODS

3.2.1 Enzymatic activity of Trp-catabolising enzymes

The *ido* expression construct was prepared as previously described (Yuasa *et al.* 2009). The coding sequences of *tdo2a* and *tdo2b* were amplified from cDNA clones MGC:171678 and MGC:63488 and blunt-end ligated into the pcDNA3.1 vector (Life Technologies). The sequences of all primers used for amplifications are listed in Table 3.1. Human Embryonic Kidney 293T (HEK293T) cells were grown in phenol red- and antibiotic-free DMEM supplemented with 10% (v/v) foetal bovine serum (FBS). Reverse transfection was performed in a 96 well plate with Lipofectamine 2000, according to the manufacturer's instructions (Life Technologies). Each well contained 0.4 μ L Lipofectamine 2000, 0.32 μ g plasmid DNA and 5×10^5 cells. Enzyme activity was measured as described in Chapter 2 (Jusof *et al.*, 2013). Briefly, the medium was replaced 24 h following transfection with culture medium supplemented with 400 μ mol/L of Trp and incubated for a further 24 h. Protein was precipitated from the medium with the addition of trichloroacetic acid (4% w/v final concentration) and centrifugation. The supernate was mixed with an equal volume of 2 % (w/v) p-dimethylaminobenzaldehyde in acetic acid and the absorbance measured at 485 nm in a spectrophotometer.

3.2.2 Fish husbandry

Wild type TAB zebrafish were maintained at 28.5°C under standard conditions (Westerfield, 2000). Embryos were collected after natural spawning as described previously (Kimmel *et al.*, 1995) and raised in embryo medium (Westerfield, 2000). All husbandry and experimental procedures were approved by the Animal Ethics Review

Committee, University of Sydney (NSW, Australia) and the Animal Ethics Committee, Macquarie University (N.S.W., Australia).

3.2.3 Reverse Transcriptase Polymerase Chain Reaction

Embryos were anaesthetised with 4 g/L Tricaine MS-222 (Sigma-Aldrich) in embryo medium prior to RNA extraction. Total RNA from 8 - 10 pooled embryos was extracted using Trizol (Life Technologies) according to the manufacturer's instructions and pellets were resuspended in RNase-free water. RNA concentrations were determined using a Nanodrop spectrophotometer (Nanodrop 2000, Thermo Scientific). For cDNA synthesis, 1 µg of RNA was denatured (70 °C, 5 min) and primed with random hexamers (0.5 µg) followed by cDNA synthesis (37 °C, 45 min) with a Tetro Reverse Transcriptase kit (Bioline) and heat denaturation (92 °C, 2 min). Gene expression was assessed using the Phusion High-Fidelity DNA Polymerase kit (New England Biolabs) according to the manufacturer's instructions. Each reaction contained cDNA equating to 50 ng of RNA starting material and 0.8 µmol/L each of reverse and forward primers. Amplification was performed on Eppendorf Mastercycler Personal with initial denaturation at 98 °C for 30 s, followed by 35 cycles of denaturation at 98 °C for 10 s, annealing at 60 °C for 30 s and elongation at 72 °C for 30 s per kb. The final elongation was at 72 °C for 5 min and amplified products were run on an agarose gel and visualized using 1 X SYBR Safe DNA gel stain (Life Technologies). For RT-quantitative PCR, amplification was performed with a Rotorgene Q (QIAGEN) using the same reaction mix and conditions, with the addition of 0.1 µL of 10 X SYBR Safe DNA gel stain to each reaction. The purity of the PCR products was assessed by melting curve analysis and expression was normalised to the *β-actin* gene.

No.	Gene	Primer design
1.	<i>tdo2a</i> (pcDNA 3.1)	5' ATGAGCGGATGTCCGATATTTTC 3' 5' CTGTATATATGTATACTCTTTA 3'
2.	<i>tdo2b</i> (pcDNA3.1)	5' ATGAGTGGATGTCCATTTTTG 3' 5' GGAAAGAGTTTAGCATTAT 3'
3.	<i>ido</i> (pCS2)	5' CTCGGATCCGATAATATGGGTACCGAAGTGAAA 3' 5' CTCGGATCCTTATTCTATGGTGAGCTC 3'
4.	<i>tdo2a</i> (ISH)	5' CATTAAACCCTCACTAAAGGGAAATTTTCAGCCATGAGCGGATG 3' 5' TAATACGACTCACTATAGGGAAGCCTGAAGCTGGTGAGAG 3'
5.	<i>tdo2b</i> (ISH)	5' CATTAAACCCTCACTAAAGGGAAGAGGAATCATCTACGGAGAC 3' 5' TAATACGACTCACTATAGGGCGATGTTAGCCTGCAGTTTA 3'
6.	<i>ido</i> (ISH)	5' CATTAAACCCTCACTAAAGGGAATCCCTCCATATTCTACGGCGTT' 3' 5' TAATACGACTCACTATAGGGCACGGGACGCTGGTATTGTG 3'.
7.	<i>ido</i> exon 1	5' ACCGAAGTGAAAGCTACAAGGAA 3' 5' CTTTGACCTCCAGGCAACGA 3'
8.	<i>ido</i> exon 9	5' TTCCCAGCGAGCTCATCAAGG 3' 5' TGGGAGGGAGGCATGTAGTC 3'
9.	<i>tdo2a</i> exon 6	5' CTCTCACCAGCTTCAGGCTT 3' 5' TTCCTCTCCGAGGCTGGT TT 3'
10.	<i>tdo2a</i> exon 3	5' CTCAGGTGCTTCAAAGTGAGC 3' 5' ATGGTTTCCAGAACGGCGAA 3'
11.	<i>tdo2b</i> exon 6	5' GCTTGACAAGGTGCTGAATGC 3' 5' GTCTGCGATTGTACGGGACT 3'
12.	<i>β-actin</i> (reference)	5' ACG AGA GAT CTT CAC TCC CCT 3' 5' GATTCAGGGGAGCCTCAGTG 3'.

Table 3.1. Primers used to amplify zebrafish *tdo2a*, *tdo2b* and *ido* mRNA and cDNA from zebrafish genome for cloning into expression vectors (1-3), for synthesis of probes for ISH (4-6) and for RT-PCR (7-12).

3.2.4 *In situ* hybridisation

Primers amplifying *tdo2a*, *tdo2b* and *ido* coding sequences were designed with a T7 or T3 promoter sequence (Table 3.1). mRNAs amplified from the zebrafish genome were run on agarose gel and purified using a QIAquick Gel Extraction Kit (Qiagen) according to the manufacturer's instructions. RNA transcription was performed in a 40 μ L reaction with 500 ng of template DNA, 1 X DIG labelling mix (Roche), 2 μ L of T7 Polymerase for antisense riboprobes or T3 Polymerase (20 U/ μ L) for sense riboprobes (Thermo Scientific), 1 X Transcription Buffer (supplied with the polymerase) and 1 μ L Ribosafe RNase inhibitor (Bioline). After 3 h incubation at 37 °C, the reaction was stopped by the addition of 4 μ L of 0.2 mol/L EDTA. Riboprobes were purified using the ISOLATE II RNA micro clean up kit (Bioline) according to the manufacturer's instructions. The concentration of RNA was measured using a Nanodrop (Nanodrop 2000, Thermo Scientific) and the probes stored at -80 °C until further use. The hybridisation procedure was performed according to Thisse *in situ* hybridisation protocol (Thisse and Thisse, 2008) with minor modifications, which included hybridising the embryos in 250 μ L hybridisation medium containing 500 ng DIG-labelled RNA probe and performing both hybridisation and post-hybridisation washes at 68 °C. After staining, embryos were rinsed in Phosphate Buffered Saline with 0.1 % (v/v) Tween 20 (PBST) and fixed in 4 % (w/v) paraformaldehyde for 2 h. At the end of fixation, embryos were rinsed in PBST twice before they were stored at 4 °C in the same solution until imaged.

3.2.5 Morpholino and *ido* mRNA microinjections

Splice-site morpholinos directed to the *ido*, *tdo2a* and *tdo* genes, as well as standard control oligonucleotides, were purchased from Gene-Tools (Table 3.2). The *ido* coding sequence for the generation of *ido* RNA transcript (rescue) was amplified using primers with BamH1 sequences and a Kozak consensus sequence upstream of the start codon (Table 3.2). After BamH1 digestion, the fragment was ligated into the pCS2 vector, then sequenced, and *ido* mRNA was transcribed finally using the SP6 mMACHINE mMESSAGING kit (Life Technologies). The mRNA was purified with the ISOLATE II RNA micro clean up kit (Bioline) according to manufacturer's instructions and the concentration of RNA measured using the Nanodrop (Nanodrop 2000, Thermo Scientific). Morpholinos were prepared with or without *ido* mRNA in RNase-free water with 10 % (v/v) phenol red and Oregon green fluorescent dye. One-cell stage *D. rerio* embryos were injected with 1.5 pmol morpholino \pm 300 pg *ido* mRNA in an approximately 3 nL bolus. Efficiency of knockdown was assessed using RT-qPCR, according to the procedures mentioned above.

No.	Gene	Morpholino design
1.	<i>ido</i> exon 1	5' AAAGAAATGACCTACAGAGATGTGA 3'
2.	<i>ido</i> exon 9	5' TTCCATCTAACAACCACAAGCAGAA 3'
3.	<i>tdo2a</i> exon 3	5' TTAGTGTTTGCGAAGCTCACCTTGA 3'
4.	<i>tdo2a</i> exon 6	5' GATGGTTTCCTCAGGTTTACCTCTA 3'
5.	<i>tdo2b</i> exon 6	5' AGATACTCCCTATAACATTCAAACA 3'

Table 3.2. Morpholino sequences targeting splice sites to knock-down gene expression

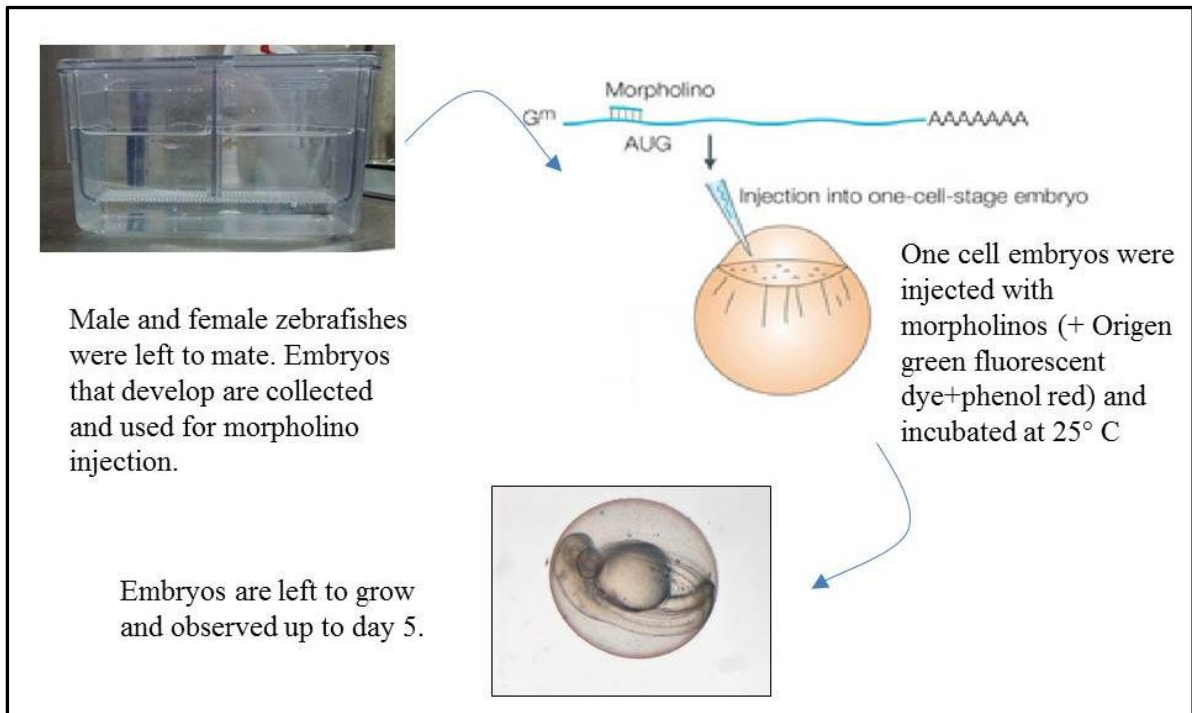


Figure 3.1. Morpholino injection protocol on one-cell stage *D. rerio* embryos. Diagram redrawn using images from (Langenau and Zon, 2005) and personal collection.

3.2.6 Microscopy and image acquisition

For live embryo imaging, embryos anaesthetised 24 hours post-fertilisation were mounted onto 3 % (w/v) methylcellulose (Sigma Aldrich) or 1 % (w/v) low melting point agarose gel (Sigma-Aldrich) and subsequently imaged. Embryos were returned to the petri dish and allowed to grow up to 5 days post-fertilisation (dpf).

For imaging of fixed embryos treated by *in situ* hybridisation, embryos were dehydrated in increasing concentrations of methanol (25, 50, 75 % v/v methanol) for 15 min each, before the final dehydration (100 % methanol, 1 h). The methanol solution was then removed and replaced with 500 µL of methysalicylate (AJAX Finechem). Embryos were allowed to sink to the bottom of the microcentrifuge tubes before they were removed and mounted in dibutylphthalate in xylene (DPX) on glass slides. These slides were imaged promptly using a Leica M165 FC stereo microscope (Leica).

3.2.7 Statistical analysis for mortality rate

The mortality rate observed in the morphants relative to uninjected wild-types and rescued morphants were analysed using repeated measures ANOVA with the Tukey post-test (GraphPad Prism) as embryo clutches differ from experiment to experiment (Kimmel et al., 1995). Therefore, the mortality rates were treated as repeated measures of different populations.

3.3 RESULTS

3.3.1 Zebrafish have three genes that encode Trp-catabolising enzymes

Amino acid sequence alignment shows that Tdo2a and Tdo2b share 76 % amino acid identity (Fig. 3.2), with their genes situated on chromosomes 11 and 14, respectively.

Database searching revealed that *Astyanax mexicanus* (Mexican tetra) also has two *tdo* genes, like *D. rerio*. Interestingly, in the phylogenetic tree (Fig. 3.3), one of *A. mexicanus* *tdo* genes is clustered with zebrafish *tdo2b*.

When introns of Tdo2a and Tdo2b were compared, it is evident that they occurred at identical positions within the coding regions of the *tdo2a* and *tdo2b* genes, suggesting that the two genes arose via a gene duplication event (Fig. 3.4A). In contrast, Ido, encoded by a gene located on chr 8, has no significant homology to the Tdo proteins. The position of introns within the coding sequence is different to the *tdo* genes, suggesting that *ido* and *tdo* do not share a common ancestral gene (Fig. 3.4A). HEK293T cells were transfected with each of the zebrafish cDNAs encoding the Tdo or Ido enzymes or with mouse IDO1, as a positive control. All of the zebrafish enzymes exhibited Trp-catabolising properties as they converted Trp in the culture medium to Kyn (Fig. 3.4B). Thus, zebrafish possess three enzymes with the ability to catabolise Trp. It is likely that the two Tdo enzymes arose through a gene duplication event while the Ido enzyme has independently evolved to have the same enzymatic activity.

Tdo2a 1 MSGCPYFQRKFLSTSKQHLKEEENDEAQTGINKASKGGLIYGDYLQLDKIVTSQVLQSEL 60
 MSGCP+ S + EE D +Q G+NKA+KGG+IYGDYLQDK++ +QVLQSE
Tdo2b 1 MSGCPFLGGTLQLLSSNPRQAEEDGSQGGVNKAAKGGIYGDYLQLDKVNAQVLQSEQ 60

Tdo2a 61 KGNKIHDEHLFIVTHQAYELWFKQVLWELDSVREIFISGHVRDERNMLKVNTRIHRIVMI 120
 KGNKIHDEHLFIVTHQAYELWFKQ+LWELDSVR++FI HVRDERNMLKV +RIHRI MI
Tdo2b 61 KGNKIHDEHLFIVTHQAYELWFKQILWELDSVRDLFIKKHVRDERNMLKVVSRIRITMI 120

Tdo2a 121 FRLLDQFAVLETMTALDFYDFRGLSPASGFQSLQFRLLNKIGVPHNQRPYNRRHYR 180
 F+LL+DQFAVLETMTALDF+DFR YLSPASGFQSLQFRLLE KIGV + RVPYNRRHYR
Tdo2b 121 FKLLVDQFAVLETMTALDFFDFREYLSPASGFQSLQFRLLEKIGVADHLRVPYNRRHYR 180

Tdo2a 181 DNFRDQESELLHSEQEPTLLQLVEQWLERTPGLEEDGFNFWGKLEKNIFEGLRREKEHI 240
 DNF +ESE LL SEQEPTLLQLVEQWLERTPGLE+DGFNFWGKL+ NI EGL+REK +
Tdo2b 181 DNFHGESEETLLSSEQEPTLLQLVEQWLERTPGLEKDGFNFWGKLQANIEEGLKREKHQV 240

Tdo2a 241 EQKPASERKEEMLAELIKQRDIFLSLFDEKRHDHLVSTGQRRLSYKALQGALMIYFYREE 300
 E+ +E K+E+L +L KQ + F +LFD KRH+HL+S G+RRLSYKALQGALMI FYREE
Tdo2b 241 EKMEDTEVKQELLEDLNKQMETFTALFDSKRHEHLLSKGERRLSYKALQGALMINFYREE 300

Tdo2a 301 PRFQVPFQLLTSLMDIDTLMTKWRYNHVCMVHRMIGRKDGTGGSSGYQLRSTVSDRYKV 360
 PRFQVPFQLLT+LM+IDTLMTKWRYNHVCMVHRMIG K GTGGSSGY YLRSTVSDRYKV
Tdo2b 301 PRFQVPFQLLTALMEIDTLMTKWRYNHVCMVHRMIGSKAGTGGSSGYHYLRSTVSDRYKV 360

Tdo2a 361 FVDLFNLATFLIPRDWVPKLPSEHTFLYMAECCDSSYCS-SSDSD 406
 FVDLFNLATFL+PR WVPKL+P+ H F Y AEC DSSY S SS+DSD
Tdo2b 361 FVDLFNLATFLVPRSWVPKLNPNIHKFPYTAECYDSSYNSSCSSEDSD 407

Fig. 3.2. An alignment of *D. rerio* Tdo2a (NP_001096086.1) and Tdo2b (NP_956150.1) proteins using T-Coffee using their FASTA sequences. Identical residues are highlighted in the middle row. The '+' sign denotes that the amino acid is conserved in charge.

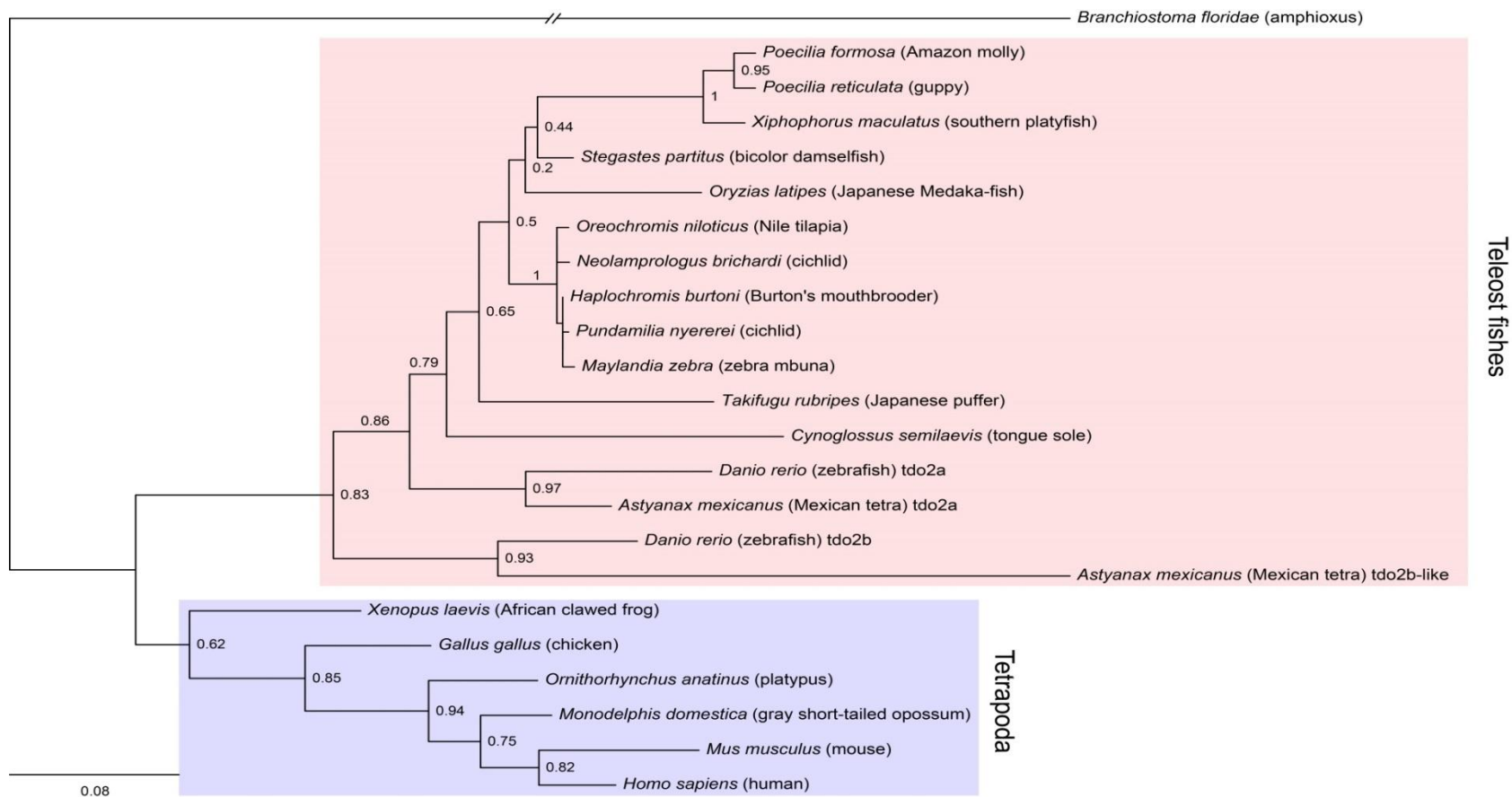
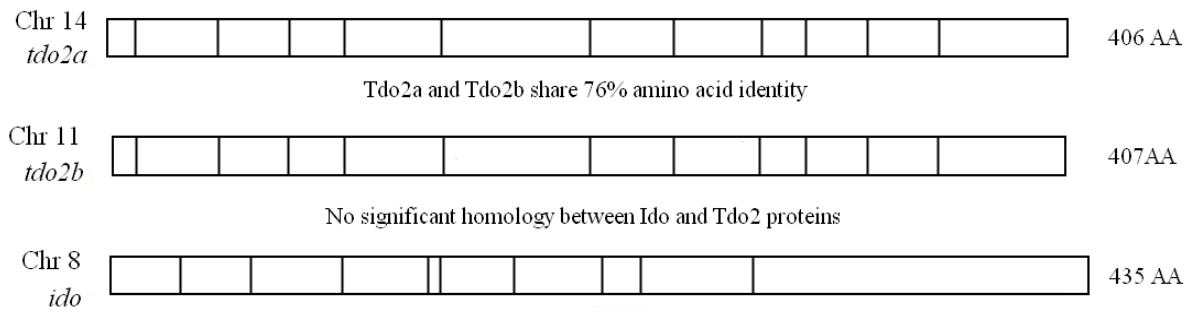


Fig. 3.3. Phylogenetic tree (maximum likelihood tree) of vertebrate TDOs. TDO is widely distributed among vertebrates, both tetrapod (highlighted in blue) and teleost fishes (highlighted in red). Each species possesses only one TDO basically, a few fishes (Danio and Astyanax) have two TDO isoforms, TDOa and TDOb. Amino acid sequences of amphioxus TDO is employed as an outgroup. The internal branch labels are bootstrap values with 100 replications. The scale bar corresponds to 0.08 substitutions per site. The tree was constructed with a help of Dr Yuasa, Kochi University, Japan.

A.



B.

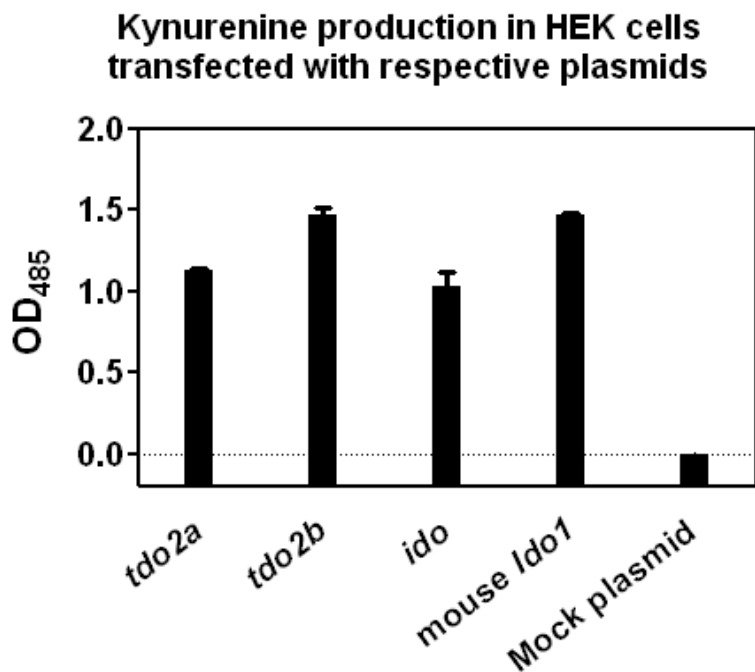


Fig 3.4. Enzymatic activity, but not sequence homology, is common to zebrafish Ido and Tdo2 proteins. **A.** A schematic representation of the intron positions in *tdo2a* (NP_001096086.1), *tdo2b* (NP_956150.1) and *ido* (NP_001077323.1) proteins and their shared homology. The vertical black lines represent the position of introns within the protein sequence. Protein sequences were aligned using T-Coffee (Notredame et al., 2000) and 76% amino acid identity was found between Tdo2a and Tdo2b. A full alignment of the Tdo2 sequences is found in Fig. 3.2. **B.** Tryptophan-catabolising enzymatic activities of zebrafish Tdo2a, Tdo2b and Ido assessed by measuring Kyn formation in the medium of transfected HEK293T cells using a spectrophotometric assay. Data shown are the mean \pm SEM from a single experiment with 6 replicates.

3.3.2 Genes coding tryptophan-catabolising enzymes are expressed in the liver and intestine of zebrafish embryos.

Expression of the three enzymes in embryonic development was examined in RNA extracted from pooled embryos by both endpoint RT-PCR and RT-qPCR (Fig. 3.5A and 3.5B). Abundant *tdo2a* mRNA expression was detected in embryos as young as 3 dpf and mRNA levels almost tripled from 3 dpf to 5 dpf. *tdo2b* mRNA was only detected from 4 dpf onwards, with approximately a 50 % increase in its expression levels from 4 to 5 dpf. The expression of *ido* was detected from 3 dpf onwards, similar to *tdo2a*. However its levels did not increase significantly from 3 to 5 dpf.

The localisation of mRNA encoding the three enzymes was examined in *D. rerio* embryos using *in situ* hybridisation. *tdo2a* mRNA was detected throughout the intestine from 3 dpf onwards, but the expression of *tdo2a* mRNA was detected in the liver only from 4 dpf (Fig. 3.6A). Likewise, *tdo2b* mRNA was detected in the liver from 4 dpf and in the intestine from 3 dpf onwards, although its expression was limited to the posterior intestine (Fig. 3.6B). *ido*, on the other hand, was detected throughout the intestine from 3 dpf onwards (Fig. 3.6C) and it was not detected in the liver (Fig. 3.6C).

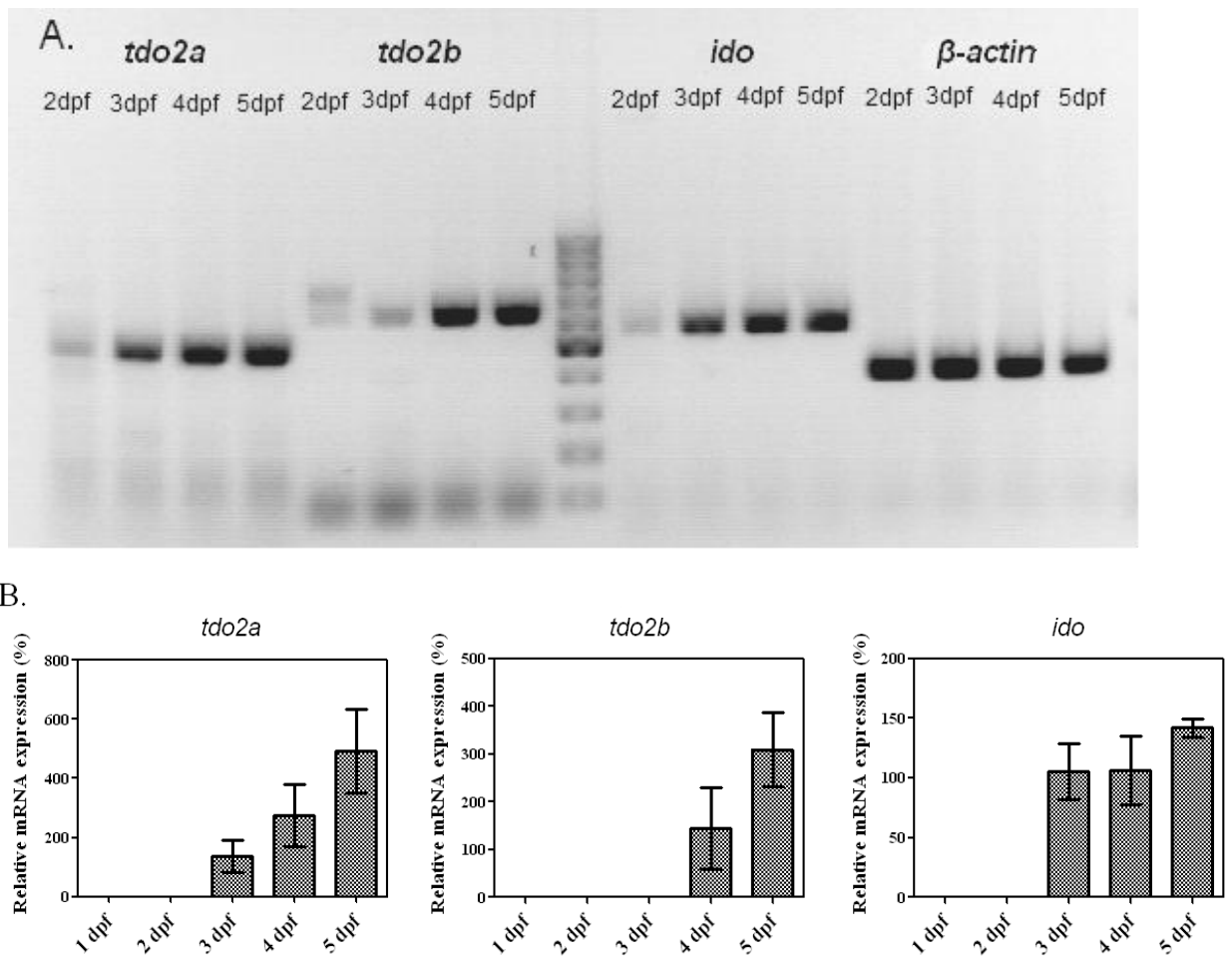
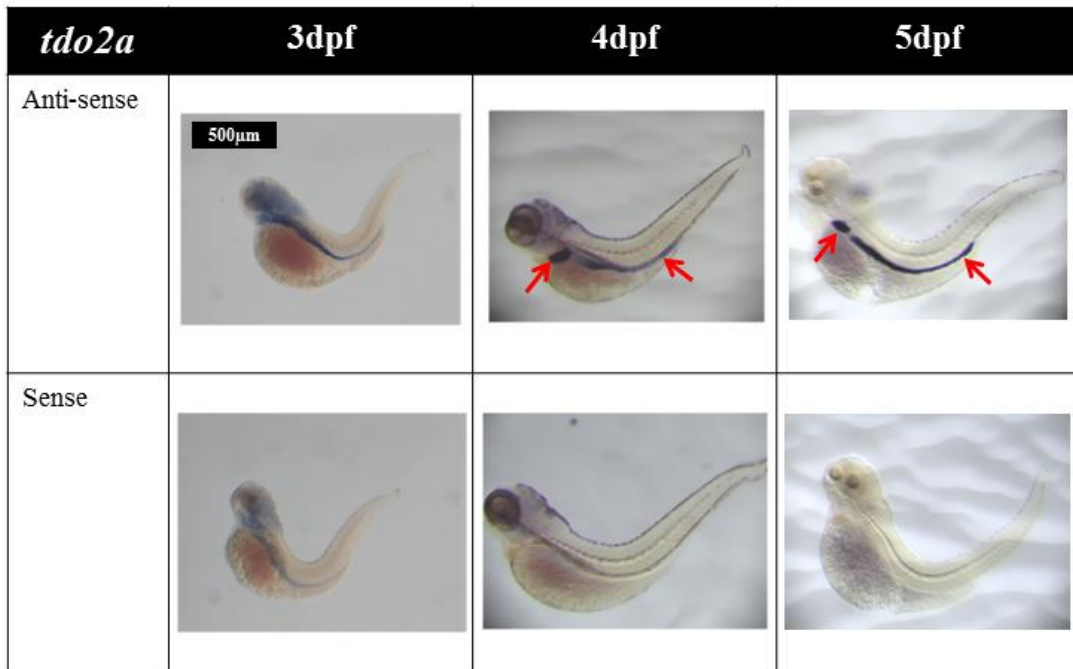
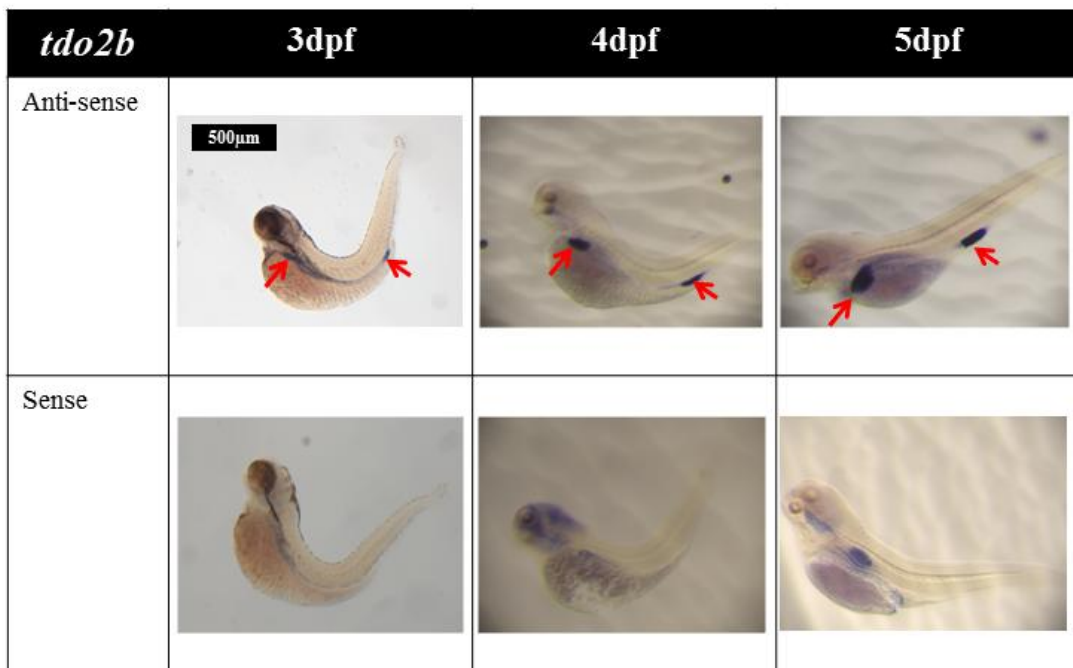


Fig. 3.5. All three genes coding for tryptophan-catabolising enzymes are expressed in zebrafish embryonic development. **A.** Expression of the three tryptophan-catabolising genes in 2 to 5 dpf *D. rerio* embryos assessed by end-point RT-PCR. A representative experiment from 10 pooled embryos is shown. **B.** *tdo2a* (left), *tdo2b* (middle) and *ido* (right) mRNA expression relative to 3 (*tdo2a*, *ido*) or 4 (*tdo2b*) dpf levels, at which point expression is first detected. Data shown for 3 to 4 dpf are from pooled samples of 10 embryos in 3 experiments whereas data shown for 1 and 2 dpf is from a single experiment. The expression of mRNA levels was relative to its own mRNA levels when it was first detected *i.e* the standard for *tdo2a* and *ido* were the expression levels of their respective mRNA at 3 dpf whereas the standard for *tdo2b* was the expression level of *tdo2b* mRNA at 4 dpf.

A.



B.



Refer to the next page for the legend

C.

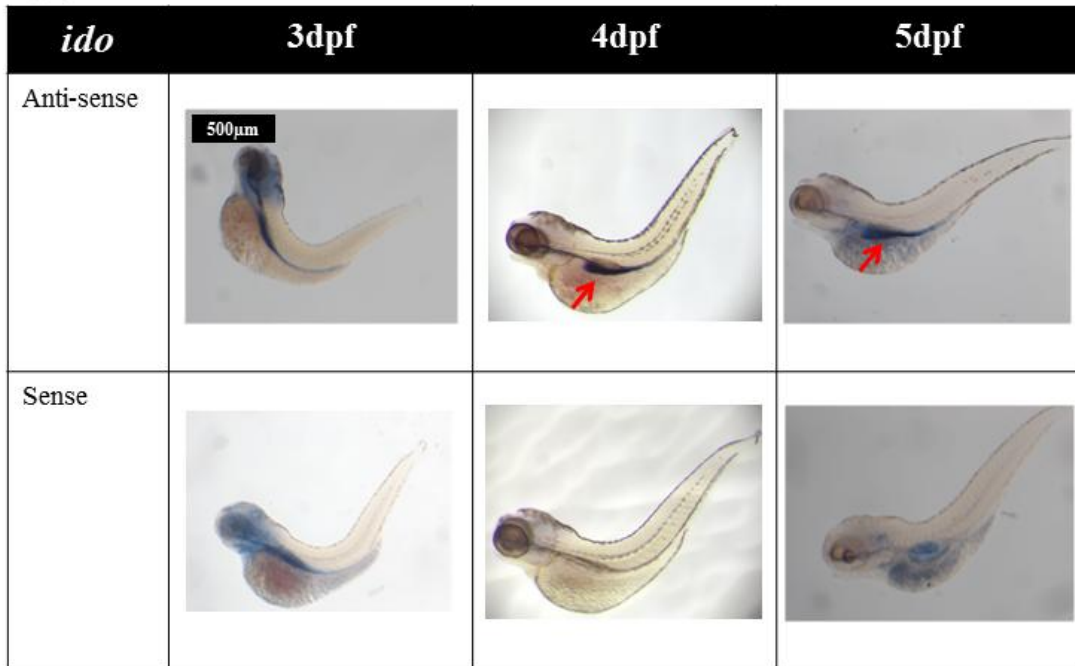


Fig 3.6. Genes coding Trp-catabolising enzymes are expressed in the zebrafish embryo intestine and liver. Images are representatives of n = 3 independent experiments in replicates of 5. **A.** *tdo2a* mRNA expression is seen in the liver and throughout the intestine from 4 and 5 dpf *D. rerio* embryos treated with *tdo2a* antisense probes, whereas no expression was seen in the negative control treated with *tdo2a* sense probes. **B.** *tdo2b* mRNA expression is seen in the liver and posterior intestine when treated with antisense probes but not with the equivalent negative control. **C.** *ido* mRNA expression is seen throughout the intestine when treated with antisense probes but not with the equivalent negative control. ISH was performed in 2 to 5 dpf embryos. However, specific staining was only evident from 4 dpf onwards. The arrows point to the tissue where targeted mRNA is detected.

3.3.3 Knocking down the *ido* gene resulted in higher mortality in the embryos.

To further investigate the Trp-catabolising genes in the *D. rerio* system, we employed the morpholino approach to transiently knockdown the expression of target genes.

An *ido* morpholino targeting exon 1 splice site successfully knocked down *ido* mRNA expression by almost 70 % relative to the uninjected wild-type embryos at 3 dpf (Fig. 3.7A). Although the levels of mRNA increased slightly at 4 and 5 dpf, they never exceeded 50 % of the mRNA levels in uninjected controls. Morphants (embryos in which target gene expression has been knocked down) that were rescued by injection with *ido* mRNA transcript had similar knockdown efficiency at 3 dpf (~70%) but the mRNA levels climbed to ~70% relative to the wild-type after 4 dpf (Fig. 3.7A). When the expression of *tdo2a* in *ido* morphants was assessed, a similar trend to *ido* expression was observed, where *tdo2a* mRNA levels were downregulated in the morphants relative to WT embryos (Fig. 3.7B).

The mortality rate was recorded on each day and the results at 5 dpf are presented in Table 3.3 (mean \pm SEM, n = 3 experiments). The morphants exhibited the highest mortality rate among the groups (55.4 ± 10.5 % from 181 morphants at 5 dpf). The mortality rate of the rescued morphants was less than half that of the morphants (21.4 ± 4.2 % in 154 embryos). There were no significant differences between the mortality rate of rescued morphants, the rescue RNA-injected embryos (22.6 ± 12.5 % in 151 embryos) and the uninjected embryos (10.1 ± 3.8 % in 307 embryos) (Fig. 3.8). Gut oedema was exhibited by 25 % (n = 20) of the *ido* morphants surviving until 5 dpf (Fig. 3.9).

Knockdown of *ido* expression in zebrafish embryos was also attempted using an alternative *ido* morpholino targeting exon 9. *ido* morphants exhibited cardiac oedema

and a general developmental retardation (Fig. 3.10A). All of the morphants also did not survive past 5 dpf. When the level of knockdown was assessed by RT-PCR and gel electrophoresis, a complete knockdown of *ido* expression was seen (Fig. 3.10E). However, alongside this knockdown, an ablation of *tdo2a* gene expression was also seen while the expression of reference gene *β-actin* remained normal. When the morphants were injected with *ido* RNA transcript (rescue), the general developmental retardation, cardiac oedema and premature death still remained (Fig. 3.10B). None of these phenotypes were observed in the rescue RNA only-injected and uninjected embryos (Fig. 3.10C & D).

3.3.4 Knocking down the *tdo2a* and *tdo2b* genes in zebrafish embryos

We successfully reduced the expression of *tdo2a* mRNA in *D. rerio* with a morpholino targeting exon 3 and 6 (Fig. 3.11A & B). However, no differences in phenotype or mortality rate were observed in the morphants compared to the wild-type uninjected embryos (Fig. 3.12). On the other hand, morpholinos designed to target splice sites in *tdo2b* mRNA were unsuccessful in knocking down gene expression (Fig. 3.11C).

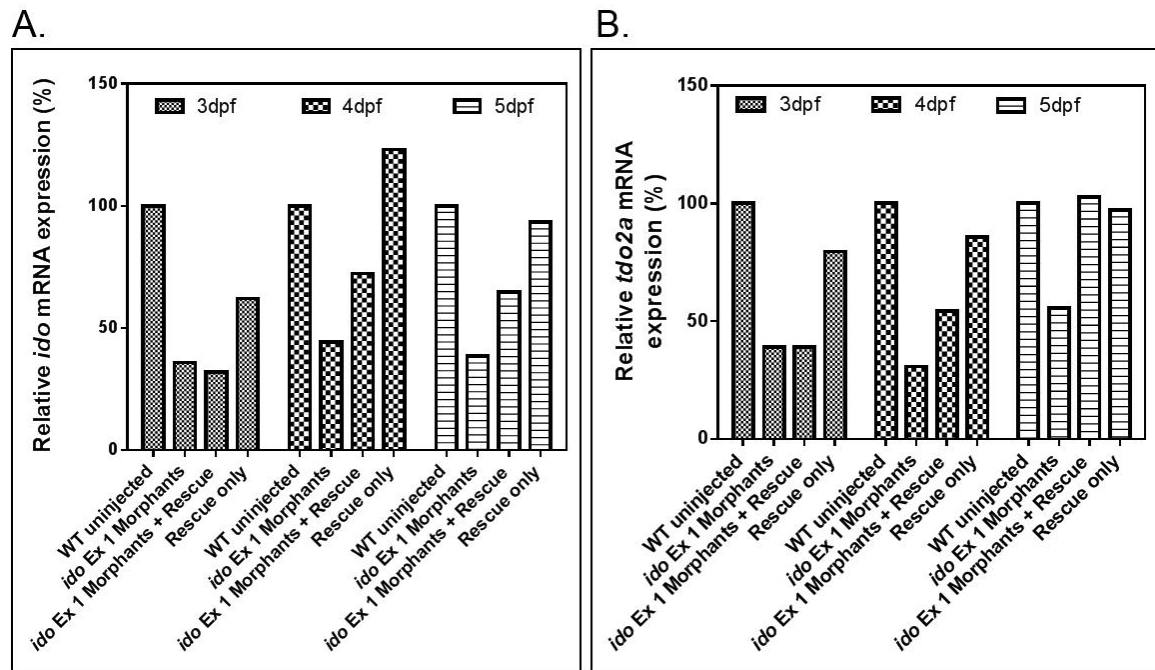


Fig. 3.7. A. *ido* gene expression can be knocked down using morpholinos. Validation of the efficiency of *ido* knockdown by morpholinos targeting exon 1 of the *ido* gene was assessed by RT-qPCR analysis in *ido* morphants, relative to uninjected wild-type embryos, at 3, 4 and 5 dpf. *Ido* expression in morphants rescued using *ido* mRNA as well as wild-type embryos injected with *ido* mRNA is also shown. **B. *tdo2a* gene expression in *ido* morphants** was assessed by RT-qPCR relative to WT embryos at 3, 4, and 5 dpf. Data are from pooled samples of 8 embryos from a single experiment.

Treatment	Total embryos alive (%)	Total embryos dead (%)	Average Mortality rate (%)
<i>ido</i> Exon 1 morpholino	80 (44)	101 (56)	55.4 ± 10.5
<i>ido</i> Exon 1 + <i>ido</i> rescue	119 (77)	34 (23)	21.4 ± 4.2
<i>ido</i> rescue only	116 (77)	35 (23)	22.6 ± 12.5
WT uninjected	274 (89)	33 (11)	10.1 ± 3.8

Table 3.3. Percentage of mortality in *ido* Exon 1 morphants, *ido* morphants rescued with *ido* mRNA, embryos injected with *ido* mRNA alone, and uninjected wild-type controls. Data shown are the total mortality rate as well as the mean mortality rate from 3 independent experiments ± SEM.

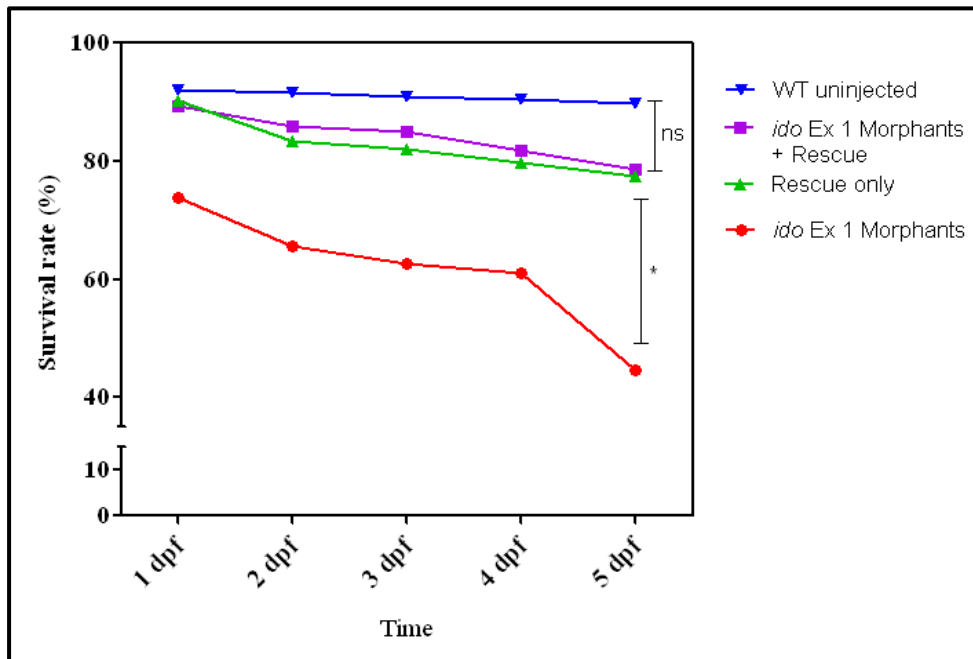


Fig. 3.8. Knockdown of *ido* gene expression increases the mortality rate in zebrafish embryos. Survival rate over 5 dpf of *ido* morphants, morphants rescued with *ido* mRNA, embryos injected with *ido* mRNA alone and uninjected wild-type embryos. Values represent the mean survival rate from 3 independent experiments. One-way repeated measures ANOVA with Tukey post-test statistical analysis showed significant differences ($p < 0.05$) in the survival rate on 5 dpf between morphants and rescued morphants (*) as well as between morphants and both rescue mRNA-injected embryos and uninjected embryos (not marked). There were no significant differences in the survival rates of uninjected embryos, rescue mRNA-injected embryos and rescued morphants (ns). Standard error of mean is not shown for clarity but were <12% of the mean values.

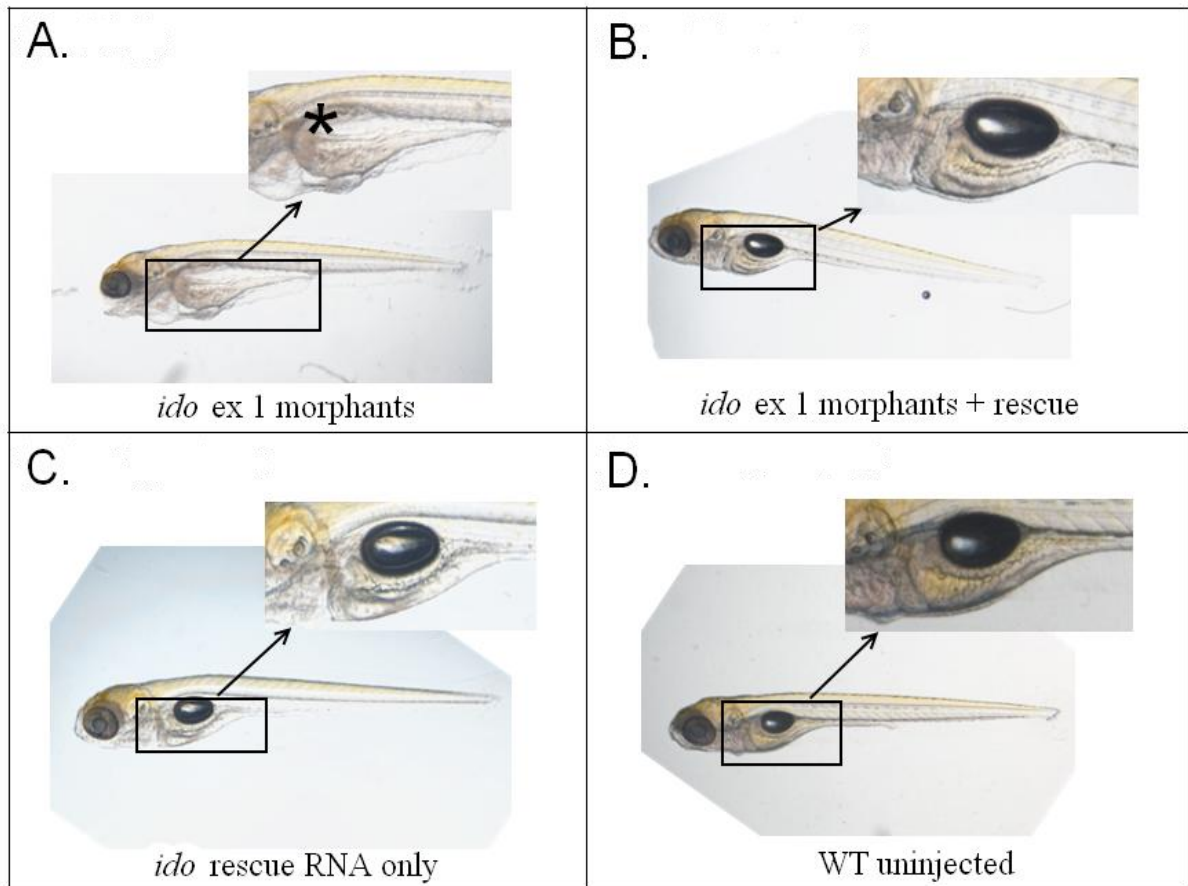


Fig. 3.9. Surviving *ido* ex 1 morphants had deformities including gut oedema. A. *ido* morphants, B. rescued morphants, C. *ido* mRNA-injected wild-type embryos and D. uninjected wild-type embryos. Images are representative of 3 independent experiments. Uninflated swim bladder (denoted by '*'), heart and gut oedema was seen in 20 % of the *ido* morphants (n=20) and was not present in the rescues.

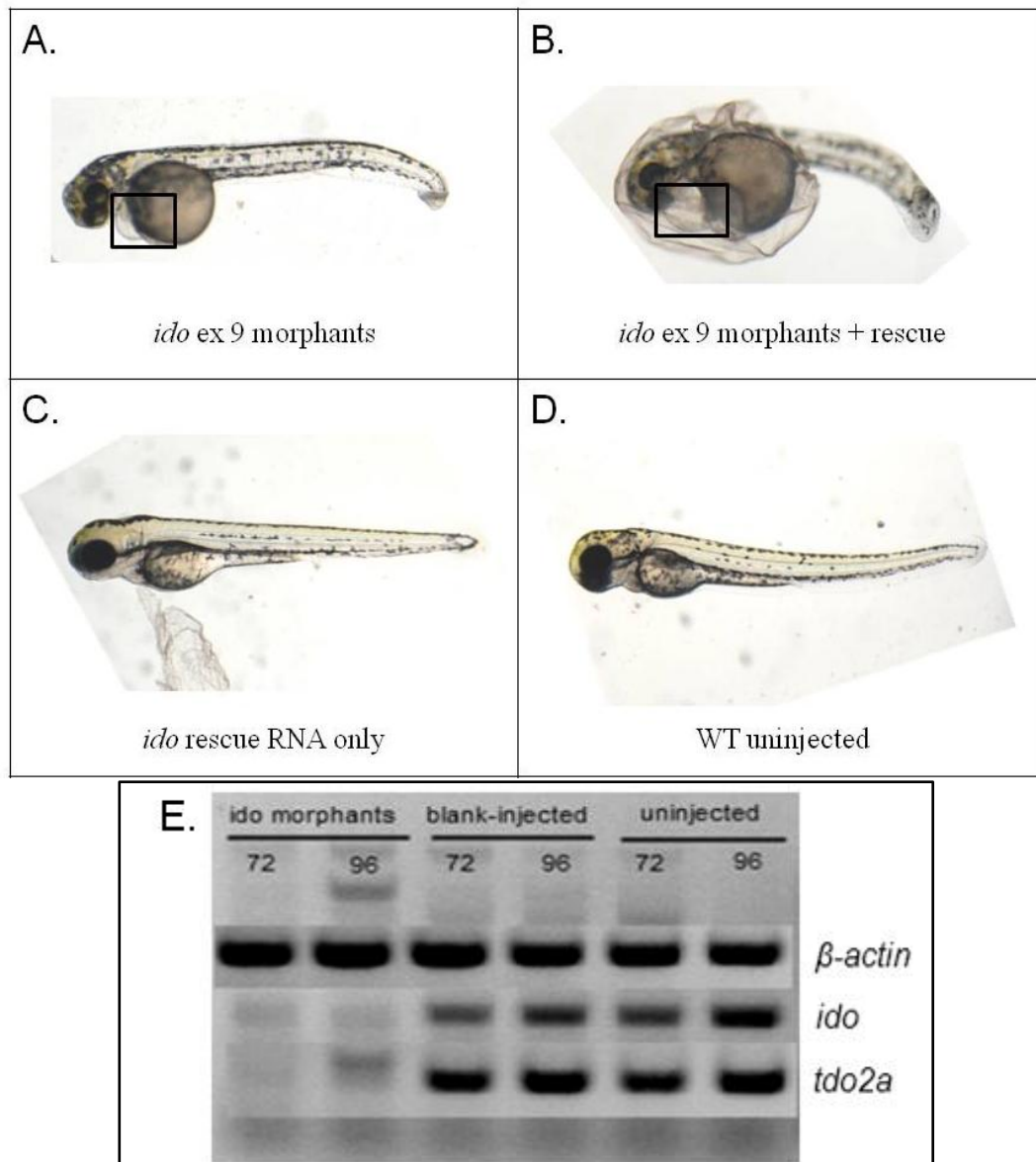


Fig. 3.10. Zebrafish embryos injected with *ido* exon 9 morpholino only (A) as well as *ido* morpholino and *ido* RNA transcript (B) at 3 dpf showed cardiac oedema (denoted by the square). Mortality rate was 100% for both *ido* morphants and rescue injected-morphants, likely indicating toxic off-target effects of the morpholino. *ido* mRNA only-injected wild-type embryos (C) and uninjected wild-type embryos (D) showed normal, healthy phenotypes. Images are representative of a single experiment.

Knockdown efficiency of *ido* exon 9 morpholino was assessed by RT-PCR and agarose gel electrophoresis (E). Although it appeared as though *ido* gene expression has been fully knocked down in *ido* morphants, the ablation of *tdo2a* gene expression in these morphants was also found. Expression of β -actin, an ubiquitously expressed gene, was normal in the morphants.

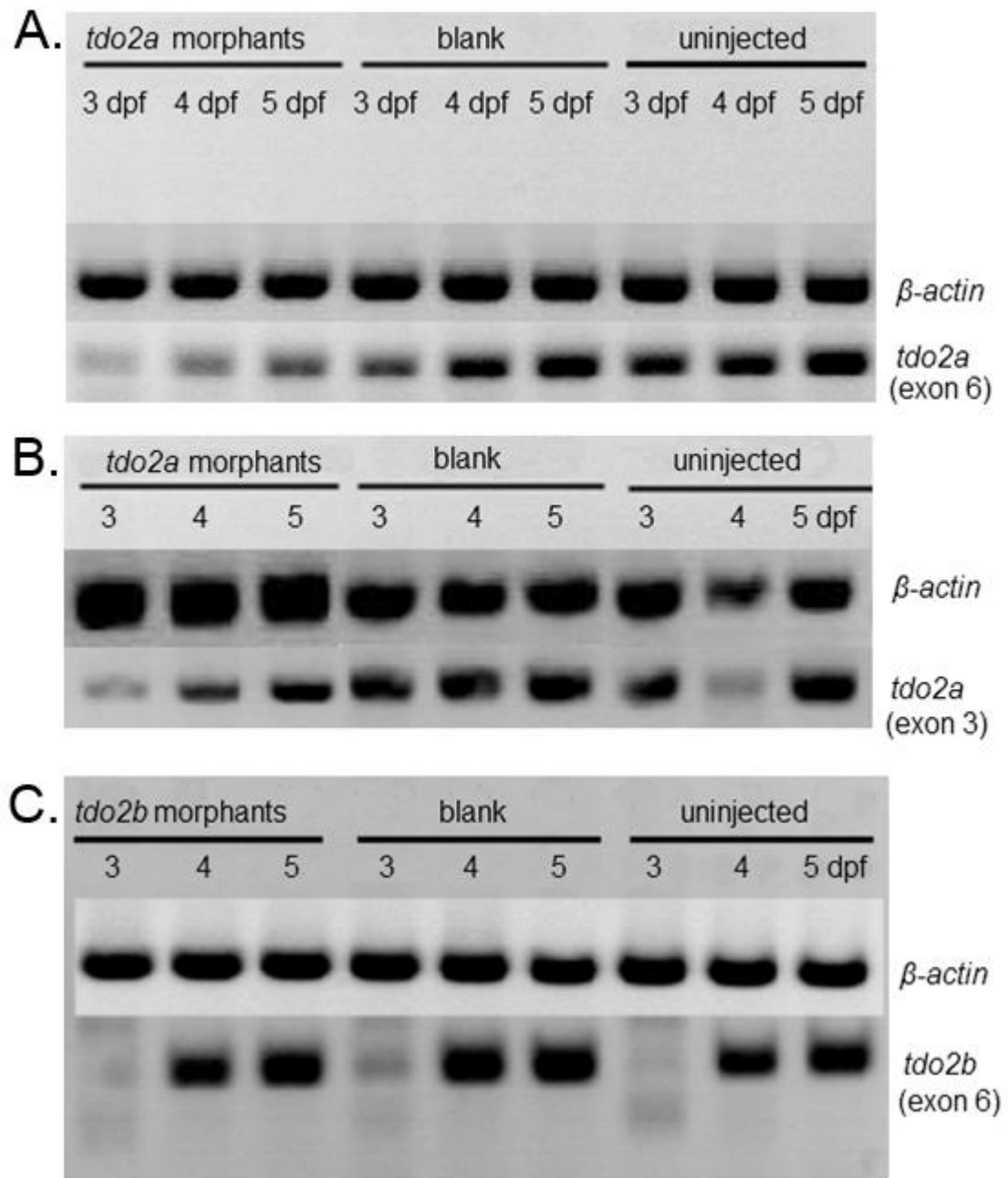


Fig. 3.11. Efficiency of *tdo2a* exon 6 (above), *tdo2a* exon 3 (middle) and *tdo2b* exon 6 (below) knockdown in morphants compared to blank-injected (RNase-free water) and uninjected embryos as assessed by RT-PCR and gel electrophoresis.

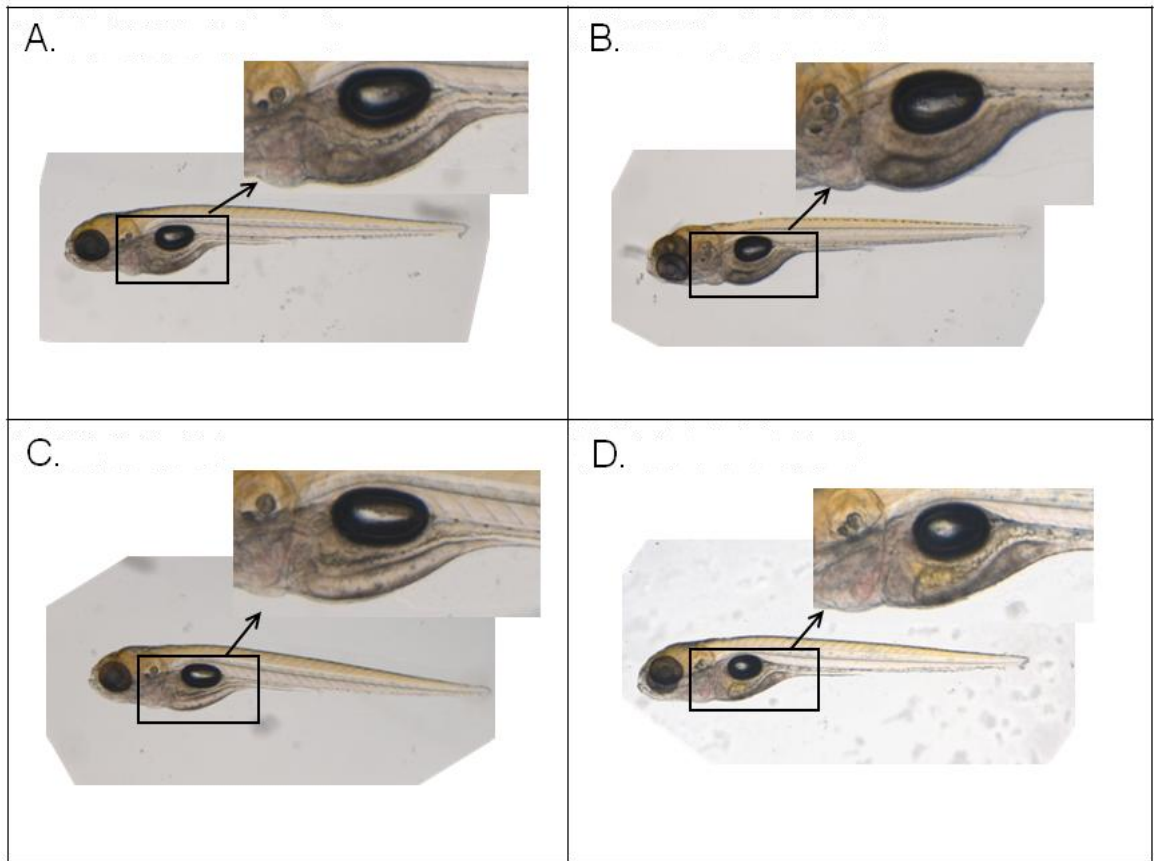


Fig. 3.12. Morphology of *tdo2a* ex 6 (A) and ex 3 (B) morphants compared to blank-injected wild-type (C) and uninjected wild-type (D) embryos at 5 dpf. No specific phenotypes seen in the morphants compared to the controls.

3.4 DISCUSSION

3.4.1 Phylogenetic analysis of tryptophan-catabolising enzymes in aquatic animals.

Ido2 is conserved throughout vertebrate evolution while *Ido1* is present in all mammals and some species of fish and turtle (Yuasa et al. manuscript submitted). *D. rerio* has lost the *Ido1* homologue but possesses an *Ido2* homologue as well as two *Tdo* homologue genes (*tdo2a* and *tdo2b*). Almost all fishes seem to have only one *Tdo* gene, showing higher identity with *tdo2a* than *tdo2b*. As one of the two *A. mexicanus* *tdo* genes is clustered with zebrafish *tdo2b* (Fig. 3.3), gene duplication might have occurred in an ancestor of the teleosts and, similar to *Ido1*, *tdo2b* has been lost in many lineages of fish. However, the unavailability of *tdo* sequences of many other fish species in the database makes it hard to ascertain the timing of the gene duplication. *D. rerio* and *A. mexicanus* are rather closely-related species, so the *tdo* gene duplication might have occurred in their common ancestor.

3.4.2 Enzyme kinetics of the three tryptophan-catabolising enzymes in zebrafish

Although the enzyme kinetics of the zebrafish TDO enzymes have not been determined, in general TDO enzymes, from invertebrates to mammals, possess a high efficiency for catabolising Trp (Yuasa & Ball, in press). In contrast, IDO2 enzymes demonstrate low/moderate efficiency for the catabolism of Trp (K_m of ~50 mM in mouse; K_m of ~30 mM in zebrafish); high efficiency for catabolising Trp, similar to TDO enzymes, has only evolved in mammalian IDO1 enzymes (K_m of ~20 μ M in mouse) (Yuasa et al., 2009; Yuasa et al., 2007); Yuasa et al. manuscript submitted). Although the results from the Kyn assay

(Fig. 1B) show similar quantities of Kyn formation by zebrafish Ido and the Tdo enzymes, this assay was performed over 24 h with a single, high concentration of L-Trp. Thus, while the assay demonstrated that each of the zebrafish enzymes has the capacity to catabolise Trp, it cannot be used to infer the enzyme kinetics of the proteins. Previous studies on the enzyme kinetics of IDO2 enzymes demonstrate that zebrafish Ido has a low efficiency for Trp catabolism compared to mammalian IDO1 enzymes (Yuasa et al, 2009). Although we have not performed a direct comparison, on the basis of these previous studies, we expect that the Trp-catabolising efficiency of zebrafish Ido would also be low compared to the zebrafish Tdo enzymes.

3.4.3 RNA expression onset and distribution of *ido*, *tdo2a* and *tdo2b* in zebrafish

The overlap in the onset of expression and distribution of *tdo2a*, *tdo2b* and *ido* in *D. rerio* is consistent with a collaborative role between the three enzymes, though this remains to be tested. Beginning at 3 dpf, all three genes were expressed in the intestine, although *tdo2b* was localized to the posterior intestine while *tdo2a* and *ido* were expressed throughout the intestine. The localisation of *tdo2b* in the posterior intestine is in agreement with a previous study (Thisse, B., Thisse, C., 2004). Both *IDO1* and *IDO2* have been reported to be expressed in the human intestine (Metz et al., 2007). More recently, we found *Ido2* mRNA in the mouse colon but not in the duodenum (Section 4.3.2). In contrast, *ido* mRNA was detected throughout the intestine in zebrafish.

Both *tdo2a* and *tdo2b* were found in the *D. rerio* liver from 4 dpf onwards, however *ido* was not detected in the liver. These results point to a difference in the expression of Trp-

catabolising genes between mammalian and zebrafish liver. Both *Tdo* and *Ido2* are expressed in the liver of humans and mice (Ball et al., 2007; Ball et al., 2014), whereas in *D. rerio* only *tdo2a* and *tdo2b* were detected in the liver. It is possible that Ido2 enzymes have evolved to have a role in the mammalian liver that does not exist in zebrafish.

3.4.4 Knocking down the expression of *ido*, *tdo2a* and *tdo2b* in zebrafish using the morpholino knockdown approach

3.4.4.1 Knocking down *ido* expression in zebrafish

The morpholino knockdown approach was used to explore the role of *ido* in zebrafish development. Morpholinos produce a transient knockdown of the targeted gene expression and are known to be stable for an average of 3 - 5 days. However, its highest knockdown efficiencies have been noted in the first two days of development (Nasevicius and Ekker, 2000). It is rare for morpholinos to be completely penetrant beyond 2 dpf. Most studies employing the morpholino knockdown approach reveal a phenotype by 3 dpf, although there have been reports of the phenotypes being stable for up to 5 days (Bill et al., 2009; Kloosterman et al., 2007; Nutt et al., 2001). Even if some percentage of knockdown is seen, the subsisting level of target mRNA can still be sufficient to produce protein with biological significance and hence, a normal phenotype may be seen (Eisen and Smith, 2008). Additionally, heterozygous mutations are unlikely to produce phenotypes (Ekker and Akimenko, 2010; Kettleborough et al., 2013). Although the *ido* gene knockdown efficiency in morphants was ~70 % on 3 dpf, this had reduced to 50 % by 4 dpf, suggesting that knockdown efficiency was decreasing and *ido* mRNA production was increasing (Fig. 3.7). In morphants injected with *ido* RNA transcript (rescue),

knockdown efficiency was ~70 % (*i.e.* 30 % of uninjected WT *ido* mRNA levels) on 3 dpf, but on 4 dpf onwards the levels of *ido* mRNA climbed to 70 % of WT RNA expression. These observations seem to indicate that the statistically significant higher mortality seen in *ido* morphants (Fig. 3.8), compared to the rescued morphants and the uninjected embryos, may be due to an off-target effect of the morpholino. There are a few indications that the apparently on-target effect of *ido* loss is likely to be off-target.

First, the significantly higher mortality rate in the morphants relative to rescued morphants and WT uninjected embryos was evident from 1 dpf onwards, a time point at which *ido* was undetectable (Fig. 3.8). This could be an off-target effect of the morpholino that causes increased mortality in the morphants, even at a time *ido* is not expressed. Although this increased mortality was rescueable by injection of *ido* RNA transcript, this does not necessarily indicate the rescue of an on-target effect. The presence of exogenous *ido* RNA could result in the improvement of the general well-being of the embryo that resulted in the reduced mortality in the rescued morphants and not necessarily be due to rescue of an on-target effect.

Secondly, both morpholino only-injected and morpholino + rescue RNA-injected embryos had high knockdown efficiency at 3 dpf and the efficiency of knockdown only diverged at 4 dpf onwards (Fig. 3.7A). In the embryos injected with both *ido* RNA transcript and morpholino, a higher level of *ido* mRNA was detected. Exogenous rescue RNA is suitable for rescuing developmental phenotypes seen in the first 24 to 48 hpf as it degrades within two to four dpf (Bill et al., 2009; Link and Megason, 2008). Therefore, the increasing levels of *ido* mRNA indicates that the knockdown effects are beginning to wear off and the significantly lower mortality rate seen in the rescued morphants is more likely due to

lower levels of morpholino in these embryos to begin with than in the morpholino only-injected embryos. In addition, the level of another gene expressed in the intestine, *tdo2a*, also was reduced (Fig. 3.7B). One could opine that this could be a result of *ido-tdo2a* interaction since both genes code Trp-catabolising enzymes that are expressed in the intestine. However, considering the former argument on the increased mortality even at 1 dpf, this reduction in *tdo2a* gene expression could be a result of an off-target effect that is affecting the development of the intestine. This could explain the gut oedema observed in the morphants.

The final observation that consolidated the finding as likely being an off-target effect was the protruding lower jaw and heart oedema seen in the morphants. These phenotypes are common off-target effects of the neural crest (Eisen and Smith, 2008). The presence of other off-target effects in tissues in which *ido* is not known to be expressed is a cause for concern and further strengthens the likelihood that the increased mortality seen in morphants is an off-target effect. What initially seemed like a 'successful' rescue of morphant phenotype of increased mortality, suggesting *ido* to play a role in the normal development of the embryos, was elucidated to be more likely an off-target effect.

Another morpholino targeting a different exon, 9, of the *ido* gene was also used to obtain knockdown of *ido* expression in zebrafish embryos. The attempt to knockdown the *ido* gene using exon 9 resulted in off-target mortality in all the injected embryos, which were not rescuable by the injection of *ido* RNA transcript (Fig. 3.10A & B). As the off-target effect included general developmental retardation, it was difficult to establish knockdown efficiency in the morphants. *ido* mRNA expression was undetectable in these morphants even from 3 dpf, while being detectable in uninjected and blank-injected zebrafish

embryos (Fig. 3.10E). The expression of *tdo2a* gene also was undetectable in these morphants. Reference gene *β -actin*, which is ubiquitously expressed in all cells and tissues, was measurable in the morphants. This outcome is similar to the morphants injected with *ido* morpholino targeting exon 1, where a knockdown of *tdo2a* also was seen in these morphants (Fig. 3.7B). Although it is possible that *ido* was knocked down efficiently in these morphants and the expression of *tdo2a* is reduced in them because of the effect of Ido deficiency on the intestinal growth or on *tdo2a* expression directly, the failure of *ido* RNA transcript to rescue the morphants suggests that the overall developmental retardation and mortality observed is an off-target effect of the morpholino.

Despite using two morpholinos targeting different exons, we were not able to elucidate the possible role of Ido in zebrafish development due to the various technical challenges encountered.

3.4.4.2 Knocking down *tdo2a* and *tdo2b* expression in zebrafish

When we attempted to knockdown *tdo2a* expression in zebrafish embryos, we were able to achieve a reduction in *tdo2a* expression by microinjection of morpholinos, but yet again we could not completely abolish gene expression. No phenotypic effects were observed as a result of knocking down *tdo2a*. As mentioned previously (Section 3.4.4.1), reduction in mRNA levels does not always translate into an equal reduction in protein levels (Eisen and Smith, 2008) and it is possible that the levels of *tdo2a* mRNA present translated into sufficient Tdo2a enzymatic activity. Alternatively, it is possible that there was loss of Tdo2a activity but either Trp catabolism is not important in embryonic

development or the loss of Tdo2a activity is compensated for by the presence of the other two enzymes. Another morpholino targeting exon five of *tdo2a* also was employed to attempt to knockdown *tdo2a* gene expression. Both these morpholinos were not able to produce sufficient mRNA knockdown to result in a phenotype. Due to the strong expression of *tdo2a* in zebrafish, transient gene knockdown approaches may be unsuitable for studying the role of Tdo2a within the zebrafish. Generating mutant fish lines using the TALENs (transcription activator-like effector nucleases), ZFN (Zinc finger nucleases) or CRISPR (clustered, regularly interspaced, short palindromic repeats)-associated Cas systems may be better alternatives, but there was insufficient time to attempt this during the current project.

The morpholinos targeting *tdo2b* were not successful in knocking down its expression. As the expression of *tdo2b* only appears at 4 dpf onwards, the morpholino approach may be unsuitable for studying the possible role of *tdo2b* in *D. rerio* embryos.

3.5 CONCLUSION

In this work, the different expression patterns of the three Trp-catabolising genes in zebrafish embryos were elucidated. However, knocking down the gene using the morpholino approach rendered misleading off-target effects which posed technical challenges to ascertaining unambiguously the possible role of the three Trp-catabolising genes in lower vertebrates.

These data point to an evident and common complication of using the morpholino approach for knocking down gene expression. Off-target effects of morpholinos are common and often can be misleading (Eisen and Smith, 2008). Even with the use of appropriate controls such as rescue RNA, blank-injected embryos or uninjected WT embryos, there is still a chance that the effects observed are off-target. A possible way to rule out off-target effects would be stringent control of the amount of morpholino delivered per embryo and the use of a number of morpholinos targeting different sites on the target gene. However, the former approach would require a more technologically advanced morpholino delivery system that does not depend on human labour for injections of the embryos, which was not available in the local zebrafish facilities. The latter suggestion, on the other hand, would be laborious and time consuming. Even with the use of multiple morpholinos, off-target effects of the morpholinos cannot be definitively avoided or resolved. In the face of an off-target effect, the remaining choice would be to utilise a different morpholino design targeting a different exon. This approach, unfortunately, could be counterproductive considering that the phenotypical changes seen in the morphants can only be ruled out as being off target after optimising and validating the knockdown itself.

The recent discovery of a double-stranded genome-editing approach, CRISPR could be a promising alternative to morpholino gene knockdown approach (Hwang et al., 2013b; Hwang et al., 2013a). However, this method also has been reported to induce a high level of off-target mutagenesis (Fu et al., 2013). Off-target effects remain a confounding aspect in more than one genome-editing approach in zebrafish. Studies to define parameters that may contribute to off-target effects may help to better refine zebrafish genome-editing approaches. More recently, a software tool to guide the selection of target sequences and validation of on- as well as off-target effects observed was developed (Hsu et al., 2013). This could help reduce the possibility of off-target effects in zebrafish genome-editing studies. Whilst the zebrafish is an excellent experimental model for fundamental localisation, developmental and organogenesis-related research, the limitation of the genome-editing techniques currently available would need to be addressed and overcome to successfully and validly answer pivotal research questions.

CHAPTER 4

EXPRESSION OF IDO2
IN VARIOUS ADULT AND
EMBRYONIC MURINE TISSUES

CHAPTER 4 EXPRESSION OF IDO2 IN VARIOUS ADULT AND EMBRYONIC MURINE TISSUES

4.1 INTRODUCTION

There are three tryptophan-catabolising enzymes that catalyse the first and rate-limiting step in the kynurenine pathway, namely TDO2, IDO1 and IDO2. These three enzymes are regulated by different factors and are expressed in different tissues, despite catalysing the same reaction. In physiological conditions, TDO2 expression is high in the liver (Knox and Auerbach, 1955), whereas IDO1 expression has been detected constitutively in epididymis, colon and placenta, although its expression is mainly induced in inflammatory conditions by IFN γ , TNF and LPS (Higuchi and Hayaishi, 1967; Pfefferkorn et al., 1986b; Yoshida and Hayaishi, 1978; Werner-Felmayer et al., 1990). IDO2 expression, on the other hand, has been reported in the liver and kidney (Ball et al., 2007; Metz et al., 2007).

All three enzymes have been implicated in various types of cancer. Increased TDO2 expression was detected in gliomas and colon, breast, ovarian and lung carcinomas (Opitz et al., 2007), whereas IDO1 expression has been detected in various human tumours such as prostatic, colorectal, pancreatic, ovarian and breast carcinomas as well as in sarcomas, lymphomas and melanomas (Uyttenhove et al., 2003). The existence of IDO2 was first reported in 2007 (Ball et al., 2007; Metz et al., 2007) and to date has been found to be associated with human pancreatic, colon, renal and gastric cancer, as well as in arthritis (Merlo et al., 2014; Witkiewicz et al., 2009; Lob et al., 2009). IDO1 also has been implicated in pregnancy, and is suggested to prevent allogeneic foetal rejection by breaking down Trp (Munn et al., 1998). It was speculated that the catabolism of Trp

resulted in the induction of maternal T-cell tolerance, which prevented allogeneic foetal rejection by inhibiting the expansion of T lymphocyte populations.

The cellular localisation pattern of TDO2 within the liver has not been reported thus far.

On the other hand, IDO1 has been reported to be localised in the columnar epithelial cells in the caput of the epididymis (Dai and Zhu, 2010; Fukunaga et al., 2012). In the digestive tract, IDO1 was detected constitutively throughout most of the tract, with the highest expression of mRNA detected in small intestine (duodenum, jejunum and ileum) (Dai and Zhu, 2010). As assessed by immunohistochemistry (IHC), IDO1 was detected in the lamina propria of villi and the glands in the duodenum, whereas in the jejunum and ileum it was found in the interstitial space of villi or the mucosal layer. The expression of IDO1 in colon and caecum was mainly in the connective tissues between the glands in the mucosal lamina propria (Dai and Zhu, 2010). A predominantly cytosolic localisation of IDO1 in syncytiotrophoblasts in the placenta also has been reported (Dai and Zhu, 2010).

Previously, IDO2 had been described in the epididymis and testes (Ball et al., 2007).

Although TDO2, IDO1 and IDO2 were all expressed in the epididymis, the pattern of cellular localisation differed (Ball et al., 2007; Britan et al., 2006; Dai and Zhu, 2010; Fukunaga et al., 2012). Some information on the possible cellular distribution of IDO2 in the liver, brain, kidney and epididymis also has been reported (Fukunaga et al., 2012).

However, the lack of a definitive negative control in the form of *Ido2*^{-/-} gene knockout mouse liver may have been a disadvantage for ascertaining accurate patterns of IDO2 cellular localisation in previous studies, as will be discussed later in this Chapter. The cellular localisation of TDO2, IDO1 and IDO2 in various tissues is summarised in Table 4.1.

To date, interactions between the expression of TDO2, IDO1 and IDO2 have not been investigated in detail. One observation is that inhibiting TDO2 enzyme activity did not alter kynurenine production by IDO1 (Opitz et al., 2007). There also have been findings indicating that IDO2 expression may be regulated by IDO1, as there were reduced levels of functional IDO2 protein, whilst alternatively-spliced IDO2 protein levels were increased, in the macrophages of *Ido1*^{-/-} mice (Metz et al., 2014). Upregulation of IDO2 in the epididymis of *Ido1*^{-/-} mice also has been reported (Fukunaga et al., 2012). Conversely, IDO1-mediated regulatory T cell generation was impaired in *Ido2*^{-/-} mice, suggesting a possible interaction between the two proteins (Metz et al., 2014). Although skin contact hypersensitivity responses were impaired in both *Ido1*^{-/-} and *Ido2*^{-/-} mice, a reduction in immune regulatory cytokines was only detected in *Ido2*^{-/-} mice, suggesting that despite an interaction between IDO1 and IDO2, there was a difference in the mechanism through which these enzymes effect change in immunity and inflammation (Metz et al., 2014).

Tissue	TDO2	IDO1	IDO2
Epididymis	Spermatozoan head (Britan et al., 2006)	Caput of epididymis (Ball et al., 2007; Britan et al., 2006; Fukunaga et al., 2012) Stereocilia of the apical epithelial epididymal cell (Dai and Zhu, 2010)	Spermatozoan tail (Ball et al., 2007) Caput, corpus and cauda (Fukunaga et al., 2012)
Testes	Intertubular tissue and late differentiating germ cell (Britan et al., 2006)	Undetected in testes (Ball et al., 2007; Britan et al., 2006)	Spermatozoa (Ball et al., 2007)
Liver	Information on cellular localisation of TDO2 has not been reported.	Undetected (Britan et al., 2006; Fukunaga et al., 2012; Dai and Zhu, 2010)	Liver hepatocyte (Fukunaga et al., 2012)
Kidney	Not reported	Localised in the blood vessels (Ball et al., 2007) Smooth muscle layer of small blood vessel (Dai and Zhu, 2010)	Tubules (Ball et al., 2007; Fukunaga et al., 2012)
Brain	Not reported	Cerebral cavity region (Dai and Zhu, 2010)	Purkinje cells of cerebellum cortex and neuronal cells of cerebrum cortex (Fukunaga et al., 2012)
Digestive tract	Not reported	Detected constitutively throughout tract. Highest expression detected in the small intestine (duodenum, jejunum and ileum) (Dai and Zhu, 2010)	Detected in human small intestine and colon (Metz et al., 2007)

Table 4.1. Summary of tissue and cellular distribution of Trp-catabolising enzymes in different tissues.

In embryonic tissues, TDO2 mRNA and protein expression have been observed as early as 5.5 days-post-coitus (dpc) in mouse concepti (embryos and extra embryonic tissues) and this was maintained up to 10.5 dpc. It also was detected strongly from 10.5 to 16.5 dpc in the placenta (Suzuki et al., 2001). In humans, *TDO2* mRNA has been reported in placental explants (Dharane Nee Ligam et al., 2010). However, the role of this enzyme in the placenta remains unknown. The expression of TDO2 in embryonic or neonatal livers has been studied in rat models where it was first detectable only in the liver of 2-week old rats (Franz and Knox, 1967). IDO1 protein has been detected in both human and mouse placenta (Suzuki et al., 2001; Yamazaki et al., 1985). The third enzyme, IDO2, has been reported only at the mRNA level both in human and mouse placenta (Metz et al., 2007; Ball et al., 2009).

Based on these earlier findings of others, we aimed to investigate more thoroughly the cellular localisation of IDO2 within different tissues of wild-type mice. We also were interested in uncovering possible interactions between the three enzymes by looking at mRNA levels of the three genes in different tissues of various single and double gene knockout mouse strains. Additionally, we examined *Tdo2*, *Ido1* and *Ido2* expression in tissues from a murine developmental series, namely the placenta, yolk sac and liver, in order to determine their patterns of expression in relation to the development of the organism.

4.2 METHODS

4.2.1 Mouse strains

C57BL/6 wildtype (WT) was the background strain of mouse used in this project. The mice were acquired from the Australian Animal Resources Centre (Perth, Australia) and were also used as the *Ido1*^{-/-} wildtype-equivalent. *Ido1*^{-/-} mice (back-crossed to C57BL/6J) were obtained from Dr Andrew Mellor (Institute for Molecular Medicine and Genetics, Medical College of Georgia) (Baban et al., 2004). *Ido2*^{-/-} mice, on the other hand, were generated in our laboratory by crossing C57BL/6J mice expressing Cre recombinase (Cre-Tg) under the influence of the Cytomegalovirus (CMV) promoter, courtesy of Prof. R. Harvey (Victor Chang Cardiac Research Institute), with C57BL/6J mice having loxP sites incorporated to either side of the exon 3 of the *Ido2* gene (courtesy of Dr. George Prendergast, Lankenau Institute of Medical Research, Philadelphia, USA). Exon 3 of the *Ido2* gene that was flanked by loxP genes was cleaved under the control of the CMV promoter, causing non-functional IDO2 enzyme production. *Ido2*^{-/-} litters were verified by genotyping.

The *Tdo2*^{-/-} mouse and its equivalent WT controls (*Tdo2*^{+/+}) consist of a mixed genetic background of C57BL/6NCr Slc x DBA/2 and were generated by intercrossing heterozygotes. The heterozygotes were obtained through germ-line transmission of the knockout allele by crossing the F1 male chimaeras (C57BL/6NCr Slc and DBA/2 parents) containing the knockout allele with C57BL/6NCr Slc females, and were obtained courtesy of Toshikazu Nakamura and Hiroshi Funakoshi (Kanai et al., 2009).

Outbred wild-type QS strain mice were courtesy of Dr Stuart Fraser (Department of Physiology, The University of Sydney).

All mice, with the exception of wild-type C57BL/6J, were bred in the Medical Foundation Building, The University of Sydney. They were housed two to five mice per cage under a 12 hour light-dark cycle with food and water available *ad libitum*.

For immunohistochemistry (IHC), liver, kidney, brain, epididymis, testes and colon tissues were collected from 8-week-old *Ido2*^{-/-} mice and the equivalent wild-type animals.

Assessment of mRNA expression in a developmental series was performed using embryos, neonates and adult tissues of outbred QS and inbred Cre transgenic mice. To study the possibility of interaction between the three genes for Trp-catabolising enzymes, the expression levels of these genes were studied in mice with single genes knocked out, *Ido1*^{-/-}, *Ido2*^{-/-} and *Tdo2*^{-/-}, alongside two double gene knockout strains (*Ido1*^{-/-} *Tdo2*^{-/-} and *Ido2*^{-/-} *Tdo2*^{-/-}) that were generated by Dr Helen Ball in the laboratory. The mRNA analysis was performed in these single and double gene knockout strains alongside their equivalent wild-type strains as shown in Table 4.2.

All studies were carried out in accordance with the New South Wales legislation governing research with animals. The protocols were approved by the University of Sydney Animal Ethics Committee.

Knockout strain	Wild-type equivalent
<i>Ido1</i> ^{-/-}	C57BL/6J
<i>Ido2</i> ^{-/-}	Transgenic <i>Ido2</i> ^{+/+} with Cre-loxP system (C57BL/6J). Also referred to as Cre-Tg.
<i>Tdo2</i> ^{-/-}	<i>Tdo2</i> ^{+/+} (DBA x C57BL/6NCr Slc)
<i>Ido1</i> ^{-/-} <i>Tdo2</i> ^{-/-}	<i>Ido1</i> ^{+/+} <i>Ido2</i> ^{+/+} <i>Tdo2</i> ^{+/+}
<i>Ido2</i> ^{-/-} <i>Tdo2</i> ^{-/-}	

Table 4.2. shows the list of knockout strains with their wild-type equivalents used for mRNA assessment of Trp-catabolising gene expression

4.2.2 Tissue collection and homogenisation

For the assessment of gene and protein expression in adult mice, tissues were collected from two, three and eight-week-old mice. For the study of gene expression in a developmental series, tissues were collected from murine embryos of outbred QS and inbred *Ido2*^{+/+} strains. Embryonic tissues such as the yolk sac and liver, as well as placenta, were collected at E12.5, E16.5, E17.5 and E18.5 dpc whereas neonatal tissues were from P1, P2, P3 and P7 neonates, *i.e.* days 1, 2, 3 and 7 post-partum. Tissues were collected in 2 mL screw-cap tubes and snap-frozen immediately in liquid nitrogen. These were stored at -80°C until processing.

On the day of homogenisation, tissues were transferred into liquid nitrogen flasks, where they were kept until they were homogenised. Tissues were transferred from the 2 mL screw cap tubes into 2 mL tubes, where 500 to 1000 µL of PBS was added to the tissue (depending on the tissue size) and homogenised using a Polytron Tissue homogeniser (PT 2100) for about 20 sec or until they were fully homogenised. Homogenates were immediately placed on ice. Subsequently, 30 µL of the homogenate was added to 350 µL RNA Lysis Buffer from the ISOLATE II RNA Mini Kit (BIOLINE). Another 400 µL of the tissue homogenate was added to another tube with an equal volume of 2X RIPA buffer for protein extraction. The remaining homogenate was aliquoted into separate tubes for other uses. All aliquots were kept frozen at -80 °C until further processed.

4.2.3 RNA extraction

RNA extraction and cDNA synthesis was performed as described previously in Chapter 2 with the exception that the RNA extraction was done using the BIOLINE ISOLATE II kit, according to the manufacturer's protocol (Jusof et al., 2013).

4.2.4 Protein extraction

An equal volume of tissue homogenate was added to 400 μ L of 2X RIPA buffer containing 50 mmol/L Tris pH 7.4, 150 mmol/L NaCl (Sigma Aldrich), 1 mmol/L EDTA (Sigma Aldrich), 1% v/v Triton X-100, 1 % w/v sodium deoxycholate (Sigma Aldrich), 0.1 % w/v sodium dodecyl sulphate (SDS) and 1:100 protease inhibitor (Sigma Aldrich) and allowed to sit on ice (4 °C) for 30 min, after which the solution was spun down at 16000 rcf at 4 °C for 15 min. The supernate was pipetted into new, clean 1.5 mL microcentrifuge tubes whereas the pellet was discarded.

4.2.5 Anti-IDO2 antibody specificity

Anti-IDO2 antibodies were obtained either commercially or from other laboratories studying IDO2. Rabbit polyclonal anti-IDO2 antibodies were obtained from Dr. Ursula Grohmann from the University of Perugia, Italy, as well as Prof. Yasuko Yamamoto from the University of Kyoto, Japan. In addition to the rabbit polyclonal anti-IDO2 antibody generated by Genscript, NJ, USA (Ball et al, 2007), two commercial anti-IDO2 antibodies were purchased from Santa Cruz Biotechnologies, one mouse monoclonal and a rabbit

polyclonal antibody. The specificity of these antibodies was tested on liver protein lysates from *Ido2*^{+/+} and *Ido2*^{-/-} mice by Western blotting.

4.2.6 SDS-PAGE and Western Blotting

Concentration of protein in the lysates was determined by bicinchoninic acid (BCA) protein assay (Pierce, IL, USA), according to the manufacturer's instructions. Once determined, the concentration of the protein was standardised to 5 µg/µL by the addition of water, before an equal volume of 2X loading buffer was added to the lysates. This was placed on a heating block at 95 °C for 2 min and 10 µL (25 µg) was transferred onto the wells of 10 % w/v SDS-Polyacrylamide Electrophoresis gels. The samples were run alongside 2 µL of pre-stained protein ladder (Pierce Life Technologies) on a MiniGel Tank in 1X Tris-Glycine-SDS electrophoresis buffer at 100 V for 110 min or until the dye front reached the bottom of the gel. The protein bands on the gel were transferred onto polyvinylidene difluoride membrane (GE Healthcare), before the membrane was incubated in 4 mL of primary antibodies (0.2 µg/mL) overnight. This was followed by 1 h incubation in 1:4000 secondary antibody (IRDye, Li-Cor) wrapped in foil. Every incubation was followed by 3 washes of the membrane in PBS with 0.1 % v/v Tween 20. The density of bands on the membrane was read on an Odyssey Infrared Imaging System (LI-COR Biosciences).

4.2.7 Immunoprecipitation and Western Blot

To every tube, 50 μL of Protein A was added and the solution was rotated at 4 $^{\circ}\text{C}$ for 1 h, before spinning down at 6000 rcf for 3 min. The supernates were retained and frozen at -80 $^{\circ}\text{C}$ until further analysis. For immunoprecipitation, Protein A was first equilibrated by spinning tubes at 6000 rcf for 3 min (40 μL of Protein A per sample). The supernate was discarded and the pellet was resuspended in 100 μL of 1X RIPA buffer (per sample). Protein lysates (200 μL) were added to 100 μL of Protein A, with 2.5 μg of IDO2 antibody. These samples were prepared alongside controls with no anti-IDO2 or an irrelevant mouse IgG antibody. The preparations were rotated overnight at 4 $^{\circ}\text{C}$ before they were spun at 6000 rcf for 3 min at 4 $^{\circ}\text{C}$. The supernates were carefully removed and the pellet was resuspended in 1 mL cold 1X RIPA buffer. This wash step was repeated twice before the pellets were finally resuspended in 1X Loading buffer and run on an SDS-PAGE gel. The antibody used for detection in the Western Blot was a different anti-IDO2 antibody, raised in a different animal species.

4.2.8 Immunohistochemistry on formalin-fixed mouse tissues using the M.O.M.

ImmPRESS system

The sections of formalin-fixed tissue were stored at 4 °C. The sections were deparaffinised by immersing them twice in xylene for 10 min each, followed by immersion in decreasing concentrations of ethanol (absolute, 95 % x 2, 70 % v/v) for 2 min each. Finally the slides were immersed in water for 2 min. Upon deparaffinisation, antigen retrieval was performed by incubating the slides in 600 mL of 0.2 mol/L citrate buffer pH 6.0 (Sigma Aldrich) at 90 ° to 95 °C for 12 min. The beaker was left to cool for 20 min in a water bath before slides were washed in 50 mmol/L TRIS-buffered saline with 0.1 % v/v Tween-20 (TBS-T) for 2 min. All subsequent washes were performed for 2 min with TBS-T unless mentioned otherwise. Peroxidase blocking was performed thereafter with 3 % v/v hydrogen peroxide (H₂O₂) in methanol for 5 min. After the slides were washed, peptide blocking was performed using Mouse on Mouse (M.O.M.) blocking reagent (Vectorlabs) for 30 min. Slides were then washed twice, and incubated with 2.5 % v/v normal horse serum (NHS) for 5 min. Primary IDO2 antibody (Santa Cruz Biotechnology) at a final concentration of 1 µg/mL, prepared in 2.5 % v/v NHS, was added to each section and incubated in a humidified container at 4 °C overnight. The next morning, the sections were washed twice before the Vector M.O.M.™ ImmPRESS reagent (Vectorlabs) was added to the sections and incubated for 10 min. Sections were then washed twice for 5 min. Dinitrophenyl (DNP) amplification reagent from the TSA™ DNP (HRP) System (Perkin Elmer) was prepared in DNP amplification reagent (from the kit) in a 1:50 v/v dilution . This was added to the sections and incubated for 5 min. Sections were washed thrice with agitation before 1:100 v/v anti-DNP-HRP (from the kit), diluted in TNB blocking

reagent, was added prior to incubation for 20 min. Sections were washed thrice with agitation before diaminobenzidine (DAB) substrate (Dako) was added and the sections incubated for 4 to 8 min (depending on the tissue type). After thorough rinsing in water, sections were stained using haematoxylin for about 2 min, subsequently washed in water, and dipped briefly in acetone before they were counterstained in Scott's blue stain. The slides were brought through an ascending concentration of ethanol (75 %, 90 % v/v and absolute ethanol for 30 sec each) and finally dipped in Histolene (2 min in each solution) before they were coverslipped and observed. All washes were performed with TBS-T for 2 min. Stained surface area and nuclei count were quantified using the MetaMorph software (Molecular Devices), after which Student's t-test was used to ascertain statistical significance using GraphPad Prism.

During the optimisation of the IHC method, various different antigen retrieval approaches were used including the pressure cooker method and water bath on a hotplate method for fixed sections with the former not being optimal for IDO2 antigen retrieval. Staining on frozen sections also was attempted. However, this method had high background staining. Despite the different approaches used, only the hotplate antigen retrieval method on formalin-fixed sections, followed by IHC with Vector M.O.M. complemented with TSA strategy yielded positive signals. Therefore, this method was used subsequently to study IDO2 expression in different tissues.

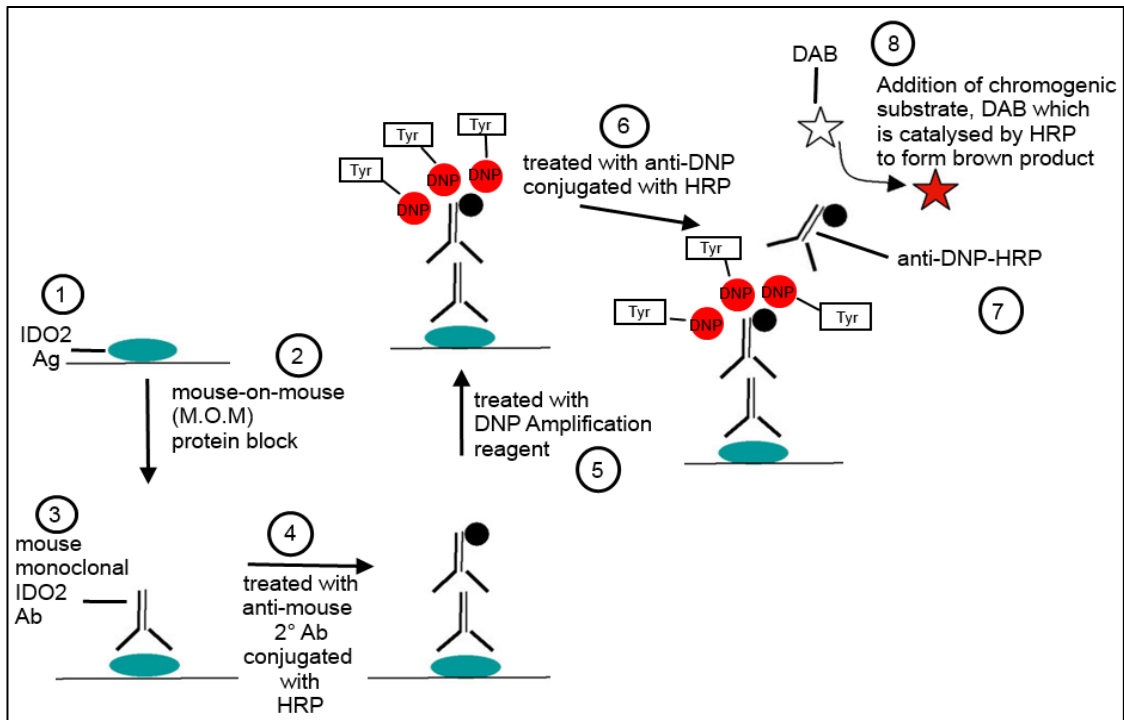


Figure 4.2. Protocol flow of IDO2 protein localisation in tissues by IHC using the Vector M.O.M. ImmPRESS kit. DNP, dinitrophenyl; Tyr, Tyramide; HRP, horse radish peroxidase; DAB, diaminobenzidine

4.2.9 Immunofluorescence

Prior to seeding with cells, Nunc 8-well permanox slides were coated with 300 μL of Poly-D-lysine (Sigma Aldrich, 25 $\mu\text{g}/\text{mL}$) and allowed to dry overnight. The next day, DNA-lipofectamine complexes were prepared in the transfection medium OPTIMEM (GIBCO) according to the ratio 80 μL OPTIMEM : 0.33 μL Lipofectamine 2000 (Invitrogen) : 0.5 μg plasmid DNA per reaction. Once the complexes had formed for 15 to 20 min, they were added to the wells – approximately 75 $\mu\text{L}/\text{well}$. A total volume of 225 μL Human Embryonic Kidney (HEK) cells at a concentration of 5×10^5 cells/mL was added to each well and swirled gently. The cells were incubated overnight to allow attachment before immunofluorescence was performed. The medium was then removed and cells were washed with 200 μL of PBS before fixation in 200 μL of 4 % v/v paraformaldehyde for 15 min. The cells were then permeabilised with 0.2 % v/v Triton-X100 (Packard Instruments) in PBS for 5 min. Protein blocking was done using 5 mg/mL BSA in PBS for 1 h. Primary antibody prepared in PBS was added to each well and incubated for 60 to 90 min. Double 5 min washing steps preceded incubation with 90 min Alexa 488 secondary antibody prepared at a concentration of 1:1000. Washing was performed similarly to the previous washing step but the chambers were incubated in the dark. The silicon beading that fastens the chamber to the slide was pulled off and chamber edges were squeezed to lift them from the surface of the slide. The gasket was gently peeled off. As much liquid as possible was removed without disturbing the cells. Finally, slides were treated with three drops of Fluoroshield mounting medium with DAPI (Sigma Aldrich) and coverslipped. The slides were refrigerated, wrapped in foil. Images were captured on a Zeiss LSM 510 Confocal Microscope at the Advanced Microscopy Facility of the Bosch Institute. Pinhole

size, detector gain, amplifier gain and amplifier offset were all standardised for each probe.

4.2.10 RT-qPCR using the standard curve method

Expression of *Ido2* was determined by the standard curve method, with normalisation to the *Ywhaz* reference gene for adult tissues and *Rpl13a* for tissues from the developmental series. These genes have similar amplification efficiencies, as assessed using serial dilutions of cDNA, and the purity of the PCR products was assessed by melting curve analysis. For the standards, cDNA for *Ido1*, *Ido2*, *Tdo2*, *Ywhaz* and *Rpl13a* genes were cloned into plasmid. Standards were serially diluted and amplified products from test samples were plotted against the standard curve to determine the relative amounts of genes of interest in the test samples.

The RT-qPCR reaction (20 µL) contained 8 µL cDNA, 0.1 µmol/L of each primer in 1x KAPA SYBR Fast Universal qPCR Master Mix (KP-KK4602). Amplification was performed in a Rotorgene 3000 (Corbett Research) with (40 cycles of 95 °C for 15 sec followed by 60 °C for 45 sec). Initially, the reference gene that was used for assessment of gene expression in tissues of murine developmental series was *Ywhaz*. However, a high variability was seen between samples. *Rpl13a* was tested and deemed to be a better reference gene for studies of embryonic tissues due to greater consistency in copy number across tissue types and age.

The primers for *Tdo2*, *Ido1*, *Ido2*, *Ywhaz* and *Rpl13a* are listed in Table 4.3.

<i>Ywhaz</i>	5' TGTCACCAACCATTCCAACCTG 3' 5' AACTGAGTGGAGCCAGAAAGA 3'
<i>Rpl13a</i>	5' CTTAGGCACTGCTCCTGTGGAT 3' 5' GGTGCGCTGTCAGCTCTCTAAT 3'
<i>Tdo2</i>	5' CTATGAGTGGGTGCCGTTT 3' 5' CACTCTGAAGTTCTTGCGCATT 3'
<i>Ido1</i>	5' AGATGAAGATGTGGGCTTTGCT 3' 5' GGCAGATTTCTAGCCACAAGGA 3'
<i>Ido2</i> (To detect transcript coding for full length protein)	5' CAAAGTCAGAGCATGACGCTG 3' 5' CGCTGCTCACGGTAACTCTTTA 3'
<i>Ido2</i> (detects C-terminus of the gene)	5' CTACATGCCGCCTTCCCATA 3' 5' AGGACCAGAGGCCAGTATGT 3'

Table 4.3. Primer sequences of genes coding Trp-catabolising enzymes and reference genes.

4.3 RESULTS

4.3.1 Detection of IDO2 protein in murine liver and kidney tissues using anti-IDO2 antibodies

In order to find a suitable antibody for the study of IDO2 protein localisation in various tissues by IHC, 5 different anti-IDO2 antibodies were tested by Western Blot on liver lysates. The rabbit polyclonal anti-IDO2 antibody from Santa Cruz Biotech (SC-292212) detected a specific IDO2 protein band at the expected band position (~44 kDa) in the wild-type liver lysates that was not present in the liver lysates of the *Ido2*^{-/-} mice (Fig. 4.3AIII). However, this antibody also detected non-specific protein bands at 50 and 85 kDa that were present in both the wild-type and *Ido2*^{-/-} liver lysates. The mouse monoclonal anti-IDO2 antibody, on the other hand, detected a single band at ~45kDa (Fig. 4.3 A-D II, which is the estimated molecular weight of IDO2 protein (Ball et al., 2007). This was present in the wild-type liver lysate but not in the corresponding *Ido2*^{-/-} lysate (Fig. 4.3AI, II). The rabbit polyclonal anti-IDO2 Ab generated by Genscript, NJ, USA (Ball et al., 2007) detected a faint band at the expected protein band location in the wild-type liver lysate but not in that of *Ido2*^{-/-} mice (Fig. 4.3BIII). However, this antibody also detected a band of a similar molecular weight to IDO2 in *Ido2*^{-/-} kidney lysates. Unexpectedly, a protein band at the position of 85 kDa was detected in both wild-type and *Ido2*^{-/-} liver lysates by the rabbit polyclonal anti-IDO2 antibody from Italy (Fig. 4.3CIII). Finally, the anti-IDO2 antibody from Prof Yasuko Yamamoto, Japan, detected a protein band at the approximate location of ~45 kDa. However, this band was present in both the wild-type and *Ido2*^{-/-} liver lysates, suggesting that the band detected is a cross-reacting protein with a similar molecular weight to that of IDO2 (Fig. 4.3DIII).

Mouse monoclonal anti-IDO2 antibody (Santa Cruz Biotech), the most specific and robust anti-IDO2 antibody of the 5 that were tested, was used to assess the presence of IDO2 protein in kidney lysates. No protein band of IDO2 was detected in wild-type or *Ido2*^{-/-} kidney lysates (Fig. 4.4) immunoprecipitated with rabbit polyclonal anti-IDO2 antibody (Genscript, NJ, USA, generated for Dr Helen Ball), despite the positive detection of IDO2 protein in the immunoprecipitated liver lysates (positive control).

Fig 4.3. Detection of IDO2 protein in liver of *Ido2*^{+/+} mice using 5 different anti-IDO2 antibodies. The first column is the combined image with both red and green detection system (AI, BI, CI and DI). The red channel (AII, BII, CII and DII) represents detection using mouse monoclonal anti-IDO2 antibody (Santa Cruz Biotech.) **AIII.** Green channel shows detection by rabbit polyclonal anti-IDO2 Ab (Santa Cruz). **BIII.** Green channel shows detection by rabbit polyclonal anti-IDO2 Ab from the Hunt laboratory (Ball et al., 2007). **CIII.** Green channel is rabbit polyclonal anti-IDO2 Ab from Dr. Ursula Grohmann, University of Perugia, Italy. **DIII.** Green channel shows detection by anti-IDO2 rabbit polyclonal antibody from Prof. Yasuko Yamamoto of the University of Kyoto, Japan. Lanes 1-3 are protein lysates from *Ido2*^{+/+} liver from 3 individual mice, whereas lanes 4-6 represent protein lysates from *Ido2*^{-/-} liver of 3 individual mice. Lane 7 is immunoprecipitated protein lysate from *Ido2*^{+/+} mouse (Images A, B and C) whereas Lane 8 is immunoprecipitated *Ido2*^{-/-} mouse liver lysate (Images A, B and C). In D, Lane 7 is immunoprecipitated *Ido2*^{-/-} mouse liver lysate whereas Lane 8 is immunoprecipitated protein lysate from *Ido2*^{+/+} mouse. Lane L shows 120 kDa pre-stained protein ladder (Pierce, ThermoFisher). Arrow indicates the expected IDO2 protein band (~44 kDa).

Figure on the next page



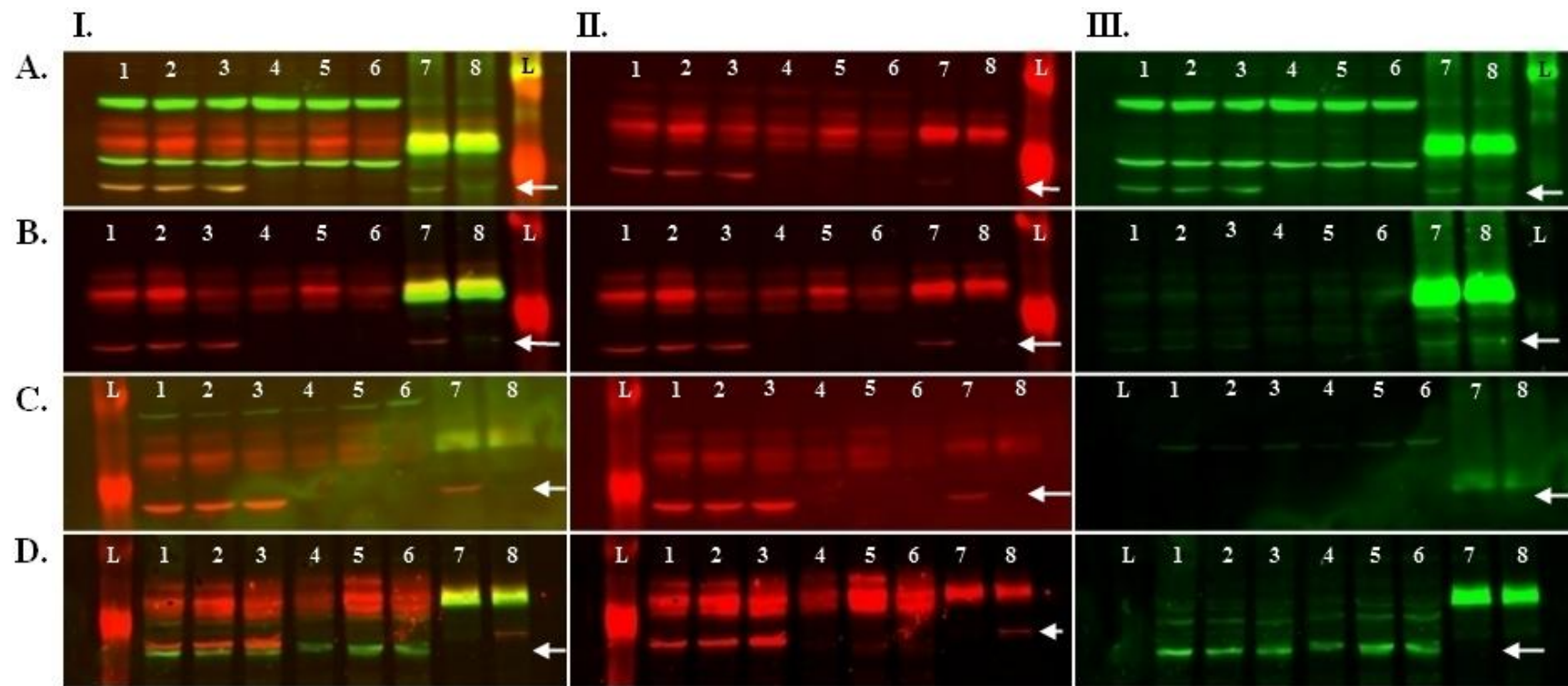


Fig. 4.3

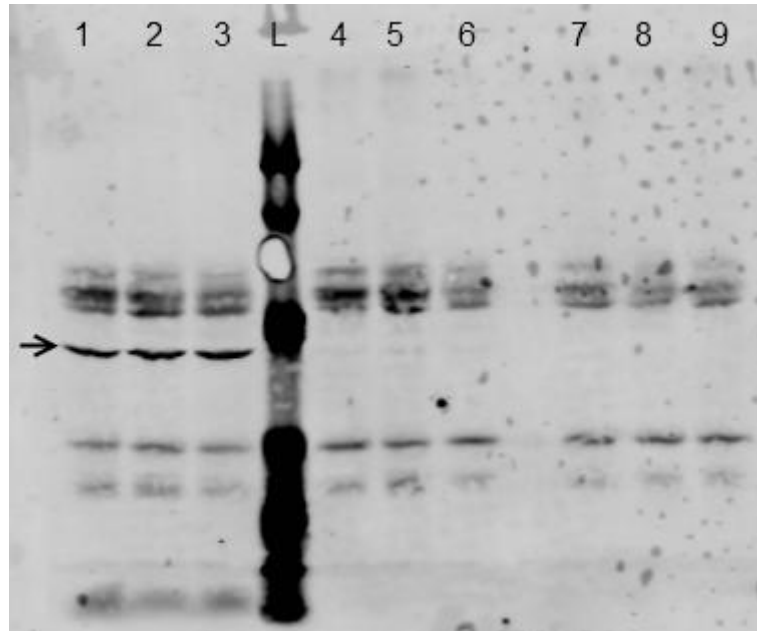


Fig 4.4. Expression of IDO2 protein in kidney lysates of *Ido2*^{+/+} (wild-type) and *Ido2*^{-/-} mouse. Specific IDO2 protein bands were detected in immunoprecipitated-protein *Ido2*^{+/+} mouse lysates from liver of 3 individual mice (lanes 1-3), whereas no bands were detected in immunoprecipitated protein lysates from *Ido2*^{+/+} mouse kidney (n=3) lanes 4-6 and *Ido2*^{-/-} mouse kidney lysates (n=3) lanes 7-9. Lane L shows 120 kDa pre-stained protein ladder (Pierce, ThermoFisher) with the arrow indicating the expected IDO2 protein band (~44 kDa). Mouse monoclonal anti-IDO2 antibody (Santa Cruz Biotech) was used for detection.

4.3.2 IDO2 protein localisation in murine tissues

The mouse monoclonal anti-IDO2 antibody was subsequently used to study the localisation of IDO2 protein in various murine tissues by immunohistochemistry (IHC). This was carried out using a staining system (Vector M.O.M. ImmPRESS kit) specialised for the detection of proteins in mouse tissues using mouse monoclonal antibodies.

In the liver, IDO2 protein appeared to be localised around the nuclei of the hepatocytes (Fig. 4.5). Though not all the nuclei were stained with a similar intensity, a significantly higher number ($p < 0.005$) of hepatocyte nuclei was stained in the wild-type liver compared to *Ido2*^{-/-} mouse liver tissue. The average nuclei surface area that was stained in the wild-type liver tissue was also significantly higher ($p < 0.001$,) than that in *Ido2*^{-/-} liver sections (Table 4.4).

When kidney tissues were analysed, no specific staining was seen in the wild-type sections, although faint non-specific staining was seen in the tubular cells of the kidney in both the wild-type and *Ido2*^{-/-} mouse tissue sections (Fig. 4.6). Staining was seen in what appears to be neuronal projections in the cerebral cortex in the wild-type mouse tissue, and this was absent in the isotype control-stained wild-type tissues (Fig. 4.7).

However, the presence of a similar staining pattern and localisation in the cerebral cortex hemisphere of an *Ido2*^{-/-} mouse brain section indicates that this is likely to be a result of non-specific staining. Similarly, in the colon, non-specific staining in the goblet cells along the intestinal mucosal layer was seen in both wild-type and *Ido2*^{-/-} mouse tissues and this was absent in the isotype control-stained tissues (Fig. 4.8). Despite low levels of IDO2 mRNA transcript being detected in testes, no specific protein staining was seen in wild-

type mouse testis sections by IHC (Fig. 4.9). A non-specific staining of the differentiating germ cells was seen both in wild-type and *Ido2*^{-/-} testes.

IDO2 mRNA was detected in substantial amounts in the epididymis. However, the epididymis showed no specific staining for IDO2 protein in this tissue (Fig. 4.10). Histology showed smaller epididymal tubules and scarcer levels of spermatozoa within the tubules in the *Ido2*^{-/-} mice compared to the equivalent wild-type animals (Fig. 4.10).

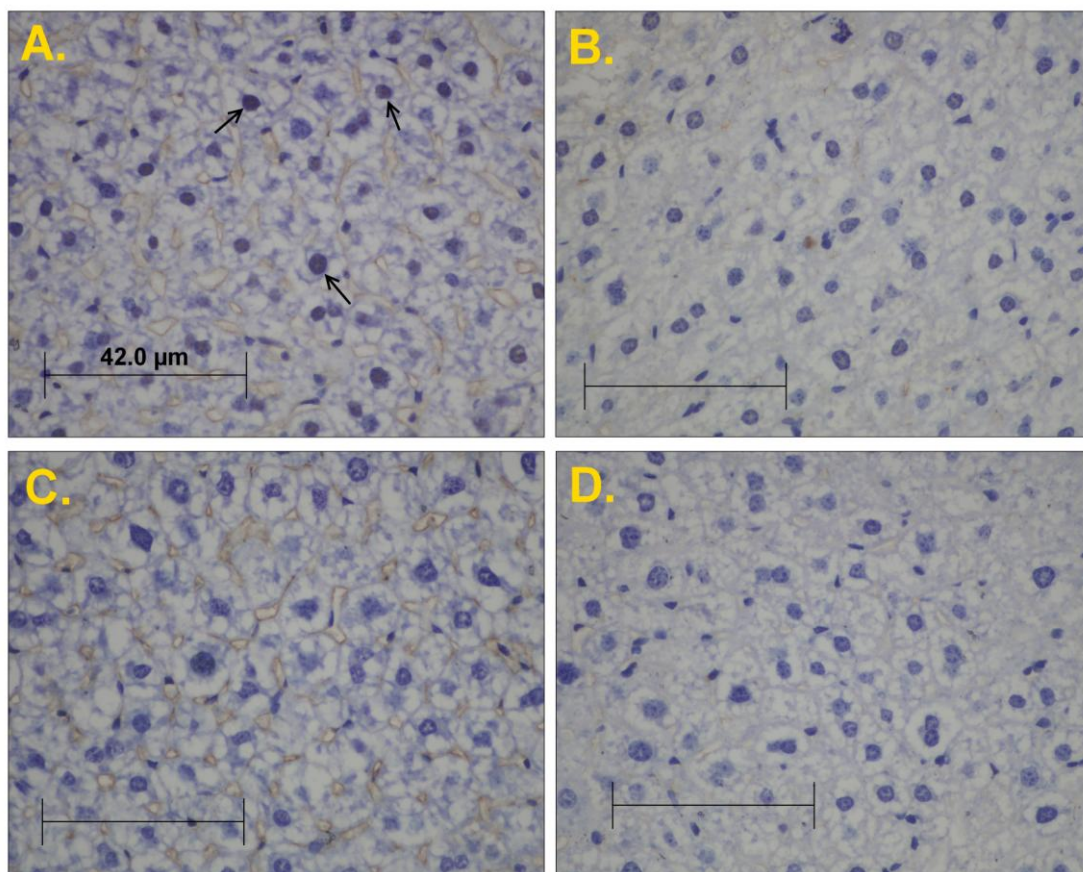


Fig. 4.5 Localisation of IDO2 protein in mouse liver. Representative image of IDO2 protein detected around the nuclei of hepatocytes in *Ido2*^{+/+} mouse liver sections (A) whereas no staining was seen in *Ido2*^{-/-} (B) when treated with mouse monoclonal anti-IDO2 antibody. No staining was seen in *Ido2*^{+/+} (C) and *Ido2*^{-/-} (D) liver sections treated with monoclonal IgG_{2A} isotype control antibody. Scale bars represent 42.0 μm.

Liver section	<i>Ido2</i> ^{+/+}	<i>Ido2</i> ^{-/-}	p-value
Average stained surface area	1731 ± 104	108 ± 108	Significant, 0.0004
Count	13 ± 2	0.0 ± 0.0	Significant, 0.0038

Table 4.4. Stained nuclei count and average surface area in livers of *Ido2*^{+/+} and *Ido2*^{-/-} mice showed a significantly higher number of stained nuclei and average stained surface area in *Ido2*^{+/+} liver than in the knockout. All values in arbitrary units. n=3 in each group with 6 random fields of view counted from each wild-type mouse liver section and 4 random fields of view from each *Ido2*^{-/-} liver section.

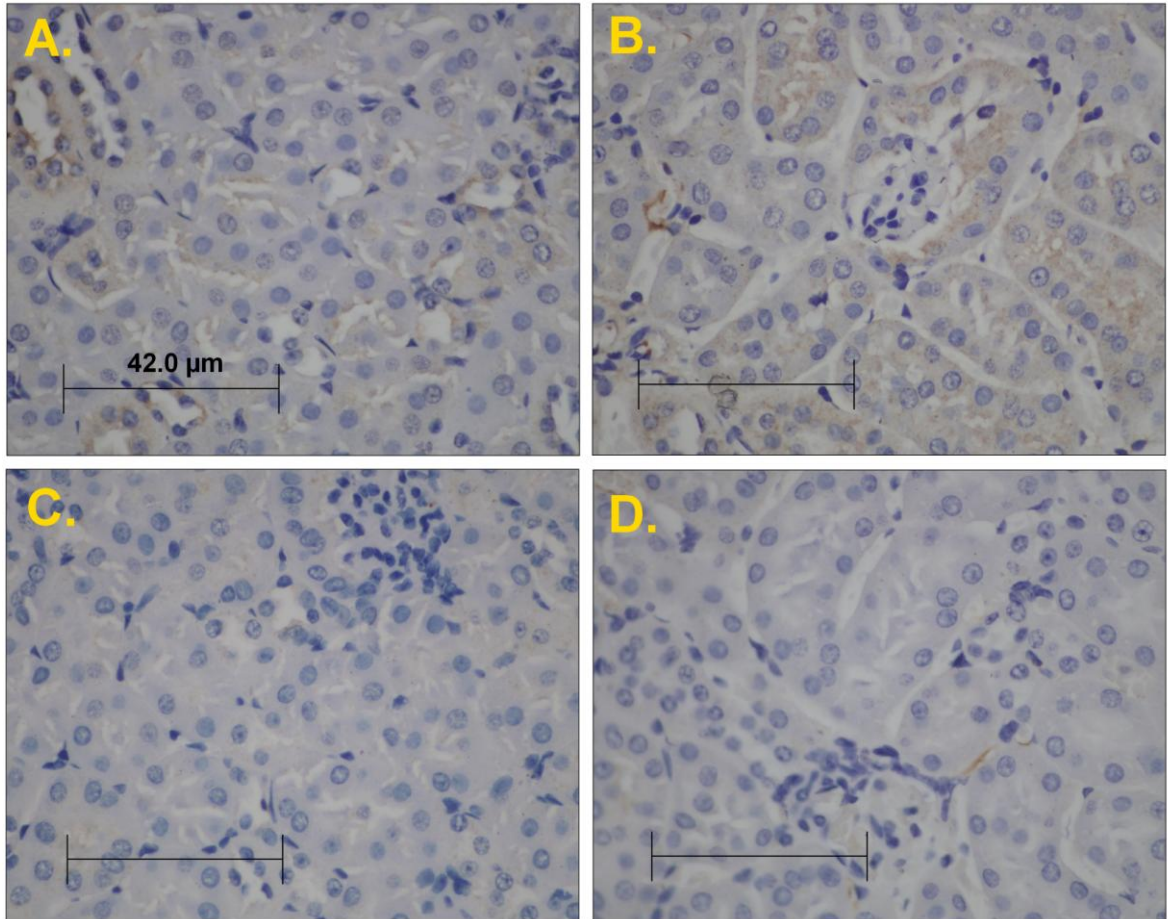


Fig. 4.6. Representative image of kidney sections stained with anti-IDO2 mouse monoclonal antibody. No specific staining seen in *Ido2*^{+/+} mouse (A) or *Ido2*^{-/-} mouse (B) kidney sections treated with mouse monoclonal anti-IDO2 antibody or in *Ido2*^{+/+} (C) and *Ido2*^{-/-} (D) mouse kidney sections treated with monoclonal IgG_{2A} isotype controls. Scale bars represent 42.0 μm.

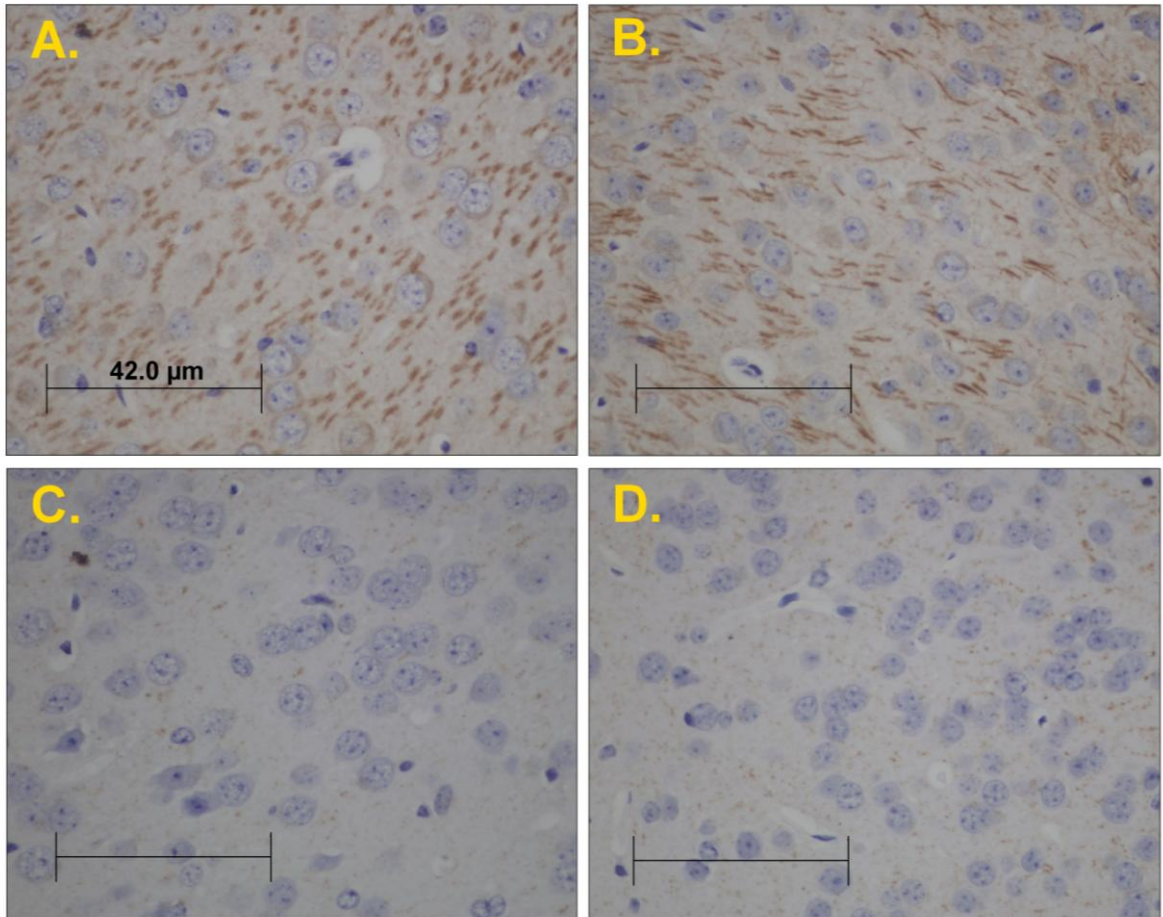


Fig. 4.7. Representative image of brain sections stained with anti-IDO2 antibody.

Non-specific staining seen in *Ido2*^{+/+} sections (A) and *Ido2*^{-/-} (B) treated with mouse monoclonal anti-IDO2 antibody. No staining seen in *Ido2*^{+/+} (C) and *Ido2*^{-/-} (D) brain sections treated with monoclonal IgG_{2A} isotype controls. Scale bars represent 42.0 μm.

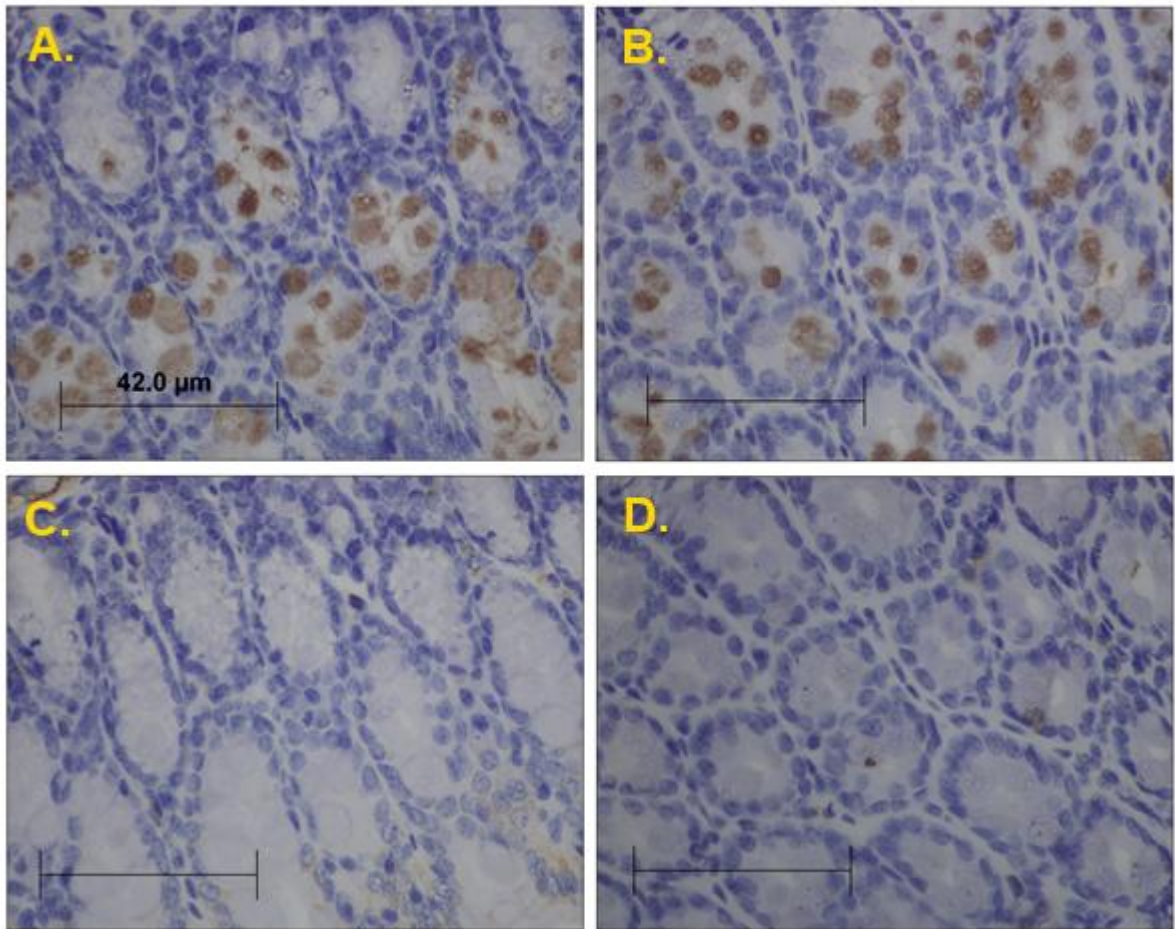


Fig. 4.8. Representative image of colon sections stained with anti-IDO2 antibody.

Non-specific staining seen in *Ido2*^{+/+} mouse (A) and *Ido2*^{-/-} mouse (B) colon sections treated with mouse monoclonal anti-IDO2 antibody. No staining seen in *Ido2*^{+/+} (C) and *Ido2*^{-/-} (D) colon sections treated with monoclonal IgG_{2A} isotype controls. Scale bars represent 42.0μm.

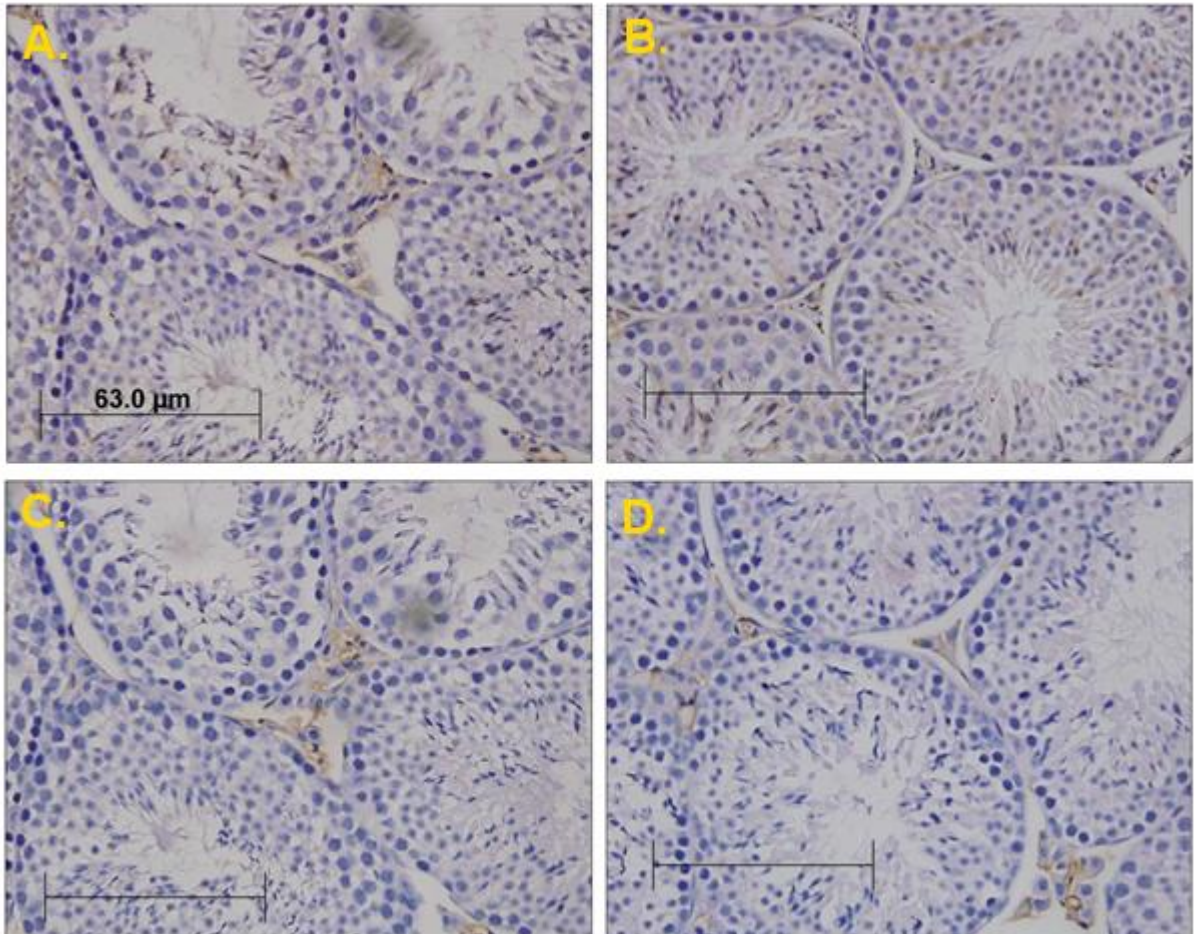


Fig. 4.9. Representative image of testis sections stained with anti-IDO2 antibody.

Non- specific staining seen in *Ido2*^{+/+} sections (A) and *Ido2*^{-/-} (B) testis sections treated with mouse monoclonal IDO2 antibody. No staining seen in *Ido2*^{+/+} (C) and *Ido2*^{-/-} (D) testis sections treated with monoclonal IgG_{2A} isotype controls. Scale bars represent 63.0 μm.

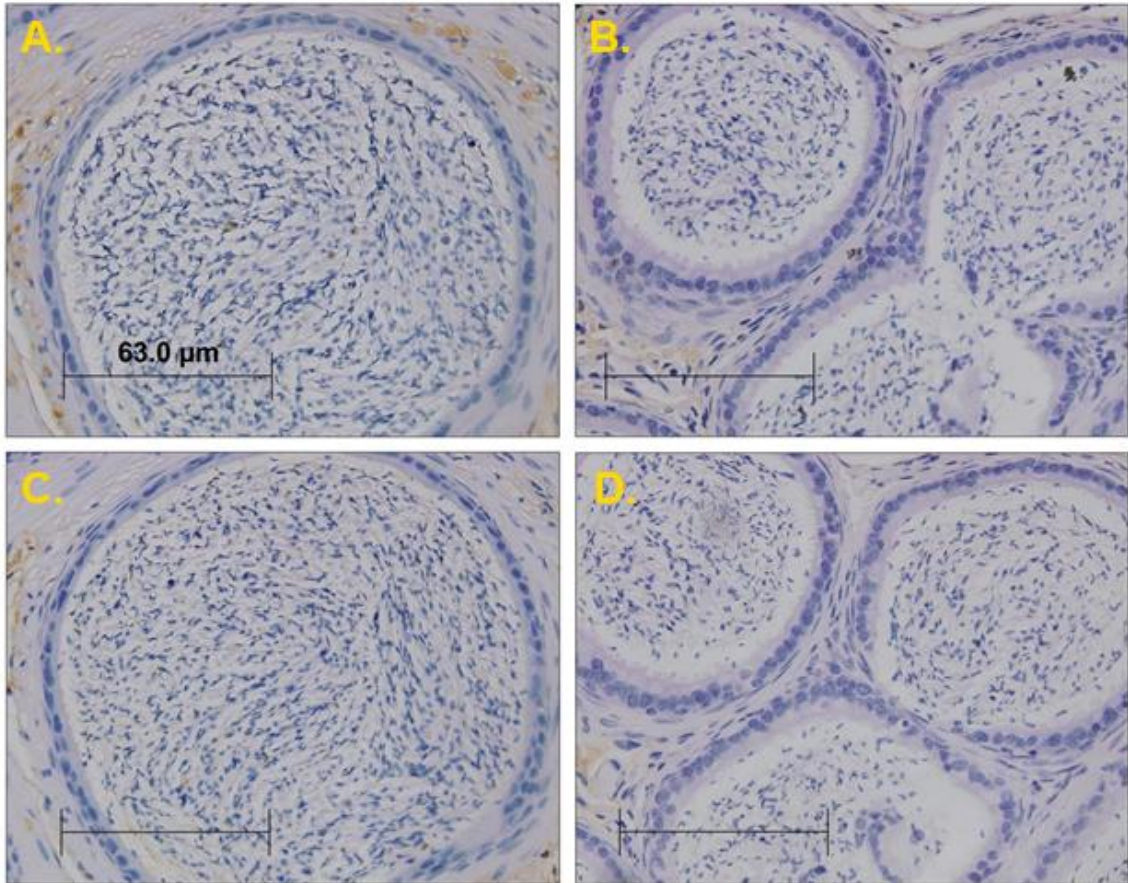


Fig. 4.10. Representative image of epididymis sections stained with anti-IDO2 antibody.

No staining seen in *Ido2*^{+/+} (A) and *Ido2*^{-/-} (B) mouse sections treated with mouse monoclonal IDO2 antibody or in *Ido2*^{+/+} (C) and *Ido2*^{-/-} (D) epididymis sections treated with monoclonal IgG_{2A} isotype controls. Scale bars represent 63.0μm.

4.3.3 IDO1 and IDO2 protein intracellular localisation in transfected Human Embryonic Kidney (HEK) cells

When HEK cells transfected with plasmids containing mouse *Ido1* and *Ido2* cDNA were assessed by immunofluorescence, both IDO1 (Fig. 4.11) and IDO2 (Fig. 4.12) transfected-HEK cells exhibited a similar protein expression pattern, which was cytoplasmic. This cytoplasmic expression pattern of both IDO1 and IDO2 in transfected HEK cells was seen in cells cultured in both Trp-deficient medium and Trp-rich medium (250 μM), similar to that in cells cultured in physiological plasma levels of Trp ($\sim 45 \mu\text{M}$).

To try to clarify this observation by examining the expression patterns of IDO1 and IDO2 protein in primary cells, we isolated hepatocytes from the liver of *Ido2*^{+/+} mice and cultured them for subsequent immunofluorescence study. However, in several experiments we found that *Ido2* mRNA expression plummeted drastically within the first 24 hours of isolation and culture (data not shown). This occurred despite variations in the isolation and culture media employed. Thus it was impossible to pursue that line of investigation.

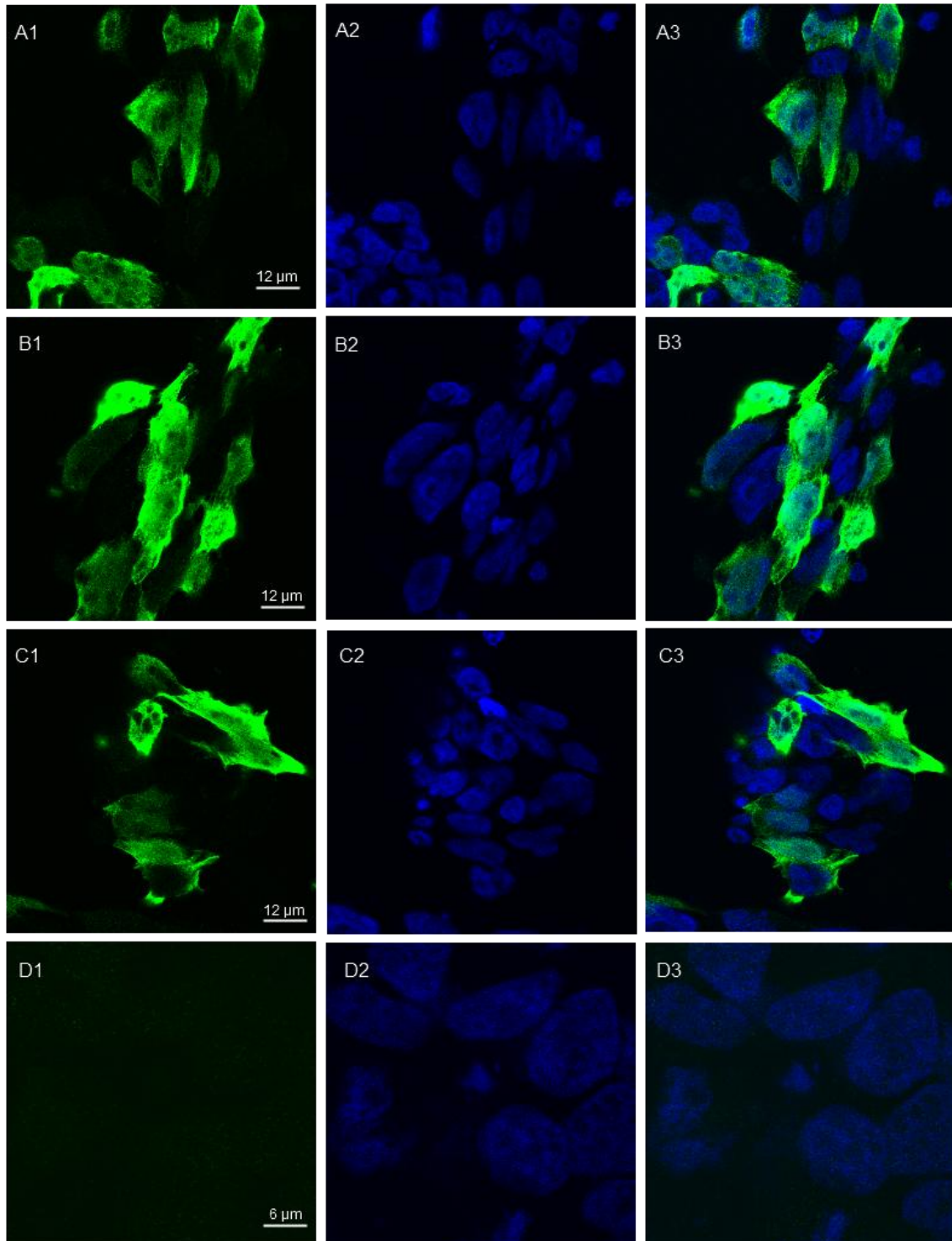


Fig. 4.11. Representative images of HEK cells transfected with plasmid carrying mouse *Ido1* cDNA. IDO1 protein expression in the transfected cells is shown on column 1, whereas column 2 shows nuclear staining (DAPI) and the third column is the merged image showing the IDO1 expression pattern along with nuclear staining. IDO1 protein expression in HEK cells grown in Trp-deficient medium (A1 – A3). The expression pattern was maintained in both HEK cells (B1 – B3) grown in medium containing physiological levels of Trp (45 $\mu\text{mol/L}$) and medium with (C1 – C3) excess Trp (250 $\mu\text{mol/L}$). Mock plasmid-transfected HEK cells treated with anti-IDO1 Ab were used as the negative control (D1 – D3).

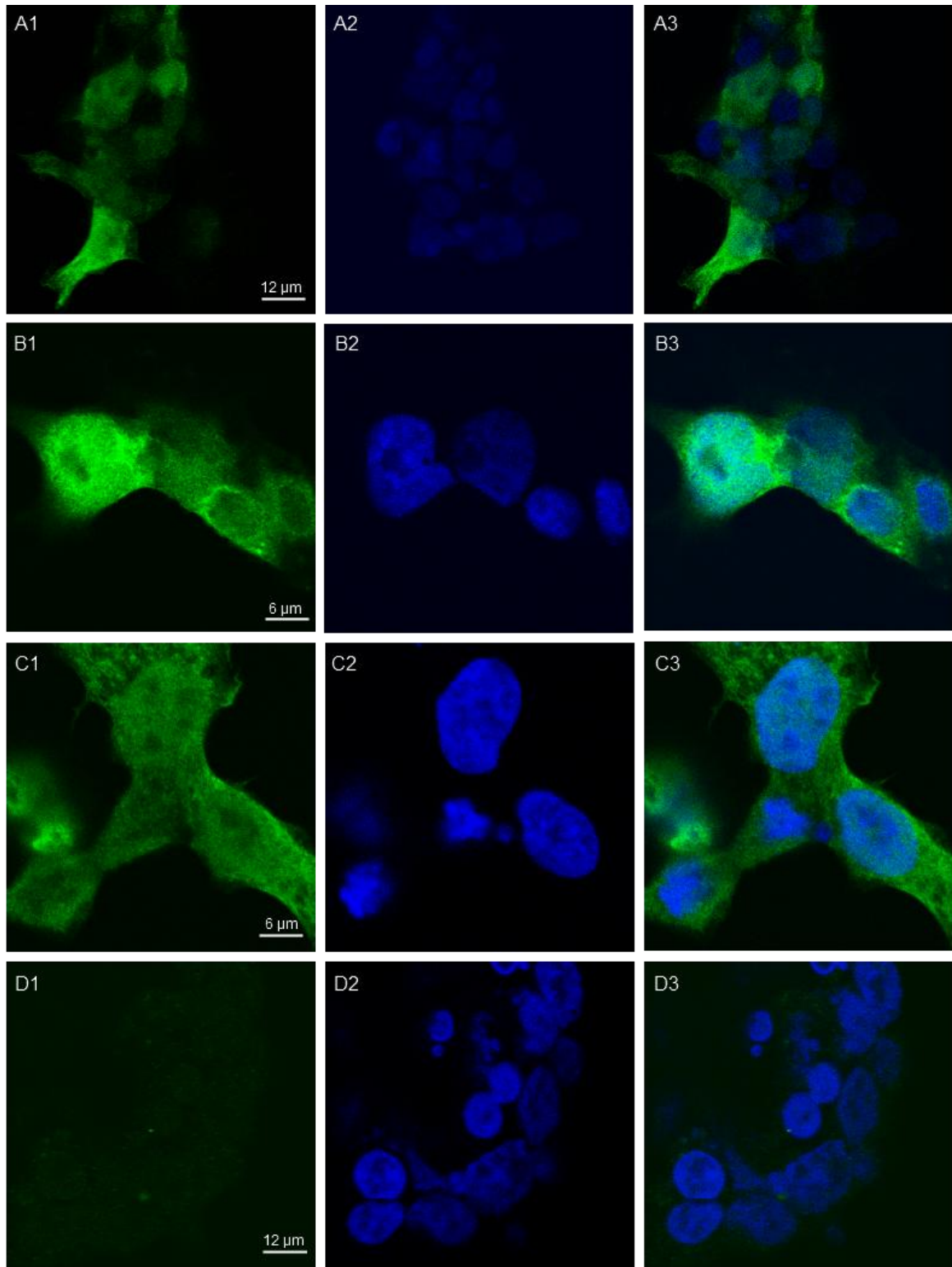


Fig. 4.12. Representative images of HEK cells transfected with mouse *Ido2* cDNA plasmid. IDO2 protein expression in HEK cells cultured in Trp-deficient medium (A1 – A3). The expression pattern was maintained in both HEK cells (B1 – B3) grown in medium containing physiological levels of Trp (45 $\mu\text{mol/L}$) and medium with (C1 – C3) excess Trp (250 $\mu\text{mol/L}$). First column shows IDO2 protein expression whereas second column shows nuclear (DAPI) staining. The third column is the combined image exhibiting both IDO2 and nuclear staining patterns.

4.3.4 Expression of genes for tryptophan-catabolising enzymes in tissues in murine developmental series

4.3.4.1 Expression of genes for tryptophan-catabolising enzymes in the placenta of developing embryos of QS strain outbred mice

The mRNA expression of all three Trp-catabolising enzymes was detected in the placenta of embryos as early as E14.5 dpc. The levels of *Ido1* (Fig. 4.13A) and *Ido2* (Fig. 4.13B) mRNA were maintained in the placenta with no significant changes throughout development. *Tdo2* mRNA, however, showed a significant increase ($p=0.0017$) between E14.5 to E16.5 dpc in placenta (Fig. 4.13C). The expression of *Tdo2* mRNA was then maintained in E17.5 dpc placenta at a similar level to that of E16.5 dpc placenta. When the ratios of the expression of *Ido1*, *Ido2* and *Tdo2* relative to reference genes were compared (Fig. 4.14), *Tdo2* had the highest mRNA expression in the placenta. The mRNA expression of both *Ido1* and *Ido2* was relatively low. However, *Ido1* was still more highly expressed than *Ido2*.

4.3.4.2 Expression of genes for tryptophan-catabolising enzymes in the yolk sac of developing embryos of QS strain outbred mice

In the yolk sac, *Ido1* and *Tdo2* mRNAs were detected as early as E12.5 dpc (Fig. 4.15). There was a significant increase in the expression *Tdo2* (Fig. 4.15C) mRNA in the yolk sac from E17.5dpc to E18.5 dpc, although expression of *Ido1* (Fig. 4.15A) and *Ido2* (Fig. 4.15B) remained relatively constant throughout development. Amongst the three Trp-

catabolising genes, *Tdo2* was the most highly expressed gene in the yolk sac, more than 30-fold higher than *Ido1* and *Ido2* (Fig 4.16).

4.3.4.3 Expression of *Ido2* and *Tdo2* in the liver of developing embryos, neonates and adult QS outbred and *Ido2*^{+/+} (Cre-Tg) transgenic mice

Due to the crossreactivity of IDO2 antibody seen in Section 4.3.2, it is best that any IDO2 protein study undertaken uses *Ido2*^{-/-} mice as the negative control. With this in mind, the later studies examining *Ido2* mRNA expression in the developmental series were done using Cre-Tg to accommodate protein studies if found necessary. However, due to relatively low levels of *Ido2* mRNA in the developmental series, protein expression studies were not pursued. The mRNA expression studies were undertaken on outbred QS strain mice as they are commonly used as the strain for studying developmental series by the collaborating laboratory (Dr. Stuart Fraser), so that gestational timing was well-established. *Tdo2* mRNA was not detected in embryonic liver in either the outbred QS (Fig. 4.17A) or inbred Cre-transgenic (Fig. 4.17B) mouse strain. The developmental stage at which *Tdo2* mRNA was first detected was P1 (neonatal liver). However, the expression level of *Tdo2* at this stage was only about 2% of adult liver expression levels. *Tdo2* mRNA expression climbed to about 10% of adult liver mRNA levels in the liver of a one-week-old neonate, before increasing almost 4-fold in the liver of 2-weeks old mice. This level was maintained in the liver of 3-week old mice before doubling in that of 8-week old mice (Fig. 4.17B).

Similarly, no *Ido2* mRNA transcript coding for full length IDO2 protein was detected in embryonic livers. *Ido2* mRNA was detected in neonatal livers, albeit at low levels (<1% of

its expression level in adult livers). In one-week old neonatal liver, *Ido2* mRNA levels were less than 5% of that in adult liver. In the following week, the mRNA expression level increased almost 6-fold. By the third week, the level of *Ido2* mRNA in the liver was about 45% of that in the adult liver. This level then doubled in the liver of adult (8-week old) mice.

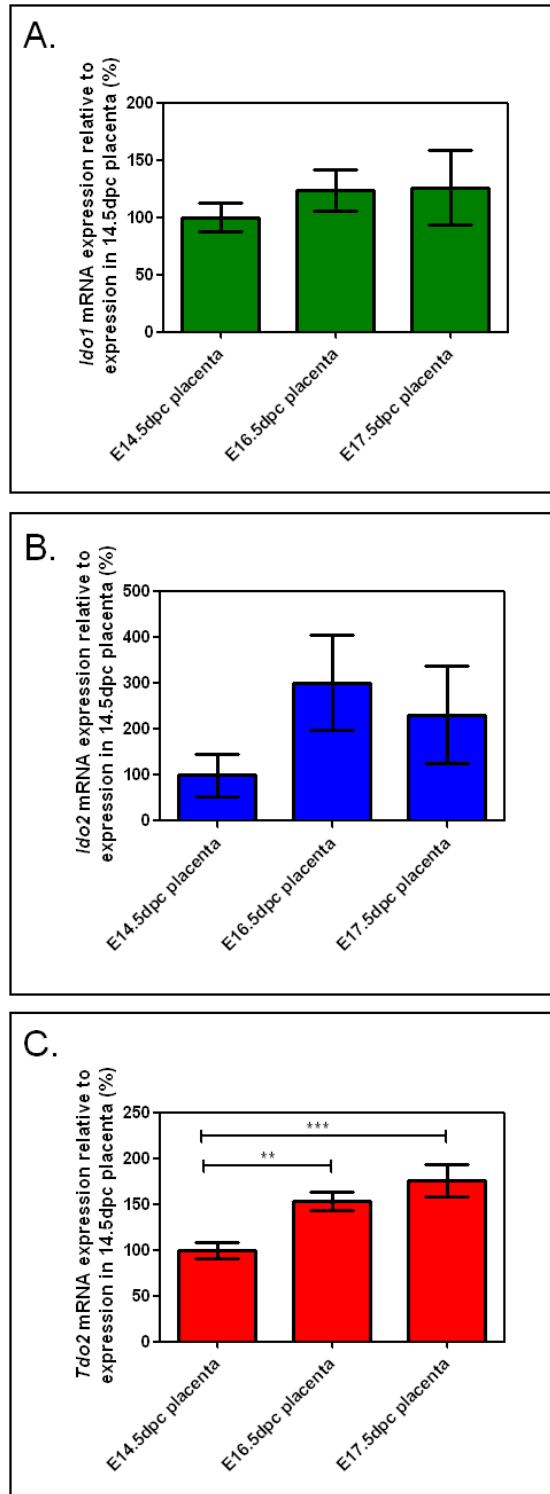


Fig. 4.13. Trp-catabolising genes *Ido1* (A), *Ido2* (B) and *Tdo2* (C) mRNA expression in placenta of developing QS strain embryos at 14.5, 16.5 and 17.5 days-post-coitus (dpc) relative to expression of the respective genes at 14.5dpc, as detected by RT-qPCR (standard curve method). Data shown are the mean percentage of expression from $N \geq 5$ individual placenta; error bars represent standard error of mean. Statistical analysis by one-way ANOVA with Tukey post-test, $p < 0.05$. Double asterisks denote $p < 0.01$ whereas triple asterisks denote $p < 0.001$.

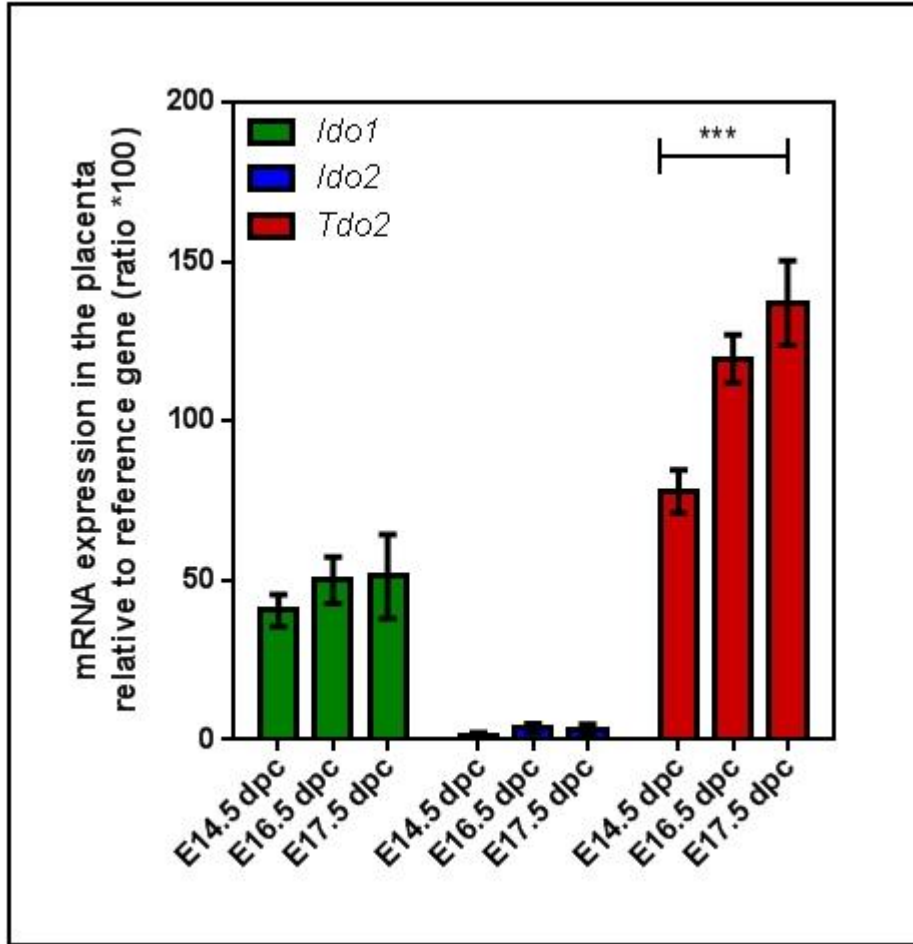


Fig. 4.14. Ratio of expression of Trp-catabolising genes *Ido1*, *Ido2* and *Tdo2* mRNA expression in placenta of developing QS strain embryos relative to the reference gene *Rpl13a*, assessed by RT-qPCR using the standard curve method. Data shown are the mean ratio of expression from $N \geq 5$ individual placentas; error bars represent standard error of mean. Statistical analysis by one-way ANOVA with Tukey post-test, $p < 0.05$. Triple asterisks denote $p < 0.001$.

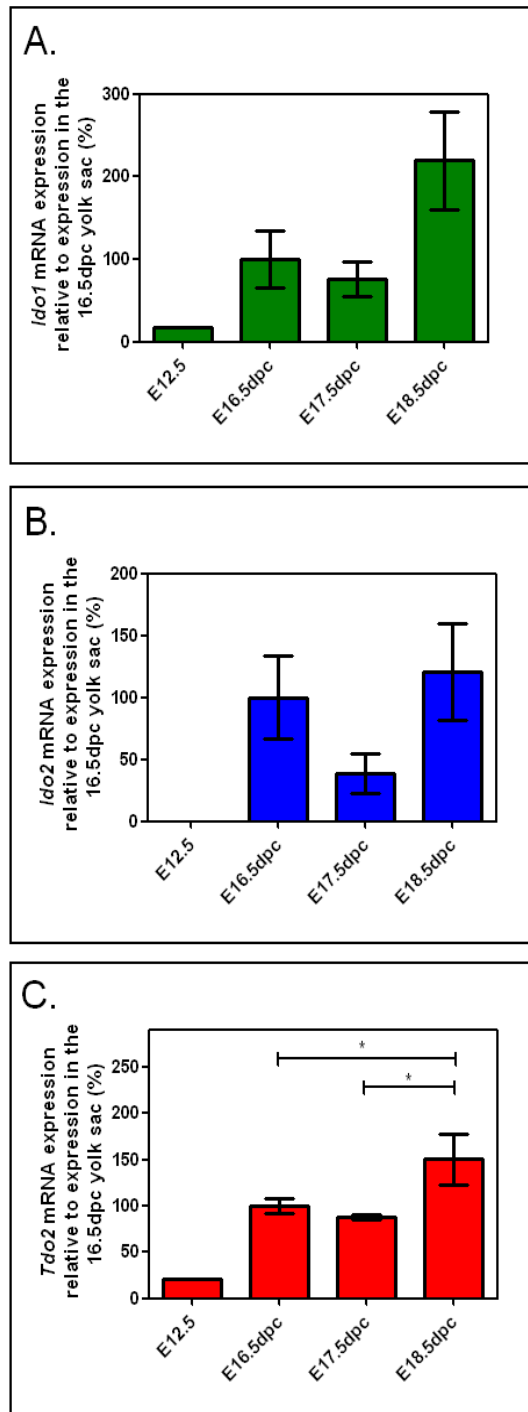


Fig 4.15. Trp-catabolising genes *Ido1* (A), *Ido2* (B) and *Tdo2* (C) mRNA expression in yolk sac of developing QS strain embryos at 12.5, 16.5, 17.5 and 18.5 dpc relative to expression of the respective genes at 16.5dpc, as detected by RT-qPCR (Standard curve method). Data shown are the mean percentage of expression from $N \geq 5$ individual yolk sacs for 16.5, 17.5 and 18.5 dpc. Percentage expression at 12.5 dpc is a result of pooled samples from $n=3$ individual yolk sacs. Statistical analysis by one-way ANOVA with Tukey post-test, $p < 0.05$ and error bars represent standard error of mean. Single asterisk denotes $p < 0.05$.

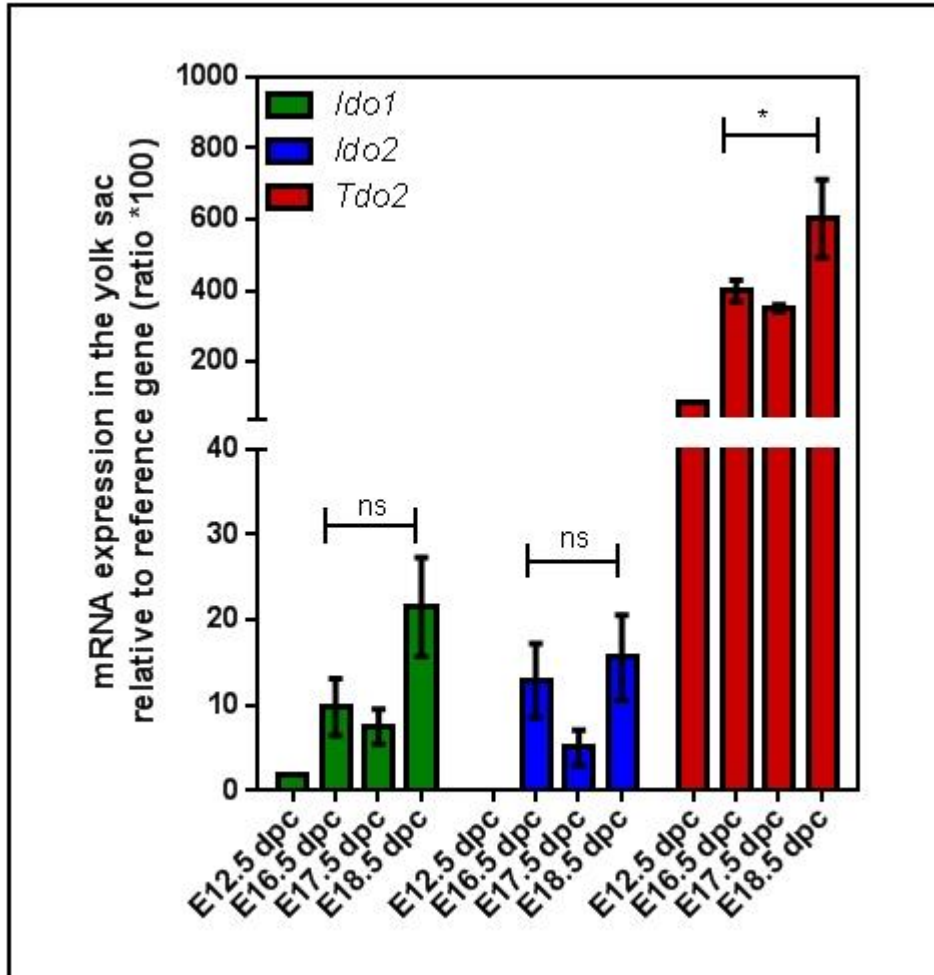


Fig. 4.16. Ratio of Trp-catabolising genes *Ido1*, *Ido2* and *Tdo2* expression in yolk sac of developing embryos relative to the reference gene *Rpl13a*, assessed by RT-qPCR using the standard curve method. Data shown are the mean ratio of expression from $N \geq 5$ individual yolk sacs for 16.5, 17.5 and 18.5 dpc. Percentage expression at 12.5 dpc is a result of pooled samples from $n=3$ individual yolk sacs. Statistical analysis by one-way ANOVA with Tukey post-test, $p < 0.05$ and error bars represent standard error of mean. Single asterisk denotes $p < 0.05$.

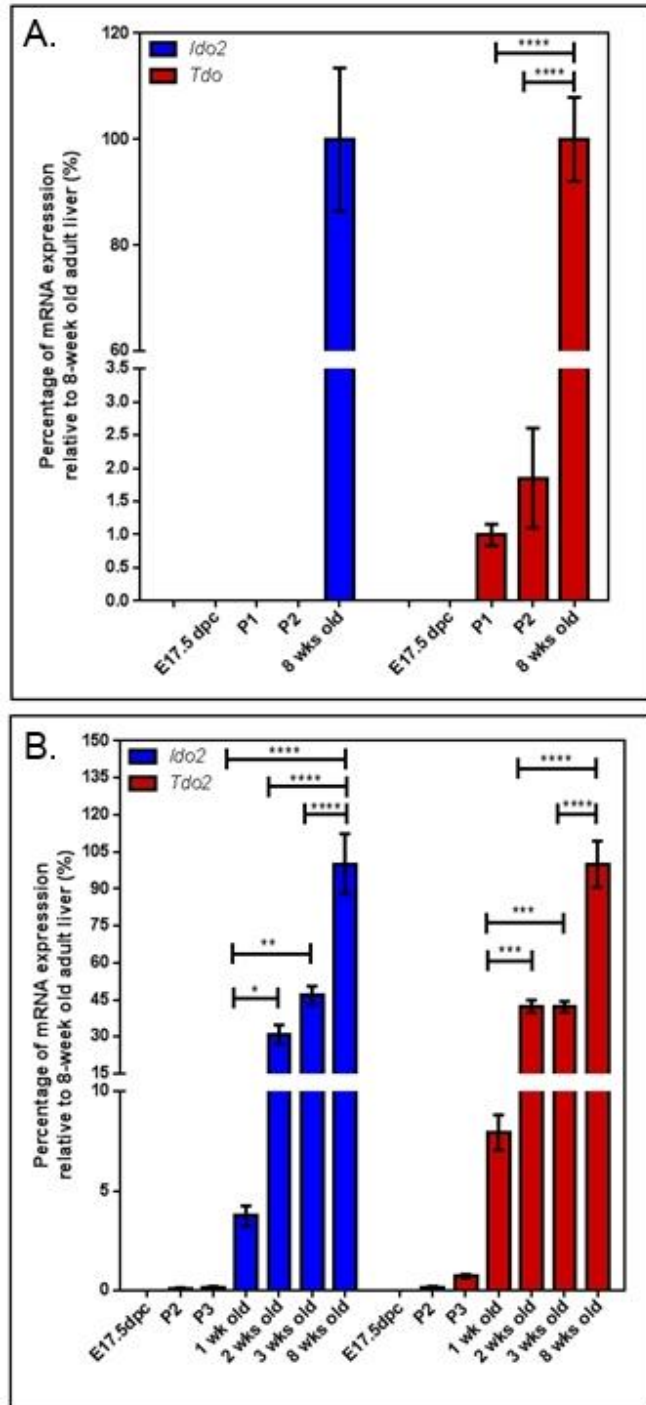


Fig. 4.17. Trp-catabolising genes *Ido2* and *Tdo2* mRNA expression in liver of embryos, neonates and adults of outbred QS mice strain (A) and inbred Cre transgenic mice strain (B) relative to the expression of the respective genes in 8-week-old adult mouse liver, as detected by RT-qPCR (standard curve method). Data shown are the mean percentage of expression from n=6; error bars represent standard error of mean. The gender of the mice at early neonatal stages (P1, P2 and P3) was not discerned. The compositions of genders for the rest of the analysis were 1-week old neonates (3♂ 3♀), 2-week old mice (2♂ 4♀), 3-week old (4♂ 2♀) and 8-week old (6♂). Statistical analysis by one-way ANOVA with Tukey post test, p<0.05. Single asterisk denotes p<0.05, double asterisks denote p<0.01, triple asterisks denote p<0.001 and quadruple asterisks denote p<0.0001.

4.3.5 Expression of genes for tryptophan-catabolising enzymes in various transgenic mouse tissues deficient for one or two tryptophan-catabolising enzymes

As mentioned previously, there have been reports suggesting possible interactions between IDO1 and IDO2 in terms of their expression. As this was of great interest, transgenic mice deficient in two Trp-catabolising enzymes were generated (in addition to the single gene knockouts) for the purpose of this study.

4.3.5.1 Liver

Both *Ido2* and *Tdo2* mRNA were detected in liver tissues, whereas no *Ido1* mRNA was detected. As expected, the expression of *Ido2* was ablated in the single *Ido2*^{-/-} as well as the double knockout *Ido2*^{-/-}*Tdo2*^{-/-} mice. *Ido2* mRNA expression levels were similar in *Ido1*^{-/-} and *Tdo2*^{-/-} mice and double knockout *Ido1*^{-/-} *Tdo2*^{-/-} mice to those of their wild type equivalent (Fig. 4.18A). The pattern of *Tdo2* mRNA levels in the various gene knockout animals was similar to that of the equivalent wild-types, with the absence of neither *Ido1* nor *Ido2* affecting *Tdo2* expression (Fig. 4.18B). No *Ido1* mRNA was detected in the liver tissues of these strains.

4.3.5.2 Kidney

Kidney was the tissue with the most abundant *Ido2* mRNA, after the liver. When *Ido2* mRNA expression level was assessed across single and double gene knockout mouse kidney tissues, significantly lower levels of *Ido2* mRNA were detected in both the single *Ido1*^{-/-} (p<0.0001) and double *Ido1*^{-/-} *Tdo2*^{-/-} (p<0.0001) kidney tissues relative to the equivalent wild types (Fig. 4.19). This pattern of lower *Ido2* mRNA in the gene knockout mice, however, was not seen in *Tdo2*^{-/-} compared to its equivalent wild-type, *Tdo2*^{+/+}.

4.3.5.3. Brain

Ido2 mRNA was detected in the brain, albeit in low levels, across the single and double gene knockout mice alongside their equivalent wild-types. A similar downregulation of *Ido2* mRNA in single *Ido1*^{-/-} (p<0.0001) and double *Ido1*^{-/-}*Tdo2*^{-/-} (p=0.0117) mice to that seen in the kidney (Section 5.3.5.2) was observed in brain tissue (Fig. 4.20A). The other Trp-catabolising gene detected in the brain was *Tdo2*, at low levels. The expression of *Tdo2* mRNA in single *Ido1*^{-/-} and *Ido2*^{-/-} mice was similar to that of their equivalent wild types, C57BL/6J and Cre transgenic respectively (Fig. 4.20B). However, *Ido1* mRNA was not detected in the brain.

4.3.5.4 Testis

The two Trp-catabolising genes expressed in the testes were *Ido1* (Fig. 4.21A) and *Tdo2* (Fig. 4.21B). Both genes were detected at low levels in the testes, and their expression patterns were maintained at a similar level in the mouse strain in which their counterpart Trp-catabolising gene had been knocked-out to that in the equivalent wild-type.

4.3.5.5 Epididymis

Both *Ido1* (Fig. 4.22A) and *Ido2* (Fig. 4.22A) mRNA were detected in the epididymis. The expression of *Ido2* in single *Ido1*^{-/-} (p<0.0001) and double *Ido1*^{-/-}*Tdo2*^{-/-} (p < 0.0001) gene knockout mice was significantly lower than in their respective wild-types. *Ido1* mRNA expression relative to the reference gene in the epididymis also was significantly higher (p < 0.0001) than that of *Ido2*.

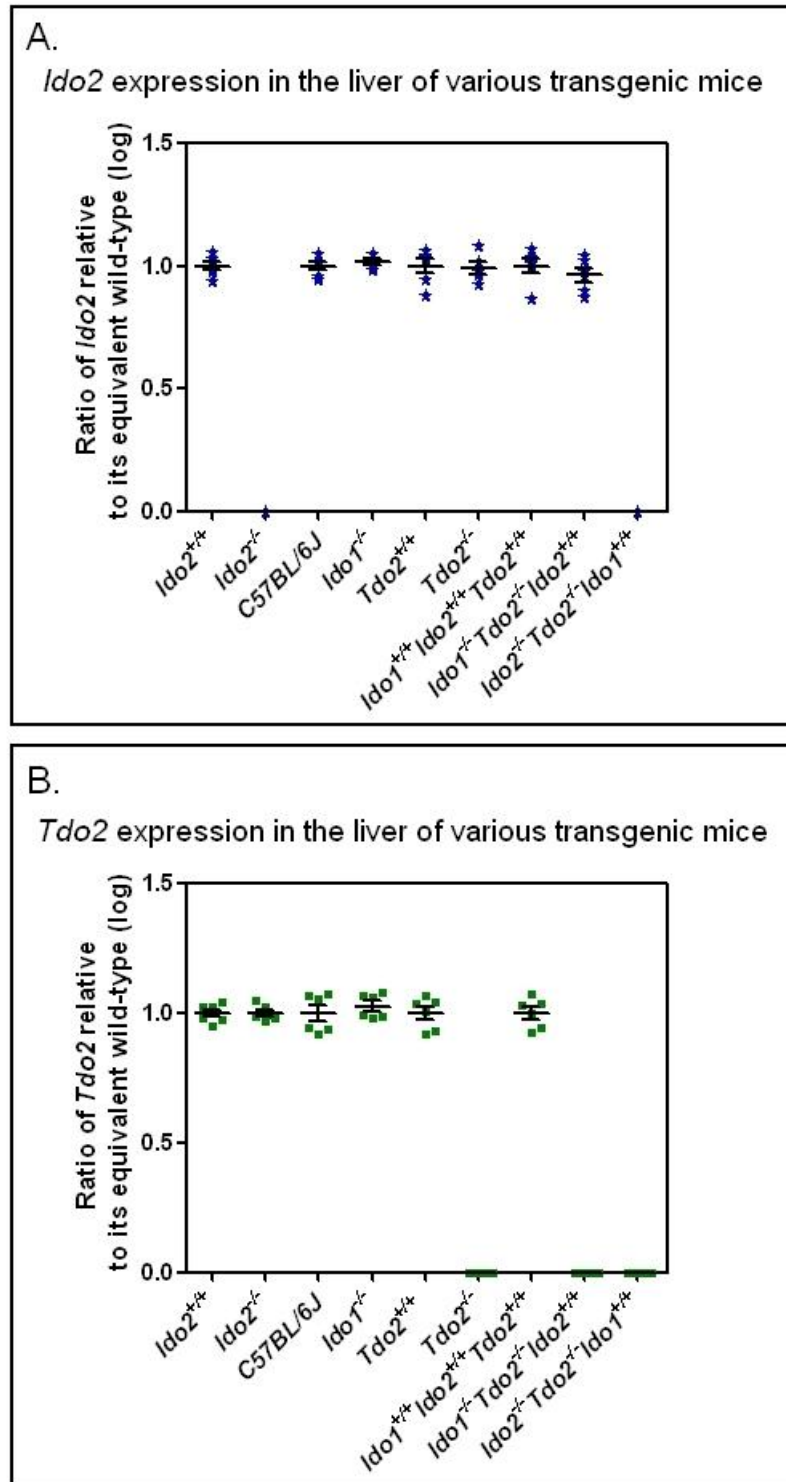


Fig. 4.18. The relative mRNA expression of *Ido2* (A) and *Tdo2* (B) in the liver tissue of nine different transgenic mouse strains, including double knockout strains *Ido1*^{-/-}*Tdo2*^{-/-} and *Ido2*^{-/-}*Tdo2*^{-/-}, relative to the equivalent wild-type mouse as assessed by RT-qPCR using the standard curve method. Error bars represent standard error of mean, n_≥5.

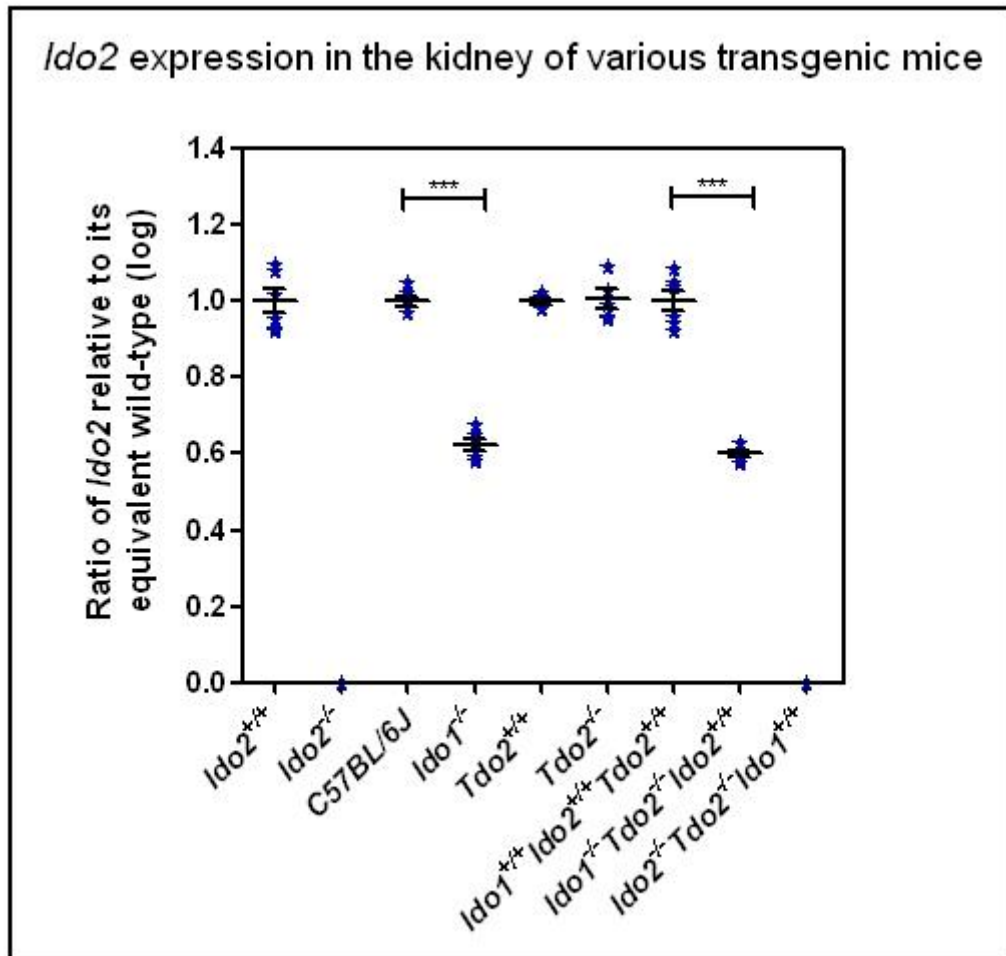


Fig. 4.19. The relative mRNA expression of *Ido2* in kidney tissues of nine different transgenic mouse strains, including double knockout strains *Ido1*^{-/-}*Tdo2*^{-/-} and *Ido2*^{-/-}*Tdo2*^{-/-}, relative to the equivalent wild-type mice as assessed by RT-qPCR using the standard curve method. *Ido2* mRNA was significantly downregulated in *Ido1*^{-/-} ($p < 0.0001$) and *Ido1*^{-/-}*Tdo2*^{-/-} ($p < 0.0001$) mice relative to their respective wild-types. No *Ido1* and *Tdo2* mRNA were detected in kidney tissues. Error bars represent standard error of mean, $n \geq 5$ whereas triple asterisks denote $p < 0.001$.

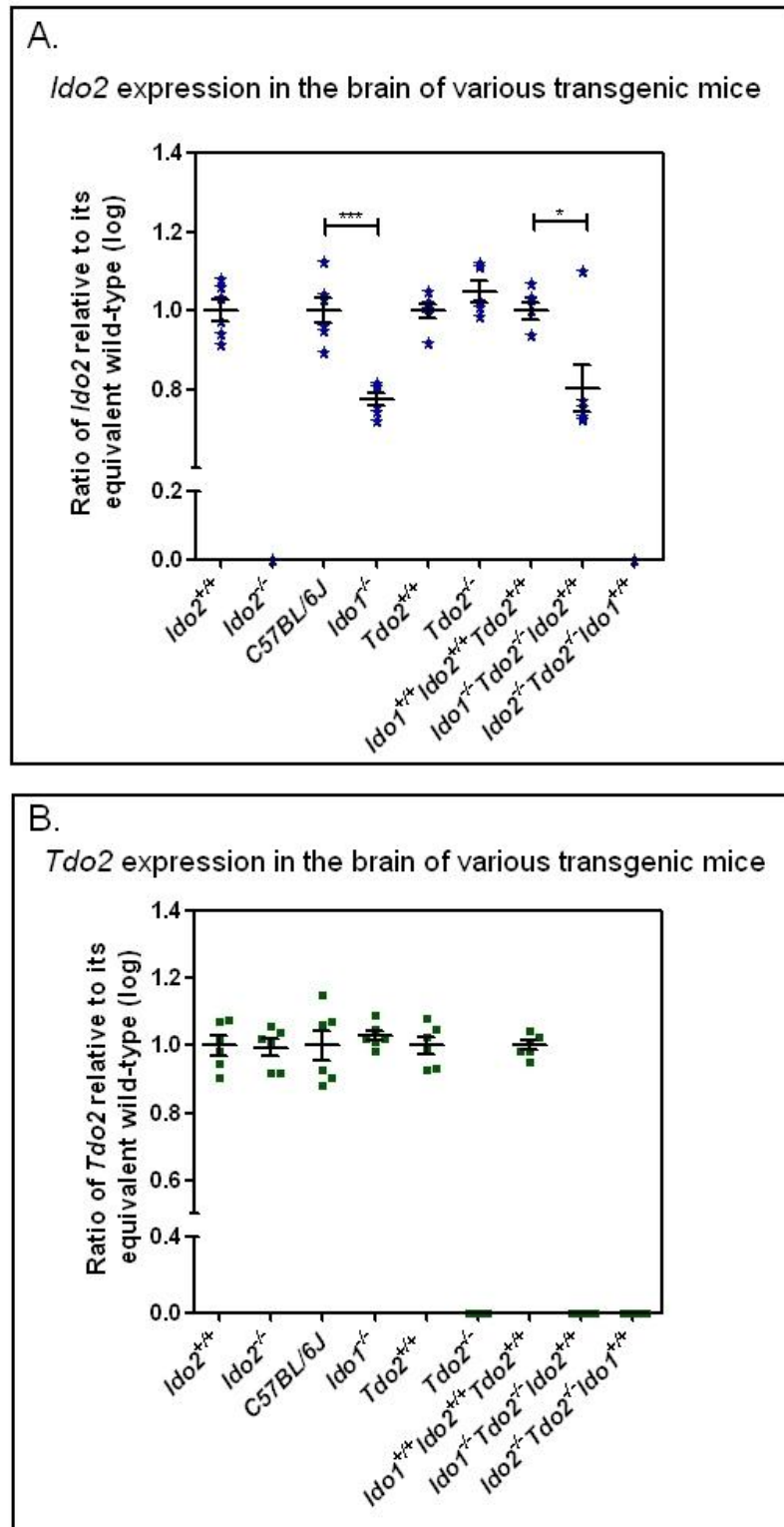


Fig. 4.20. The relative mRNA expression of *Ido2* (A) and *Tdo2* (B) in brain tissues of nine different transgenic mouse strains, including double knockout strains *Ido1*^{-/-}*Tdo2*^{-/-} and *Ido2*^{-/-}*Tdo2*^{-/-}, relative to the equivalent wild-type mouse as assessed by RT-qPCR using the standard curve method. *Ido2* mRNA was significantly downregulated in *Ido1*^{-/-} ($p < 0.0001$) and *Ido1*^{-/-}*Tdo2*^{-/-} ($p = 0.0117$) relative to their respective wild-types. No *Ido1* mRNA was detected in brain tissues. Error bars represent standard error of mean, $n \geq 5$. Single asterisk denotes $p < 0.05$ whereas triple asterisks denote $p < 0.001$.

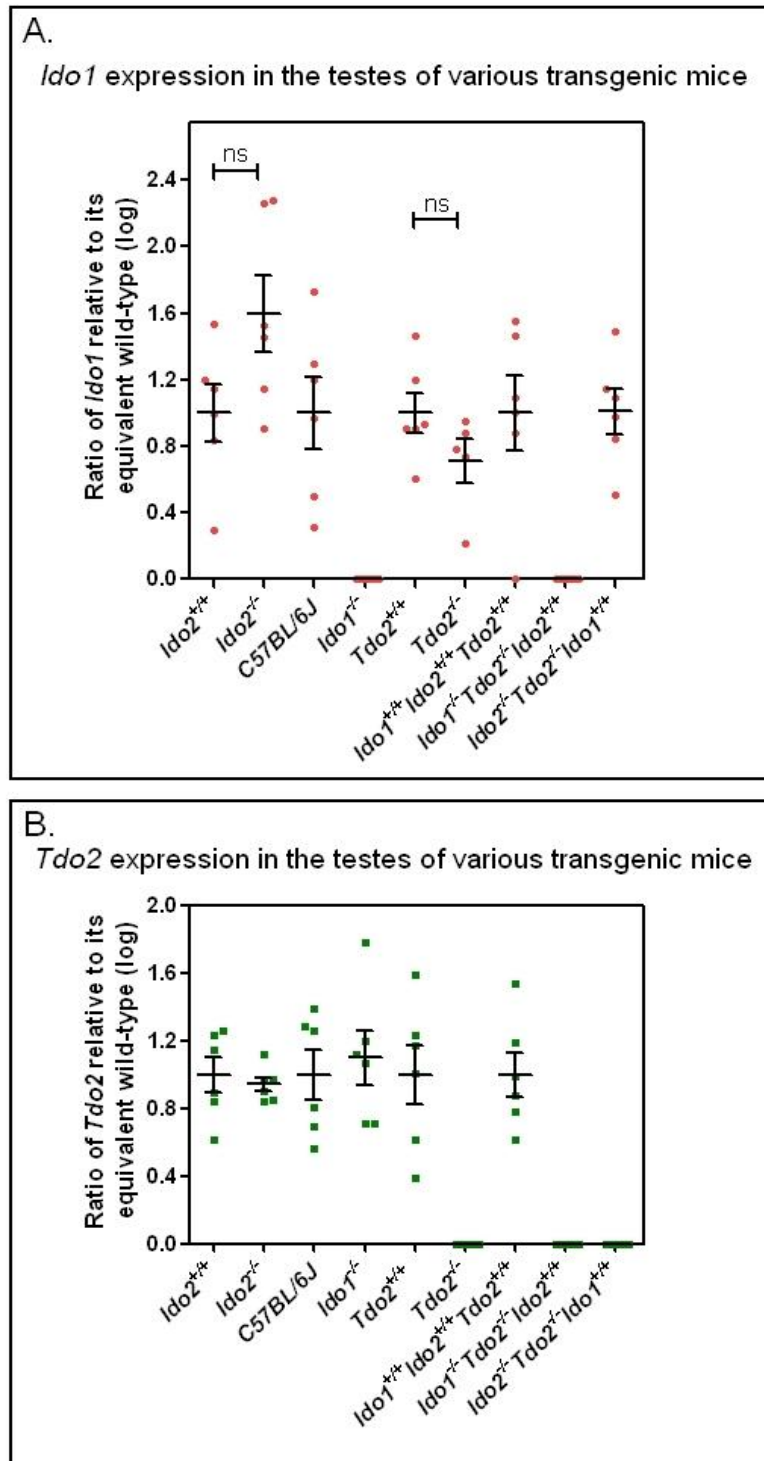


Fig. 4.21. The relative mRNA expression of *Ido1* and *Tdo2* in testes tissues of nine different transgenic mouse strains, including double knockout strains *Ido1*^{-/-}*Tdo2*^{-/-} and *Ido2*^{-/-}*Tdo2*^{-/-}, relative to the equivalent wild-type mouse as assessed by RT-qPCR using the standard curve method. No *Ido2* mRNA transcript coding for full length IDO2 protein was detected in testis tissues. Error bars represent standard error of mean, n_≥5.

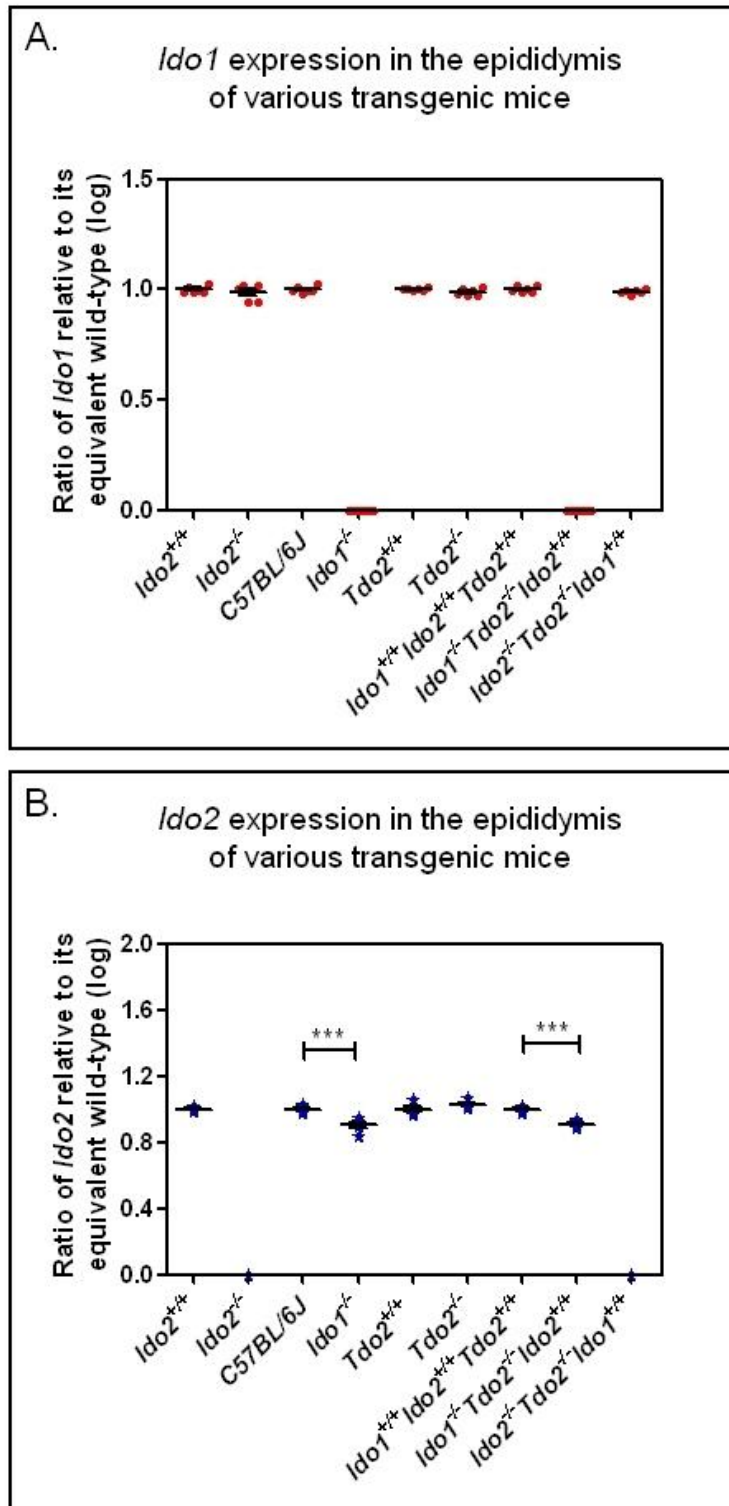


Fig. 4.22. The relative mRNA expression of *Ido1* (A) and *Ido2* (B) in epididymis of nine different transgenic mouse strains, including double knockout strains *Ido1*^{-/-}*Tdo2*^{-/-} and *Ido2*^{-/-}*Tdo2*^{-/-}, relative to the equivalent wild-type mouse as assessed by RT-qPCR using the standard curve method. *Ido2* mRNA was significantly downregulated in *Ido1*^{-/-} (p=0.0001) and *Ido1*^{-/-}*Tdo2*^{-/-} (p<0.0001) relative to their respective wild-types. No *Tdo2* mRNA was detected in epididymis. Error bars represent standard error of mean, n_≥5. Triple asterisks denote p<0.001.

4.4 DISCUSSION

In this chapter, we aimed to investigate the tissue and cellular distribution of IDO2 within adult and developmental series murine tissues and to elucidate possible interactions between the three Trp-catabolising genes within various murine adult tissues.

4.4.1 IDO2 protein detection in Western Blot

Five different anti-IDO2 antibodies were tested by Western Blot on liver lysates of wild-type and *Ido2*^{-/-} mice to validate their specificity (Section 4.3.2). Although four out of five anti-IDO2 antibodies detected a band with a molecular weight of ~45 kDa (the estimated molecular weight of IDO2), two out of these four antibodies detected similar bands in livers from *Ido2*^{-/-} mice. Notably, the two non-specific anti-IDO2 antibodies were rabbit polyclonal antibodies. The detection of a non-specific band of a similar molecular weight in the liver tissues of both wild-type and *Ido2*^{-/-} mice indicates an issue of antibody cross-reactivity, which only became evident in the presence of a true negative control in the form of gene knockout mouse tissues. The use of a cell line or tissue known to not express the protein, or loading buffer without the sample, are commonly used as negative controls in Western blotting and IHC. However, based on the current observations, the best negative control to determine specificity of an antibody, for Western Blot or IHC, is protein lysates or sections from the same tissue of the appropriate gene knockout mice. The anti-IDO2 antibody made for the Hunt laboratory by Genscript (USA), while being specific on liver lysates, was not specific for kidney, as it detected a similar-sized band in *Ido2*^{-/-} kidney lysates. This adds to the complexity of validating the presence of IDO2 in tissues by Western Blot and IHC as antibodies may be specific for

some tissues, but not so for others. This issue of non-specificity did not arise for IDO2 detection in HEK cells transfected with IDO2 plasmids (data not shown), using the same antibodies. As HEK cells are of human origin, it is possible that the anti-IDO2 does not react with other proteins in human cells but does do so in murine cells. Apart from that, there could be a difference in terms of cellular expression, whereby no cross reacting protein is present in embryonic kidney cells that may be present in other cell types. In addition, this could be an issue more relevant to testing the presence of proteins in whole tissue lysates. Therefore, when elucidating the presence of a protein in whole tissues using Western Blot, it is highly desirable to have a negative control in the form of an equivalent tissue from a gene knockout mouse. Obviously, this is not feasible for other mammalian species.

The antibody that was specific, whereby no bands were detected in *Ido2*^{-/-} mouse liver, was a commercial mouse monoclonal anti-IDO2 antibody (Santa Cruz). This antibody, however, did not detect any IDO2 protein in kidney lysates. This suggests a higher specificity of mouse monoclonal antibodies compared to polyclonal antibodies, as would be expected, and, therefore, better applicability to protein detection, especially for IHC. Despite higher specificity of mouse monoclonal antibodies, technical challenges that arise when using mouse monoclonal antibodies on mouse tissues in IHC will need to be overcome before analysis can be done, as is described in the next section.

4.4.2 Cellular distribution of IDO2 within various murine tissues

4.4.2.1 IHC techniques for detecting mouse protein using mouse monoclonal antibody

As the only antibody that was specific for IDO2 was a mouse monoclonal antibody, IHC techniques to detect the subcellular localisation of IDO2 within mouse tissue required a more specialised approach to prevent high background and/or non-specific staining. The Vector M.O.M. (Mouse-on-mouse) kit gave no staining initially. When the Vector M.O.M. approach was complemented with tyramide signal amplification (TSA) there was a detectable positive signal in the tissue (Section 4.3.2). This shows that although a relatively abundant level of *Ido2* mRNA was detected in liver tissues by RT-qPCR (Section 4.3.1), this did not seem to translate into protein detection, when assessed by IHC. IDO2 protein was not detectable by conventional IHC and required the TSA approach for the expression pattern to become evident. The relatively low and detectable IDO2 protein signal in the liver sections could be due to a number of possible reasons. I. The antigen retrieval method is not optimal and antigen epitopes remain masked by formalin fixation. II. Limitations of the Vector M.O.M. method, in that the blocking Fc segments of endogenous mouse antibodies in the method could also block the Fc segments of the primary IDO2 antibodies, which are necessary for the binding of the secondary antibodies. III. Low levels of IDO2 protein in the liver

With regard to the first possibility, various different antigen retrieval approaches were used (as mentioned in Section 4.2.8) and none but the hotplate antigen retrieval method on formalin-fixed sections, followed by IHC with Vector M.O.M. complemented with TSA strategy yielded positive signals. This indicates that it is more likely that IDO2 protein was absent in the liver or was present at a low level that was not detectable by conventional

IHC methods. While reason (II) is a possibility, this method has been optimised with its own specialised secondary antibody, which has been reported to yield specific staining with its secondary without affecting its ability to bind to the Fc segment of the primary mouse antibody, rendering it highly specific without affecting the binding effectiveness of the secondary antibody. Due to this, we conclude that low levels of IDO2 protein (III) in the liver are the most likely cause for the weak staining seen in the liver tissues.

4.4.2.2 Cellular localisation of IDO2 in various tissues

IDO2 protein was detected in the liver, often located around the nuclei of hepatocytes. However, not all hepatocytes showed this staining. There also was variability in the intensity of staining between different cells. Its localisation around and over the nuclei could suggest that IDO2 is either a nuclear protein or is stored around the nucleus until its use is triggered by other factors. Although the preliminary data on intracellular localisation of IDO2 in transfected HEK cells showed a cytoplasmic distribution (Section 4.3.3), the localisation of IDO2 may differ according to tissue type. An *in vitro* system also may not necessarily represent the distribution of IDO2 *in vivo* as the gene is artificially expressed in a cell line in which it would not otherwise be expressed. Although the mouse monoclonal IDO2 antibody did not detect any non-specific bands of a similar molecular weight to IDO2 in *Ido2*^{-/-} mouse liver lysates, while detecting a specific band in the wild-type by Western Blot, it did bind to other non-specific proteins of higher molecular weight. Non-specific staining by IHC was seen in a number of other tissues from *Ido2*^{-/-} mice. No staining was seen in the kidney and epididymis. However, in the brain, colon and testes, staining was seen in the wild-type and *Ido2*^{-/-} sections treated with anti-IDO2

antibody that was absent in the sections treated with mouse monoclonal IgG_{2A} isotype control. Within the brain, what seemed like positive staining of cells with the characteristics of nerve fibres in the wild-type, was actually non-specific staining that was also present in the *Ido2*^{-/-} mouse brain. Similarly in the colon, staining was seen in the goblet cells along the crypts of the colon in both the wild-type and *Ido2*^{-/-} mouse sections, despite being absent in sections treated with an isotype control antibody. Positive staining was observable in the differentiating germ cells within the testes. However, as was seen in the case of brain and colon tissue, similar staining was observable in testis sections from *Ido2*^{-/-} mice. No staining was observed in the small intestine of any mouse (data not shown). This non-specific staining could be high molecular weight proteins detected by the mouse monoclonal IDO2 antibody (Fig. 4.3). This outcome is one of the limitations of using mouse monoclonal antibodies on mouse sections as cross reactivity is a common issue. While the Vector M.O.M. system uses a blocking approach that significantly reduces this, it is possible that some cross-reactivity still occurs resulting in the staining of non-specific proteins. Without the knockout tissue, the staining patterns observed could easily have been interpreted as specific staining denoting IDO2 expression within the different tissues, as the staining pattern observed in the wild-type mouse tissue treated with anti-IDO2 antibody was absent in the sections treated with isotype control. Both previous papers reporting the cellular localisation of IDO2 within tissues (Ball et al., 2007; Fukunaga et al., 2012) did not have the advantage of tissues from gene knockout mice as negative control. Therefore, the results reported in these two papers will need to be validated with tissues from knockout mice. Ball et al. (2007) reported IDO2 by IHC in the epididymis, testis and kidney and Fukunaga et al. (2012) found IDO2 in the brain, liver, kidney and epididymis. Both publications agreed that the

distribution of IDO2 within the kidney was localised to the tubules. However, the data on cellular distribution of IDO2 in the epididymis differed between the two publications as the earlier paper reported IDO2 localised in the tail of spermatozoa (Ball et al., 2007) whereas the latter found it expressed in the caput, corpus and cauda cells of the epididymis (Fukunaga et al., 2012). Another consideration is that the antibody was indeed staining for IDO2, but a truncated version of the protein that might or might not be enzymatically active. Both the mouse and human *IDO2* genes have various alternatively spliced transcripts (Metz et al., 2007; Ball et al., 2007). These possess the potential to translate into variant forms of IDO2 proteins. More recently, a truncated version of IDO2 has been reported that possesses lower Trp-catabolising activity (Metz et al., 2014). The IDO2 antibodies available commercially do not distinguish between full-length and variant forms of IDO2 that may exist. It is possible that the protein we detected both by Western Blots and IHC is one of the variant forms of the IDO2 protein. With this in mind, for future directions, it will be necessary to generate antibodies that are either specific to the enzymatically active protein or the truncated protein.

4.4.3 Intracellular localisation of IDO1 and IDO2 within transfected HEK cells

We hypothesised that the intracellular localisation of IDO1 and IDO2 may differ, and that this might change in different conditions (Trp-rich vs physiological Trp vs Trp-deficient medium). We initially explored this question by transfecting HEK with plasmids containing *Ido1* and *Ido2* cDNA. When assessed by immunofluorescence, no gross differences between the distribution pattern of IDO1 and IDO2 within the cells in the three different conditions tested were observed (Fig 4.11 and 4.12). This lack of difference need not

necessarily be a true representation of the distribution pattern of these two enzymes. As HEK cells were transfected with plasmids expressing these enzymes, we would not expect to be able to detect meaningful differences in levels of IDO1 and IDO2 expression. It is possible that IDO1 or IDO2 expression in primary cells would be influenced by extracellular Trp concentration. In addition, HEK cells are embryonic kidney cells in which IDO1 and IDO2 proteins are not detectable constitutively. *In vivo*, only IDO2 has been detected in adult kidney cells (Ball et al., 2007; Fukunaga et al., 2012). IDO1, on the other hand, is not present in kidney cells constitutively (Section 4.3.2) (Theate et al., 2015). Furthermore, as mentioned previously, the localisation of IDO2 within transfected HEK cells differed to that in hepatocytes since the intracellular localisation of IDO2 in the former appeared cytoplasmic whereas in the liver hepatocytes, it had a perinuclear localisation (Section 4.3.2). Therefore, the apparent cytoplasmic intracellular localisation of both IDO1 and IDO2 needed to be validated by assessment of the distribution pattern of these proteins in primary cells.

When we attempted to study intracellular localisation in primary hepatocytes, isolated from wild-type and *Ido2*^{-/-} liver tissues, we encountered a number of obstacles. First, the expression levels of *Ido2* mRNA dropped drastically within the first 24 hours of isolation, conforming with previous reports of a marked loss of DNA and of protein expression in hepatocyte monocultures during the first 48 hours (Bissell and Guzelian, 1980; Crane and Miller, 1977; Clayton and Darnell, 1983). Secondly, the long-term stability of functional primary hepatocytes has been difficult to establish (Hewitt et al., 2007; Martinez et al., 2010). This made studying the expression pattern of the protein unfeasible unless a way to extend the stability of hepatocytes could be found. Different approaches, such as co-

culturing hepatocytes with liver endothelial cells or fibroblasts (Ukairo et al., 2013; Fraslin et al., 1985) or culturing the hepatocytes in a sandwich collagen gel formation (Choi and Choi, 2013), have been recommended. Although we attempted to co-culture the hepatocytes with fibroblasts, overgrowth of the fibroblasts impeded the growth of the hepatocytes. Due to all these technical challenges, this aspect could not be further pursued.

4.4.4 Expression of genes for tryptophan-catabolising enzymes in murine developmental series

Although the expression of Trp-catabolising genes in embryonic developmental tissues has been investigated before, all the studies (Suzuki et al., 2001; Yamazaki et al., 1985; Dharane Nee Ligam et al., 2010) focused primarily on placenta, and most did not compare the expression of the three genes in embryonic tissues. One group reported the expression patterns of TDO2 and IDO1 in embryonic and extraembryonic tissues (from 5.5 to 9.5 dpc) as well as in placenta (10.5 to 18.5 dpc), comparing protein levels and activity and semi-quantitative analysis of mRNA levels by Northern Blot (Suzuki et al., 2001). High Trp-degrading activity was detected in early concepti (5.5 dpc), which was attributed to TDO2. This high activity was not maintained throughout embryonic developmental stages and dropped after 6.5 dpc to basal levels comparable to those detectable in placenta. On the other hand, neither IDO1 mRNA nor protein was detectable in the early developmental stages (5.5 to 9.5 dpc) (Suzuki et al., 2001). However, IDO1 has been reported in both human and mouse placenta, specifically in the endothelial cells of villous chorion in the placental vasculature (Blaschitz et al., 2011;

Metz et al., 2007). Unlike earlier suggestions that IDO1 plays a key role in preventing allogeneic foetus rejection by depriving the microenvironment of Trp and, thus, suppressing T-cell proliferation (Munn et al., 1998), it was proposed that TDO plays this role (Suzuki et al., 2001).

In this study, we determined the expression of Trp-catabolising enzyme genes in embryonic tissues, namely the visceral yolk sac and liver as well as the foetomaternal tissue, placenta (Section 4.3.4). The high expression of *Tdo2* in early concepti in a previous report (Suzuki et al., 2001) could have been contributed to by the yolk sac, as yolk sac had the highest expression of Trp-catabolising enzyme genes, compared to the other tissues we tested. The expression of all three Trp-catabolising genes in the yolk sac might suggest that Trp catabolism is occurring actively in the yolk sac during development. Based on previous reports on the significance of Trp catabolism in preventing foetal rejection (Munn et al., 1998; Mellor et al., 2001), Trp catabolism in the embryonic tissues could be regulating the immune response at the foetal-maternal interface for precisely this role. However, this could be a collaborative function of the three Trp-catabolising enzymes and this would need to be further investigated. Although both placenta and endoderm yolk sac are responsible for transport of nutrients from the mother to the foetus, the types of nutrients transported by the two tissues differ. Immunoglobulins, as well as important nutrients such as cholesterol, lipids, iron, folic acid, retinoic acid and vitamin B12, are passed on to the foetus through the yolk sac (Jollie, 1990; Lloyd et al., 1996; Zohn and Sarkar, 2010; Brambell, 1966; Kozyraki and Gofflot, 2007). The yolk sac is also believed to be important for nutrient transfer during organogenesis (Ambroso et al., 1997; Beckman et al., 1998; Christensen and Birn, 2002).

In the placenta, on the other hand, glucose transporters (GLUTs), Ca²⁺ transporters and amino acid transporters have been reported, suggesting that it may play an essential role in the transport of these nutrients (Watson and Cross, 2005; Lager and Powell, 2012). It has been suggested that the transport of nutrients depends on the yolk sac in the earlier stages of development, after which this role is played by placenta, based on the high expression of certain genes in the early yolk sac which eventually decreases, while the expression of the same genes in the placenta is detected and climbs in later developmental stages (Freyer and Renfree, 2009; Jauniaux et al., 2004). However, this was not true of *Tdo2* as its expression in the yolk sac was consistently higher than in the placenta even in the later developmental stages (16.5 to 18.5 dpc) (Fig. 4.14 and Fig. 4.16). *Tdo2* could be playing a key role in the transport and catabolism of Trp during developmental stages, supporting organogenesis in the embryos. As both *Ido1* and *Ido2* were expressed at similar levels to each other in the yolk sac, both enzymes also could be involved in this process. Similar to *Tdo2*, the levels of *Ido2* were higher in the yolk sac than in the placenta. Whether its expression in the yolk sac is pointing to a role in nutrient transport or immunity is an interesting aspect for future investigation. Although we did not observe any gross phenotypical abnormalities in *Tdo2*^{-/-}, *Ido1*^{-/-} and *Ido2*^{-/-} mouse offspring compared to their respective wild-types, a more in-depth analysis of the levels of glucose, cholesterol, lipids and other major nutrients will be crucial to better understanding the role of these enzymes in embryonic development. The mechanism through which they support embryonic development and the possible differences in the roles of each Trp-catabolising enzyme will also need to be further investigated.

In the placenta, *Ido1*, *Ido2* and *Tdo2* mRNA were all detectable. *Tdo2* again had the highest expression. Unlike *Tdo2*, *Ido1* was more highly expressed in the placenta than the yolk sac. To date, it has been believed that *Ido1* plays a pivotal role in preventing allogeneic foetal rejection (Munn et al., 1998), as a significant decrease in the mean number of concepti in IDO-sufficient pregnant mice treated with the IDO inhibitor 1-methyl-tryptophan (1-MT) was found. However, this study did not distinguish between IDO1 and IDO2 activity. 1-MT was later shown to inhibit both IDO1 and IDO2 (Austin et al., 2010; Yuasa et al., 2010). Therefore, while it has been established that IDO is a key player in preventing allogeneic foetal rejection in pregnancy, whether this role is driven by IDO1 or IDO2 remains an open question that requires further investigation. The immunomodulatory role of IDO in pregnancy also could be mediated more through the placenta than the yolk sac.

Suzuki et al. (2001) speculated that it was TDO2 that was responsible for the increase in Trp catabolic activity in earlier embryonic stages (5.5 to 9.5 dpc) by demonstrating that the use of 1-MT did not significantly alter Trp-degrading activity in the earlier stages, but only in the later stages (12.5 dpc onwards). This is worthy of further study.

The unavailability of appropriate anti-mouse-TDO2 antibodies impeded us from studying the localisation of TDO2 in embryonic and adult tissues, which could shed light on its possible role within the yolk sac and placenta. It would also be interesting to compare the localisation of TDO2 within the placenta to that of IDO1, as it may inform our understanding on the roles of IDO1 and TDO2 in embryonic development.

Both *Ido2* and *Tdo2* mRNA were undetectable in embryonic liver, however. The absence of Trp-catabolising activity in embryonic liver has been documented in rats (Franz and

Knox, 1967). Although Trp-catabolising activity within neonatal liver was detectable in P7 neonates following induction with hydrocortisone, basal Trp-catabolising activity without stimulation was only detected in 2-week old rats. It was rather surprising that although both IDO2 and TDO2 were highly expressed in adult murine livers, mRNAs coding for these proteins were undetectable in embryonic livers. In early neonatal liver (P1 – P3) of outbred QS mice, *Tdo2* was detectable at very low levels, although *Ido2* was not. Although *Ido2* was detectable in in-bred *Ido2*^{+/+} mice in early neonatal liver (P2 and P3), the level of mRNA was very low. At all timepoints, the expression of *Tdo2* in the liver was higher than that of *Ido2*. The inferred absence of Trp-catabolising enzymes in embryonic liver suggests that Trp degradation is not performed in the liver until much later after birth. Perhaps, during the embryonic stage, Trp catabolism is performed mainly, if not solely, by the placenta and the yolk sac. It would be interesting to investigate whether the activity of *Tdo2* and *Ido2* is triggered post-partum by an intrinsic factor or the feeding process (suckling, solid food).

4.4.5 Expression of genes for tryptophan-catabolising enzymes in various transgenic mice deficient for one or two tryptophan-catabolising enzymes

There is some published evidence suggesting that the expression of *Ido2* is regulated by *Ido1*. In the epididymis, an upregulation of IDO2 was seen in *Ido1*^{-/-} mice (Fukunaga et al., 2012). There was also downregulation of regulatory T cells mediated by IDO1 in *Ido2*^{-/-} mice (Metz et al., 2014). This points to a possible regulatory relationship between IDO1 and IDO2. Whether TDO2 was involved in regulation of the other two Trp-catabolising enzymes in other tissues has not been explored to date.

In the liver, there were no differences in either *Tdo2* or *Ido2* expression between the various gene knockout mouse strains. The mRNA expression level of *Tdo2* in the liver was unchanged in the single gene knockouts *Ido1*^{-/-} and *Ido2*^{-/-} as well as the double knockouts *Ido1*^{-/-}*Tdo2*^{-/-} and *Ido2*^{-/-}*Tdo2*^{-/-} relative to their respective wild-types, suggesting that *Tdo2* expression in the liver is neither dependent on, nor influenced by, the other two Trp-catabolising enzymes. The same can be said for *Ido2* in the liver, as both single and double gene knockout mouse livers had similar mRNA levels of *Ido2* to those in their respective wild-types. This is consistent with the argument that IDO2 has a function apart from its Trp-catabolic activity, a role independent of TDO2.

The presence of two Trp-catabolic enzymes in the same tissue did raise some questions about the possibility that these two proteins interact to maintain Trp homeostasis within the liver. However, the lack of a significant difference at the mRNA level, in the absence of the other enzyme, suggests that this would be unlikely. It needs to be noted, however, that the lack of differences in mRNA levels (*i.e.* transcription) may not necessarily denote lack of differences at the level of protein expression (*i.e.* translation). This is an aspect that needs further investigation.

A significant downregulation of *Ido2* mRNA, however, was seen in single *Ido1*^{-/-} and double *Ido1*^{-/-}*Tdo2*^{-/-} kidney, brain and epididymis tissues. However, it is possible that the downregulation seen could be an artefact resulting from knocking out *Ido1*, as *Ido2* is located immediately adjacent to *Ido1* on chromosome 8. The absence of *Ido1* in wild-type kidney and brain supports this argument. Since there was no *Ido1* in the wild-type kidney and brain to begin with, any downregulation of *Ido2* seen in the knockout tissues are very unlikely to be a functional effect caused by the absence of IDO1

The epididymis may be different, however, as both IDO1 and IDO2 are present there. Fukunaga et al. (2012) reported an upregulation of IDO2 in *Ido1*^{-/-} mouse epididymis by Western Blot and IHC. Differences in mRNA levels were unreported. We, however, saw a downregulation of *Ido2* mRNA in *Ido1*^{-/-} epididymis. The limitation in the Fukunaga et al. (2012) study is the lack of *Ido2*^{-/-} mice to validate their data. We demonstrated in the results, and discussed in the previous section, the importance of validating the specificity of IDO2 antibodies using *Ido2*^{-/-} mouse tissues as negative control due to the recurrent issue of cross-reactivity. Therefore, in the absence of a negative control in the form of *Ido2*^{-/-} tissues, the observation made regarding upregulation of IDO2 in *Ido1*^{-/-} epididymis (Fukunaga et al., 2012) may not be truly representative of the condition in the tissue. When we obtained anti-IDO2 antibodies from the Yamamoto group and validated them, a non-specific band of a similar molecular weight to IDO2 was detected not only in *Ido2*^{+/+} liver lysates but also in *Ido2*^{-/-} liver lysates. It is possible that the downregulation of *Ido2* seen in the kidney, brain and epididymis of mice deficient in IDO1 is caused by the disruption of regulatory elements of *Ido2* genes, a possible by-product of deletion of a part of the *Ido1* gene as the *Ido1* and *Ido2* genes are situated adjacent to each other. These regulatory elements, however, would also have tissue-specific roles. A different approach may be necessary to elucidate whether the downregulation of *Ido2* in *Ido1*^{-/-} and *Ido1*^{-/-}*Ido2*^{-/-} (Figures 4.22) is caused by the absence of IDO1. An example of such an approach would be to determine IDO2 expression in the epididymis of mice treated with an IDO1-selective inhibitor or by utilising transient knockdown approaches such as siRNA. Metz et al. (2014) demonstrated an upregulation of *Ido2* RNA in primary peritoneal macrophages from *Ido1*^{-/-} tissues, stimulated with LPS. The pattern of *Ido2* regulation in the absence of *Ido1* could be a tissue-specific phenomenon that may also differ in

physiological compared to pathological conditions. Of the tissues analysed, almost all had two Trp-catabolising enzymes present except kidney, where only *Ido2* was detected. The presence of only *Ido2* mRNA in kidney tissues could imply that *Ido2* may play a specialised role in the kidney. IDO2 protein, however, was not detectable in *Ido2*^{+/+} kidney tissues by either Western Blot of immunoprecipitated lysates or IHC on kidney sections. Metz et al. (2014), however, reported the presence of IDO2 in wild-type kidney by Western Blot, and this was absent in *Ido2*^{-/-} mice. It is possible that the method we employed was not as sensitive as that of Metz and colleagues who used immunoprecipitation beads of higher sensitivity. Another consideration is the epitope at which the antibody is directed. The mouse monoclonal IgG₁ antibody employed by Metz et al. on murine kidney lysates was generated by immunising mice with human IDO2, produced in HEK293T cells, and was recommended for human IDO2 detection. On the other hand, we used an IgG_{2A} mouse monoclonal generated by immunising mice with murine C-9 terminus IDO2. The existence of alternatively-spliced transcripts for both human and mouse *IDO2* genes that have been reported previously (Metz et al., 2007) could suggest that proteins encoded by these transcripts may interact with a subset of IDO2 antibodies. In such a case, there is a need to differentiate between the full-length protein and truncated proteins when assessing the presence of IDO2 in tissues by Western Blot or IHC. Elucidating whether the protein present in the kidney and epididymis is the full-length or truncated IDO2 protein would give us a better understanding of the possible roles of IDO2 within these tissues.

In the testes, only *Ido1* and *Tdo2* were detected and there were no differences in the mRNA expression level of the respective genes in the single and double knockout mice relative to the respective wild-types. Despite an earlier report (Ball et al., 2007) claiming

the presence of IDO2 in the testes, the absence of mRNA transcript coding for full-length protein in the testes could imply either the presence of truncated proteins of uncertain enzymatic function, or cross-reactivity of the anti-IDO2 antibody used.

4.5 SUMMARY

Although an isotype control is the most commonly used negative control in IHC analysis, we found that mouse gene knockout tissues were the most suitable negative control, differentiating specific antibodies from those that were not. Out of the five anti-IDO2 antibodies we tested for specificity by Western Blot, the mouse monoclonal anti-IDO2 antibody was the most specific, detecting a single band of the expected molecular weight in wild-type mouse liver lysate, which was absent in *Ido2*^{-/-} lysates. However, it did not detect any IDO2 protein bands in the wild-type kidney lysates.

IDO2 was found localised around the hepatocyte nuclei in the liver when detected using mouse monoclonal IDO2 antibody by an optimised IHC approach. However, the localisation of IDO2 in transfected HEK cells appeared cytoplasmic. Despite conferring high sensitivity by Western Blot, non-specific staining was evident by IHC in a number of other tissues, namely the brain, colon and testes, where a similar staining pattern was seen in *Ido2*^{-/-} to that present in *Ido2*^{+/+} mice, while the isotype control showed negative staining.

In the murine embryonic development series, *Tdo2* was the most highly expressed gene in both the placenta and yolk sac. Whether the role of *Tdo2* in murine embryos is purely nourishment and NAD⁺ production, or if it may also be playing a role in inducing immune tolerance to prevent foetal rejection, will need to be further investigated. *Ido1* mRNA expression in the placenta and yolk sac was higher than that of *Ido2*. As *Ido2* was present only at very low levels in the embryonic tissues, it is unlikely that *Ido2* is playing a pivotal role in embryonic development. Despite being present in abundant amounts in adult

liver, neither *Ido2* nor *Tdo2* were present in embryonic liver and were only detectable in low levels in early neonates, suggesting that Trp metabolism is not performed by the liver until much later in murine development. Finally, the absence of the other Trp-catabolising enzymes did not affect the expression levels of *Ido2* within the liver. Although *Ido2* was downregulated in *Ido1*^{-/-} and *Ido1*^{-/-}*Tdo2*^{-/-} kidney, brain and epididymis, it is likely that these were artefacts as *Ido1* was not present in wild-type kidney and brain in the first place. Whether the downregulation of *Ido2* seen in *Ido1*^{-/-} and *Ido1*^{-/-}*Tdo2*^{-/-} epididymis is due to the absence of IDO1 will need to be further investigated by using transient knockdowns or an siRNA approach.

CHAPTER 5

IDO2- AND TDO2-REGULATED
PATHWAYS IN MURINE LIVER

CHAPTER 5: IDO2- AND TDO2-REGULATED PATHWAYS IN MURINE LIVER

5.1 INTRODUCTION

The tryptophan catabolic capacity of IDO2 and TDO2 via the kynurenine pathway has been well established (Knox and Auerbach, 1955; Ball et al., 2007; Metz et al., 2007). However, the roles these two enzymes may play outside this pathway and the expression of genes regulated by one or both of these enzymes have not been investigated before.

Apart from regulation of dietary tryptophan and supplying NAD⁺ (Badawy, 1981), TDO2 also has been suggested to play a role in facilitating immunotolerance in allogeneic liver transplantation (Schmidt et al., 2009) as well as in cancer (Pilotte et al., 2012). Increased anxiety also has been reported in mice deficient of TDO2 (Kanai et al., 2009) and an upregulation of TDO2 activity was observed in post-mortem analysis of the cortex of individuals with schizophrenia and bipolar disorder (Miller et al., 2006). In addition to the possible role of TDO2 in these conditions, only the differential regulation of downstream enzymes of the kynurenine and TPH pathway in the absence of TDO2 has been studied previously. The role of TDO2 outside of these two pathways has not been investigated before.

The second tryptophan-catabolising enzyme present in human and murine liver is IDO2. *In vivo*, the tryptophan catabolic activity of IDO2 in the liver is relatively low as the K_m of mouse IDO2 was more than 400 times higher than that of mouse IDO1 (Austin et al., 2010), suggesting lower affinity of IDO2 towards tryptophan. It has been proposed that some effects of IDO2 may be mediated through a mechanism unrelated to tryptophan catabolism/kynurenine production (Ball et al., 2014). To date, the physiological roles of

IDO2 have not been well established. Apart from some reports on the upregulation of *IDO2* seen in human cancer cell lines (Lob et al., 2009; Witkiewicz et al., 2009), nothing more is known on the specific role of human IDO2. Metz and colleagues more recently suggested that IDO2 plays a role in contact hypersensitivity, one that is mechanistically distinct from IDO1 (Metz et al., 2014). Its possible role as an important mediator of autoantibody production in autoimmune diseases also has been discussed (Merlo et al., 2014). However, nothing more is known about the role of IDO2 or the mechanism of its action.

In this chapter, microarray analysis of differentially expressed genes in mice deficient for one or two genes coding for tryptophan-catabolising enzymes, relative to their respective wild-type strain, was undertaken. As two tryptophan-catabolising enzymes, IDO2 and TDO2, are expressed in the liver, the possibility of a redundancy in their roles needed to be considered. With this in mind, we aimed to investigate whether the absence of either or both of these enzymes affects a distinct or overlapping set of genes, which may provide insights into the interaction between TDO2 and IDO2, as well as alternative roles they may be playing in the liver.

5.2 METHODS

5.2.1 Liver collection and homogenisation

Liver was collected from *Ido2^{+/+}*, *Ido2^{-/-}*, *Tdo2^{+/+}*, *Tdo2^{-/-}*, *Ido2^{+/+}Tdo2^{+/+}* and *Ido2^{-/-}Tdo2^{-/-}* mice and homogenised as described in Section 4.2.2.

5.2.2 RNA extraction

RNA extraction was performed as described in Section 4.2.3. Part of the RNA was used for cDNA synthesis (as described in Section 4.2.3) and the remainder was used for microarray analysis.

5.2.3 RNA quality assessment using the Nanodrop and Bioanalyser

The quality of RNA of each sample was assessed with a Nanodrop 2000 (Thermoscientific) and an RNA 6000 Nano Assay chip on an Agilent 2100 Bioanalyser as per the manufacturer's instructions. Samples with 260:280 and 260:230 ratios of above 1.8 as well as RNA Integrity Number (RIN) of above seven were deemed acceptable for microarray analysis (Thompson et al., 2007; Schroeder et al., 2006).

5.2.4 Illumina mouse (WG-6) microarray

Samples ($n \geq 5$) of each mouse strain were pooled for microarray analysis such that each individual mouse contributed an equivalent amount of RNA (200 ng) to the pooled sample with a final concentration of 100 ng/ μ L and total amount of 1000 – 1200 ng. Pooled samples were assayed by the Ramaciotti Centre for Genomics, UNSW, using the

Illumina mouse (WG-6) BeadChip array system according to the manufacturer's instructions.

5.2.5 Microarray data analysis

Illumina microarray data were extracted using Genome Studio with the addition of a Partek plug-in to facilitate the analysis of data on Partek software. Data were analysed using Partek Genomics Suite 6.6 software to identify differentially-expressed genes. Each array from a gene knockout mouse strain was compared to its respective control strain and a differentially-expressed gene was defined as having a greater than 2-fold change. As each array represented pooled samples no statistical test was performed. Instead, selected genes, *i.e.* those having at least a two-fold change in expression, were further validated using RT-qPCR on samples from individual mice with appropriate statistical tests. Partek Pathway software was used for detecting the different pathways implicated by the global genes that were differentially regulated in the samples.

5.2.6 RT-qPCR

The expression of some of the genes differentially regulated in the microarray analysis was validated by RT-qPCR. The reaction (20 μ L) contained 8 μ L cDNA and 0.1 μ mol/L of each primer in 1x KAPA SYBR Fast Universal qPCR Master Mix. Amplification was performed in a Rotorgene 3000 (Corbett Research) with 40 cycles of 95 °C for 15 sec followed by 60 °C for 45 sec. *Ywhaz* was used as the housekeeping gene. The relative expression of genes was calculated using the $\Delta\Delta$ Ct method with normalisation to *Ywhaz* (Livak and Schmittgen, 2001; Jusof et al., 2013). The primer sequences for the genes are listed in Table 5.1.

<i>Ywhaz</i>	5' TGTCACCAACCATTCCAACCTTG 3' 5' AACTGAGTGGAGCCAGAAAGA 3'
<i>Fam25c (2200001I15Rik)</i>	5' AAGCACGCTCTTCCAGTCTGAG 3' 5' TCCACTGCGTGAAGTCTGCTC 3'
<i>Bcl7c</i>	5' GAATTCGGCACGAGGCTCA 3' 5' TTCTCCCATCTCCGGACCTT 3'
<i>Bmf</i>	5' GCGGGCGTATTTTGGAAACA 3' 5' CAGGGTCCAGGGTGAAGAAC 3'
<i>Cdc37</i>	5' CACCGGGTTGGGGATACAAA 3' 5' GGTCACCCTCTGCCTCAAA 3'
<i>Cyp4a14</i>	5' TTGCTCACGAGCACACAGAT 3' 5' TCTTCTTCTGGCCTTCTGC 3'
<i>Ehd3</i>	5' CACATCTAGGCTCCGAGCAG 3' 5' GCAGTGCCCTATGGAGGTTT 3'
<i>Acot1</i>	5' GGTGCCAACATCACCTTTGG 3' 5' TTTCCCAACCTCCAAACCA 3'
<i>Acot3</i>	5' AGCTCTTGACCTTGCTGTCTG 3' 5' AGTCAATGGGCAGGGAGTTG 3'
<i>Acot4</i>	5' TCGGGTACATGCTTCGACAT 3' 5' GCGGAATCATGGTCTGCTTG 3'
<i>Lcn2</i>	5' AATGTCACCTCCATCCTGGTCA 3' 5' CCCTGGAGCTTGAACAAATG 3'
<i>Saa1</i>	5' ATCACCAGATCTGCCAGGA 3' 5' CCTTGGAAAGCCTCGTGAAC 3'
<i>Steap3</i>	5' ACCCAGGGTTAAGGAGAACCT 3' 5' ACTCCAGCTCACCAGGTCTA 3'
<i>Nrep (DOH4S114F)</i>	5' CAGGCCTGGTTCGCTACAA 3' 5' ATGAAAGGCAGGAGTGGACC 3'
<i>Gjb3</i>	5' CAGCCAGAGGGAGGCTTTAC 3' 5' CTGCTAGCCACACTTGCTCT 3'
<i>Moxd1</i>	5' ACAACGCAGAGTGGTCGATT 3'

	5' CTTTCTCGCACACCAGAGGT 3'
<i>Igfbp1</i>	5' CGCCGACCTCAAGAAATGGA 3' 5' GACACACCAGCAGAGTCCAG 3'
<i>G0s2</i>	5' CAAAGCCAGTCTGACGCAAG 3' 5' AACTGCCAGCACGTATAG 3'
<i>Ankar</i>	5' ACCTTCGGGAAAATTTAGCA 3' 5' GAACGAGCATCATCCTTGGC 3'
<i>Psmb5</i>	5' CCATGGGCACCATGATCTGT 3' 5' CGTAAGCATAACGGAGCCA 3'
<i>Adam33</i>	5' AAACCGAGATGCCTTCCCCT 3' 5' AGAATGTTGGGAGCTGGTAGCAC 3'
<i>Gdf15</i>	5' ACTCAGGACACAAGCGACAT 3' 5' GGGTCGCTGTTTCAGGCATT 3'
<i>8430408G22Rik</i>	5' GCCTGGATGACTACGTCAGG 3' 5' GCCTGGATGACTACGTCAGG 3'

Table 5.1. Lists of primers for genes of interest validated by RT-qPCR.

5.2.7 Statistical test

Data were log-transformed and the unpaired t-test was used to detect significant differences in expression of an individual gene in the knockout strain relative to its equivalent wild-type using GraphPad Prism software.

5.3 RESULTS

5.3.1 Genes differentially regulated in liver lysates of *Ido2*^{-/-} mice relative to *Ido2*^{+/+} and their associated pathways.

A total of 73 genes was found to be differentially regulated in the *Ido2*^{-/-} liver relative to its equivalent wild-type (*Ido2*^{+/+}) using microarray analysis. Of these, 10 genes have been withdrawn from PubMed Gene due to lack of sufficient evidence for their existence and were therefore not further considered. Of the remaining 63 genes that were found to be differentially regulated, 26 were upregulated (Table 5.2) and 37 downregulated (Table 5.3) in *Ido2*^{-/-} relative to *Ido2*^{+/+}. The functions or nomenclatures of five of these have yet to be validated. A list of pathways that were implicated by the genes that were differentially-regulated was generated by Partek Pathway and the top 30 pathways are listed in Table 5.4. Pathways related to lipid metabolism (elongation, biosynthesis and degradation of fatty acids as well as peroxisome proliferator-activated receptor [PPAR] signalling pathway) were implicated in the absence of *Ido2*, as were the purine metabolism, asthma, JAK-STAT, p53, chemokine and cytokine-cytokine receptor signalling pathways. All these pathways were to some degree related to insulin resistance, oxidative stress, the immune response or inflammation. Although these pathways were implicated by the Partek analysis, only a small number of genes in each pathway was detected as being differentially regulated. For example, although there are 22 genes involved in encoding proteins for the fatty acid elongation pathway, only one was found by microarray to be differentially regulated. Similarly, in purine metabolism, only 2 genes were differentially regulated although 173 genes are involved in this pathway.

Fourteen out of the 26 upregulated genes were evaluated by RT-qPCR (Table 5.5), out of which seven genes (*Xdh*, *Acot1*, *Cyp4a14*, *Ehd3*, *Gdf15*, *Igfbp1* and *Fam25c*) were found to be significantly upregulated in the *Ido2*^{-/-} liver compared to the wild-type. Among the list of downregulated genes, the expression of six genes was assessed by RT-qPCR and only *Moxd1* was significantly (p=0.0108) downregulated. *Xdh*, *Ehd3* and *Fam25c* (all p<0.0001) were most significantly upregulated in *Ido2*^{-/-} liver compared to wild-type, followed by *Acot1* (p<0.01), *Cyp4a14*, *Gdf15* and *Igfbp1* (p<0.05) (Fig. 5.1).

	Symbol	Definition	Chromosome	Fold-Change (<i>Ido2</i> ^{-/-} vs. <i>Ido2</i> ^{+/+})
1.	<i>Fam25c</i> (2200001I15Rik)	RIKEN cDNA 2200001I115 gene (2200001I15Rik), mRNA. Now known as Fam25c (family with sequence similarity 25, member C)	14	7.00087
2.	<i>Cyp4a14</i>	Cytochrome P450, family 4, subfamily a, polypeptide 14 (Cyp4a14), mRNA.	4	5.12023
3.	<i>Xdh</i>	Xanthine dehydrogenase (Xdh), mRNA.	17	3.7886
4.	<i>Ehd3</i>	EH-domain containing 3 (Ehd3), mRNA.	17	3.6572
5.	<i>G0s2</i>	G0/G1 switch gene 2 (G0s2), mRNA.	1	3.53331
6.	<i>Bcl7c</i>	B cell CLL/lymphoma 7C; associated with certain types of lymphoma and leukemias	7	3.19183
7.	<i>8430408G22Rik</i>	RIKEN cDNA 8430408G22 gene (8430408G22Rik), mRNA.	6	3.01383
8.	<i>Ankar</i>	Ankyrin and armadillo repeat containing (Ankar), mRNA.	1	3.01383
9.	<i>Psmb5</i>	Proteasome (prosome, macropain) subunit, beta type 5 (Psmb5), mRNA.	14	2.98575
10.	<i>Igfbp1</i>	Insulin-like growth factor binding protein 1 (Igfbp1), mRNA.	11	2.72639
11.	<i>Gdf15</i>	Growth differentiation factor 15 (Gdf15), mRNA.	8	2.54065
12.	<i>Tas2r125</i>	Taste receptor, type 2, member 125 (Tas2r125), mRNA.	6	2.46006
13.	<i>Bmf</i>	BCL2 modifying factor	2	2.45616
14.	<i>Cox7a2l</i>	Cytochrome c oxidase subunit VIIa polypeptide 2-like	17	2.42212
15.	<i>Yipf4</i>	Yip1 domain family, member 4 (Yipf4), mRNA.	17	2.39514
16.	<i>Cxcl1</i>	Chemokine (C-X-C motif) ligand 1 (Cxcl1), mRNA.	5	2.27302
17.	<i>Ppp1r3g</i> (1600032L17Rik)	Validated as <i>Ppp1r3g</i> (protein phosphatase 1, regulatory (inhibitor) subunit 3G)	13	2.2632
18.	<i>Gjb3</i>	Gap junction protein, beta 3 (Gjb3), mRNA.	4	2.2448
19.	<i>Supt16h</i>	Suppressor of Ty 16 homolog (S. cerevisiae) (Supt16h), mRNA.	14	2.19184
20.	<i>Lars2</i>	Leucyl-tRNA synthetase, mitochondrial (Lars2), nuclear gene encoding mitoc	9	2.1552

21.	<i>Krt1-2</i>	Keratin 32	11	2.14519
22.	<i>Ms4a2</i>	Membrane-spanning 4-domains, subfamily A, member 2 (<i>Ms4a2</i>), mRNA.	19	2.13687
23.	<i>Il13ra2</i>	Interleukin 13 receptor, alpha 2 (<i>Il13ra2</i>), mRNA.	X	2.12012
24.	<i>Prob1</i> (<i>Gm1614</i>)	PREDICTED: gene model 1614, (NCBI) (<i>Gm1614</i>), mRNA. Validated as proline rich basic protein 1 (<i>Prob1</i>)	18	2.12001
25.	<i>Itga9</i>	Integrin alpha 9 (<i>Itga9</i>), mRNA.	9	2.10595
26.	<i>Acot1</i>	Acyl-CoA thioesterase 1 (<i>Acot1</i>), mRNA.	12	2.01911

Table 5.2. Genes upregulated (n=26) in mouse liver lysates of *Ido2*^{-/-} (pooled from n=6) relative to *Ido2*^{+/+} (also pooled from n=6), where genes are ranked according to decreasing fold-change values as determined by Illumina microarray analysis. mRNA expression of genes in bold font subsequently was assessed further by RT-qPCR. Data were extracted and analysed using Partek Genomics Suite 6.6 software

	Symbol	Definition	Chromosome	Fold-Change (<i>Ido2</i> ^{-/-} vs. <i>Ido2</i> ^{+/+})
1.	<i>Adam33</i>	A disintegrin and metallopeptidase domain 33 (<i>Adam33</i>), mRNA.	2	-6.77354
2.	<i>Cdc37</i>	Cell division cycle 37 homolog (<i>S. cerevisiae</i>) (<i>Cdc37</i>), mRNA.	9	-5.49856
3.	<i>OTTMUSG00000010433</i>	Predicted gene, OTTMUSG00000010433 (OTTMUSG00000010433), mRNA.	4	-4.05319
4.	<i>Gadd45g</i>	Growth arrest and DNA-damage-inducible 45 gamma (<i>Gadd45g</i>), mRNA.	13	-3.8463
5.	<i>Moxd1</i>	Monooxygenase, DBH-like 1 (<i>Moxd1</i>), mRNA.	10	-3.79386
6.	<i>Cish</i>	Cytokine inducible SH2-containing protein (<i>Cish</i>), mRNA.	9	-3.68348
7.	<i>Lrrc18</i>	Leucine rich repeat containing 18 (<i>Lrrc18</i>), mRNA.	14	-3.5994
8.	<i>Lmln</i>	Leishmanolysin-like (metallopeptidase M8 family) (<i>Lmln</i>), mRNA.	16	-3.58725
9.	<i>Foxq1</i>	Forkhead box Q1 (<i>Foxq1</i>), mRNA.	13	-3.34803
10.	<i>Degs2</i>	Degenerative spermatocyte homolog 2 (<i>Drosophila</i>), lipid desaturase (<i>Degs2</i>)	12	-2.79156
11.	<i>Hhex</i>	Hematopoietically expressed homeobox (<i>Hhex</i>), mRNA.	19	-2.70547
12.	<i>Hist1h1c</i>	Histone cluster 1, H1c	13	-2.65215
13.	<i>Mela</i>	Melanoma antigen	8	-2.60853
14.	<i>Tom1</i>	Target of myb1 homolog (chicken) (<i>Tom1</i>), mRNA.	8	-2.59949
15.	<i>Phlda1</i>	Pleckstrin homology-like domain, family A, member 1 (<i>Phlda1</i>), mRNA.	10	-2.56321
16.	<i>Slbp</i>	Stem-loop binding protein (<i>Slbp</i>), mRNA.	5	-2.46028
17.	<i>Lrrc3b</i>	Leucine rich repeat containing 3B (<i>Lrrc3b</i>), mRNA.	14	-2.44217
18.	<i>Cisd2</i>	CDGSH iron sulfur domain 2 (<i>Cisd2</i>), mRNA.	3	-2.43887
19.	<i>Klf1</i>	Kruppel-like factor 1 (erythroid) (<i>Klf1</i>), mRNA.	8	-2.41683
20.	<i>Ccr4</i>	Chemokine (C-C motif) receptor 4 (<i>Ccr4</i>), mRNA.	9	-2.40598

21.	<i>Tmbim1</i> (2310061B02Rik)	Validated as (<i>Tmbim1</i>) transmembrane BAX inhibitor motif containing 1	1	-2.39888
22.	<i>Pde6h</i>	Phosphodiesterase 6H, cGMP-specific, cone, gamma (<i>Pde6h</i>), mRNA.	6	-2.38854
23.	<i>EG241041</i>	Predicted gene, EG241041 (EG241041), non-coding RNA.	1	-2.3572
24.	<i>Iqcf4</i>	IQ motif containing F4 (<i>Iqcf4</i>), mRNA.	9	-2.35017
25.	<i>Axud1</i>	AXIN1 up-regulated 1 (<i>Axud1</i>), mRNA.	9	-2.30655
26.	<i>Nhedc2</i>	Na ⁺ /H ⁺ exchanger domain containing 2 (<i>Nhedc2</i>), mRNA.	3	-2.27656
27.	<i>5033411D12Rik</i>	RIKEN cDNA 5033411D12 gene (5033411D12Rik), mRNA.	13	-2.26891
28.	<i>Mstn</i>	Myostatin (<i>Mstn</i>), mRNA.	1	-2.23966
29.	<i>C87499</i>	Expressed sequence C87499 (C87499), mRNA.	4	-2.19228
30.	<i>Ctse</i> (C920004C08Rik)	Validated as <i>Ctse</i> (cathepsin E)	1	-2.16718
31.	<i>Nrep</i> (D0H4S114)	DNA segment, human D4S114 (D0H4S114), mRNA. Now known as <i>Nrep</i> (Neuronal regeneration-related protein)	18	-2.14232
32.	<i>Per2</i>	Period homolog 2 (<i>Drosophila</i>) (<i>Per2</i>), mRNA. Also known as Period circadian clock 2	1	-2.14048
33.	<i>Asns</i>	Asparagine synthetase (<i>Asns</i>), mRNA.	6	-2.08855
34.	<i>Olf97</i>	Olfactory receptor 97 (<i>Olf97</i>), mRNA.	17	-2.06431
35.	<i>LOC100039496</i>	Predicted: hypothetical protein LOC100039496 (LOC100039496), mRNA.	8	-2.03371
36.	<i>Dusp1</i>	Dual specificity phosphatase 1 (<i>Dusp1</i>), mRNA.	17	-2.03146
37.	<i>Duoxa1</i>	Dual oxidase maturation factor 1 (<i>Duoxa1</i>), mRNA.	2	-2.02541

Table 5.3. Genes downregulated (n=37) in mouse liver lysates of *Ido2*^{-/-} mice (pooled from n=6) relative to *Ido2*^{+/+} (also pooled from n=6), where genes are ranked according to decreasing fold-change values as determined by Illumina microarray analysis. mRNA expression of genes in bold font subsequently was evaluated further by RT qPCR. Data were extracted and analysed using Partek Genomics Suite 6.6 Software.

	Pathway Name	No. genes in list	No. in pathway
1.	Caffeine metabolism	1	4
2.	Maturity onset diabetes of the young	1	21
3.	Fatty acid elongation	1	22
4.	Biosynthesis of unsaturated fatty acids	1	23
5.	Asthma	1	24
6.	Jak-STAT signaling pathway	2	147
7.	Alanine, aspartate and glutamate metabolism	1	30
8.	Energy Metabolism	2	155
9.	Circadian rhythm	1	31
10.	Purine metabolism	2	163
11.	Transcriptional misregulation in cancer	2	169
12.	Chemokine signaling pathway	2	170
13.	Fatty acid degradation	1	42
14.	Proteasome	1	43
15.	Aminoacyl-tRNA biosynthesis	1	44
16.	Drug metabolism - other enzymes	1	45
17.	Sphingolipid metabolism	1	46
18.	NOD-like receptor signaling pathway	1	55
19.	Legionellosis	1	56
20.	Taste transduction	1	60
21.	Cytokine-cytokine receptor interaction	2	238
22.	p53 signaling pathway	1	67
23.	Cardiac muscle contraction	1	68
24.	Fc epsilon RI signaling pathway	1	69
25.	MAPK signaling pathway	2	248
26.	Arrhythmogenic right ventricular cardiomyopathy (ARVC)	1	70
27.	Prolactin signaling pathway	1	71
28.	RNA degradation	1	72
29.	PPAR (peroxisome proliferator-activated receptor) signaling pathway	1	73
30.	Salmonella infection	1	75

Table 5.4. List generated by Partek Pathway of top 30 pathways implicated by genes differentially-regulated in *Ido2*^{-/-} (n=6, pooled sample) relative to *Ido2*^{+/+} (n=6, pooled sample) mouse liver lysates. mRNA expression of some genes involved in the pathways indicated with bold font subsequently was analysed further by RT-qPCR.

	Gene	Changes relative to <i>Ido2</i> ^{+/+}
1.	<i>Xdh</i>	+
2.	<i>Acot1</i>	+
3.	<i>Cyp4a14</i>	+
4.	<i>Ehd3</i>	+
5.	<i>Gdf15</i>	+
6.	<i>IgfbP1</i>	+
7.	<i>Fam25c</i>	+
8.	<i>Moxd1</i>	-
9.	<i>Cdc37</i>	ns
10.	<i>G0s2</i>	ns
11.	<i>Psmb5</i>	ns
12.	<i>Ankar</i>	ns
13.	<i>Adam33</i>	ns
14.	<i>Gjb3</i>	ns
15.	<i>Acot3</i>	ns
16.	<i>Acot4</i>	ns
17.	<i>Nrep</i>	ns
18.	<i>Bcl7c</i>	ns
19.	<i>Bmf</i>	ns
20.	<i>Ccr4</i>	ns
21.	<i>8430408G22Rik</i>	ns
22.	<i>Saa1</i>	ns
23.	<i>Lcn2</i>	ns

Table 5.5. Gene expression in *Ido2*^{-/-} relative to *Ido2*^{+/+} mouse liver, evaluated by RT-qPCR from the list of genes differentially regulated according to microarray analysis.

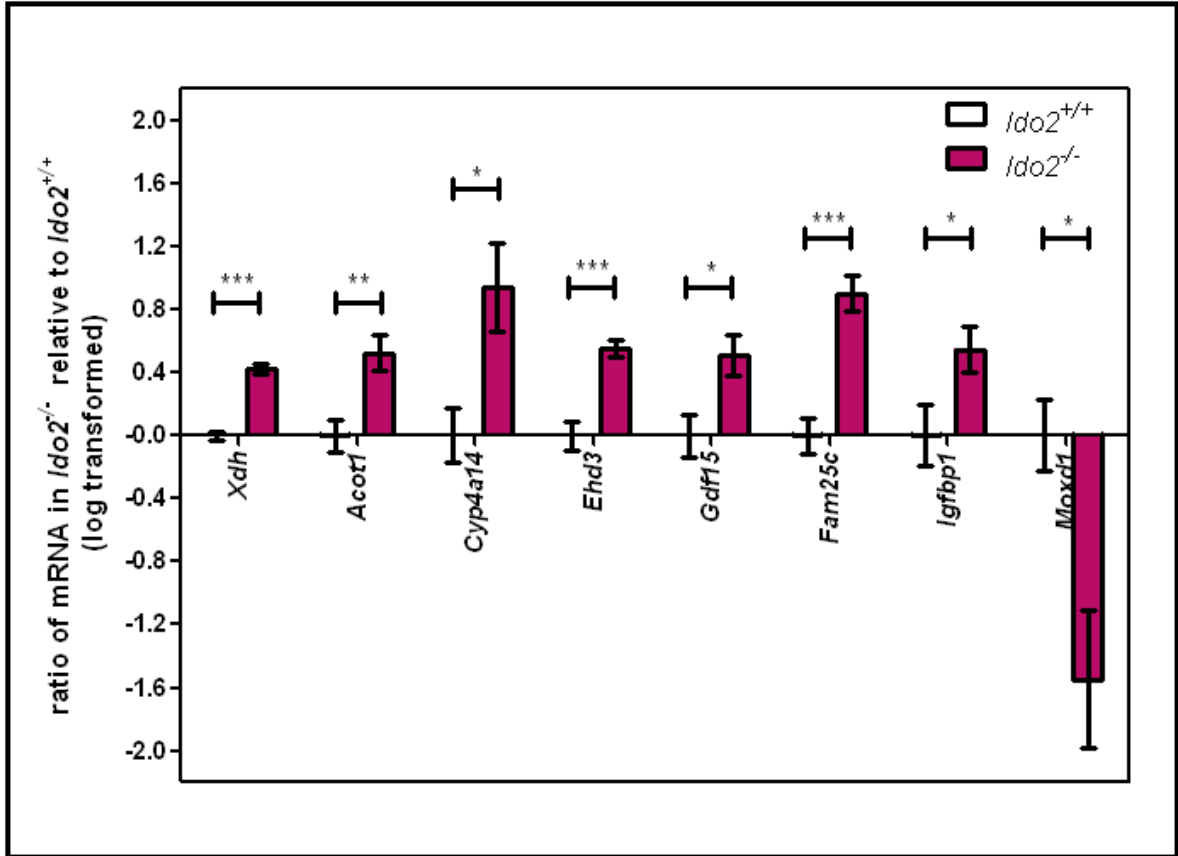


Figure 5.1. Genes that were significantly differentially regulated in *Ido2*^{-/-} mouse liver relative to *Ido2*^{+/+} as assessed by RT-qPCR. Three asterisks denote $p < 0.0001$, double asterisks $0.0001 < p < 0.001$, whereas one asterisk denotes $0.001 < p < 0.05$. $N = 6$ in each case.

5.3.2 Genes differentially regulated in liver lysates of *Tdo2*^{-/-} mice relative to *Tdo2*^{+/+} and the pathways implicated.

A total of 95 genes were differentially regulated in *Tdo2*^{-/-} compared to *Tdo2*^{+/+} mouse liver as assessed by microarray analysis. Of these, 15 genes were either not defined or withdrawn from the Entrez Gene (NCBI database for gene-specific information) (Maglott et al., 2005), leaving 80 potential genes for further validation. Six out of the 80 differentially-regulated genes in *Tdo2*^{-/-} mice were either predicted genes that have yet to be validated or validated genes whose function or role have yet to be classified.

When the list of differentially-regulated genes was assessed using the Partek Pathway software, lipid metabolism-related pathways were most commonly implicated in the absence of *Tdo2*, similar to what was observed in *Ido2*^{-/-} animals (Table 5.8). Four out of 70 genes associated with the PPAR signalling pathway were differentially regulated (*Acot3*, *Acot4*, *Cyp7a1*, *Cyp4a14*), while in the fatty acid elongation pathway, two out of 21 genes were differentially regulated (*Acot3* and *Acot4*).

The expression of six out of the 54 upregulated genes (Table 5.6) was further analysed by RT-qPCR and only *Cyp4a14* was found to be significantly upregulated using this technique. Of the 26 downregulated genes (*Tdo2* included) (Table 5.7), the expression of three was further assessed and only *Moxd1* was found to be significantly downregulated. In addition to these, the expression levels of seven genes that were differentially regulated in *Ido2*^{-/-} were also analysed in the *Tdo2*^{-/-} mice relative to the equivalent wild-type (*Tdo2*^{+/+}) (Table 5.9). However, none of these was found to be differentially regulated in *Tdo2*^{-/-} mouse liver. The expression patterns of both *Cyp4a14* and *Moxd1* were similar to their expression in *Ido2*^{-/-} mice, as *Cyp4a14* was significantly

upregulated ($p= 0.0488$) and *Moxd1* was significantly downregulated ($p=0.0268$) in *Tdo2*^{-/-} mouse liver relative to its wild-type counterpart (Fig. 5.2).

	Symbol	Definition	Chromosome	Fold-Change (<i>Tdo2</i> ^{-/-} vs. <i>Tdo2</i> ^{+/+})
1.	<i>Accn5</i>	Amiloride-sensitive cation channel 5, intestinal (<i>Accn5</i>), mRNA.	3	7.7863
2.	<i>Steap3</i>	STEAP family member 3, mRNA.	1	4.59505
3.	<i>Acot3</i>	Acyl-CoA thioesterase 3, mRNA.	12	4.34048
4.	<i>Rad54l2</i> (<i>Srisnf2l</i>)	Validated as <i>Rad54l2</i> (RAD54 like 2 (<i>S. cerevisiae</i>))	9	4.23291
5.	<i>Cyp7a1</i>	Cytochrome P450, family 7, subfamily a, polypeptide 1 (<i>Cyp7a1</i>), mRNA.	4	3.62802
6.	<i>Mr1</i>	Major histocompatibility complex, class I-related	1	3.23201
7.	<i>Cyp4a14</i>	Cytochrome P450, family 4, subfamily a, polypeptide 14 (<i>Cyp4a14</i>), mRNA.	4	3.1853
8.	<i>Myoz1</i>	Myozenin 1 (<i>Myoz1</i>), mRNA.	14	3.09084
9.	<i>Nrep</i> (<i>D0H4S114</i>)	DNA segment, human D4S114 (<i>D0H4S114</i>), mRNA. Now known as <i>Nrep</i> (Neuronal regeneration-related protein).	18	2.99895
10.	<i>Tmco2</i>	Transmembrane and coiled-coil domains 2 (<i>Tmco2</i>), mRNA.	4	2.69164
11.	<i>Agk</i>	Acylglycerol kinase (<i>Agk</i>), mRNA.	6	2.65009
12.	<i>Bmf</i>	BCL2 modifying factor	2	2.56819
13.	<i>Edn2</i>	Endothelin 2 (<i>Edn2</i>), mRNA.	4	2.55954
14.	<i>Rgs16</i>	Regulator of G-protein signaling 16, mRNA.	1	2.50613
15.	<i>Rshl2a</i>	Radial spokehead-like 2A, mRNA.	17	2.47821
16.	<i>Prei4</i>	Preimplantation protein 4, transcript variant 3, mRNA.	2	2.42365
17.	<i>Crtc2</i> (<i>4632407F12Rik</i>)	Validated as <i>Crtc2</i> (CREB regulated transcription coactivator 2)	3	2.39501

18.	<i>Tiam2</i>	T-cell lymphoma invasion and metastasis 2 (<i>Tiam2</i>), mRNA.	17	2.39175
19.	<i>Usp2</i>	Ubiquitin specific peptidase 2 (<i>Usp2</i>), transcript variant 2, mRNA.	9	2.38705
20.	<i>D1Ertd622e</i>	DNA segment, Chr 1, ERATO Doi 622, expressed (<i>D1Ertd622e</i>), mRNA.	1	2.28648
21.	<i>Mmd2</i>	Monocyte to macrophage differentiation-associated 2 (<i>Mmd2</i>), mRNA.	5	2.26695
22.	<i>Exph5</i> (<i>Slac2b</i>)	Validated as <i>Exph5</i> (exophilin 5)	9	2.24818
23.	<i>Pdk1</i> (<i>D530020C15Rik</i>)	Validated as <i>Pdk1</i> (pyruvate dehydrogenase kinase, isoenzyme 1)	2	2.23418
24.	<i>Cndp1</i>	Carnosine dipeptidase 1 (metallopeptidase M20 family) (<i>Cndp1</i>), mRNA.	18	2.20074
25.	<i>Per3</i>	Period circadian clock 3	4	2.19626
26.	<i>2610020H08Rik</i>	RIKEN cDNA 2610020H08 gene	7	2.16727
27.	<i>Pcsk4</i>	Proprotein convertase subtilisin/kexin type 4, mRNA.	10	2.14789
28.	<i>Pdk1</i>	Pyruvate dehydrogenase kinase, isoenzyme 1, nuclear gene encoding m	2	2.14561
29.	<i>P2ry1</i>	Purinergic receptor P2Y, G-protein coupled , mRNA.	3	2.14393
30.	<i>Hamp2</i>	Hepcidin antimicrobial peptide 2, mRNA.	7	2.14239
31.	<i>LOC194360</i>	PREDICTED: Mus musculus hypothetical LOC194360 (LOC194360), mRNA. Gm4744 predicted gene 4744	6	2.13307
32.	<i>BC016495</i>	cDNA sequence BC016495 (BC016495), mRNA.	19	2.13036
33.	<i>Sema4d</i>	Sema domain, immunoglobulin domain (Ig), transmembrane domain (TM) and short cytoplasmic domain, (semaphorin) 4D	13	2.12925
34.	<i>Prmt8</i>	Protein arginine N-methyltransferase 8 (<i>Prmt8</i>), mRNA.	6	2.12476
35.	<i>LOC666168</i>	PREDICTED: Mus musculus similar to cytochrome P450, family 4, subfamily a, polypeptide	4	2.10826
36.	<i>Olfr1212</i>	Olfactory receptor 1212 (<i>Olfr1212</i>), mRNA.	2	2.10776

37.	<i>Gm129</i>	Gene model 129, (NCBI) (Gm129), mRNA. XM_907670 XM_920513 XM_920520 XM_920	3	2.09879
38.	<i>Ell3</i>	Elongation factor RNA polymerase II-like 3 (Ell3), mRNA.	2	2.08376
39.	<i>Olf1412</i>	Olfactory receptor 1412	1	2.07623
40.	<i>Mll5</i>	Lysine (K)-specific methyltransferase 2E	5	2.06649
41.	<i>Emp2</i>	Epithelial membrane protein 2 (Emp2), mRNA.	16	2.05973
42.	<i>Plac9a</i> (MGC41689)	<i>Plac9a</i> (placenta specific 9a)	14	2.05766
43.	<i>Lrtm1</i>	Leucine-rich repeats and transmembrane domains 1, mRNA.	14	2.05602
44.	<i>Bhlhb9</i>	Basic helix-loop-helix domain containing, class B9, mRNA.	X	2.05379
45.	<i>Cyp2c54</i>	Cytochrome P450, family 2, subfamily c, polypeptide 54, mRNA.	19	2.04421
46.	<i>Fam108b</i>	Family with sequence similarity 108, member B, mRNA.	19	2.04263
47.	<i>Serpina6</i>	Serine (or cysteine) peptidase inhibitor, clade A, member 6, mR	12	2.03427
48.	<i>Acot4</i>	Acyl-CoA thioesterase 4, mRNA.	12	2.0333
49.	LOC100042018	PREDICTED: Mus musculus hypothetical protein LOC100042018 (LOC100042018), mRNA. Gm3627 predicted gene 3627	4	2.02483
50.	<i>Gjb3</i>	Gap junction protein, beta 3, mRNA.	4	2.02265
51.	<i>Olf1813</i>	Olfactory receptor 813, mRNA.	10	2.00893
52.	<i>Tnpo2</i>	Transportin 2 (importin 3, karyopherin beta 2b), mRNA.	8	2.00813
53.	<i>Gm906</i>	Gene model 906, (NCBI) (Gm906), mRNA.	13	2.00575
54.	<i>Rnf186</i>	Ring finger protein 186, mRNA.	4	2.0041

Table 5.6. Genes upregulated (n=54) in liver lysates of *Tdo2*^{-/-} mice (pooled from n=5) relative to *Tdo2*^{+/+} mice (pooled from n=6), where genes are ranked according to the fold-change values as assessed by Illumina microarray analysis. mRNA expression of genes in bold font subsequently was assessed further by RT-qPCR. Data were extracted and analysed using Partek Genomics Suite 6.6 Software.

	Symbol	Definition	Chromosome	Fold-Change (<i>Tdo2</i> ^{-/-} vs. <i>Tdo2</i> ^{+/+})
1.	<i>LOC666403</i>	PREDICTED: Mus musculus similar to ribosomal protein S2 (LOC666403), misc RNA.	11	-18.0343
2.	<i>Tdo2</i>	Tryptophan 2,3-dioxygenase, mRNA.	3	-11.1854
3.	<i>Saa2</i>	Serum amyloid A 2, mRNA.	7	-7.74417
4.	<i>Saa1</i>	Serum amyloid A 1, mRNA.	7	-5.85553
5.	<i>Tbkbp1</i>	TBK1 binding protein 1, mRNA.	11	-5.02919
6.	<i>Polr2c</i>	Polymerase (RNA) II (DNA directed) polypeptide C, mRNA.	8	-5.02492
7.	<i>Selenbp2</i>	Selenium binding protein 2, mRNA.	3	-4.26395
8.	<i>Erdr1</i>	Erythroid differentiation regulator 1, mRNA.	Y	-4.15712
9.	<i>Lcn2</i>	Lipocalin 2 (Lcn2), mRNA.	2	-3.66235
10.	<i>1700012A03Rik</i>	RIKEN cDNA 1700012A03 gene (1700012A03Rik), mRNA.	6	-3.45047
11.	<i>Atp4b</i>	ATPase, H ⁺ /K ⁺ exchanging, beta polypeptide (Atp4b), mRNA.	8	-3.17338
12.	<i>Ep</i>	Hermansky-Pudlak syndrome 1 homolog	19	-2.80116
13.	<i>Rps3a</i>	Ribosomal protein S3a, mRNA.	3	-2.79031
14.	<i>Hsd3b5</i>	Hydroxy-delta-5-steroid dehydrogenase, 3 beta- and steroid delta-isomerase	3	-2.77053
15.	<i>Sept12</i>	Septin 12 (Sept12), mRNA.	16	-2.6386
16.	<i>Szt2</i> (<i>BC059842</i>)	Seizure threshold 2, mRNA	4	-2.46092
17.	<i>Try4</i>	trypsin 4 (Try4), mRNA.	6	-2.41999
18.	<i>AU018091</i>	Expressed sequence AU018091 (AU018091), mRNA.	7	-2.35656
19.	<i>Moxd1</i>	Monooxygenase, DBH-like 1 (Moxd1), mRNA.	10	-2.28549

20.	<i>Syk</i>	Spleen tyrosine kinase (Syk), mRNA.	13	-2.24069
21.	<i>Olf414</i>	Olfactory receptor 414 (Olf414), mRNA.	1	-2.19227
22.	<i>Gab2</i>	Growth factor receptor bound protein 2-associated protein 2 (Gab2), mRNA.	7	-2.1782
23.	<i>Lbp</i>	Lipopolysaccharide binding protein (Lbp), mRNA.	2	-2.12514
24.	<i>Setbp1</i> (C130092E12)	Validated as <i>Setbp1</i> (SET binding protein 1)	18	-2.06874
25.	<i>Apcs</i>	Serum amyloid P-component (Apcs), mRNA.	1	-2.0158
26.	<i>B4galnt3</i>	Beta-1,4-N-acetyl-galactosaminyl transferase 3 (B4galnt3), mRNA.	6	-2.0082

Table 5.7. Genes downregulated (n=26) in mouse liver lysates of *Tdo2*^{-/-} mice (pooled from n=5) relative to *Tdo2*^{+/+} (pooled from n=6), where genes are ranked according to the fold-change values as analysed by Illumina microarray analysis. mRNA expression of genes in bold font subsequently was assessed further by RT-qPCR. Data were extracted and analysed using Partek Genomics Suite 6.6 Software.

	Pathway Name	No. genes in list	No. in pathway
1.	PPAR signaling pathway	4	70
2.	Fatty acid elongation	2	21
3.	Biosynthesis of unsaturated fatty acids	2	22
4.	Steroid hormone biosynthesis	3	80
5.	beta-Alanine metabolism	2	27
6.	Metabolic pathways	11	1131
7.	Fatty acid degradation	2	41
8.	Tryptophan metabolism	2	41
9.	Lysine degradation	2	45
10.	Fc epsilon RI signaling pathway	2	68
11.	Retinol metabolism	2	80
12.	Arachidonic acid metabolism	2	83
13.	Fc gamma R-mediated phagocytosis	2	84
14.	NF-kappa B signaling pathway	2	88
15.	Primary bile acid biosynthesis	1	14
16.	HIF-1 signaling pathway	2	103
17.	Butanoate metabolism	1	22
18.	Osteoclast differentiation	2	118
19.	Collecting duct acid secretion	1	24
20.	Propanoate metabolism	1	26
21.	RNA polymerase	1	26
22.	Histidine metabolism	1	28
23.	Circadian rhythm	1	31
24.	Linoleic acid metabolism	1	45
25.	Tuberculosis	2	172
26.	Arginine and proline metabolism	1	47
27.	Valine, leucine and isoleucine degradation	1	47
28.	Fatty acid metabolism	1	48
29.	Glycerolipid metabolism	1	55
30.	Ovarian steroidogenesis	1	57

Table 5.8. List of top 30 pathways implicated by genes differentially-regulated in *Tdo2*^{-/-} (n=5) relative to *Tdo2*^{+/+} (n=6) liver lysates. mRNA expression of some genes involved in the pathways shown with bolded font subsequently was evaluated further by RT-qPCR. The list was generated using microarray data analysed using Partek Pathway software.

	Gene	Changes relative to <i>Tdo2</i> ^{+/+}
1.	<i>Cyp4a14</i>	+
2.	<i>Moxd1</i>	-
3.	<i>Acot3</i>	ns
4.	<i>Steap3</i>	ns
5.	<i>Nrep</i>	ns
6.	<i>Acot4</i>	ns
7.	<i>Gjb3</i>	ns
8.	<i>Lcn2</i>	ns
9.	<i>Saa1</i>	ns
10.	<i>Xdh</i>	ns
11.	<i>Ehd3</i>	ns
12.	<i>Gdf15</i>	ns
13.	<i>Fam25c</i>	ns
14.	<i>IgfbP1</i>	ns
15.	<i>G0s2</i>	ns
16.	<i>Acot1</i>	ns

Table 5.9. Gene expression in *Tdo2*^{-/-} relative to *Tdo2*^{+/+}, analysed by RT-qPCR from the list of genes differentially regulated by microarray analysis.

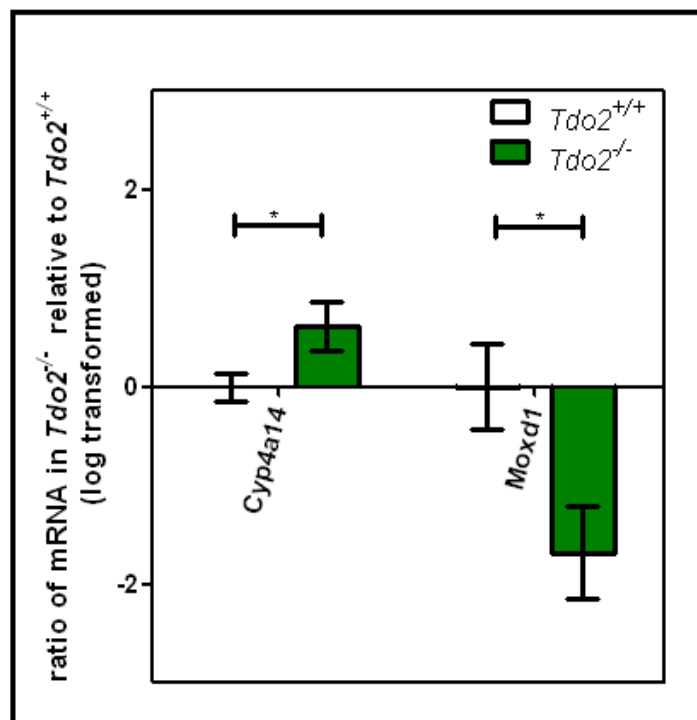


Fig. 5.2. *Cyp4a14* ($p=0.0488$) and *Moxd1* ($p=0.0268$) were significantly differentially regulated in *Tdo2*^{-/-} mouse liver lysates relative to *Tdo2*^{+/+}, where $p<0.05$, as assessed by RT-qPCR. $N \geq 5$ in each case.

5.3.3 Global gene expression in liver lysates of *Ido2^{-/-}Tdo2^{-/-}* mouse liver relative to *Ido2^{+/+}Tdo2^{+/+}* and the pathways implicated

A total of 123 global genes were differentially regulated in *Ido2^{-/-}Tdo2^{-/-}* mouse liver relative to its wild-type counterpart. However, only 111 genes were verifiable in Pubmed Gene. The remaining 12 genes were either not found or withdrawn from the database due to insufficient evidence. Two out of 66 upregulated genes (Table 5.10) were further validated by RT-qPCR and both *Lcn2* and *Saa1* were found to be significantly upregulated (Fig 5.3). From the list of genes downregulated in liver, three out of 45 genes were further validated (Table 5.11). *Nrep* and *Acot4* were significantly downregulated (Fig 5.3) in *Ido2^{-/-}Tdo2^{-/-}* mice as compared to their wild-type counterparts. The expression levels of an additional eight genes that were differentially regulated in either *Ido2^{-/-}* or *Tdo2^{-/-}* mice were also assessed in these double knockout animals (Table 5.13) and none of the genes tested were found to be significantly differentially regulated in *Ido2^{-/-}Tdo2^{-/-}* relative to *Ido2^{+/+}Tdo2^{+/+}*. Although *Cyp4a14* was upregulated in the liver tissue deficient for *Ido2* and *Tdo2* individually, this upregulation was not observed in liver tissue of mice deficient in both *Ido2* and *Tdo2*.

Pathways that were implicated by the differentially-regulated genes were again lipid metabolism-related genes, namely fatty acid elongation and biosynthesis of unsaturated fatty acids pathways. In the former pathway, three (*Elovl6*, *Acot3* and *Acot4*) out of 20 genes were differentially regulated. Three out of 70 genes related to the PPAR signalling pathway were also implicated due to the downregulation of *Cyp7a1* as well as *Acot3* and *Acot4* (Table 5.12). Other noteworthy pathways that were implicated by the differentially regulated genes in the *Ido2^{-/-}Tdo2^{-/-}* mouse liver were the

cytokine-related pathways such as the Jak-STAT signalling pathway and the malaria pathway.

	Symbol	Definition	Chr	Fold-Change (<i>Ido2</i> ^{-/-} <i>Tdo2</i> ^{-/-} vs. <i>Ido2</i> ^{+/+} <i>Tdo2</i> ^{+/+})
1.	<i>Saa2</i>	Serum amyloid A 2, mRNA.	7	18.0424
2.	<i>Lcn2</i>	Lipocalin 2, mRNA.	2	18.0381
3.	<i>Saa1</i>	Serum amyloid A 1, mRNA.	7	13.4714
4.	<i>Orm2</i>	Orosomucoid 2	4	6.16559
5.	<i>Trpa1</i>	Transient receptor potential cation channel, subfamily A, member 1	1	6.07971
6.	<i>Hcrt</i>	Hypocretin, mRNA.	11	6.07137
7.	<i>Tnfsf15</i>	Tumor necrosis factor (ligand) superfamily, member 15, mRNA.	4	5.73186
8.	<i>Jdp2</i>	Jun dimerization protein 2, mRNA.	12	5.35209
9.	<i>Taar7e</i>	Trace amine-associated receptor 7E, mRNA.	10	4.75828
10.	<i>Hhat1</i>	Hedgehog acyltransferase-like, mRNA.	9	4.69441
11.	<i>Accn5</i>	Amiloride-sensitive cation channel 5, intestinal, mRNA.	3	4.6359
12.	<i>Saa3</i>	Serum amyloid A 3, mRNA.	7	4.36359
13.	<i>7420426K07Rik</i>	RIKEN cDNA 7420426K07 gene, mRNA.	9	3.89435
14.	<i>Thbs2</i>	Thrombospondin 2 (Thbs2), mRNA.	17	3.14326
15.	<i>Bhlhb4</i>	Basic helix-loop-helix domain containing, class B4, mRNA.	2	3.13176
16.	<i>Incenp</i>	Inner centromere protein, mRNA.	19	3.12555
17.	<i>Myom1</i>	Myomesin 1, mRNA.	17	3.10907
18.	<i>Mt1</i>	Metallothionein 1, mRNA.	8	3.07366
19.	<i>Rnase10</i>	Ribonuclease, RNase A family, 10 (non-active), mRNA.	14	3.05756
20.	<i>Bglap1</i>	Bone gamma carboxyglutamate protein 1, transcript variant 1, mRNA	3	3.03914

21.	<i>Kctd1</i>	Potassium channel tetramerisation domain containing 1, mRNA. XM_97	18	2.99579
22.	<i>Ureb1</i>	Also known as Huwe1 (HECT, UBA and WWE domain containing 1)	X	2.95686
23.	<i>Atat1</i> (2610110G12Rik)	Validated as <i>Atat1</i> (alpha tubulin acetyltransferase 1)	17	2.94559
24.	<i>Ptbp2</i>	Polypyrimidine tract binding protein 2	3	2.81686
25.	<i>Il23a</i>	Interleukin 23, alpha subunit p19, mRNA.	10	2.7915
26.	<i>Myt1</i>	Myelin transcription factor 1, mRNA.	2	2.68917
27.	<i>Phf14</i> (4932409F11Rik)	Validated as <i>Phf14</i> (PHD finger protein 14)	6	2.68316
28.	<i>Adam33</i>	A disintegrin and metallopeptidase domain 33, mRNA.	2	2.60281
29.	<i>Prr7</i>	Proline rich 7 (synaptic), mRNA.	13	2.56205
30.	<i>Col23a1</i>	Collagen, type XXIII, alpha 1	11	2.56146
31.	<i>Cd276</i>	CD276 antigen, mRNA.	9	2.5208
32.	<i>Rhbdd3</i>	Rhomboid domain containing 3, mRNA.	11	2.51229
33.	<i>Fam64a</i> (6720460F02Rik)	RIKEN cDNA 6720460F02 gene (6720460F02Rik), mRNA. Also known as <i>Fam64a</i> (family with sequence similarity 64, member A)	11	2.50221
34.	<i>4932443I19Rik</i>	PREDICTED: RIKEN cDNA 4932443I19 gene, transcript variant 2 (4932443I19Rik)	8	2.49155
35.	<i>Lrrc30</i>	Leucine rich repeat containing 30, mRNA.	17	2.46812
36.	<i>Actc1</i>	Actin, alpha, cardiac muscle 1, mRNA.	2	2.44374
37.	<i>Srek1</i> <i>SRRP86</i>	Also known as <i>Srek1</i> (splicing regulatory glutamine/lysine-rich protein 1)	13	2.43596
38.	<i>Pif1</i>	PIF1 5'-to-3' DNA helicase homolog (<i>S. cerevisiae</i>) (<i>Pif1</i>), mRNA.	9	2.43347
39.	<i>Orly</i>	Validated as <i>Orly</i> (oppositely-transcribed, rearranged locus on the Y)	Y	2.41987

	(4930529H12Rik)			
40.	<i>Klhl24</i> (LOC100046372)	Validated as <i>Klhl24</i> (kelch-like 24)	16	2.41608
41.	<i>Lrp11</i>	Low density lipoprotein receptor-related protein 11, mRNA.	10	2.39417
42.	<i>Apcs</i>	Serum amyloid P-component, mRNA.	1	2.38877
43.	<i>Pmch</i>	Pro-melanin-concentrating hormone, mRNA.	10	2.38749
44.	<i>Scara5</i>	Scavenger receptor class A, member 5 (putative), mRNA.	14	2.34509
45.	<i>Vps37b</i>	Vacuolar protein sorting 37B (yeast), mRNA.	5	2.30027
46.	<i>Bcl6</i>	B-cell leukemia/lymphoma 6, mRNA.	16	2.2668
47.	<i>Nmnat2</i>	Nicotinamide nucleotide adenylyltransferase 2, mRNA.	1	2.25532
48.	<i>Zfp353</i>	Zinc finger protein 353, mRNA.	8	2.25321
49.	<i>Mtvr2</i>	Mammary tumor virus receptor 2, transcript variant 2, mRNA.	19	2.20975
50.	<i>Slc41a2</i>	Solute carrier family 41, member 2, mRNA.	10	2.17968
51.	<i>Olfir780</i>	Olfactory receptor 780, mRNA.	10	2.17843
52.	<i>Pnlip</i>	Pancreatic lipase, mRNA.	19	2.17612
53.	<i>Rnuxa</i>	RNA U, small nuclear RNA export adaptor, mRNA.	18	2.17186
54.	<i>Recq15</i>	RecQ protein-like 5, mRNA.	11	2.17092
55.	<i>Enho</i> (2310040A07Rik)	Validated as <i>Enho</i> (energy homeostasis associated)	4	2.14905
56.	<i>Reg3g</i>	Regenerating islet-derived 3 gamma, mRNA.	6	2.10547
57.	<i>Olfir11</i>	Olfactory receptor 11, mRNA.	13	2.10102
58.	<i>Rilpl1</i>	Rab interacting lysosomal protein-like 1, mRNA.	5	2.09711
59.	<i>Pira6</i>	Paired-Ig-like receptor A6, transcript variant 2, mRNA.	7	2.09638
60.	<i>Nnmt</i>	Nicotinamide N-methyltransferase	9	2.08966

61.	<i>Olfml3</i>	Olfactomedin-like 3, mRNA.	3	2.0817
62.	<i>Olf460</i>	Olfactory receptor 460, mRNA.	6	2.06781
63.	<i>Plekhg3</i> (BC030417)	Validated as <i>Plekhg3</i> (pleckstrin homology domain containing, family G)	12	2.05746
64.	<i>Myo1f</i>	Myosin IF, mRNA.	17	2.04977
65.	<i>Cdh3</i>	Cadherin 3, transcript variant 1, mRNA.	8	2.02131
66.	<i>BC048671</i>	cDNA sequence BC048671 (BC048671), mRNA.	6	2.00031

Table 5.10. Genes upregulated (n=66) in liver lysates of *Ido2^{-/-}Tdo2^{-/-}* mice (pooled from n=6) relative to *Ido2^{+/+}Tdo2^{+/+}* mice (pooled from n=6), where genes are ranked according to the fold-change values as evaluated by Illumina microarray analysis. mRNA expression of genes in bold font subsequently was assessed further by RT-qPCR. Data were extracted and analysed using Partek Genomics Suite 6.6 Software.

	Symbol	Definition	Chr	Fold-Change (<i>Ido2</i> ^{-/-} vs. <i>Ido2</i> ^{+/+})
1.	<i>Tdo2</i>	Tryptophan 2,3-dioxygenase, mRNA.	3	-12.7669
2.	<i>Selenbp2</i>	Selenium binding protein 2, mRNA.	3	-4.39624
3.	<i>Rps3a</i>	Ribosomal protein S3a, mRNA.	3	-4.23152
4.	<i>Sucnr1</i>	Succinate receptor 1, mRNA.	3	-4.09805
5.	<i>Cib3</i>	PREDICTED: Calcium and integrin binding family member 3, transcript varian	8	-3.99612
6.	<i>Acot3</i>	Acyl-CoA thioesterase 3, mRNA.	12	-3.26252
7.	<i>Thrsp</i>	Thyroid hormone responsive	7	-3.17541
8.	<i>Krt79</i>	Keratin 79, mRNA.	15	-3.13334
9.	<i>LOC669658</i>	PREDICTED: similar to melanoma antigen, mRNA.	18	-3.08308
10.	<i>Hsd3b5</i>	Hydroxy-delta-5-steroid dehydrogenase, 3 beta- and steroid delta-isomerase	3	-2.91359
11.	<i>Nrep</i> (<i>D0H4S114</i>)	DNA segment, human D4S114 (D0H4S114), mRNA. Now known as <i>Nrep</i> (Neuronal regeneration-related protein).	18	-2.84185
12.	<i>Ces1</i>	Carboxylesterase 1, mRNA.	8	-2.69296
13.	<i>Elovl6</i>	ELOVL family member 6, elongation of long chain fatty acids (yeast)	3	-2.64572
14.	<i>Hamp2</i>	Hepcidin antimicrobial peptide 2, mRNA.	7	-2.6271
15.	<i>Sult1c2</i>	Sulfotransferase family, cytosolic, 1C, member 2	17	-2.61046
16.	<i>Dbp</i>	D site albumin promoter binding protein, mRNA.	7	-2.60059
17.	<i>Ppp1r3g</i> <i>1600032L17Rik</i>	Validated as <i>Ppp1r3g</i> (protein phosphatase 1, regulatory (inhibitor) subunit 3G)	13	-2.54774

18.	<i>9130409I23Rik</i>	RIKEN cDNA 9130409I23 gene, mRNA.	1	-2.48669
19.	<i>Ptgds</i>	Prostaglandin D2 synthase	2	-2.44528
20.	<i>Cish</i>	Cytokine inducible SH2-containing protein, mRNA.	9	-2.44116
21.	<i>Krtap4-16</i> <i>OTTMUSG00000002196</i>	Predicted gene, OTTMUSG00000002196, mRNA. Also known as <i>Krtap4-16</i> (keratin associated protein 4-16)	11	-2.3801
22.	<i>Rgs16</i>	Regulator of G-protein signaling 16, mRNA.	1	-2.29596
23.	<i>Acot4</i>	Acyl-CoA thioesterase 4, mRNA.	12	-2.28633
24.	<i>Pdk1</i>	Pyruvate dehydrogenase kinase, isoenzyme 1, nuclear gene encoding m	2	-2.2666
25.	<i>Aacs</i>	Acetoacetyl-CoA synthetase, mRNA.	5	-2.23187
26.	<i>Cyp7a1</i>	Cytochrome P450, family 7, subfamily a, polypeptide 1, mRNA.	4	-2.22223
27.	<i>Abcc3</i>	ATP-binding cassette, sub-family C (CFTR/MRP), member 3, mRNA.	11	-2.22062
28.	<i>Ccrn4l</i>	CCR4 carbon catabolite repression 4-like (<i>S. cerevisiae</i>), mRNA.	3	-2.1556
29.	<i>Gstm6</i>	Glutathione S-transferase, mu 6	3	-2.15109
30.	<i>Mtfr1l</i> <i>2410166I05Rik</i>	Validated as <i>Mtfr1l</i> (mitochondrial fission regulator 1-like)	4	-2.13669
31.	<i>Mod1</i>	Malic enzyme, supernatant, mRNA.	9	-2.13567
32.	<i>A530017F20</i>	PREDICTED: Gm2447 predicted gene 2447	3	-2.11981
33.	<i>Necab1</i>	N-terminal EF-hand calcium binding protein 1, mRNA.	4	-2.10211
34.	<i>Srebf1</i>	Sterol regulatory element binding factor 1, mRNA.	11	-2.08173
35.	<i>Olig1</i>	Oligodendrocyte transcription factor 1, mRNA.	16	-2.07964
36.	<i>Pnpla3</i>	Patatin-like phospholipase domain containing 3, mRNA.	15	-2.05922
37.	<i>Ugt2a3</i>	UDP glucuronosyltransferase 2 family, polypeptide A3, mRNA.	5	-2.05416
38.	<i>Nudcd2</i>	NudC domain containing 2, mRNA.	11	-2.0449

39.	<i>Nampt</i>	Nicotinamide phosphoribosyltransferase, mRNA.	12	-2.03617
40.	<i>Slc17a8</i>	Solute carrier family 17 (sodium-dependent inorganic phosphate cotransport	10	-2.0341
41.	<i>Serpina7</i>	Serine (or cysteine) peptidase inhibitor, clade A (alpha-1 antiproteinase,	X	-2.03341
42.	<i>Bdh2</i>	3-hydroxybutyrate dehydrogenase, type 2, mRNA.	3	-2.03296
43.	<i>Cd1d1</i>	CD1d1 antigen, mRNA.	3	-2.02001
44.	<i>Acly</i>	ATP citrate lyase, mRNA.	11	-2.0157
45.	<i>Ces5</i>	Carboxylesterase 5, mRNA.	8	-2.00567

Table 5.11. Genes downregulated (n=45) in liver lysates of *Ido2^{-/-}Tdo2^{-/-}* mice (pooled from n=6) relative to *Ido2^{+/+}Tdo2^{+/+}* mice (pooled from n=6), where genes are ranked according to the fold-change values as assessed by Illumina microarray analysis. mRNA expression of genes in bold font subsequently was assessed further by RT-qPCR. Data were extracted and analysed using Partek Genomics Suite 6.6 Software.

	Pathway Name	No. genes in list	No. in pathway
1.	Fatty acid elongation	3	20
2.	Biosynthesis of unsaturated fatty acids	3	21
3.	Nicotinate and nicotinamide metabolism	3	27
4.	Metabolic pathways	16	1126
5.	Primary bile acid biosynthesis	2	13
6.	Butanoate metabolism	2	21
7.	Steroid hormone biosynthesis	3	80
8.	Drug metabolism - other enzymes	2	44
9.	Glycerolipid metabolism	2	54
10.	Synthesis and degradation of ketone bodies	1	7
11.	Metabolism of xenobiotics by cytochrome P450	2	62
12.	Drug metabolism - cytochrome P450	2	63
13.	Bile secretion	2	68
14.	PPAR signaling pathway	2	72
15.	Chemical carcinogenesis	2	86
16.	Vitamin digestion and absorption	1	23
17.	Ascorbate and aldarate metabolism	1	26
18.	Citrate cycle (TCA cycle)	1	31
19.	Pentose and glucuronate interconversions	1	33
20.	Nicotine addiction	1	36
21.	Pyruvate metabolism	1	37
22.	Fat digestion and absorption	1	37
23.	Porphyrin and chlorophyll metabolism	1	40
24.	Tryptophan metabolism	1	42
25.	Jak-STAT signaling pathway	2	147
26.	Malaria	1	43
27.	Cell adhesion molecules (CAMs)	2	151
28.	Sphingolipid metabolism	1	46
29.	ABC transporters	1	46
30.	Mineral absorption	1	46

Table 5.12. List of top 30 pathways implicated by genes differentially regulated in *Ido2*^{-/-} *Tdo2*^{-/-} (n=6) relative to *Ido2*^{+/+} *Tdo2*^{+/+} (n=6) mouse liver lysates. mRNA expression of some genes involved in the pathways, indicated with bold font, subsequently was assessed further by RT-qPCR. The list was generated using microarray data analysed with Partek Pathway software.

	Gene	Changes relative to <i>Ido2^{+/+}Tdo2^{+/+}</i>
1.	<i>Lcn2</i>	+
2.	<i>Saa1</i>	+
3.	<i>Acot4</i>	-
4.	<i>Nrep</i> (previously known as D0H4S114)	-
5.	<i>Xdh</i>	ns
6.	<i>Ehd3</i>	ns
7.	<i>Gdf15</i>	ns
8.	<i>Fam25c</i> (previously known as 2200001115Rik)	ns
9.	<i>IgfbP1</i>	ns
10.	<i>Acot1</i>	ns
11.	<i>Acot3</i>	ns
12.	<i>Cyp4a14</i>	ns

Table 5.13. Gene expression in *Ido2^{-/-}Tdo2^{-/-}* relative to *Ido2^{+/+}Tdo2^{+/+}* mouse liver, analysed by RT-qPCR from the list of genes differentially regulated in microarray analysis.

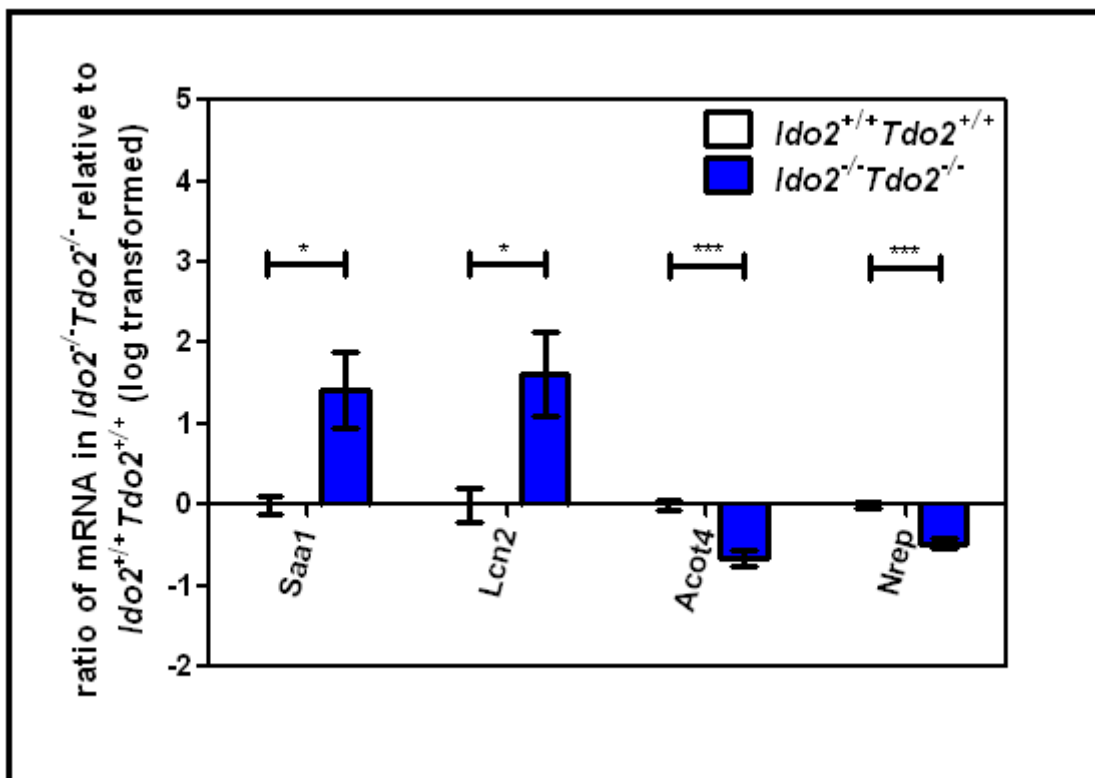


Fig. 5.3. *Saa1* and *Lcn2* were significantly upregulated while *Acot4* and *Nrep* were significantly downregulated in *Ido2^{-/-}Tdo2^{-/-}* mouse liver lysates relative to *Ido2^{+/+}Tdo2^{+/+}* as determined by RT-qPCR. A single asterisk denotes statistical significance of p < 0.05 whereas triple asterisks denote statistical significance of p < 0.0001. N = 6 in each case.

5.3.4 Overlapping gene expressions in *Ido2*^{-/-}, *Tdo2*^{-/-} and *Ido2*^{-/-} *Tdo2*^{-/-} mice relative to their equivalent wild-types.

Upon validation by RT-qPCR, the expression of only two genes were differentially regulated in the liver of both *Ido2*^{-/-} and *Tdo2*^{-/-} single knockouts, where *Cyp4a14* was upregulated (Fig. 5.4) and *Moxd1* was downregulated (Fig. 5.5). Very surprisingly, no genes were differentially expressed in all the three transgenic mouse strains deficient for one or two tryptophan-catabolising genes tested (relative to their respective wild-types), *i.e.* *Ido2*^{-/-}, *Tdo2*^{-/-} and *Ido2*^{-/-}*Tdo2*^{-/-} (Fig. 5.6).

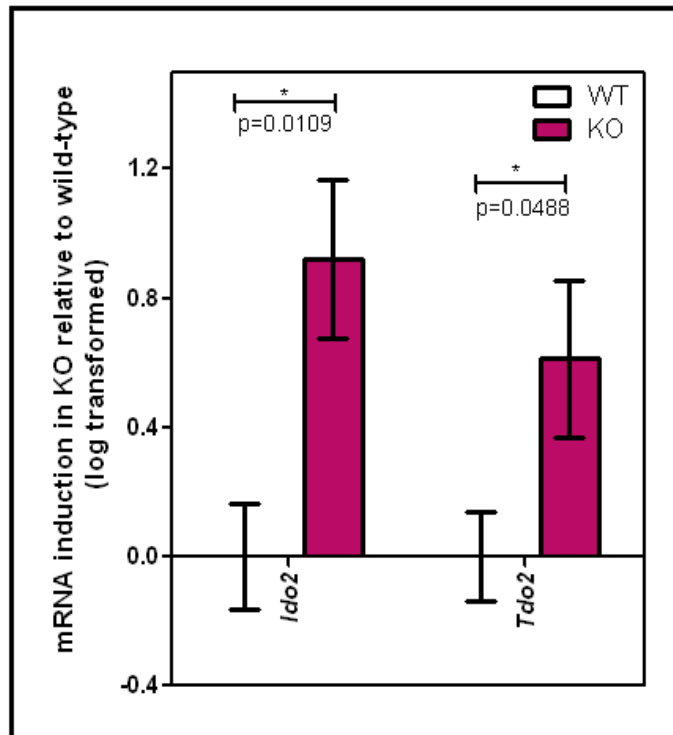


Fig. 5.4. *Cyp4a14* was upregulated in the liver of both *Ido2*^{-/-} and *Tdo2*^{-/-} single knockouts (n_≥5 each group) as determined by RT-qPCR. This upregulation, however, was not seen in the *Ido2*^{-/-}*Tdo2*^{-/-} double knockouts (Fig. 5.3).

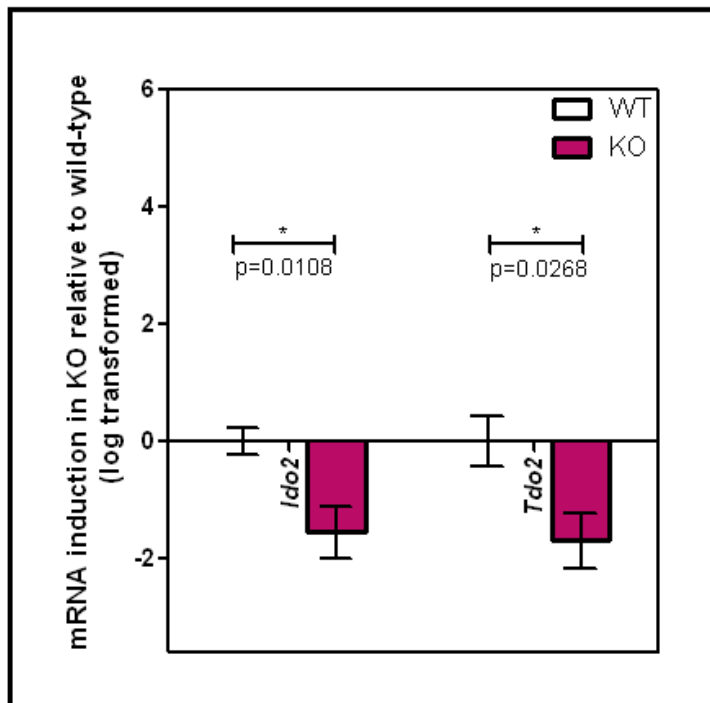


Fig. 5.5. *Moxd1* was downregulated in the liver of both *Ido2*^{-/-} and *Tdo2*^{-/-} single knockouts (n_≥5 each group) as determined by RT-qPCR. However, this gene was not differentially regulated in the *Ido2*^{-/-}*Tdo2*^{-/-} double knockouts (Fig. 5.3).

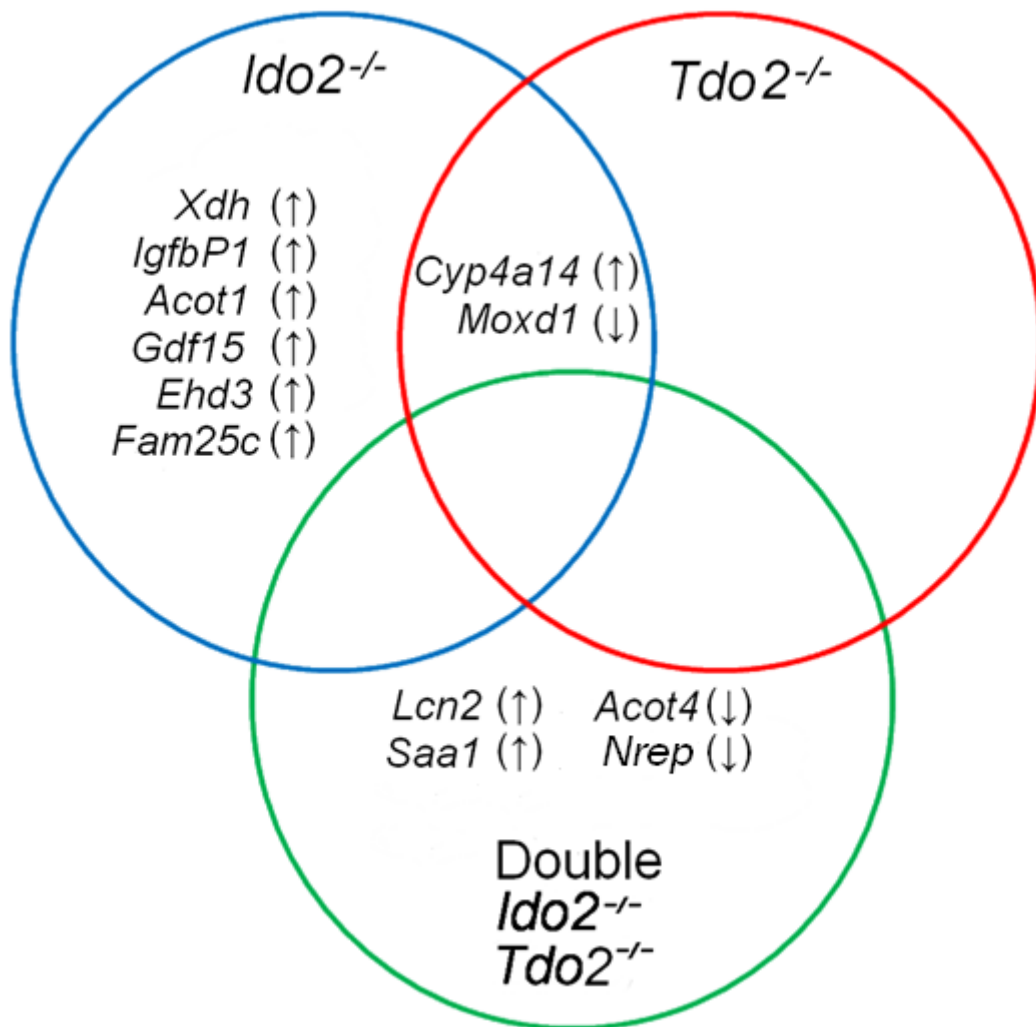


Fig. 5.6. Venn diagram depicting differentially-regulated genes in liver lysates of single *Ido2*^{-/-} and *Tdo2*^{-/-} as well as *Ido2*^{-/-}*Tdo2*^{-/-} double knockout mouse strains based on RT-qPCR analysis.

5.4 DISCUSSION

To validate the findings of the microarray analysis, the mRNA levels of genes that were differentially regulated (in microarray) in the liver lysates of mice deficient for one or two Trp-catabolic enzymes were assessed by RT-qPCR. Although we were interested to assess the protein levels and/or activity of the differentially regulated genes that were validated by RT-qPCR, time constraints meant that this could not be pursued. Therefore, in this section, the changes in mRNA levels will be discussed as indicative of changes in protein expression and/or activity. However, the above caveat needs to be kept in mind.

5.4.1 Differentially-regulated genes in *Ido2*^{-/-} mouse liver lysates relative to the wild-type counterparts (*Ido2*^{+/+})

The upregulation of eight (*Xdh*, *Acot1*, *Cyp4a14*, *Gdf15*, *Igf1bp1*, *Moxd1*, *Ehd3* and *Fam25c*) metabolism-related enzymes (Table 5.4) in the absence of *Ido2*^{-/-} indicates a potentially significant role for *Ido2* in maintenance of the normal metabolism of various elements in murine liver.

Xanthine dehydrogenase (*Xdh*) was one of the genes upregulated in *Ido2*^{-/-} mouse liver relative to *Ido2*^{+/+}. XDH, one of the interconvertible forms of xanthine oxidoreductase (XOR), is an NAD-dependent cytosolic dehydrogenase. Both XDH and xanthine oxidase (XO) are capable of metabolising hypoxanthine to xanthine, which is then converted to uric acid (Pacher et al., 2006). *In vivo*, XOR exists predominantly as XDH (Hille and Nishino, 1995; Hille, 2006) and is converted to XO by sulphhydryl oxidation or limited proteolysis (Pacher et al., 2006; Zhang et al., 1998). Conversion of XDH to XO has been

documented in ischaemia, atherosclerosis and inflammation (Tan et al., 1995; Houston et al., 1999; White et al., 1996). While both NAD^+ and O_2 can reduce XOR, XDH has a greater affinity for NAD^+ as its electron acceptor, generating NADH, while the converse is true for XO, with superoxide anions being the by-product (Nishino, 1994). Both human XDH and XO also have been shown to oxidise accumulated NADH and hypoxanthine, generating reactive oxygen species in the presence of oxygen. However, XDH prefers NADH as its reducing agent whereas XO favours hypoxanthine (Zhang et al., 1998). It also is known that the NADH generated by XDH can eventually be consumed by XDH itself to regenerate NAD^+ (Harris and Massey, 1997). NAD^+ is a common denominator between the kynurenine and purine pathways, since the former generates NAD^+ as one of its final products whereas XDH activation is dependent on NAD^+ and is upregulated by it. It is possible that the observed upregulation of *Xdh* in *Ido2*^{-/-} mouse liver relative to *Ido2*^{+/+} is indirectly caused by an elevation in XO or NAD^+ . However, if IDO2 plays a role in generating NAD^+ it is likely that NAD^+ deficiency, rather than accumulation, is observed in the absence of the enzyme. It previously has been reported that the absence of IDO2 did not cause any significant change in serum kynurenine levels (Metz et al., 2014), which suggests that it is likely that no changes in NAD^+ levels will be observed in the absence of IDO2.

A product of the XO-mediated reaction, superoxide anion radical, has been speculated to act as a cofactor that activates IDO1 in enterocytes, since the presence of the XO substrates hypoxanthine, inosine and adenosine was shown to increase IDO1 activity (Taniguchi et al., 1977). One possibility is that the relationship of XO with IDO2 is similar to that postulated between XO and IDO1, where products of XO activity, namely

superoxide anion radicals, result in increased activity of the IDO1 enzyme. The absence of IDO2 enzyme appears to lead to upregulation of XDH, which could attempt to compensate for the lack of IDO2 activity by driving the synthesis of its cofactor, superoxide anion radical. However, there is no evidence that superoxide can affect the expression of *Ido1* or *Ido2*. Furthermore, the claim that the superoxide anion radical is a physiological IDO1 cofactor was refuted by a recent publication (Maghzal et al., 2008). Maghzal and colleagues demonstrated that although inosine upregulated IDO1 activity, this was entirely dependent on the presence of methylene blue in the cell-free assay system and, when an XO inhibitor, oxypurinol, was added to the reaction, IDO1 activity was unaffected. This and other evidence showed that superoxide anion radical was not acting as a cofactor of the IDO1 enzyme in cells. It was suggested that cytochrome_{b5} was the physiological co-factor for IDO1. Subsequently, Austin and colleagues showed parallels with the activation of IDO2 in a cell-free system (Austin et al., 2010). Therefore, there are no grounds for postulating that the upregulation of *Xdh* seen in *Ido2*^{-/-} mouse liver is related to the superoxide anion radical-generating characteristic of XOR.

In fact, the relationship between XDH and IDO2 may not be within the kynurenine pathway but rather through an independent alternative pathway (Figure 5.7).

Hypoxanthine, one of the substrates of XDH (the gene upregulated in the absence of IDO2), was found increased at rest and after exercise in the plasma of obese subjects, relative to their healthy, normal body weight counterparts (Saiki et al., 2001) (Figure 5.7). *Xdh* mRNA and activity also were found upregulated in obese mice (Cheung et al., 2007). Regulatory T cells have been shown to play an important role in averting obesity, whereas macrophages are key mediators of inflammation and insulin resistance in

obesity (Feuerer et al., 2009; O'Rourke et al., 2012). In mouse models of obesity, increased numbers of CD8⁺ effector T cells, reduced numbers of CD4⁺ regulatory T cells and accumulation of macrophages in adipose tissue were noted (Nishimura et al., 2009; Yang et al., 2010). The former study also showed reduced cell counts of CD8⁺ and CD4⁺ T cells in peripheral blood. An important player in the activation and differentiation of regulatory T cells, which in turn suppress antigen-specific T cells, is IDO1 (Baban et al., 2009; Mellor and Munn, 2008; Sharma et al., 2007). This IDO1-dependent T cell regulation requires IDO2, since in the absence of IDO2 proliferation of T cells is not suppressed (Metz et al., 2014). It is interesting to speculate whether this role of IDO2 in IDO1-dependent T cell regulation may lead to obesity (Fig. 5.7). Given the relationship between IDO2 and T_{regs}, it seems important to ascertain its possible role in contributing to the onset of obesity, a condition in which T_{regs} are reportedly decreased and hypoxanthine levels elevated (Nishimura et al., 2009; Saiki et al., 2001; Yang et al., 2010). In addition to impaired activation of regulatory T cells as previously reported (Metz et al., 2014), levels of T_{regs} could be decreased in the plasma and/or liver in the absence of IDO2. Although Metz and colleagues found no difference in the numbers of T_{regs} in the spleen and lymph nodes in their experimental contact sensitivity model (Metz et al., 2014), it would be worth investigating whether their numbers are reduced in peripheral blood, adipose tissue and liver of *Ido2*^{-/-} mice. Absence of IDO2 conceivably could contribute to the onset of obesity, through the dysregulation of T_{reg} functions. This putative onset of obesity could then be marked by an increase in hypoxanthine levels, and consequently *Xdh* levels (Figure 5.7).

Another interesting feature of XOR is the induction of *Xdh* mRNA expression and the consequent conversion of XDH to XO, increasing XO activity, by proinflammatory cytokines like IFN γ , LPS, TNF, IL-1 and IL-6 (Reiners et al., 1990; Terao et al., 1992; Ghezzi et al., 1984; Ghezzi et al., 1986; Rinaldo et al., 1994; Pfeffer et al., 1994). IL-1, IL-6 and TNF are increased in the plasma and adipose tissues of obese humans (Jung and Choi, 2014; Ouchi et al., 2011) while, in addition to these cytokines, IFN γ also was found elevated in the visceral adipose tissue of obese humans (O'Rourke et al., 2009). Here, then, we speculate that the absence of IDO2 could be triggering the onset of obesity-related inflammation concurrent with increases in proinflammatory cytokines, such as IFN γ , IL-1, IL-6 and TNF, which in turn could be upregulating *Xdh* (Fig. 5.7). Whether the upregulation of *Xdh* seen in the liver of *Ido2*^{-/-} mice is contributed to by any of the proinflammatory cytokines will need to be further investigated by assessing their protein levels. Although no upregulation of these cytokines in liver was detected at the molecular level by microarray, it is worth considering that the cytokines might be produced elsewhere and carried in the circulation to the liver.

Hyperuricaemia, a product of increased XO activity, has been noted to be correlated with insulin resistance as well as dyslipidaemia (Facchini et al., 1991; Zavaroni et al., 1993; Pacher et al., 2006). These latter observations also are consistent with our hypothesis that the absence of IDO2 might trigger obesity, through T cell dysregulation (as discussed above) and release of inflammatory mediators that switch on XDH/XO, which could contribute to insulin resistance and dyslipidaemia (Fig. 5.7). This, however, will need to be further investigated by analysing inflammatory biomarkers, insulin and triglyceride levels in IDO2-deficient mice. Although in a previous report the absence of

IDO2 attenuated skin inflammatory responses and IFN γ , TNF and IL-6 levels in the ear (Metz et al., 2014), this could be a tissue-specific phenomenon. The expression of these inflammatory factors should be analysed at the protein level in liver tissues and blood samples of IDO2-deficient mice, but there was insufficient time to do this during this project.

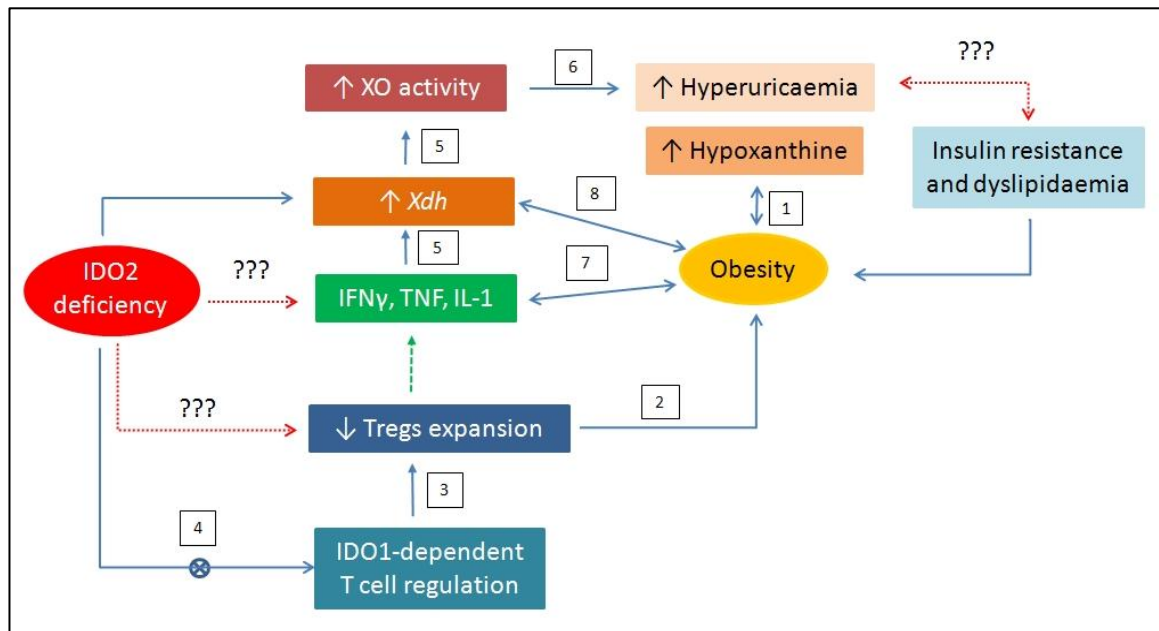


Fig. 5.7. Possible mechanism through which IDO2 deficiency leads to *Xdh* upregulation, and its implications. XO, xanthine oxidase; *Xdh*, xanthine dehydrogenase; IFN γ , interferon gamma; TNF, tumour necrosis factor; T_{regs}, regulatory T cells. Numbers in the diagram refer to the supporting references listed below. Blue solid lines denote established findings, green dashed lines implied outcomes and red dotted lines postulated relationships that have not been studied to date.

1. (Saiki et al., 2001)
2. (Feurerer et al., 2009; O'Rourke et al., 2012; Nishimura et al., 2009; Yang et al., 2010)
3. (Baban et al., 2009; Mellor and Munn, 2008; Sharma et al., 2007)
4. (Metz et al., 2014)
5. (Reiners et al., 1990; Pfeffer et al., 1994)
6. (Facchini et al., 1991; Pacher et al., 2006; Zavaroni et al., 1993)
7. (Jung and Choi, 2014; Ouchi et al., 2011)
8. (Cheung et al., 2007)

Another two genes that were differentially regulated in *Ido2*^{-/-} mouse liver lysates relative to *Ido2*^{+/+} were also related to lipid metabolism and/or decreased insulin bioavailability. *Cyp4a14* and *Acot1*, both upregulated in the absence of IDO2, are respectively involved in fatty acid degradation and biosynthesis of unsaturated fatty acid. These are lipid metabolic processes modulated by the PPAR α signalling pathway. Ligand-activated transcription factors, PPARs trigger the transcription of genes involved in a number of processes such as inflammation, as well as lipid and glucose metabolism (Patsouris et al., 2006). Most commonly, PPARs induce proliferation of peroxisomes, an organelle involved in fatty acid oxidation (Issemann and Green, 1990). The CYP4 family of cytochrome P450s catalyses metabolism of saturated branched chain and unsaturated fatty acids by ω -hydrolysis. In hepatocytes, the products are transported into peroxisomes as either free fatty acids or dicarboxylic acids following the hydrolysis, after which they are esterified by acyl-CoA synthetase. Upregulation of *Cyp4a14* mRNA has been reported in obese and/or nutritionally diabetic (Type II) mice (Cheng et al., 2008; Enriquez et al., 1999). However, this PPAR α -dependent gene was suggested to play a protective role in liver inflammation, where its upregulation was shown to increase lipid turnover and prevent steatohepatitis, a condition marked by inflammation and accumulation of fat in the liver (Ip et al., 2003). *Cyp4a14* expression also is increased in immune-deficient mice that lack mature T and B lymphocytes (Nyagode et al., 2012). The study by Nyagode and colleagues, however, did not differentiate between regulatory and cytotoxic T cells, which makes it difficult to ascertain whether the upregulation of *Cyp4a14* is related to the downregulation of T_{regs} specifically. As mentioned previously, a defect in IDO1-mediated T cell regulation was observed in IDO2-deficient mice (Metz et al., 2014). Unfortunately, a literature search did not yield much useful information on the effect of pro-inflammatory cytokines on

Cyp4a14. However, LPS, an endotoxin, does induce *Cyp4a14* expression in a TLR4-dependent manner in specific mouse strains (Chaluvadi et al., 2009) and this effect could be mediated through cytokines such as TNF, IL-1, IL-6, IL-8, the production of which is known to be stimulated by LPS (Segura et al., 2002; Harris et al., 2007). As *Cyp4a14* is increased in obese and/or diabetic mice as well as in immune deficient mice, we speculate that the upregulation of *Cyp4a14* could be caused by a dysregulation of T cells in this mouse strain, concurrent with an onset of obesity, a condition marked by release of proinflammatory cytokines and reduced levels of T cells in the blood (Jung and Choi, 2014; Nishimura et al., 2009). The upregulation of *Cyp4a14* in the absence of IDO2 also could be a biomarker for a possible obesity-related inflammation occurring in the liver of *Ido2*^{-/-} mice. However, as an increase of *Cyp4a14* mRNA expression in murine liver also was shown to prevent steatohepatitis – fatty liver disease – its upregulation in the liver of IDO2-deficient mice may play a protective role in averting the putative inflammation or the worsening of it. Our speculation of the onset of obesity-related inflammation in the absence of IDO2 contradicts an earlier report which suggested that the absence of IDO2 ameliorates inflammation, in the skin at least (Metz et al., 2014). In the face of these contradictory results, one has to consider that the phenomenon may be tissue-specific and requires more examination at the molecular, and especially protein, levels to acquire better understanding.

After fatty acids or dicarboxylic acids are esterified, they are hydrolysed further by acyl-CoA thioesterases (ACOTs) (Hardwick, 2008). *Acot1*, a gene upregulated in *Ido2*^{-/-} mouse liver, codes for ACOT1 (cytosolic acyl-coenzyme A thioesterase I), previously referred to as CTE-1 or ACH2. This enzyme hydrolyses long chain fatty acids into free fatty acids and

coenzyme A (CoA). In diabetic heart, an accumulation of long chain acyl CoA is seen. ACOT1 renders protection against cardiac dysfunction in the diabetic heart by reducing long chain fatty acid CoA overload by hydrolysing them (Yang et al., 2012). In the liver, *Acot1* is upregulated when treated with PPAR agonists (Yamada et al., 1994; Lindquist et al., 1998; Hunt et al., 1999) and in diabetic rats (Kurooka et al., 1971), suggesting that ACOT1 could be participating in lipid disposal by channelling free fatty acids to ω -oxidation when experiencing fatty acid overload (Yi et al., 2013; Pashaj et al., 2013; Hunt and Alexson, 2002). It previously was reported that PPAR α deficiency contributes to improved protection against diet-induced glucose intolerance and insulin resistance (Finck et al., 2005; Tordjman et al., 2001). Whether ACOT1 plays a similar protective role in diabetic or pre-diabetic liver to that reported in the heart (Yang et al., 2012), by removing long chain acyl-CoAs, thereby suppressing PPAR α signalling, is not yet known but is certainly a possibility. Collectively, these observations illustrate that PPAR α signalling can induce expression of ACOT1, which subsequently suppresses the activity of the pathway by removing the long chain acyl CoA agonists of PPAR α . An insufficiency in PPAR α signalling pathway activity has been shown to circumvent glucose intolerance and insulin resistance (Finck et al., 2005; Tordjman et al., 2001). This indicates that ACOT1 possibly plays a protective role against the lipid overload that may occur when PPAR α signalling is activated. Therefore, the upregulation of *Acot1* detected in the liver of *Ido2*^{-/-} mice could be pointing to a possible activation of PPAR α signalling. However, as ACOT1 then feeds back negatively to suppress this PPAR α signalling, it is more likely that its upregulation indicates a protective response to circumvent the long-chain fatty acid overload and onset of insulin resistance and glucose intolerance that otherwise would have been triggered by the activation of the PPAR α signalling pathway (Fig. 5.8). Although

there were no differences in the expression of other genes regulated by this signalling pathway in the liver of *Ido2*^{-/-} mice relative to WT, this does not necessarily mean that the PPAR α signalling pathway is unaffected by *Acot1*. It is possible that although their mRNA expression was unaffected in the liver of IDO2-deficient mice, the activity or the localisation of the proteins regulated by this pathway could be altered. Therefore, it would be relevant to analyse expression of proteins regulated by the PPAR α signalling pathway to better understand the mechanism behind the upregulation of *Acot1* and the involvement of PPAR α signalling in this tissue.

Thus, expression of *Cyp4a14* and *Acot1*, both coding for proteins involved in protective responses against diabetes (Cheng et al., 2008; Enriquez et al., 1999; Yang et al., 2012), was increased in the liver of *Ido2*^{-/-} mice. This could be a marker of inflammation leading to dyslipidaemia, eventually resulting in diabetes or obesity in these mice when older. However, due to time constraints, we were not able to measure plasma lipid or glucose levels or analyse cytokines in the liver tissue of these mice to confirm this possibility.

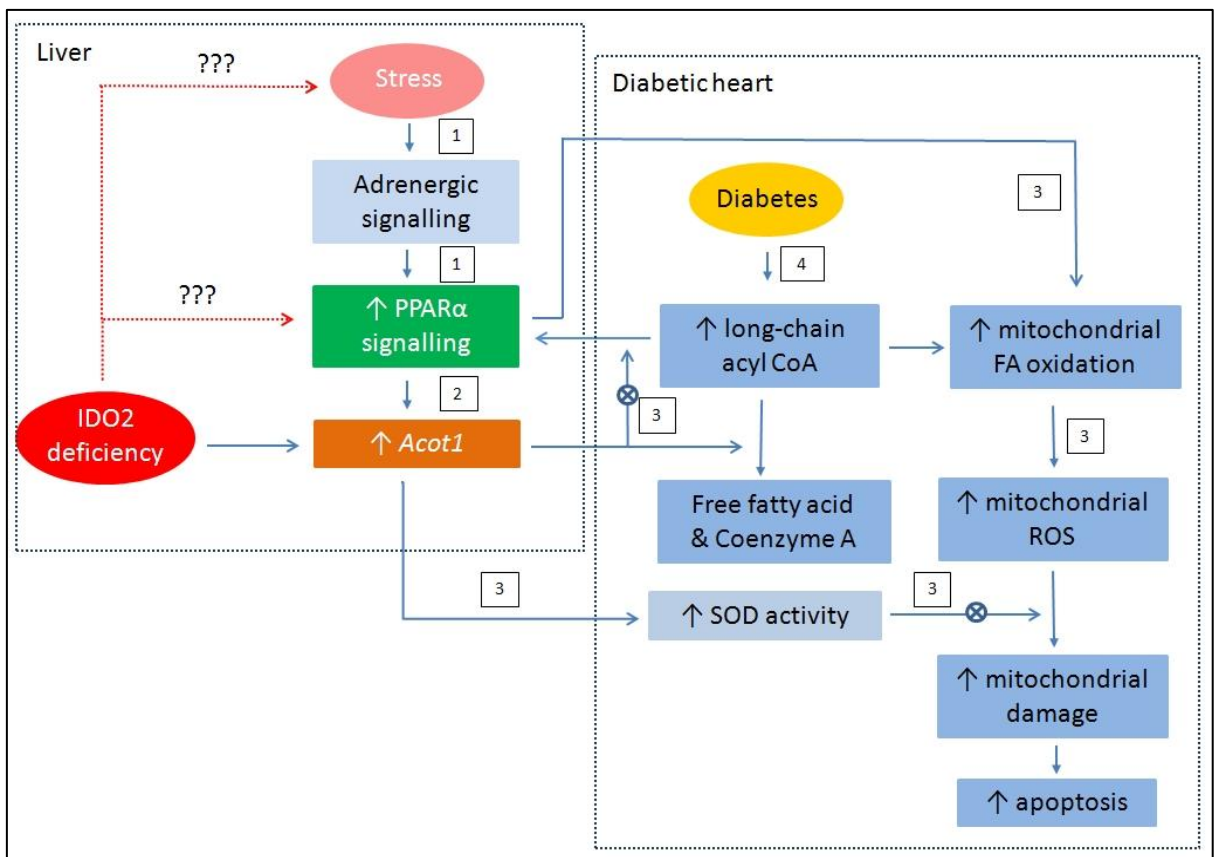


Fig. 5.8. Possible mechanism through which *Acot1* is upregulated in the liver of IDO2-deficient mice, and its implications. PPAR α , peroxisome proliferator-activated receptors alpha; *Acot1*, acyl CoA thioesterase 1; SOD, superoxide dismutase; FA, fatty acid; ROS, reactive oxygen species. Changes that have been demonstrated in liver and heart are indicated. Numbers on the diagram refer to the supporting references given below. Blue solid lines denote established findings and red dotted lines possible relationships that have not been studied to date.

1. (Konstandi et al., 2013)
2. (Hunt et al., 1999; Lindquist et al., 1998; Yang et al., 2012)
3. (Yang et al., 2012)
4. (Jagasia and McNulty, 2003)

Gdf15, also found upregulated in *Ido2*^{-/-} mouse liver lysates relative to *Ido2*^{+/+}, is the murine orthologue of the human macrophage inhibitory cytokine-1 (MIC-1). MIC-1/GDF15 were discovered as a divergent member of the transforming growth factor β (TGF β) superfamily (Bootcov et al., 1997). Although constitutively its expression is low, GDF15 is induced in malignancy or injury, leading to speculation about its possible role in inflammation (Fairlie et al., 1999; Welsh et al., 2003; Zimmers et al., 2006). More recently, its expression also was reported in adipocytes and it was shown to enhance the release of adiponectin, suggesting a possible role for this cytokine in modulation of adipose tissue function and insulin-sensitivity (Ding et al., 2009). Proinflammatory factors such as phorbol myristate acetate (PMA), IL-1, TNF and macrophage colony-stimulating factor (M-CSF), as well as the anti-inflammatory factor TGF- β , were shown to stimulate MIC-1 in human culture-derived macrophages (Fairlie et al., 1999; Bootcov et al., 1997). However, IFN γ and LPS were found to exert no effect on the expression of this protein. It has been suggested that its induction by proinflammatory cytokines acts as a protective factor, limiting later phases of macrophage activation (Bootcov et al., 1997; Xu et al., 2006), suggesting that it could contribute to the aversion of inflammation. IDO2 has been implicated in inflammation, since skin contact hypersensitivity responses were reduced in mice deficient for IDO2 (Metz et al., 2014). Increased levels of GDF15 also have been reported in rheumatoid arthritis and cancer (Brown et al., 2007; Brown et al., 2003; Brown et al., 2006; Koopmann et al., 2006) while IDO2 was shown to be critical for progression of autoimmune arthritis (Merlo et al., 2014).

Reports of *Ido2*^{-/-} mice exhibiting ameliorated inflammatory responses in skin contact hypersensitivity (Metz et al., 2014) and alleviation of rheumatoid arthritis (Merlo et al.,

2014) suggest that the absence of IDO2 mitigates inflammatory responses. This conflicts with our report on the upregulation of *Gdf15* in liver lysates of *Ido2*^{-/-} mice relative to its WT, which would be consistent with the occurrence of inflammation in the absence of IDO2. As speculated previously, this difference might indicate tissue-specific roles of IDO2, which could depend on the balance of other pro- and anti-inflammatory factors.

More recently, GDF15 was proposed as a marker for obesity and diabetes (Hong et al., 2014; Kempf et al., 2012) as there were markedly higher levels of serum GDF15 in obese than non-obese humans as well as in Type II diabetic patients compared to their healthy counterparts (Ding et al., 2009; Dostalova et al., 2009). Therefore, the upregulation of *Gdf15* seen in *Ido2*^{-/-} relative to *Ido2*^{+/+} mouse liver also could be indicative of obesity or Type II diabetes in older mice, with an underlying inflammation.

Two other genes that were differentially regulated in the liver tissue of *Ido2*^{-/-} mice are *Igfbp1* and *Moxd1*. Both genes were reported to be markers of reduced insulin bioavailability (Jee et al., 2007; Zhang et al., 2007a). Insulin-like growth factors (IGFs) are involved in maintaining glucose homeostasis by inhibiting glucose-stimulated insulin secretion at higher concentrations (Hill et al., 1997) and stimulating insulin release at lower concentrations (Guler et al., 1989). This action is modulated by IGFBPs (insulin-like growth factor binding proteins) through the sequestration of IGFs (Firth and Baxter, 2002), limiting their hypoglycaemic effects. Proinsulin and insulin were shown to both play a role in suppressing hepatic IGFBP1 and levels of this protein were reduced in obese and Type II diabetic humans (Conover et al., 1992; George et al., 2002; Kamoda et al., 2006). In Type I diabetes, insulin secretion is reduced and hence an upregulation of IGFBP1 has been reported (Hedman et al., 2004). The upregulation of *Igfbp1* seen in the

liver of *Ido2*^{-/-} mice could be hinting at the possibility of reduced levels of insulin and/or proinsulin. However, this observation does not agree well with the upregulation of the other genes, *Cyp4a14* and *Gdf15*, which were implicated in Type II diabetes, although XDH has been associated with both Type I and II diabetes (Butler et al., 2000; Desco et al., 2002).

Interestingly, the proinflammatory factors IL-1 β , IL-6 and TNF were found to induce IGFBP1 secretion in mice as well as in a human hepatoma cell line (Samstein et al., 1996; Fan et al., 1996; Fan et al., 1995). The upregulation of *Igfbp1* in the liver lysates of *Ido2*^{-/-} mice could indicate the presence of proinflammatory factors that trigger inflammation, which could eventually lead to obesity and/or diabetes. However, deeper investigation will need to be undertaken before this relationship can be established.

Unlike *Igfbp1*, which has been studied extensively since the 1970s, very little is known about *Moxd1*, a gene whose expression was downregulated in the liver of *Ido2*^{-/-} mice, as it was discovered only 17 years ago (Chambers et al., 1998). The literature shows that *Moxd1* expression was decreased in mice with reduced insulin bioavailability (Jee et al., 2007). Thus, downregulation of *Moxd1* and upregulation of *Igfbp1* both occur in cases of reduced insulin bioavailability, which is characteristic of diabetes and/or obesity, consistent with their expression pattern in *IDO2*^{-/-} mice.

Collectively, the absence of IDO2 switched on a number of genes that were reported to be inducible by pro-inflammatory factors such as IFN γ , TNF, IL-1 and IL-6. The cytokines IFN γ , TNF and IL-1 are secreted by macrophages (Darwich et al., 2009; Beuscher et al., 1990; Stow et al., 2009) whereas IL-6 is secreted secondary to the synthesis of the former two cytokines by either macrophages or local stromal cells (Uhlir and Whitehead, 1999;

Martin and Dorf, 1991). The fact that macrophages commonly express a number of the genes seen upregulated in the liver of *Ido2*^{-/-} mice is indeed interesting, considering that expression of IDO2 is readily detectable in these immune cells. The liver contains a high number of Kupffer cells of the macrophage lineage. Whether the secretion of proinflammatory cytokines is defective in IDO2-deficient macrophages can be further investigated. Although these pro-inflammatory factors were not differentially regulated when assessed by microarray, it is worth considering that such changes may occur at the protein level as they may be synthesised extrahepatically and transported into the liver. The genes *Xdh*, *Cyp4a14* and *Gdf15*, expression of which was upregulated in the liver of *Ido2*^{-/-} mice relative to the WT, were implicated previously in type II diabetes and/or obesity, although *Xdh* also has been implicated in Type I diabetes, as was *Igf1*. While *Moxd1* has not been implicated directly in diabetes, its downregulation in mice with reduced insulin bioavailability is consistent with a role for this gene in diabetes-related conditions. Collectively, this could be pointing to a possible role of IDO2 in regulating inflammation, a process that can result in Type II diabetes or obesity. However, this will need to be further confirmed by measuring cytokine levels in the serum as well as glucose, insulin, lipid, fatty acid and cholesterol levels in the *Ido2*^{-/-} mice relative to *Ido2*^{+/+}, which has not been studied to date. Although previously no significant differences were found in plasma glucose levels of *Ido2*^{-/-} mice relative to its WT, this was analysed in mice ranging from 8 to 23 weeks old (Bakmiwewa, 2011). Plasma glucose levels in a group of older mice (>30 weeks) may be a better indicator of the glycaemic status in these mice. The mechanism through which the absence of IDO2 might result in these conditions also would need to be investigated. Although there were no significant differences between the body weights of *Ido2*^{-/-} and WT mice up to 12 weeks of age (HJ

Ball, personal communication), it is possible that any dyslipidaemia that might be occurring in the *Ido2*^{-/-} animals has not by that age translated into changes in body weight, considering that the differentially regulated genes have been implicated in maturity onset, rather than juvenile, diabetes (Pacher et al., 2006; Enriquez et al., 1999; Hur, 2014). It would be interesting to determine body weight as well as blood glucose, insulin, cholesterol and lipid levels in older mice to determine whether any differences are evident.

The upregulation of *Ehd3* and *Fam25c*, however, does not seem to fall into any of the potential disease categories discussed above. *Ehd3* has been implicated in endocytic recycling and tubular structures, directing their motility (Galperin et al., 2002). It also has been suggested to play a role in cardiac membrane protein trafficking and physiology (Curran et al., 2014). In mice, *Ehd3* has been detected only in the brain and kidney (Galperin et al., 2002). The upregulation of *Ehd3* in the absence of IDO2 will require further in-depth analysis. The least understood protein in the list is *Fam25c*, which is a predicted sequence with no reports on its structure or role having been made thus far.

5.4.2 Differentially-regulated genes in *Tdo2*^{-/-} mouse liver lysates relative to the wild-type counterparts (*Tdo2*^{+/+})

Upon validation of the microarray results by RT-qPCR, only *Cyp4a14* and *Moxd1* were differentially regulated in *Tdo2*^{-/-} liver lysates compared to *Tdo2*^{+/+}. As discussed in the previous section (Section 5.4.1), *Cyp4a14* is involved in fatty acid degradation and an upregulation of this enzyme is seen in diabetic and obese mice, whereas *Moxd1* is

downregulated in rats with decreased insulin bioavailability, suggesting the possibility of a form of dyslipidaemia resulting in an onset of obesity and/or diabetes in *Tdo2*^{-/-}.

However, as there was no difference in the expression of the other lipid metabolism-related genes that were upregulated in *Ido2*^{-/-}, if any dyslipidaemia is occurring in *Tdo2*^{-/-}, it would be less severe than that previously postulated to occur in *Ido2*^{-/-}, relative to their respective wild-types, and likely occurring through a different pathway.

5.4.3 Differentially-regulated genes in liver lysates of *Ido2*^{-/-} *Tdo2*^{-/-} murine liver relative to *Ido2*^{+/+} *Tdo2*^{+/+}

In *Ido2*^{-/-}*Tdo2*^{-/-} liver, *Saa1* and *Lcn2* were significantly upregulated, while *Acot4* and *Nrep* were significantly downregulated, relative to *Ido2*^{+/+} *Tdo2*^{+/+}.

SAA1 is an acute phase apolipoprotein (Kushner, 1982), expressed primarily in the liver as a response to infection or inflammation (Marhaug and Dowton, 1994; Baumann et al., 1984; Marhaug et al., 1983; Benson and Cohen, 1979; Meek and Benditt, 1986). An elevation of SAA1 levels is seen in obese women and correlates positively with their body mass indices (BMI) (Yang et al., 2006). Correlation between excess body fat and metabolic as well as cardiovascular diseases has been well documented, although this link is not clear at the level of the molecular and cellular interactions (Yang et al., 2006). Increased expression of proinflammatory cytokines such as TNF and IL-6 was observed in adipose tissue of obese humans and mice, indicating an 'inflamed' tissue (Lehrke and Lazar, 2004; Emanuela et al., 2012; Nishimura et al., 2009). The expression of human SAA1 is inducible by IL-1, IL-6 and TNF (Thorn and Whitehead, 2002; Hagihara et al., 2004; Thorn et al.,

2004; Thorn et al., 2003). As none of these factors were upregulated at the mRNA level when analysed by microarray, we must consider the possibility that they are produced elsewhere, as discussed earlier. Elevated levels of SAA1 in the liver tissue of *Ido2^{-/-}Tdo2^{-/-}* suggest an underlying inflammation in the liver of these mice. As the liver is the main site of SAA1 production, inflammation could be occurring elsewhere, and circulating cytokines could be triggering the transcription of *Saa1* in the liver. The presence of inflammation in *Ido2^{-/-}* mice would need to be confirmed by examining protein levels of inflammatory cytokines in the liver and plasma. While no significant difference between the weight of the *Ido2^{-/-}Tdo2^{-/-}* and *Ido2^{+/+}Tdo2^{+/+}* mice was observed in both genders up to 12 weeks of age (HJ Ball, personal communication), in the case that an inflammatory pathology is observed through liver histology or analysis of inflammatory markers, there will need to be investigation as to whether this inflammation translates into obesity or diabetes in mature animals. Interestingly, *Saa1* was not upregulated in the *Ido2^{-/-}* mouse liver lysates relative to their equivalent wild-type. Although we speculated that onset of inflammation may be occurring in the liver of IDO2-deficient mice, the lack of *Saa1* upregulation in their liver suggests that the mechanism through which inflammation might be occurring in *Ido2^{-/-}* and *Ido2^{-/-}Tdo2^{-/-}* may differ.

Complementing *Saa1* expression is the upregulation of another gene, *Lcn2*, coding for an inflammatory marker and acute phase protein, lipocalin-2 (LCN), in the mutant mice deficient in genes coding for both Trp-catabolising enzymes. Expression of LCN2, also known as neutrophil gelatinase-associated lipocalin, is stimulated by IL-1 β , IL-6 and TNF in hepatocytes, similar to SAA1 (Borkham-Kamphorst et al., 2011). However, it was also shown that in the absence of *Lcn2*, the levels of the same proinflammatory cytokines

were elevated, suggesting that while *Lcn2* expression is induced by IL-1 β , IL-6 and TNF (Borkham-Kamphorst et al., 2013), the synthesis of LCN2 acts in a negative feedback manner protecting the liver from further injury by suppressing the expression of these cytokines. This finding is further consolidated by the observation that the absence of LCN2 (*Lcn2*^{-/-} mice) resulted in worsening of insulin resistance and glucose homeostasis, increasing inflammation in the tissue, leading to the proposal of a protective role for LCN2 during inflammation (Guo et al., 2010). In addition to this, *Lcn2* also has been reported to be upregulated in the adipose and liver tissue of genetically obese mice (Zhang et al., 2008). Similar to *Saa1*, despite being upregulated in *Ido2*^{-/-}*Tdo2*^{-/-} liver compared to *Ido2*^{+/+}*Tdo2*^{+/+}, there were no significant differences in the levels of *Lcn2* in the liver of *Ido2*^{-/-} mice relative to its wild-type. First and foremost, whether 'true' inflammation is occurring in these liver tissues deficient for two Trp-catabolising enzymes will need to be confirmed by liver histology as well as analysis of LCN2 and inflammatory cytokine protein expression. As speculated previously, despite the possible inflammatory onsets that could be occurring in the liver tissues of both *Ido2*^{-/-} and *Ido2*^{-/-}*Tdo2*^{-/-} mice, the inflammation-related genes that were dysregulated in these animals differ, suggesting that the mechanisms through which inflammation might occur are likely to be distinct.

Two genes that were downregulated in *Ido2*^{-/-}*Tdo2*^{-/-} liver compared to their equivalent wild-types were *Acot4* and *Nrep*. Although both ACOT1 and ACOT4 hydrolyse fatty acids to form free fatty acids, they hydrolyse different types of fatty acid chains. Described for the first time in 2005 (Westin et al., 2005), the latter is responsible for catabolising medium chain fatty acids such as succinyl CoA into free fatty acids via ω -oxidation, whereas the former does so more with long chain fatty acids via β -oxidation (Hunt et al.,

2012; Westin et al., 2005). There are no reports on factors that regulate ACOT4. Therefore, the downregulation of *Acot4* in *Ido2^{-/-}Tdo2^{-/-}* mouse liver in contrast to the upregulation of *Acot1* seen in single *Ido2^{-/-}* is perplexing, in view of the differential regulation of other inflammation-related genes. We can only speculate that some form of dysregulation of lipid metabolism could be occurring. However, the process that is leading to this difference in regulation will need to be studied in detail before any conclusions can be made concerning the mechanisms involved.

Nrep, also known as *DOH4S114* and *P311*, was reported to be expressed constitutively in hepatocytes, liver sinusoidal endothelial cells and in activated hepatic stellate cells (Guimaraes et al., 2015). Apart from its earlier reported roles in neuronal regeneration (Fujitani et al., 2004) and distal lung generation (Zhao et al., 2006), *Nrep* also has been shown to upregulate a number of genes involved in lipid synthesis and metabolism, increase cellular cholesterol and triglyceride level and induce lipid droplet accumulation mediated by retinoic acid (Leung et al., 2008). Plasma *Nrep* is downregulated postprandially in rats fed with an olive oil-rich diet (Martinez-Beamonte et al., 2011). This could be suggesting a role for NREP in regulating lipid homeostasis in the liver. If the downregulation of *Nrep* seen in *Ido2^{-/-}Tdo2^{-/-}* mouse liver relative to *Ido2^{+/+}Tdo2^{+/+}* is also seen at the protein level, the decrease could be a protective response to control the production of cholesterol and triglyceride. Again, due to time constraints, we were not able to confirm the expression of *Nrep* at the protein level. Further investigations will need to be done to determine whether dyslipidaemia and inflammation occur in *Ido2^{-/-}Tdo2^{-/-}* mouse liver.

5.4.4 Genes that were differentially expressed in *Ido2*^{-/-}, *Tdo2*^{-/-} and *Ido2*^{-/-} *Tdo2*^{-/-} mouse liver relative to the equivalent wild-types.

There were only two genes (*Cyp4a14*, *Moxd1*) whose differential expression was similar in the liver lysates of both *Ido2*^{-/-} and *Tdo2*^{-/-} mice relative to their equivalent WT (Fig. 5.9). Other genes such as *Xdh*, *Acot1*, *Gdf15*, *Igf1*, *Ehd3* and *Fam25* were upregulated only in the liver of *Ido2*^{-/-} mice. Similarly, *Saa1*, *Lcn2*, *Acot4* and *Nrep* were differentially regulated only in the liver of *Ido2*^{-/-} *Tdo2*^{-/-} mice, with no changes in expression in either *Ido2*^{-/-} or *Tdo2*^{-/-} animals. Therefore, it is likely that the mechanism through which TDO2 and IDO2 may exert their putative effects on inflammation, lipid and/or glucose metabolism are different. Upon RT-qPCR validation, there were a greater number of genes that were differentially regulated in the absence of IDO2 than there was in the absence of TDO2 or IDO2 and TDO2 together. This could be suggesting that the absence of IDO2 may exert a greater effect on inflammation in the liver, if there is any, than the absence of either TDO2 alone or both IDO2 and TDO2. Whether this inflammation is actually occurring and if it could lead to obesity or Type II diabetes will need to be further investigated by looking at cytokine levels in these genetically-modified mice, as well as insulin, glucose and lipid metabolism.

Surprisingly, there was no common gene that was regulated in a similar manner in all the three transgenic mouse strains deficient for one or two Trp-catabolising enzymes (Fig. 5.6). This further consolidates the view that while the absence of TDO2 and IDO2 individually may result in similar outcomes, such as obesity and/or diabetes as postulated here, the mechanism leading to this outcome differs between the two cases.

5.4.5 RT-qPCR assessment of genes differentially expressed according to microarray analysis in IDO2- and/or TDO2-deficient mice

Despite the relatively high number of genes reported to be differentially regulated in the liver lysates of *Ido2*^{-/-}, *Tdo2*^{-/-} and *Ido2*^{-/-}*Tdo2*^{-/-} mice relative to their equivalent wild-types by microarray analysis, only a fraction was further assessed by RT-qPCR due to time constraints. Out of these re-assessed genes, only a small number was validated, as shown in Table 5.14.

Mouse strain	Percentage of genes assessed by RT-qPCR (total number of genes assessed by RT-qPCR / total number of genes differentially regulated in microarray analysis)	Percentage of genes validated by RT-qPCR (total number of genes validated by RT-qPCR / total number of genes differentially regulated in microarray analysis)	Percentage genes with the same outcome in RT-qPCR analysis as microarray analysis
<i>Ido2</i> ^{-/-}	31.7 % (20/63)	12.7 % (8/63)	40.0 % (8/20)
<i>Tdo2</i> ^{-/-}	11.2 % (9/80)	2.5 % (2/80)	22.2 % (2/9)
<i>Ido2</i> ^{-/-} <i>Tdo2</i> ^{-/-}	4.5 % (5/111)	3.6% (4/111)	80.0 % (4/5)

Table 5.14. Percentage of genes assessed by RT-qPCR from the total number of genes differentially regulated by Illumina microarray analysis

In some cases, a difference was seen in the fold expression of genes differentially expressed in the liver of *Ido2*^{-/-}, *Tdo2*^{-/-} and *Ido2*^{-/-}*Tdo2*^{-/-} mice relative to their equivalent wild types by RT-qPCR analysis that did not attain statistical significance. As we were using pooled samples in microarray analysis, what seemed like a substantial change in gene expression in the liver of *Ido2*^{-/-}, *Tdo2*^{-/-} and *Ido2*^{-/-}*Tdo2*^{-/-} mice relative to their equivalent wild-type was not statistically significant in fold-change when assessed in

samples from individual animals by RT-qPCR. Such was the case for *G0s2*, *Psmb5* and *Ccr4* expression in *Ido2*^{-/-}, *Acot3*, *Nrep* and *Saa1* in *Tdo2*^{-/-} and *Acot3* in *Ido2*^{-/-}*Tdo2*^{-/-} mice relative to their respective wild-type. In some cases, the presence of an individual mouse outlier within the pooled sample may have resulted in the detection of falsely 'upregulated' or 'downregulated' genes by microarray analysis.

Finally, there were quite a number of genes with very low expression, which could contribute to 'noise' in microarray analysis. A small change in these genes can cause large differences in fold expression when assessed by microarray analysis. *Bcl7*, *Bmf* and *Cdc* are some of these genes that were expressed at very low levels in liver lysates when analysed by RT-qPCR, yet were indicated as being differentially regulated by microarray analysis.

These observations reiterate the need to further assess genes that are apparently differentially-regulated in microarray samples, in order to validate the expression patterns observed. Initially this can be achieved by RT-qPCR. This is even truer when performing microarray analysis using pooled samples, a common procedure given the high cost of the process. Using pooled samples for microarray analysis and validating the differentially-regulated genes by RT-qPCR is perhaps the most cost-effective method to study global gene expression in various conditions.

5.4.6 Pathways implicated in mice deficient for one or two Trp-catabolising enzymes

Although quite a number of pathways were implicated in *Ido2*^{-/-}, *Tdo2*^{-/-} and *Ido2*^{-/-}*Tdo2*^{-/-} mouse liver lysates, the percentage of genes differentially regulated in each pathway (number of genes differentially regulated in the pathway / total number genes involved in the pathway) in these genetically-modified mice was rather low. The question why the absence of IDO2, TDO2 or both only affects the expression of a low number of genes per pathway, while the others remain unaffected, requires deeper investigation. Certainly, there is considerable redundancy between pathways as defined by the Partek analysis software and, indeed, between signal transduction pathways in biological systems. For example, based on the genes differentially regulated in the liver of *Ido2*^{-/-}*Tdo2*^{-/-} mice, the “malaria pathway” was implicated by the Partek Pathway software. However, this “pathway” comprises a number of other pathways such as JAK-STAT and Trp metabolism, both of which were separately listed as involved pathways by the software.

Only a small number of genes from each individual pathway was implicated in the absence of IDO2 and TDO2, and most of the genes affected by the absence of one or two of the enzymes differed. While this could be a result of the different backgrounds of *Ido2*^{-/-}, *Tdo2*^{-/-} and their equivalent wild-type strains, it also could be suggesting that the absence of either could be inducing distinct key inflammatory mediators, which then affect the expression of different genes from a variety of pathways. This suggests that the mechanisms through which either IDO2 or TDO2 contribute to inflammation (if this does occur) also are likely to be different.

5.5 SUMMARY

In conclusion, the absence of either of the tryptophan-catabolising enzymes seems to impact upon the expression of genes that have been implicated in inflammation, dyslipidaemia, diabetes and/or obesity (Fig 5.9), suggesting that IDO2 and TDO2 could be involved in lipid homeostasis and inflammation in the liver.

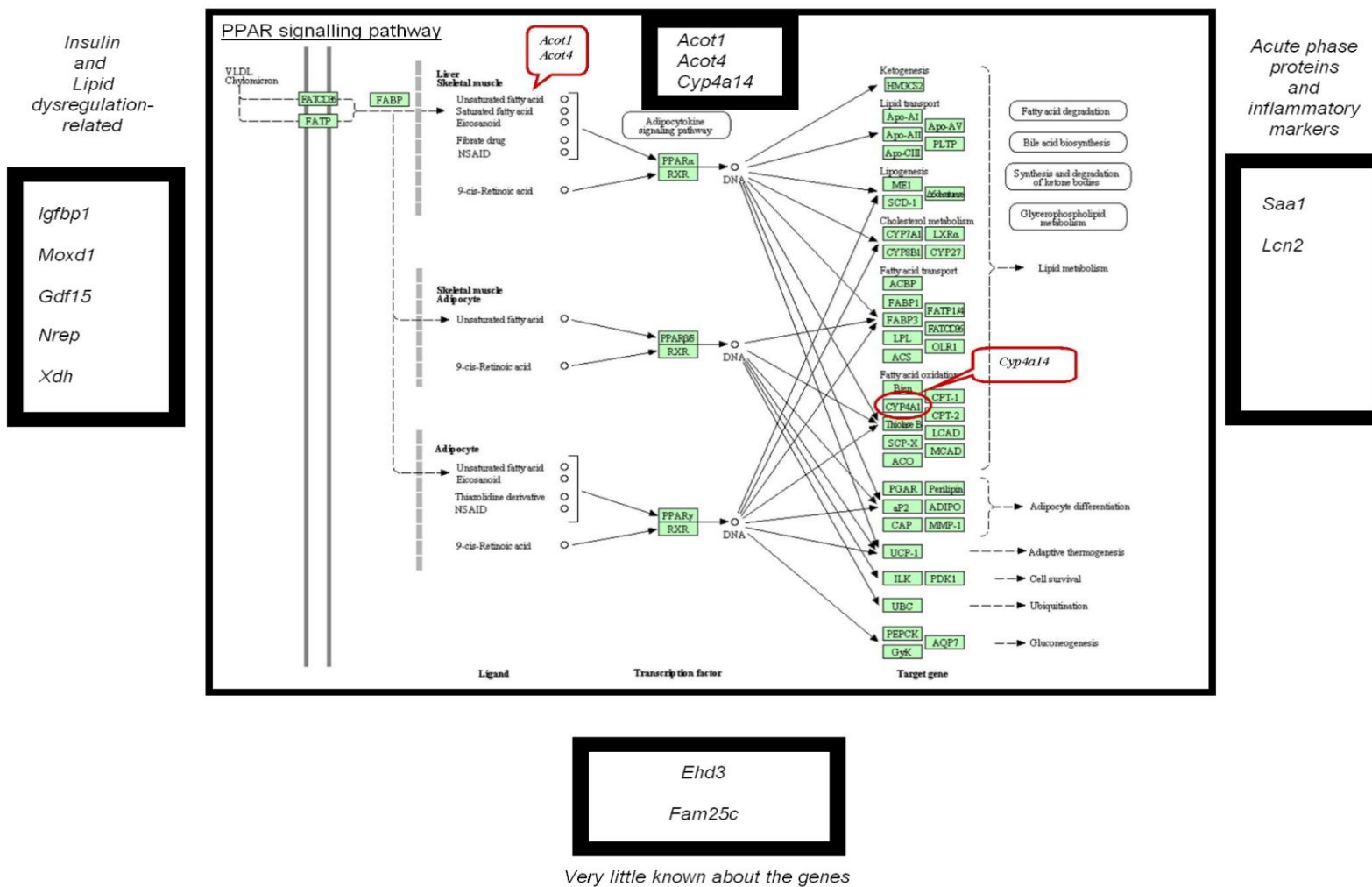


Fig. 5.9. Diagram summarising the validated, differentially-regulated genes in *Ido2^{-/-}*, *Tdo2^{-/-}* and *Ido2^{-/-}Tdo2^{-/-}* relative to their respective wild-types, and their roles. The diagram was taken from PPAR signalling pathway illustration of Kyoto Encyclopedia of genes and genome (KEGG).

CHAPTER 6

GENERAL DISCUSSION AND
FUTURE DIRECTIONS

CHAPTER 6: GENERAL DISCUSSION & FUTURE DIRECTIONS

6.1 GENERAL DISCUSSION

Tryptophan is an essential amino acid. Trp-catabolic enzymes play a prominent immunomodulatory role in the physiological process of pregnancy, protection against infections, as well as in the pathophysiology of a number of autoimmune conditions such as cancer, asthma and rheumatoid arthritis (Schmidt et al., 2009; Szanto et al., 2007; Hayashi et al., 2004; Pilotte et al., 2012; Uyttenhove et al., 2003; Munn et al., 1998). Their roles in other physiological processes are as yet incompletely understood.

Very little is known about the biological roles of the most recently discovered Trp-catabolic isozyme, IDO2, although it has been implicated in inflammatory responses as well as in autoimmune disorders (Merlo et al., 2014; Metz et al., 2014). IDO2, the existence of which was first reported by Dr Helen Ball (Ball et al., 2007), from our laboratory, has been the main focus in this project. Discovered in 2007 in mice as the paralogue of IDO1 and later detected in other mammals such as humans, chimpanzees, dog, cow and rats, the characteristics and role of mammalian IDO2 remain to be explored. The presence of two other Trp-degrading enzymes, TDO2 and IDO1, led researchers to question whether the roles of these enzymes are redundant, if they possess overlapping functions, or have their own specialised function distinct from the other Trp-catabolic enzymes. Understanding this will be fundamental in the field of Trp research.

The zebrafish was viewed as the canonical vertebrate due to its position in the evolutionary timeline. It also possesses several features that make it easy to study,

including optical transparency of its embryos, *ex utero* fertilisation and rapid breeding with high numbers of offspring. Due to the presence in the zebrafish of only one *ido* gene, which is more similar to *Ido2* than *Ido1* (Yuasa et al., 2007), this animal model appeared very suitable for the study of the possible role of IDO2 in development.

The low Trp-catabolic activity of IDO2 has led investigators to speculate that it also may possess a role independent of its enzymatic activity (Fatokun et al., 2013; Yuasa et al., 2009; Metz et al., 2007). Downregulation of functional IDO2 has been reported in macrophages from *Ido1*^{-/-} mice, while an upregulation in IDO2 expression was described in IDO1-deficient epididymis (Metz et al., 2014; Fukunaga et al., 2012). Apart from these dysregulations, the relationship between IDO1 and IDO2 has not been extensively investigated.

While the role of IDO1 in preventing allogeneic foetus rejection in pregnancy is widely agreed upon, the role of IDO2 in pregnancy is still under debate (Munn et al., 1998; Suzuki et al., 2001). Despite being expressed in the placenta, the role of the third Trp-catabolic isozyme, IDO2, in pregnancy remains to be explored (Metz et al., 2007; Ball et al., 2009).

During this project, we first developed a convenient and simple human IFN γ bioassay that can be adapted for use in different applications such as testing human biological samples for the pro-inflammatory cytokine. This assay is based on the ability of the cytokine to induce the expression of IDO1 in human endothelial cells. We then acquired useful information on the expression patterns of genes coding for Trp-catabolic enzymes during development in zebrafish and mouse (Table 6.1). In addition, we investigated the distribution of IDO2 within various murine tissues. We also examined the intracellular

expression of both IDO1 and IDO2 in a transfected cell system. The expression of genes in the absence of one or two Trp-degrading enzymes also was uncovered by studying the mRNA expression of *Tdo2*, *Ido1* and *Ido2* in different tissues from a variety of transgenic mouse strains, *Ido1^{-/-}*, *Ido2^{-/-}* and *Tdo2^{-/-}*. Furthermore, *Ido1^{-/-}Tdo2^{-/-}* and *Ido2^{-/-} Tdo2^{-/-}* and their equivalent WT mice were generated to acquire additional data on the expression of genes coding Trp-catabolic enzymes in the absence of two (of the three) enzymes. Finally, we assessed global gene expression in liver tissue deficient in IDO2, TDO2, or both.

6.1.1 Distribution and role of IDO2 in development of genes coding for Trp-catabolising enzymes

In this project, we ascertained the distribution of genes coding for Trp-catabolising enzymes in both murine and zebrafish developmental series. When the distributions of *tdo2a*, *tdo2b* and *ido* of zebrafish were compared to those of the genes coding Trp-catabolic enzymes in mouse (*Tdo2*, *Ido1* and *Ido2*), differences in the distribution patterns between the TDO and IDO homologues were evident (Fig. 6.1).

TDO2 in the liver has been shown to be pivotal for the normal regulation of dietary Trp (Knox and Auerbach, 1955) as well as to confer tolerogenic properties to the liver, modulating immunotolerance in transplantation (Schmidt et al., 2009). In the zebrafish, *tdo2a* and *tdo2b* both were expressed in the liver from 4 dpf (Fig. 3.6). As the liver develops by 3 dpf, with medial expansion by 4 dpf (Field et al., 2003), it can be postulated that the expression of *tdo2a* and *tdo2b* in the liver is concurrent with the maturation of the liver in zebrafish embryos. In contrast, the expression of both *Ido2* and *Tdo2* mRNA

was undetectable in murine embryonic liver (Fig. 4.17), despite being detected at relatively high levels in adult livers, suggesting that Trp degradation in murine embryos is not activated at the embryonic stage, in the liver at least. The functions of TDO2 and IDO2 in murine liver are switched on perhaps only after birth. Genes coding Trp-catabolic enzymes were detected in zebrafish liver from 4 dpf onwards, after hatching occurs (~3 dpf). While no synonymy between zebrafish hatching and mouse birth has been established, it would be interesting to investigate the factors that switch on the genes coding Trp-catabolic enzymes in the zebrafish and mouse.

Genes coding Trp-catabolising enzymes also were found in zebrafish intestine, where *tdo2a* was distributed throughout (seen at 3 dpf) and *tdo2b* localised in the posterior intestine (visible at 4 dpf) (Fig. 3.6). This is consistent with gut development, where the lumen of the intestine is evident by 3 dpf, followed by differentiation of intestinal epithelium (~4 dpf) and compartmentalisation of the tract into three distinct sections, intestinal bulb, mid-intestine and posterior intestine (by 5 dpf) (Ng et al., 2005). This pattern could be suggesting that the Trp-catabolic genes are switched on as part of the development of the intestine and may even be necessary for normal intestinal development and functioning, similar to the situation in the liver.

The knocking down of *ido* and *tdo2a* genes in zebrafish embryos did not yield reliable information on the role of these genes in embryonic development due to the unsuitability of the morpholino approach for studying the role of these genes in zebrafish embryos since they are expressed relatively late during development (3 dpf onwards). However, the localisation and onset of gene expression suggest that the expression of these Trp-catabolic enzymes is concurrent with liver and intestinal development/maturation.

The only intestinal Trp-catabolising enzyme reported thus far is IDO1, which is found constitutively in the jejunum and ileum (small intestine) of rabbit and mouse (Higuchi and Hayaishi, 1967; Dai and Zhu, 2010), while also being upregulated in inflammatory diseases of the gut in mouse and human (Ciorba, 2013; Ohyama et al., 2007; Clarke et al., 2009). Although Metz and colleagues reported *Ido2* mRNA in the colon, another publication was not able to detect any in the same tissue (Metz et al., 2007; Fukunaga et al., 2012). While we, too, were able to detect *Ido2* mRNA in the colon, specific IDO2 protein staining was undetectable in this tissue (Fig. 4.8). The presence of TDO2 in the adult mouse intestine has not been reported. As neither IDO2 nor TDO2 protein have been reported in the intestine thus far, we speculate that these two Trp-catabolic enzymes may be absent in embryonic gut as well. While we cannot rule out the possibility that IDO1 is expressed in embryonic gut, we speculate that, like IDO2 and TDO2 that were only expressed postnatally, IDO1 may be expressed only after birth. However, this needs to be confirmed by direct measurements of protein expression.

In the murine developmental series, the genes coding for Trp-degrading enzymes were detected in the yolk sac and placenta (Table 6.1). Therefore, it is quite possible that the murine Trp-catabolising homologues, while providing nutrients to the embryo through the yolk sac, also have evolved to play an immunomodulatory role in development, as was the case of IDO1 in murine placenta (Munn et al., 1998). It is rather unlikely that the zebrafish homologues of Trp-degrading enzymes play this role in embryonic development as fertilisation and maturation of embryos occur *ex utero*. However, whether these enzymes play a role in immune responses to foreign material or infection requires further investigation as the genes coding for these enzymes were detected in the liver and

intestine, tissues that are involved in not only metabolic and digestive processes but also in immune responses (Forn-Cuni et al., 2015; Goldsmith and Jobin, 2012). While all three genes coding for Trp-degrading enzymes were detected in murine yolk and placenta, *Tdo2* was the most highly expressed. While it is IDO1 that has been implicated in inducing local immune suppression to prevent allogeneic foetal rejection in mice, the high expression of *Tdo2* mRNA in the yolk sac and placenta indicates that *Tdo2* also could be playing roles in murine embryonic development. Whether these roles are related to nutrient supply, immunomodulation, or both, warrants further investigation. The absence of TDO2, IDO1 or IDO2, or both IDO1 and TDO2 or IDO2 and TDO2, proteins did not affect breeding outcomes significantly (HJ Ball, personal communication). This suggests that while genes coding for these enzymes are detected in key embryonic developmental tissues, these proteins are not essential for normal syngeneic pregnancy, where compensatory mechanisms may make up for the absence of Trp-catabolic enzymes. It has been shown, however, that IDO is necessary to prevent foetal rejection in allogeneic pregnancies of IDO-sufficient parents (Munn et al., 1998). However, no distinction between IDO1 and IDO2 activity was made in this experiment. When parents were IDO1-deficient, no significant differences in pregnancy failure rates were seen in either allogeneic or syngeneic foetuses (Baban et al., 2004). Baban and colleagues suggested that in IDO1-deficient parents compensatory mechanisms may exist to make up for the absent immunomodulatory role of IDO1 in pregnancy. This compensatory mechanism may be IDO2-related considering that 1-MT, the inhibitor used in the former study, was reported to inhibit both IDO1 and IDO2 (Metz et al., 2007). Although the mRNA levels of *Ido2* were relatively low in both yolk sac and placenta of WT mice, this does not necessarily imply a lack of role for IDO2 in immunomodulation in pregnancy. It is worth

considering that maternal IDO2 from other tissues may contribute to facilitate immune tolerance during pregnancy. Breeding rates of syngeneic pregnancies in *Ido2*^{-/-}, *Tdo2*^{-/-} and *Ido2*^{-/-}*Tdo2*^{-/-} mice were studied and no differences were found (H. Ball, personal communication). The role of IDO2 and TDO2 in allogeneic pregnancy rates in either IDO2- and/or TDO2-deficient mice should be examined next. Whether the absence of these enzymes during embryonic development affects the mice as they age, predisposing them to other conditions, also should be further examined. Furthermore it will be interesting to investigate whether the functions of the three Trp-catabolic proteins in these tissues overlap or if they play different, specialised roles. The factors that trigger the expression of the genes coding Trp-degrading proteins in these tissues also are worth identifying.

It is quite striking to observe that the expression patterns of the *tdo2s* in zebrafish were different to those in embryonic and adult mouse. As discussed previously (Section 3.4.1), *tdo2b* was initially duplicated from *tdo2a* in an ancestor of teleosts but was eventually lost in many fish lineages. The absence of TDO2 in mammalian intestine could be suggesting that although TDO contributed to Trp-catabolising activity in the intestine in early evolution, this role was eventually performed by IDO1 alone, which is the Trp-degrading enzyme expressed highly in the intestine of mouse and humans (Yamazaki et al., 1985; Yoshida et al., 1980). While these early reports did not distinguish between IDO1 and TDO2, the Trp-degrading enzyme reported in the murine intestine had a broad substrate specificity and required the presence of methylene blue for its activity, both of which are characteristic of IDO1. This led researchers to conclude that IDO1 is responsible for Trp catabolism in intestinal tissues, ruling out a role for extra-intestinal TDO2 or IDO2.

However, TDO2, to date, has not been conclusively proven to be absent in the intestine by assessment of its molecular or protein expression.

Although the *ido* gene in zebrafish is the murine orthologue of IDO2, it was undetectable in zebrafish liver while murine IDO2 is expressed strongly in mouse liver. On the other hand, zebrafish *ido* was expressed throughout the intestine, a distribution pattern similar to IDO1 in mammalian intestine. Therefore, while being structurally more similar to IDO2, the zebrafish IDO homologue exhibited greater similarity to mammalian IDO1 in terms of its distribution pattern. Also, zebrafish *ido* mRNA was detected constitutively only in the intestine while mammalian *Ido2* (coding for full-length IDO2 protein) has been reported in the liver, colon, kidney, brain and epididymis (Ball et al., 2007; Metz et al., 2007).

Human IDO activity was detected readily in post mortem small intestine, lung, epididymis, and placenta (Yamazaki et al., 1985). The wider distribution of IDOs in mammals also indicates that the role of the two enzymes in the more complex mammalian system could be more extensive and diverse than the role of the homologue in the fish.

While the zebrafish appears a promising experimental model for the study of Trp-degrading enzymes, especially the IDO2 homologue, the challenges in gene knockdown or knockout approaches in zebrafish remain a major concern. With high rates of off-target effects, one has to carefully pick a suitable knockdown/knockout approach with the least probability of off-target effects, as well as approaches suitable for studying genes that are expressed at later time points in development. This is discussed further in Section 6.4.

6.1.2 IDO2 distribution within murine tissue

Taking into account the differential distribution of IDO2 intracellularly in transfected HEK cells and WT liver sections, with the former appearing cytoplasmic and the latter perinuclear, it could be speculated that the distribution pattern of the protein may differ according to tissue type. Of course, the apparent difference in intracellular localisation also could be related to the fact that the HEK cells were transfected, or to species differences. Although the distribution of IDO2 in transfected HEK cells did not change when incubated in different concentrations of Trp, whether this is also the case *in vivo* should be investigated to acquire more understanding of the distribution of IDO2 in physiological circumstances. *In vivo*, we found that, at physiological Trp levels, IDO2 was localised perinuclearly in liver hepatocytes. This distribution pattern could suggest a role for IDO2 in signal transduction, perhaps affecting the expression of other genes through a transduction pathway. While this is purely speculative, it would be worth investigating given the precedent set by another haem enzyme, haem oxygenase 1 (HO-1), which possesses nuclear distribution in its truncated form (Lin et al., 2007). While HO-1 itself is not a conventional transcription factor, its nuclear localisation suggested a possible signalling role for the enzyme. Upon trans-signal array analysis, this faster migrating HO-1 was found to activate a number of transcription factors such as AP-1, STAT1 and NF- κ B (Lin et al., 2007). It would also be interesting to investigate the distribution pattern of IDO2 in primary hepatocytes in Trp-rich conditions *in vivo*. One way to investigate IDO2 expression in hepatocytes in Trp-rich conditions *in vivo* could be by studying by IHC the distribution patterns of IDO2 in the liver of *Tdo2*^{-/-} mice relative to *Tdo2*^{+/+} mice, since the plasma level of Trp is elevated (~10x) in IDO2-deficient mice (Kanai et al., 2009).

Although *Ido2* mRNA was detectable in a number of tissues, namely, the liver, kidney, brain, epididymis and colon (Ball et al., 2007; Fukunaga et al., 2012; Metz et al., 2007), there was no specific protein staining detected in any of these organs, except liver, when tissues from *Ido2*^{-/-} mice were used as negative controls (Table 6.1). The *Ido2*^{-/-} mice have exons 9 and 10 deleted, resulting in the absence of full-length IDO2 protein and enzymatic activity (Metz et al., 2014). The existence of alternatively spliced *Ido2* mRNA transcripts (Ball et al., 2009; Metz et al., 2007) suggests that there is the potential for variant forms of IDO2 proteins, with at least one less active form having been described (Metz et al., 2014). If a variant IDO2 protein is recognized by an IDO2 antibody, but does not contain exon 9 onwards, then it is possible that it will still be detectable in the *Ido2*^{-/-} mice. Thus our results suggest that while specific staining of full-length protein is only apparent in the liver, other tissues may still possess variant IDO2 proteins that are recognisable by anti-IDO2 antibodies. It would be a methodological milestone to be able to generate different antibodies that differentiate between the full-length and truncated IDO2 proteins. Only the full-length IDO2 protein is considered likely to possess Trp-catabolic activity (albeit possessing only low activity), as truncated IDO2 protein possessed only a small fraction of the Trp-catabolic activity of the full length protein (Metz et al., 2014). However, the presence of substantial amounts of mRNA transcripts in the kidney, brain, epididymis and colon but no specific IDO2 staining (when tissues from *Ido2*^{-/-} mice were used as negative controls) forces us to consider other roles the possible alternative protein forms of IDO2 may play in these tissues. While mRNA transcripts coding for full-length IDO2 protein were undetectable in embryonic liver (Section 4.3.4.3), an alternatively spliced *Ido2* variant that may encode IDO2 isoforms was found in these livers (data not shown). Whether these splice forms of *Ido2* mRNA code alternative IDO2

proteins that possess actions independent of its enzymatic activity remains to be explored.

6.1.3 Expression of genes in the liver of IDO2- and/or TDO2-deficient mice

While a number of genes were differentially regulated (Fig. 6.1), as determined by microarray analysis, in liver lysates of mice deficient for one or two Trp-catabolic enzymes only a few genes were differentially regulated in the liver lysates of all the three transgenic mice analysed, *Ido2*^{-/-}, *Tdo2*^{-/-} and *Ido2*^{-/-}*Tdo2*^{-/-} (Section 5.3.4), when validated by RT-qPCR. It is intriguing that the genes differentially regulated in the liver of single *Ido2*^{-/-} and double *Ido2*^{-/-}*Tdo2*^{-/-} were different and no one gene was differentially regulated in the liver of both mouse models (Section 5.4.4). This could suggest that TDO2 may in some way be necessary for the dysregulation of the genes differentially regulated in IDO2-deficient mice and, in the absence of both TDO2 and IDO2, the expression of those genes was not affected. Similarly, the expression of the two genes that were dysregulated in the liver of *Tdo2*^{-/-} mice, in which IDO2 is constitutively expressed, namely *Cyp4a14* and *Moxd1*, was unaffected in the liver of *Ido2*^{-/-}*Tdo2*^{-/-} mice. The converse may also be possible, where IDO2 is necessary for the dysregulation of *Cyp4a14* and *Moxd1* seen in TDO2-deficient mice. This will need to be investigated in more detail by analysing by RTqPCR and IHC the expression of a greater number of genes found dysregulated in the liver of *Tdo2*^{-/-} mice by microarray. Despite the possible interdependence of TDO2 and IDO2 in the liver, it is worth considering that the mechanism through which the postulated inflammation is triggered, or metabolic processes are perturbed, in the liver of these mice differs as there were only two genes that differentially regulated in a similar

manner in the liver of both *Tdo2*^{-/-} and *Ido2*^{-/-} mice (Section 5.4.4). There were no genes similarly regulated in all the three mutant mice deficient for one or two Trp-degrading enzymes, which is consistent with this speculation. mRNA expression of neither *Ido2* nor *Tdo2* was affected in the absence of the other in various murine tissues (liver, brain, kidney, testes and epididymis) (Section 4.3.5). However, whether either is required to dysregulate other genes in the absence of their counterpart necessitates further investigation. While a downregulation of *Ido2* was seen in the kidney, brain and epididymis of *Ido1*^{-/-} and *Ido1*^{-/-}*Tdo2*^{-/-} mice, such a dysregulation was not seen in the liver, where *Ido2* is detected constitutively (Table 6.1). This is an interesting observation. It is possible that the expression of *Ido2* is only affected by the absence of IDO1 in tissues in which IDO1 was constitutively expressed. In tissues where IDO1 is not constitutively expressed, *i.e.* the liver, such regulation of *Ido2* mRNA may not occur, as indeed might be expected. However, the attenuation of *Ido2* mRNA expression in the kidney of *Ido1*^{-/-} and *Ido1*^{-/-}*Tdo2*^{-/-} mice is an anomaly to this hypothesis as its expression is downregulated despite the absence of constitutive expression of IDO1 and TDO2 in this tissue (Section 4.3.5.2).

Collectively, as we were unable to detect specific IDO2 protein staining in WT kidney, brain and epididymis, IDO1 regulation of IDO2 in these tissues will be challenging to study at the level of protein expression (Table 6.1). Perhaps, while the mRNA is present constitutively, the expression of IDO2 protein is only triggered in certain pathological conditions, due to stimulation by specific factors, as yet unidentified. Given the proposed roles of IDO2 in inflammation (Metz et al., 2014), perhaps the expression of IDO2 protein

in these tissues from WT, *Ido1*^{-/-} and *Ido2*^{-/-} mice in inflammatory conditions would be worth investigating.

6.2 FUTURE DIRECTIONS

The findings of this project have opened new doors on the roles of Trp-catabolic enzymes, especially in murine models, giving leads to possible alternative roles of IDO2 and TDO2 physiologically and pathophysiologically.

1. We discovered the expression patterns of genes coding Trp-degrading enzymes in a zebrafish developmental series. While the roles of these enzymes in zebrafish physiology remain to be uncovered, their expression patterns suggest that they may have roles different to those in mammalian systems, exemplified here by the mouse. The roles of Trp-catabolic enzymes in zebrafish embryos and adult fishes should be investigated using a permanent genome-editing approach such as TALENs or CRISPR-Cas (Gupta and Musunuru, 2014; Hwang et al., 2013a; Clark et al., 2011). Essential amino acids (which need to be acquired from the diet) in fish are similar to those in mammals, with Trp being necessary for the optimal growth of some species of fish, though not all (Ketola, 1982). Despite this similarity, understanding the roles of these enzymes in the development of zebrafish can provide information on the roles of these enzymes in early evolution. As we speculate that the roles of the Trp-catabolic enzymes in fish differ from those in mammals, it would be interesting to investigate whether there was divergence in the roles of these enzymes throughout evolution.
2. The expression of the Trp-catabolic enzymes TDO2, IDO1 and IDO2 should be confirmed at the protein level in murine developmental tissues (yolk sac and placenta). The Trp-catabolic activities of these enzymes also should be assessed. The roles of TDO2 and IDO2 in adult mice, separated from those during mouse development, could be investigated by a conditional knockout approach where

genes coding for Trp-catabolic enzymes would be only knocked out during adulthood by administration or feeding of factors that activate regulatory elements that clip the genes (Friedel et al., 2011). This approach can also be used to induce knockouts in specific cell types. The conditional knockout method may be more specific, with fewer off-target effects, than utilising either siRNA or selective inhibitors for TDO2 and IDO2. No difference in breeding numbers was found in *Ido2*^{-/-} or *Tdo2*^{-/-} litters (data not shown), suggesting that if the enzymes have roles in syngeneic embryonic development, other mechanisms may exist to compensate for the lack of these enzymes during development. Breeding rates of allogeneic fetuses from parents deficient for TDO2 and IDO2 should be observed and compared to those of TDO2-, IDO1- and IDO2-sufficient parents in whom the Trp-catabolic activity is antagonised by conditional knockout given the precedent that IDO was necessary for allogeneic pregnancies in IDO-sufficient parents, although this did not distinguish between IDO1 and IDO2 (Baban et al., 2004). Breeding rates of syngeneic offsprings of IDO1, IDO2 and TDO2-sufficient parents whose Trp-catabolic activity was ablated by selective inhibitors also could be acquired to better elucidate the possible role of these enzymes in pregnancy.

3. IDO2 protein was detectable only in liver and, in the absence of IDO2, a number of inflammation- and metabolism-related genes were differentially regulated in this tissue (Section 5.3.1). The biological significance of this observation merits further study. It was suggested (Section 5.4.1) that these changes in young mice might flag the early stages of an inflammatory response that might in turn induce a metabolic dysregulation with some similarities to Type 2 diabetes. Assessment of inflammatory markers in the plasma and different cell populations, especially immune cells, of

IDO2-deficient mice as well as the histology of the liver at different age points may provide essential information on the health status of the mice in the absence of IDO2. Examining similar parameters in *Tdo2*^{-/-} and *Ido2*^{-/-} *Tdo2*^{-/-} mice also may provide pivotal information on the consequences of the absence of IDO2 and TDO2 for the normal physiology of mice.

4. We speculated (Section 5.4.1) that the absence of IDO2 results in dysregulation of inflammatory mediators, which could lead eventually to obesity or diabetes. If changes in pro-inflammatory factors were confirmed, switching off their expression either by long-acting neutralising antibodies or conditional knockout could help us elucidate the changes that are triggered in the absence of IDO2. Assessment of obesity and diabetes also should be done in older mice (>20 wks of age) by examining their plasma lipid, glucose, cholesterol and body weights.
5. Another possibility is to study the expression of IDO2 in immune/inflammatory models in *Ido2*^{-/-} and WT mice, e.g. models of liver transplantation, viral hepatitis, alcohol-induced steatohepatitis or non-alcoholic fatty liver disease, all of which involve, to some extent, inflammation of the liver. This may provide some valuable insights into the role of IDO2 in acute or chronic liver injury/inflammation as well as immunotolerance in transplantation.
6. It has been established previously that, *in vivo*, Trp-rich conditions activate TDO2 (Knox and Auerbach, 1955), while IDO1 expression is inhibited by elevated serum Trp and stimulated more by immunological signals (Yoshida et al., 1980). However, the regulation of IDO2 by Trp *in vivo* has not been investigated as yet. While studying the distribution of IDO2 in different Trp concentrations was attempted in this project (Section 4.3.3), it only could be tested in HEK cells transfected with mouse *Ido2*

plasmids and not in primary hepatocytes as *Ido2* signals in the latter plunged dramatically within the first 24 hours. Also, other factors that regulate IDO2 expression are not known. Examining the activity and distribution of IDO2 in various tissues when fed Trp-rich or –deficient diets would be a good approach. However, it must be recalled that *Ido2* mRNA expression did not change in *Tdo2*^{-/-} mice (Section 4.3.5), which have elevated serum Trp concentrations (Kanai et al., 2009).

Understanding the expression of IDO2 in the presence of different concentrations of its primary substrate, Trp, could help us better understand the role of IDO2 in murine physiology.

7. Although the analysis of gene expression of Trp-catabolic enzymes in the colon was not pursued, since we did not detect any specific IDO2 protein staining there (despite the presence of mRNA), the mRNA expression of the Trp-degrading enzymes in the intestine of *Ido1*^{-/-}, *Ido2*^{-/-}, *Tdo2*^{-/-}, *Ido1*^{-/-}*Tdo2*^{-/-}, *Ido2*^{-/-} *Tdo2*^{-/-} mice and their equivalent WTs is worth investigating. IDO1 has been reported in the human and mouse intestine (Yoshida et al., 1980; Yamazaki et al., 1985) while *Ido2* mRNA has been detected in both human (Metz et al., 2007) and mouse colon (Section 4.3.2). Any findings of IDO2 expression in the colon can be compared with the expression of zebrafish Trp-catabolic enzymes (Section 3.2.2). Global gene expression in the colon of mice deficient for IDO1 or IDO2 also could be investigated to ascertain whether the two enzyme isoforms play an interdependent role in this tissue.
8. Truncated IDO2 protein, coded for by the splice form of *Ido2* mRNA, has been reported and was shown to possess a much lower Trp-catabolic activity than the full length protein (Ball et al., 2009; Metz et al., 2014). It has been speculated that this truncated protein may possess alternative biological roles despite diminished

enzymatic activity. Sequencing of 'non-specific' proteins detectable by mouse IDO2 antibodies, especially in tissues in which staining by IHC was evident, could be pursued. If indeed the non-specific protein detected is the truncated form of IDO2 protein, uncovering its role in mouse physiology by knocking out its expression using a conditional knockout approach might yield interesting outcomes.

9. While we validated by RT-qPCR the mRNA expression of some of the genes found by microarray analysis to be dysregulated in the liver of mice deficient for IDO2, TDO2, or both, we were not able to validate the mRNA levels of many other genes found differentially regulated in this analysis due to time constraints. We also were not able to confirm the dysregulation of the genes at the protein level. Ascertaining the expression of proteins of the genes found dysregulated by RT-qPCR should be pursued as it can provide insight into whether the absence of IDO2, TDO2 or both affects the expression of other genes at the posttranslational level. The expression of other genes, especially those related to the ones found differentially regulated in the liver of *Ido2*^{-/-} and/or *Tdo2*^{-/-} mice by RT-qPCR, should be assessed to uncover more players in the possible pathophysiology of the liver in the absence of IDO2, TDO2 or both.

6.3 FINAL CONCLUSION

Collectively, these findings show a difference in the expression patterns of TDO and IDO homologues in zebrafish and mouse, which suggests differences in the roles of these homologues in embryonic development of the two species. In the adult mouse, IDO2 was found localised perinuclearly in hepatocytes. In the absence of the enzyme a number of inflammatory mediator-induced genes were differentially regulated, suggesting the possibility of a pre-inflammatory state in the liver in the absence of IDO2 in young adult mice. In the absence of both TDO2 and IDO2, a divergent set of inflammation-related genes was differentially regulated, suggesting mechanistic differences in how inflammation might be induced in these models. We speculate on a possible role for IDO2 in mediating inflammation and that, in the absence of the protein, inflammation-driven obesity and/or diabetes may result.

Zebrafish (Section 3.3.2)	<i>tdo2a</i>	<i>tdo2a</i>	<i>ido</i>
	<ul style="list-style-type: none"> i. Expressed in the liver and throughout the intestine. ii. Expressed from 3 dpf onwards iii. Possible role not ascertained as morpholino approach was unsuitable for knockdown 	<ul style="list-style-type: none"> i. Expressed in the liver and posterior intestine ii. Expressed 4 dpf onwards iii. Possible role not ascertained due to unsuitability of morpholino approach 	<ul style="list-style-type: none"> i. Expressed throughout the intestine ii. Expressed from 3 dpf onwards iii. Despite increased mortality in <i>ido</i> morphants, which was rescueable by the injection of <i>ido</i> RNA transcript, it was later deemed likely to be an off-target effect of the morpholino
Mouse	<i>Tdo2</i>	<i>Ido1</i>	<i>Ido2</i>
Embryonic (Section 4.3.4)	<ul style="list-style-type: none"> i. mRNA expressed highly in yolk sac and placental tissue in a developing murine embryo. Among the three genes coding for Trp-catabolising enzymes, <i>Tdo2</i> was expressed the highest. No expression detectable in murine liver while neonatal liver expressed very low levels of <i>Tdo2</i> gene. 	<ul style="list-style-type: none"> i. mRNA expressed at low levels in yolk sac and placenta 	<ul style="list-style-type: none"> i. mRNA expressed at low levels in yolk sac and placenta. Expression levels were also lower than <i>Ido1</i>. mRNA coding for full length protein was undetectable in both embryonic and neonatal liver
Adult			
Cellular and intracellular distribution (Section 4.3.2 and 4.3.3)	<ul style="list-style-type: none"> i. Neither cellular nor intracellular localisation of TDO2 in tissues were examined due to the lack of a suitable antibody 	<ul style="list-style-type: none"> i. Cellular distribution of IDO1 was not studied as it has been investigated thoroughly by previous researchers (Britan et al., 2006; Ball et al., 2007; 	<ul style="list-style-type: none"> i. For cellular distribution, IDO2 protein detected in the liver, distributed perinuclearly in hepatocytes, which was different to the distribution

		<p>Dai and Zhu, 2010; Fukunaga et al., 2012).</p> <p>ii. Intracellular localisation of IDO1 showed cytoplasmic distribution in HEK cells transfected with plasmid containing <i>Ido1</i> cDNA.</p>	<p>reported by an earlier group (Fukunaga et al., 2012). Colon, brain, testis and kidney tissues exhibited non-specific staining that was present in both WT and <i>Ido2</i>^{-/-} mice, challenging the findings of previous publications (Ball et al., 2007; Fukunaga et al., 2012).</p> <p>ii. IDO2 also exhibited cytoplasmic expression intracellularly in HEK cells transfected with plasmid carrying <i>Ido2</i> cDNA.</p>
<p>Expression in liver, kidney, brain, epididymis and testis tissue of different mutant mice deficient for one or two Trp-catabolising enzymes and their equivalent WT (<i>Ido2</i>^{-/-}, <i>Ido2</i>^{+/+}, <i>Ido1</i>^{-/-}, <i>Ido1</i>^{+/+}, <i>Tdo2</i>^{-/-}, <i>Tdo2</i>^{+/+}, <i>Ido2</i>^{-/-}<i>Tdo2</i>^{-/-}, <i>Ido1</i>^{-/-}<i>Tdo2</i>^{-/-} and <i>Ido1</i>^{+/+}<i>Ido2</i>^{+/+}<i>Tdo2</i>^{+/+}) (Section 4.3.5)</p>	<p>i. <i>Tdo2</i> mRNA was detectable in the liver, brain and testis of all the genetically-modified mouse strains except in <i>Tdo2</i>^{-/-}, <i>Ido2</i>^{-/-}<i>Tdo2</i>^{-/-} and <i>Ido1</i>^{-/-}<i>Tdo2</i>^{-/-}</p> <p>ii. <i>Tdo2</i> mRNA was not differentially regulated in the above mentioned tissues in mouse strains deficient for either IDO1 or IDO2, suggesting that the absence of the two genes does not affect the expression of <i>Tdo2</i>.</p>	<p>i. <i>Ido1</i> mRNA expression was found in the testis and epididymis of all mouse strains except <i>Ido1</i>^{-/-} and <i>Ido1</i>^{-/-}<i>Tdo2</i>^{-/-}</p> <p>ii. The mRNA levels were unaffected in these tissues from mice deficient for IDO2 and/or TDO2.</p>	<p>i. <i>Ido2</i> mRNA was detected in the liver, kidney, brain, testis and epididymis in all mouse strains except <i>Ido2</i>^{-/-} and <i>Ido2</i>^{-/-}<i>Tdo2</i>^{-/-}.</p> <p>ii. <i>Ido2</i> mRNA levels were attenuated in the kidney, brain and epididymis of <i>Ido1</i>^{-/-} and <i>Ido1</i>^{-/-}<i>Tdo2</i>^{-/-} mice, suggesting a possible downregulation of <i>Ido2</i> mRNA in the absence of <i>Ido1</i>. Possibility that the effects seen are artefact also was considered.</p>

<p>Assessment of global gene expressions by microarray in liver lysates of <i>Ido2</i>^{-/-}, <i>Ido2</i>^{+/+}, <i>Tdo2</i>^{-/-}, <i>Tdo2</i>^{+/+}, <i>Ido2</i>^{-/-}<i>Tdo2</i>^{-/-} and <i>Ido1</i>^{+/+}<i>Ido2</i>^{+/+}<i>Tdo2</i>^{+/+}) (Chapter 5)</p>	<ul style="list-style-type: none"> i. Absence of TDO2 in <i>Tdo2</i>^{-/-} lead to the upregulation of <i>Cyp4a14</i> and downregulation of <i>Moxd1</i>. ii. <i>Cyp4a14</i> is a PPARα signalling pathway-dependent gene, involved in lipid and fatty acid metabolism while also implicated in a hepatoprotective role in ameliorating inflammation in the liver. iii. <i>Moxd1</i> was reportedly downregulated in mice with reduced insulin bioavailability. This suggests a possible role for TDO2 in lipid metabolism. 	<ul style="list-style-type: none"> i. Not studied 	<ul style="list-style-type: none"> i. <i>Xdh</i>, <i>Acot1</i>, <i>Cyp4a14</i>, <i>Gdf15</i>, <i>Igf1</i>, <i>Moxd1</i>, <i>Ehd3</i> and <i>Fam25c</i> were differentially regulated in liver tissue of <i>Ido2</i>^{-/-} mice relative to <i>Ido2</i>^{+/+}. ii. <i>Xdh</i>, <i>Acot1</i>, <i>Cyp4a14</i>, <i>Gdf15</i>, <i>Igf1</i>, <i>Ehd3</i> and <i>Fam25c</i> were all upregulated in IDO2-deficient mice whereas <i>Moxd1</i> was downregulated. iii. <i>Xdh</i>, <i>Acot1</i>, <i>Cyp4a14</i>, <i>Gdf15</i> and <i>Igf1</i> were all implicated in inflammatory responses while also reported in obesity and obesity-related diabetes. Proinflammatory cytokines such as IFNγ, TNF, IL-1 and IL-6 have been shown to upregulate some of these genes. iv. <i>Moxd1</i> was downregulated in <i>Ido2</i>^{-/-} relative to <i>Ido2</i>^{+/+} mice, similar to its reduction in liver lysates of <i>Tdo2</i>^{-/-} mice relative to the WT.
--	--	--	---

	<p>i. In the absence of both TDO2 and IDO2 in the liver, four genes were found differentially regulated, namely, <i>Saa1</i>, <i>Lcn2</i>, <i>Acot4</i> and <i>Nrep</i>.</p> <p>ii. Both <i>Saa1</i> and <i>Lcn2</i> were downregulated in liver lysates of <i>Ido2</i>^{-/-}<i>Tdo2</i>^{-/-} relative to <i>Ido1</i>^{+/+}<i>Ido2</i>^{+/+}<i>Tdo2</i>^{+/+}. Both these genes code for acute-phase proteins that are upregulated by TNF, IL-1 and IL-6. Both SAA1 and LCN2 also have been implicated in inflammation and obesity. The lack of such upregulation in mice deficient for only one Trp-catabolising enzyme, IDO2 or TDO2, could be suggesting that the presence of at least one Trp-degrading enzyme is necessary to avert acute inflammatory responses, if inflammation is indeed occurring in the liver of these mice.</p>
--	---

Table 6.1 Summary of all findings

Fig. 6.1 Diagrammatic summary of findings

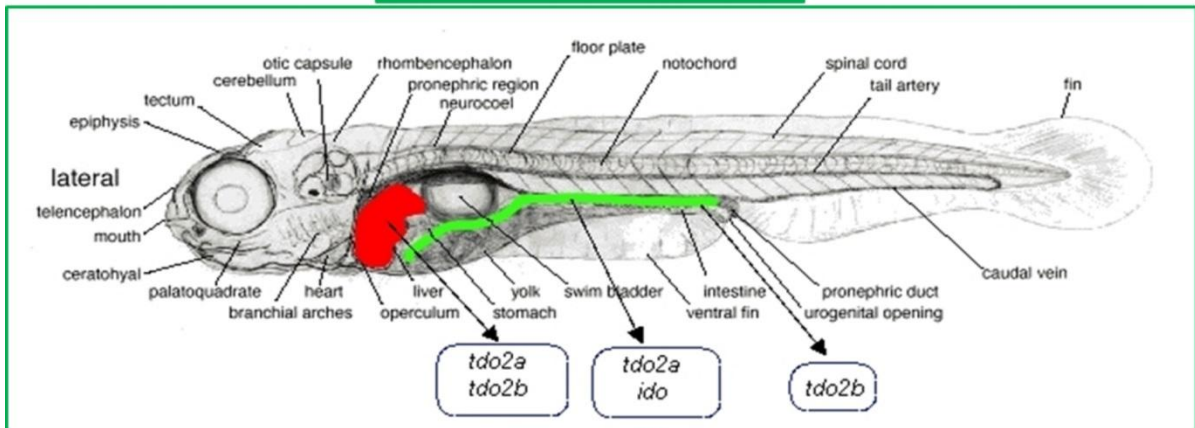
Zebrafish image taken from (Haffter et al., 1996) and murine embryo image from (Mikkola and Orkin, 2006). The image of the liver was taken from

[\(http://www.pinkjooz.com/index.php/virtual-liver-product-by-iisc-professor-patented-in-us/\)](http://www.pinkjooz.com/index.php/virtual-liver-product-by-iisc-professor-patented-in-us/)

LPS - lipopolysaccharide; IFN γ - interferon gamma; TNF - tumour necrosis factor; IL-1 - interleukin 1; IL-6 - interleukin 6; IL-4 - interleukin 4; *Xdh* - xanthine oxidoreductase/dehydrogenase; *Acot1* - acyl CoA thioesterase 1; *Igfbp1* - insulin-like growth factor binding protein 1; *Gdf15* - growth differentiation factor 15; *Cyp4a14* - cytochrome P450 family 4, subfamily a, polypeptide 14; *Moxd1* – monooxygenase DBH-like 1; *Saa1* – Serum amyloid A 1; *Lcn2* – Lipocalin 2



Danio rerio (zebrafish)

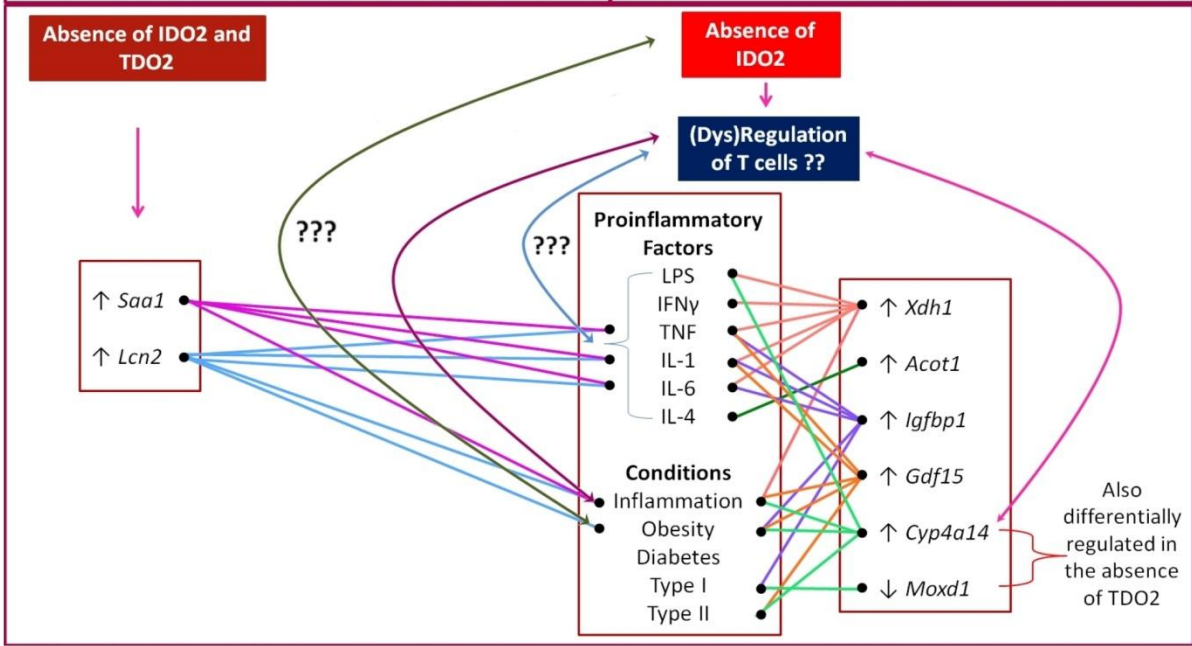


tdo2a
tdo2b
tdo2a
ido
tdo2b

Trp-catabolising enzymes

Mus musculus (Mouse)

<p>Embryonic development (<i>Tdo2</i>><i>Ido1</i>><i>Ido2</i>)</p> <p>Placenta Yolk sac Foetal liver (No genes coding Trp-catabolic enzymes detected)</p> <p>Trp-catabolising enzymes in embryonic gut??</p>	<p>Adult (7-9 weeks old)</p> <p>IDO2 detected perinuclearly in hepatocytes.</p> <div style="border: 1px solid red; border-radius: 50%; padding: 10px; width: fit-content; margin-left: auto;"> <p>IDO2 in kidney, brain, colon, epididymis??</p> </div>
---	--



REFERENCES

- ADAMS, O., BESKEN, K., OBERDORFER, C., MACKENZIE, C. R., TAKIKAWA, O. & DAUBENER, W. 2004. Role of indoleamine-2,3-dioxygenase in alpha/beta and gamma interferon-mediated antiviral effects against herpes simplex virus infections. *J Virol*, 78, 2632-6.
- AGUET, M., DEMBIC, Z. & MERLIN, G. 1988. Molecular cloning and expression of the human interferon-gamma receptor. *Cell*, 55, 273-80.
- AKBAR, S. M., INABA, K. & ONJI, M. 1996. Upregulation of MHC class II antigen on dendritic cells from hepatitis B virus transgenic mice by interferon-gamma: abrogation of immune response defect to a T-cell-dependent antigen. *Immunology*, 87, 519-27.
- ALEXANDER, A. M., CRAWFORD, M., BERTERA, S., RUDERT, W. A., TAKIKAWA, O., ROBBINS, P. D. & TRUCCO, M. 2002. Indoleamine 2,3-dioxygenase expression in transplanted NOD Islets prolongs graft survival after adoptive transfer of diabetogenic splenocytes. *Diabetes*, 51, 356-65.
- AMBROSO, J. L., LARSEN, S. V., BRABEC, R. K. & HARRIS, C. 1997. Fluorometric analysis of endocytosis and lysosomal proteolysis in the rat visceral yolk sac during whole embryo culture. *Teratology*, 56, 201-9.
- ANDERSSON, O., ADAMS, B. A., YOO, D., ELLIS, G. C., GUT, P., ANDERSON, R. M., GERMAN, M. S. & STAINIER, D. Y. 2012. Adenosine signaling promotes regeneration of pancreatic beta cells in vivo. *Cell Metab*, 15, 885-94.
- ASTIGIANO, S., MORANDI, B., COSTA, R., MASTRACCI, L., D'AGOSTINO, A., RATTO, G. B., MELIOLI, G. & FRUMENTO, G. 2005. Eosinophil granulocytes account for indoleamine 2,3-dioxygenase-mediated immune escape in human non-small cell lung cancer. *Neoplasia*, 7, 390-6.
- AUSTIN, C. J., MAILU, B. M., MAGHZAL, G. J., SANCHEZ-PEREZ, A., RAHLFS, S., ZOCHER, K., YUASA, H. J., ARTHUR, J. W., BECKER, K., STOCKER, R., HUNT, N. H. & BALL, H. J. 2010. Biochemical characteristics and inhibitor selectivity of mouse indoleamine 2,3-dioxygenase-2. *Amino Acids*, 39, 565-78.
- BABAN, B., CHANDLER, P., MCCOOL, D., MARSHALL, B., MUNN, D. H. & MELLOR, A. L. 2004. Indoleamine 2,3-dioxygenase expression is restricted to fetal trophoblast giant cells during murine gestation and is maternal genome specific. *J Reprod Immunol*, 61, 67-77.
- BABAN, B., CHANDLER, P. R., SHARMA, M. D., PIHKALA, J., KONI, P. A., MUNN, D. H. & MELLOR, A. L. 2009. IDO activates regulatory T cells and blocks their conversion into Th17-like T cells. *J Immunol*, 183, 2475-83.
- BABCOCK, T. A. & CARLIN, J. M. 2000. Transcriptional activation of indoleamine dioxygenase by interleukin 1 and tumor necrosis factor alpha in interferon-treated epithelial cells. *Cytokine*, 12, 588-94.
- BACH, E. A., AGUET, M. & SCHREIBER, R. D. 1997. The IFN gamma receptor: a paradigm for cytokine receptor signaling. *Annu Rev Immunol*, 15, 563-91.
- BADAWY, A. A. 1981. Possible involvement of the enhanced tryptophan pyrrolase activity in the corticosterone- and starvation-induced increases in concentrations of nicotinamide-adenine dinucleotides (phosphates) in rat liver. *Biochem J*, 196, 217-24.
- BAKER, K., WARREN, K. S., YELLEN, G. & FISHMAN, M. C. 1997. Defective "pacemaker" current (I_h) in a zebrafish mutant with a slow heart rate. *Proc Natl Acad Sci U S A*, 94, 4554-9.
- BAKMIWEWA, S. M. 2011. *Indoleamine 2,3 Dioxygenase 2 : Developing tools to discover its biological role*. Bachelor of Medical Science (Hons) Honours, The University of Sydney.
- BAKMIWEWA, S. M., FATOKUN, A. A., TRAN, A., PAYNE, R. J., HUNT, N. H. & BALL, H. J. 2012. Identification of selective inhibitors of indoleamine 2,3-dioxygenase 2. *Bioorganic & Medicinal Chemistry Letters*, 22, 7641-6.
- BALL, H. J., JUSOF, F. F., BAKMIWEWA, S. M., HUNT, N. H. & YUASA, H. J. 2014. Tryptophan-catabolizing enzymes - party of three. *Front Immunol*, 5, 485.

- BALL, H. J., SANCHEZ-PEREZ, A., WEISER, S., AUSTIN, C. J., ASTELBAUER, F., MIU, J., MCQUILLAN, J. A., STOCKER, R., JERMIIN, L. S. & HUNT, N. H. 2007. Characterization of an indoleamine 2,3-dioxygenase-like protein found in humans and mice. *Gene*, 396, 203-13.
- BALL, H. J., YUASA, H. J., AUSTIN, C. J., WEISER, S. & HUNT, N. H. 2009. Indoleamine 2,3-dioxygenase-2; a new enzyme in the kynurenine pathway. *Int J Biochem Cell Biol*, 41, 467-71.
- BANGE, F. C., FLOHR, T., BUWITT, U. & BOTTGER, E. C. 1992. An interferon-induced protein with release factor activity is a tryptophanyl-tRNA synthetase. *FEBS Lett*, 300, 162-6.
- BAUMANN, H., HELD, W. A. & BERGER, F. G. 1984. The acute phase response of mouse liver. Genetic analysis of the major acute phase reactants. *J Biol Chem*, 259, 566-73.
- BECKMAN, D. A., LLOYD, J. B. & BRENT, R. L. 1998. Quantitative studies on the mechanisms of amino acid supply to rat embryos during organogenesis. *Reprod Toxicol*, 12, 197-200.
- BECKMAN, D. A., PUGARELLI, J. E., JENSEN, M., KOSZALKA, T. R., BRENT, R. L. & LLOYD, J. B. 1990. Sources of amino acids for protein synthesis during early organogenesis in the rat. I. Relative contributions of free amino acids and of proteins. *Placenta*, 11, 109-21.
- BECKMAN, D. A., PUGARELLI, J. E., KOSZALKA, T. R., BRENT, R. L. & LLOYD, J. B. 1991. Sources of amino acids for protein synthesis during early organogenesis in the rat. 2. Exchange with amino acid and protein pools in embryo and yolk sac. *Placenta*, 12, 37-46.
- BENDER, D. A. & OLUFUNWA, R. 1988. Utilization of tryptophan, nicotinamide and nicotinic acid as precursors for nicotinamide nucleotide synthesis in isolated rat liver cells. *Br J Nutr*, 59, 279-87.
- BENSON, M. D. & COHEN, A. S. 1979. Serum amyloid A protein in amyloidosis, rheumatic, and neoplastic diseases. *Arthritis Rheum*, 22, 36-42.
- BERGER, M., GRAY, J. A. & ROTH, B. L. 2009. The expanded biology of serotonin. *Annu Rev Med*, 60, 355-66.
- BEUSCHER, H. U., GUNTHER, C. & ROLLINGHOFF, M. 1990. IL-1 beta is secreted by activated murine macrophages as biologically inactive precursor. *J Immunol*, 144, 2179-83.
- BEVILACQUA, E. M. & ABRAHAMSOHN, P. A. 1989. Trophoblast invasion during implantation of the mouse embryo. *Arch Biol Med Exp (Santiago)*, 22, 107-18.
- BILL, B. R., PETZOLD, A. M., CLARK, K. J., SCHIMMENTI, L. A. & EKKER, S. C. 2009. A primer for morpholino use in zebrafish. *Zebrafish*, 6, 69-77.
- BILLIAU, A. & MATTHYS, P. 2009. Interferon-gamma: a historical perspective. *Cytokine Growth Factor Rev*, 20, 97-113.
- BISSELL, D. M. & GUZELIAN, P. S. 1980. Phenotypic stability of adult rat hepatocytes in primary monolayer culture. *Ann N Y Acad Sci*, 349, 85-98.
- BLASCHITZ, A., GAUSTER, M., FUCHS, D., LANG, I., MASCHKE, P., ULRICH, D., KARP, E., TAKIKAWA, O., SCHIMEK, M. G., DOHR, G. & SEDLMAYR, P. 2011. Vascular endothelial expression of indoleamine 2,3-dioxygenase 1 forms a positive gradient towards the fetomaternal interface. *PLoS One*, 6, e21774.
- BODAGHI, B., GOUREAU, O., ZIPETO, D., LAURENT, L., VIRELIZIER, J. L. & MICHELSON, S. 1999. Role of IFN-gamma-induced indoleamine 2,3 dioxygenase and inducible nitric oxide synthase in the replication of human cytomegalovirus in retinal pigment epithelial cells. *J Immunol*, 162, 957-64.
- BOEHM, U., KLAMP, T., GROOT, M. & HOWARD, J. C. 1997. Cellular responses to interferon-gamma. *Annu Rev Immunol*, 15, 749-95.
- BOOTCOV, M. R., BAUSKIN, A. R., VALENZUELA, S. M., MOORE, A. G., BANSAL, M., HE, X. Y., ZHANG, H. P., DONNELLAN, M., MAHLER, S., PRYOR, K., WALSH, B. J., NICHOLSON, R. C., FAIRLIE, W. D., POR, S. B., ROBBINS, J. M. & BREIT, S. N. 1997. MIC-1, a novel macrophage inhibitory cytokine, is a divergent member of the TGF-beta superfamily. *Proc Natl Acad Sci U S A*, 94, 11514-9.

- BORKHAM-KAMPHORST, E., DREWS, F. & WEISKIRCHEN, R. 2011. Induction of lipocalin-2 expression in acute and chronic experimental liver injury moderated by pro-inflammatory cytokines interleukin-1beta through nuclear factor-kappaB activation. *Liver Int*, 31, 656-65.
- BORKHAM-KAMPHORST, E., VAN DE LEUR, E., ZIMMERMANN, H. W., KARLMARK, K. R., TIHAA, L., HAAS, U., TACKE, F., BERGER, T., MAK, T. W. & WEISKIRCHEN, R. 2013. Protective effects of lipocalin-2 (LCN2) in acute liver injury suggest a novel function in liver homeostasis. *Biochim Biophys Acta*, 1832, 660-73.
- BOTTING, N. P. 1995. Chemistry and neurochemistry of the kynurenine pathway of tryptophan metabolism. *Chemical Society Reviews*, 24, 401-&.
- BRAMBELL, F. W. 1966. The transmission of immunity from mother to young and the catabolism of immunoglobulins. *Lancet*, 2, 1087-93.
- BRANCA, A. A. & BAGLIONI, C. 1981. Evidence that types I and II interferons have different receptors. *Nature*, 294, 768-70.
- BRANDACHER, G., PERATHONER, A., LADURNER, R., SCHNEEBERGER, S., OBRIST, P., WINKLER, C., WERNER, E. R., WERNER-FELMAYER, G., WEISS, H. G., GOBEL, G., MARGREITER, R., KONIGSRAINER, A., FUCHS, D. & AMBERGER, A. 2006. Prognostic value of indoleamine 2,3-dioxygenase expression in colorectal cancer: effect on tumor-infiltrating T cells. *Clin Cancer Res*, 12, 1144-51.
- BRITAN, A., MAFFRE, V., TONE, S. & DREVET, J. R. 2006. Quantitative and spatial differences in the expression of tryptophan-metabolizing enzymes in mouse epididymis. *Cell Tissue Res*, 324, 301-10.
- BROWN, D. A., MOORE, J., JOHNEN, H., SMEETS, T. J., BAUSKIN, A. R., KUFFNER, T., WEEDON, H., MILLIKEN, S. T., TAK, P. P., SMITH, M. D. & BREIT, S. N. 2007. Serum macrophage inhibitory cytokine 1 in rheumatoid arthritis: a potential marker of erosive joint destruction. *Arthritis Rheum*, 56, 753-64.
- BROWN, D. A., STEPHAN, C., WARD, R. L., LAW, M., HUNTER, M., BAUSKIN, A. R., AMIN, J., JUNG, K., DIAMANDIS, E. P., HAMPTON, G. M., RUSSELL, P. J., GILES, G. G. & BREIT, S. N. 2006. Measurement of serum levels of macrophage inhibitory cytokine 1 combined with prostate-specific antigen improves prostate cancer diagnosis. *Clin Cancer Res*, 12, 89-96.
- BROWN, D. A., WARD, R. L., BUCKHAULTS, P., LIU, T., ROMANS, K. E., HAWKINS, N. J., BAUSKIN, A. R., KINZLER, K. W., VOGELSTEIN, B. & BREIT, S. N. 2003. MIC-1 serum level and genotype: associations with progress and prognosis of colorectal carcinoma. *Clin Cancer Res*, 9, 2642-50.
- BUTLER, R., MORRIS, A. D., BELCH, J. J., HILL, A. & STRUTHERS, A. D. 2000. Allopurinol normalizes endothelial dysfunction in type 2 diabetics with mild hypertension. *Hypertension*, 35, 746-51.
- BYRNE, G. I., LEHMANN, L. K., KIRSCHBAUM, J. G., BORDEN, E. C., LEE, C. M. & BROWN, R. R. 1986a. Induction of tryptophan degradation in vitro and in vivo: a gamma-interferon-stimulated activity. *J Interferon Res*, 6, 389-96.
- BYRNE, G. I., LEHMANN, L. K. & LANDRY, G. J. 1986b. Induction of tryptophan catabolism is the mechanism for gamma-interferon-mediated inhibition of intracellular Chlamydia psittaci replication in T24 cells. *Infect Immun*, 53, 347-51.
- CAPECE, L., ARRAR, M., ROITBERG, A. E., YEY, S. R., MARTI, M. A. & ESTRIN, D. A. 2010. Substrate stereo-specificity in tryptophan dioxygenase and indoleamine 2,3-dioxygenase. *Proteins*, 78, 2961-72.
- CARLIN, J. M., BORDEN, E. C., SONDEL, P. M. & BYRNE, G. I. 1987. Biologic-response-modifier-induced indoleamine 2,3-dioxygenase activity in human peripheral blood mononuclear cell cultures. *J Immunol*, 139, 2414-8.

- CARNAUD, C., LEE, D., DONNARS, O., PARK, S. H., BEAVIS, A., KOEZUKA, Y. & BENDELAC, A. 1999. Cutting edge: Cross-talk between cells of the innate immune system: NKT cells rapidly activate NK cells. *J Immunol*, 163, 4647-50.
- CHALUVADI, M. R., NYAGODE, B. A., KINLOCH, R. D. & MORGAN, E. T. 2009. TLR4-dependent and -independent regulation of hepatic cytochrome P450 in mice with chemically induced inflammatory bowel disease. *Biochem Pharmacol*, 77, 464-71.
- CHAMBERS, K. J., TONKIN, L. A., CHANG, E., SHELTON, D. N., LINSKENS, M. H. & FUNK, W. D. 1998. Identification and cloning of a sequence homologue of dopamine beta-hydroxylase. *Gene*, 218, 111-20.
- CHANG, M. Y., SMITH, C., DUHADAWAY, J. B., PYLE, J. R., BOULDEN, J., SOLER, A. P., MULLER, A. J., LAURY-KLEINTOP, L. D. & PRENDERGAST, G. C. 2011. Cardiac and gastrointestinal liabilities caused by deficiency in the immune modulatory enzyme indoleamine 2,3-dioxygenase. *Cancer Biol Ther*, 12, 1050-8.
- CHENG, Q., ALEKSUNES, L. M., MANAUTOU, J. E., CHERRINGTON, N. J., SCHEFFER, G. L., YAMASAKI, H. & SLITT, A. L. 2008. Drug-metabolizing enzyme and transporter expression in a mouse model of diabetes and obesity. *Mol Pharm*, 5, 77-91.
- CHEUNG, K. J., TZAMELI, I., PISSIOS, P., ROVIRA, I., GAVRILOVA, O., OHTSUBO, T., CHEN, Z., FINKEL, T., FLIER, J. S. & FRIEDMAN, J. M. 2007. Xanthine oxidoreductase is a regulator of adipogenesis and PPARgamma activity. *Cell Metab*, 5, 115-28.
- CHOI, H. J. & CHOI, D. 2013. Successful mouse hepatocyte culture with sandwich collagen gel formation. *J Korean Surg Soc*, 84, 202-8.
- CHRISTENSEN, E. I. & BIRN, H. 2002. Megalin and cubilin: multifunctional endocytic receptors. *Nat Rev Mol Cell Biol*, 3, 256-66.
- CIORBA, M. A. 2013. Indoleamine 2,3 dioxygenase in intestinal disease. *Curr Opin Gastroenterol*, 29, 146-52.
- CLARK, K. J., VOYTAS, D. F. & EKKER, S. C. 2011. A TALE of two nucleases: gene targeting for the masses? *Zebrafish*, 8, 147-9.
- CLARKE, G., FITZGERALD, P., CRYAN, J. F., CASSIDY, E. M., QUIGLEY, E. M. & DINAN, T. G. 2009. Tryptophan degradation in irritable bowel syndrome: evidence of indoleamine 2,3-dioxygenase activation in a male cohort. *BMC Gastroenterol*, 9, 6.
- CLAYTON, D. F. & DARNELL, J. E., JR. 1983. Changes in liver-specific compared to common gene transcription during primary culture of mouse hepatocytes. *Mol Cell Biol*, 3, 1552-61.
- CLEROUX, J., VAN NGUYEN, P., TAYLOR, A. W. & LEENEN, F. H. 1989. Effects of beta 1- vs. beta 1 + beta 2-blockade on exercise endurance and muscle metabolism in humans. *J Appl Physiol* (1985), 66, 548-54.
- COLLART, M. A., BELIN, D., VASSALLI, J. D., DE KOSSODO, S. & VASSALLI, P. 1986. Gamma interferon enhances macrophage transcription of the tumor necrosis factor/cachectin, interleukin 1, and urokinase genes, which are controlled by short-lived repressors. *J Exp Med*, 164, 2113-8.
- CONNICK, J. H., CARLA, V., MORONI, F. & STONE, T. W. 1989. Increase in kynurenic acid in Huntington's disease motor cortex. *J Neurochem*, 52, 985-7.
- CONOVER, C. A., LEE, P. D., KANALEY, J. A., CLARKSON, J. T. & JENSEN, M. D. 1992. Insulin regulation of insulin-like growth factor binding protein-1 in obese and nonobese humans. *J Clin Endocrinol Metab*, 74, 1355-60.
- CRANE, L. J. & MILLER, D. L. 1977. Plasma protein synthesis by isolated rat hepatocytes. *J Cell Biol*, 72, 11-25.
- CRIADO, G., SIMELYTE, E., INGLIS, J. J., ESSEX, D. & WILLIAMS, R. O. 2009. Indoleamine 2,3 dioxygenase-mediated tryptophan catabolism regulates accumulation of Th1/Th17 cells in the joint in collagen-induced arthritis. *Arthritis Rheum*, 60, 1342-51.
- CROITORU-LAMOUREY, J., LAMOUREY, F. M., CARISTO, M., SUZUKI, K., WALKER, D., TAKIKAWA, O., TAYLOR, R. & BREW, B. J. 2011. Interferon-gamma regulates the proliferation and

- differentiation of mesenchymal stem cells via activation of indoleamine 2,3 dioxygenase (IDO). *PLoS One*, 6, e14698.
- CROSS, J. C., WERB, Z. & FISHER, S. J. 1994. Implantation and the placenta: key pieces of the development puzzle. *Science*, 266, 1508-18.
- CURRAN, J., MAKARA, M. A., LITTLE, S. C., MUSA, H., LIU, B., WU, X., POLINA, I., ALECUSAN, J. S., WRIGHT, P., LI, J., BILLMAN, G. E., BOYDEN, P. A., GYORKE, S., BAND, H., HUND, T. J. & MOHLER, P. J. 2014. EHD3-dependent endosome pathway regulates cardiac membrane excitability and physiology. *Circ Res*, 115, 68-78.
- CURZON, G., FRIEDEL, J. & KNOTT, P. J. 1973. The effect of fatty acids on the binding of tryptophan to plasma protein. *Nature*, 242, 198-200.
- CURZON, G., JOSEPH, M. H. & KNOTT, P. J. 1972. Effects of immobilization and food deprivation on rat brain tryptophan metabolism. *J Neurochem*, 19, 1967-74.
- DAHME, T., KATUS, H. A. & ROTTBAUER, W. 2009. Fishing for the genetic basis of cardiovascular disease. *Dis Model Mech*, 2, 18-22.
- DAI, W. & GUPTA, S. L. 1990. Regulation of indoleamine 2,3-dioxygenase gene expression in human fibroblasts by interferon-gamma. Upstream control region discriminates between interferon-gamma and interferon-alpha. *J Biol Chem*, 265, 19871-7.
- DAI, X. & ZHU, B. T. 2010. Indoleamine 2,3-dioxygenase tissue distribution and cellular localization in mice: implications for its biological functions. *J Histochem Cytochem*, 58, 17-28.
- DARWICH, L., COMA, G., PENA, R., BELLIDO, R., BLANCO, E. J., ESTE, J. A., BORRAS, F. E., CLOTET, B., RUIZ, L., ROSELL, A., ANDREO, F., PARKHOUSE, R. M. & BOFILL, M. 2009. Secretion of interferon-gamma by human macrophages demonstrated at the single-cell level after costimulation with interleukin (IL)-12 plus IL-18. *Immunology*, 126, 386-93.
- DAUBENER, W., SPORS, B., HUCKE, C., ADAM, R., STINS, M., KIM, K. S. & SCHROTEN, H. 2001. Restriction of *Toxoplasma gondii* growth in human brain microvascular endothelial cells by activation of indoleamine 2,3-dioxygenase. *Infect Immun*, 69, 6527-31.
- DESCO, M. C., ASENSI, M., MARQUEZ, R., MARTINEZ-VALLS, J., VENTO, M., PALLARDO, F. V., SASTRE, J. & VINA, J. 2002. Xanthine oxidase is involved in free radical production in type 1 diabetes: protection by allopurinol. *Diabetes*, 51, 1118-24.
- DHARANE NEE LIGAM, P., MANUELPIILLAI, U., WALLACE, E. & WALKER, D. W. 2010. NFkappaB-dependent increase of kynurenine pathway activity in human placenta: inhibition by sulfasalazine. *Placenta*, 31, 997-1002.
- DING, Q., MRACEK, T., GONZALEZ-MUNIESA, P., KOS, K., WILDING, J., TRAYHURN, P. & BING, C. 2009. Identification of macrophage inhibitory cytokine-1 in adipose tissue and its secretion as an adipokine by human adipocytes. *Endocrinology*, 150, 1688-96.
- DONG, J., QIU, H., GARCIA-BARRIO, M., ANDERSON, J. & HINNEBUSCH, A. G. 2000. Uncharged tRNA activates GCN2 by displacing the protein kinase moiety from a bipartite tRNA-binding domain. *Mol Cell*, 6, 269-79.
- DOSTALOVA, I., ROUBICEK, T., BARTLOVA, M., MRAZ, M., LACINOVA, Z., HALUZIKOVA, D., KAVALKOVA, P., MATOULEK, M., KASALICKY, M. & HALUZIK, M. 2009. Increased serum concentrations of macrophage inhibitory cytokine-1 in patients with obesity and type 2 diabetes mellitus: the influence of very low calorie diet. *Eur J Endocrinol*, 161, 397-404.
- DUNN, A. J. 1992. Endotoxin-induced activation of cerebral catecholamine and serotonin metabolism: comparison with interleukin-1. *J Pharmacol Exp Ther*, 261, 964-9.
- DURR, S. & KINDLER, V. 2013. Implication of indoleamine 2,3 dioxygenase in the tolerance toward fetuses, tumors, and allografts. *J Leukoc Biol*, 93, 681-7.
- EISEN, J. S. & SMITH, J. C. 2008. Controlling morpholino experiments: don't stop making antisense. *Development*, 135, 1735-43.
- EKKER, M. & AKIMENKO, M.-A. 2010. Reverse genetics: Morpholino knockdown and TILLING. *Fish Physiology: Zebrafish*. First ed. United States of America: Academic Press Publications.

- EMANUELA, F., GRAZIA, M., MARCO DE, R., MARIA PAOLA, L., GIORGIO, F. & MARCO, B. 2012. Inflammation as a Link between Obesity and Metabolic Syndrome. *J Nutr Metab*, 2012, 476380.
- ENRIQUEZ, A., LECLERCQ, I., FARRELL, G. C. & ROBERTSON, G. 1999. Altered expression of hepatic CYP2E1 and CYP4A in obese, diabetic ob/ob mice, and fa/fa Zucker rats. *Biochem Biophys Res Commun*, 255, 300-6.
- FACCHINI, F., CHEN, Y. D., HOLLENBECK, C. B. & REAVEN, G. M. 1991. Relationship between resistance to insulin-mediated glucose uptake, urinary uric acid clearance, and plasma uric acid concentration. *JAMA*, 266, 3008-11.
- FAIRLIE, W. D., MOORE, A. G., BAUSKIN, A. R., RUSSELL, P. K., ZHANG, H. P. & BREIT, S. N. 1999. MIC-1 is a novel TGF-beta superfamily cytokine associated with macrophage activation. *J Leukoc Biol*, 65, 2-5.
- FALLARINO, F., GROHMANN, U., VACCA, C., BIANCHI, R., ORABONA, C., SPRECA, A., FIORETTI, M. C. & PUC CETTI, P. 2002. T cell apoptosis by tryptophan catabolism. *Cell Death Differ*, 9, 1069-77.
- FALLARINO, F., GROHMANN, U., YOU, S., MCGRATH, B. C., CAVENER, D. R., VACCA, C., ORABONA, C., BIANCHI, R., BELLADONNA, M. L., VOLPI, C., FIORETTI, M. C. & PUC CETTI, P. 2006. Tryptophan catabolism generates autoimmune-preventive regulatory T cells. *Transpl Immunol*, 17, 58-60.
- FAN, J., CHAR, D., BAGBY, G. J., GELATO, M. C. & LANG, C. H. 1995. Regulation of insulin-like growth factor-I (IGF-I) and IGF-binding proteins by tumor necrosis factor. *Am J Physiol*, 269, R1204-12.
- FAN, J., WOJNAR, M. M., THEODORAKIS, M. & LANG, C. H. 1996. Regulation of insulin-like growth factor (IGF)-I mRNA and peptide and IGF-binding proteins by interleukin-1. *Am J Physiol*, 270, R621-9.
- FARBER, S. A., PACK, M., HO, S. Y., JOHNSON, I. D., WAGNER, D. S., DOSCH, R., MULLINS, M. C., HENDRICKSON, H. S., HENDRICKSON, E. K. & HALPERN, M. E. 2001. Genetic analysis of digestive physiology using fluorescent phospholipid reporters. *Science*, 292, 1385-8.
- FATOKUN, A. A., HUNT, N. H. & BALL, H. J. 2013. Indoleamine 2,3-dioxygenase 2 (IDO2) and the kynurenine pathway: characteristics and potential roles in health and disease. *Amino Acids*, 45, 1319-29.
- FAVRE, D., MOLD, J., HUNT, P. W., KANWAR, B., LOKE, P., SEU, L., BARBOUR, J. D., LOWE, M. M., JAYAWARDENE, A., AWEEKKA, F., HUANG, Y., DOUEK, D. C., BRENCHLEY, J. M., MARTIN, J. N., HECHT, F. M., DEEKS, S. G. & MCCUNE, J. M. 2010. Tryptophan catabolism by indoleamine 2,3-dioxygenase 1 alters the balance of TH17 to regulatory T cells in HIV disease. *Sci Transl Med*, 2, 32ra36.
- FERNSTROM, J. D. & FERNSTROM, M. H. 2006. Exercise, serum free tryptophan, and central fatigue. *J Nutr*, 136, 553S-559S.
- FERNSTROM, J. D. & WURTMAN, R. J. 1971. Brain serotonin content: physiological dependence on plasma tryptophan levels. *Science*, 173, 149-52.
- FERNSTROM, M. H. & FERNSTROM, J. D. 1993. Large changes in serum free tryptophan levels do not alter brain tryptophan levels: studies in streptozotocin-diabetic rats. *Life Sci*, 52, 907-16.
- FEUERER, M., HERRERO, L., CIPOLLETTA, D., NAAZ, A., WONG, J., NAYER, A., LEE, J., GOLDFINE, A. B., BENOIST, C., SHOELSON, S. & MATHIS, D. 2009. Lean, but not obese, fat is enriched for a unique population of regulatory T cells that affect metabolic parameters. *Nat Med*, 15, 930-9.
- FIELD, H. A., OBER, E. A., ROESER, T. & STAINIER, D. Y. 2003. Formation of the digestive system in zebrafish. I. Liver morphogenesis. *Dev Biol*, 253, 279-90.
- FINCK, B. N., BERNAL-MIZRACHI, C., HAN, D. H., COLEMAN, T., SAMBANDAM, N., LARIVIERE, L. L., HOLLOSZY, J. O., SEMENKOVICH, C. F. & KELLY, D. P. 2005. A potential link between

- muscle peroxisome proliferator- activated receptor- α signaling and obesity-related diabetes. *Cell Metab*, 1, 133-44.
- FINKELMAN, F. D., KATONA, I. M., MOSMANN, T. R. & COFFMAN, R. L. 1988. IFN- γ regulates the isotypes of Ig secreted during in vivo humoral immune responses. *J Immunol*, 140, 1022-7.
- FIRTH, S. M. & BAXTER, R. C. 2002. Cellular actions of the insulin-like growth factor binding proteins. *Endocr Rev*, 23, 824-54.
- FISHMAN, M. C. 2001. Genomics. Zebrafish--the canonical vertebrate. *Science*, 294, 1290-1.
- FLAISHON, L., HERSHKOVIZ, R., LANTNER, F., LIDER, O., ALON, R., LEVO, Y., FLAVELL, R. A. & SHACHAR, I. 2000. Autocrine secretion of interferon gamma negatively regulates homing of immature B cells. *J Exp Med*, 192, 1381-8.
- FORN-CUNI, G., VARELA, M., FERNANDEZ-RODRIGUEZ, C. M., FIGUERAS, A. & NOVOA, B. 2015. Liver immune responses to inflammatory stimuli in a diet-induced obesity model of zebrafish. *J Endocrinol*, 224, 159-70.
- FOROUHAR, F., ANDERSON, J. L., MOWAT, C. G., VOROBIEV, S. M., HUSSAIN, A., ABASHIDZE, M., BRUCKMANN, C., THACKRAY, S. J., SEETHARAMAN, J., TUCKER, T., XIAO, R., MA, L. C., ZHAO, L., ACTON, T. B., MONTELIONE, G. T., CHAPMAN, S. K. & TONG, L. 2007. Molecular insights into substrate recognition and catalysis by tryptophan 2,3-dioxygenase. *Proc Natl Acad Sci U S A*, 104, 473-8.
- FOX, C. J., HAMMERMAN, P. S. & THOMPSON, C. B. 2005. The Pim kinases control rapamycin-resistant T cell survival and activation. *J Exp Med*, 201, 259-66.
- FRANZ, J. M. & KNOX, W. E. 1967. The effect of development and hydrocortisone on tryptophan oxygenase, formamidase, and tyrosine aminotransferase in the livers of young rats. *Biochemistry*, 6, 3464-71.
- FRASLIN, J. M., KNEIP, B., VAULONT, S., GLAISE, D., MUNNICH, A. & GUGUEN-GUILLOUZO, C. 1985. Dependence of hepatocyte-specific gene expression on cell-cell interactions in primary culture. *EMBO J*, 4, 2487-91.
- FREEMAN, S. J. & LLOYD, J. B. 1983. Evidence that protein ingested by the rat visceral yolk sac yields amino acids for synthesis of embryonic protein. *J Embryol Exp Morphol*, 73, 307-15.
- FREYER, C. & RENFREE, M. B. 2009. The mammalian yolk sac placenta. *J Exp Zool B Mol Dev Evol*, 312, 545-54.
- FRIEDEL, R. H., WURST, W., WEFERS, B. & KUHN, R. 2011. Generating conditional knockout mice. *Methods Mol Biol*, 693, 205-31.
- FRUCHT, D. M., FUKAO, T., BOGDAN, C., SCHINDLER, H., O'SHEA, J. J. & KOYASU, S. 2001. IFN- γ production by antigen-presenting cells: mechanisms emerge. *Trends Immunol*, 22, 556-60.
- FRUMENTO, G., ROTONDO, R., TONETTI, M., DAMONTE, G., BENATTI, U. & FERRARA, G. B. 2002. Tryptophan-derived catabolites are responsible for inhibition of T and natural killer cell proliferation induced by indoleamine 2,3-dioxygenase. *J Exp Med*, 196, 459-68.
- FU, Y., FODEN, J. A., KHAYTER, C., MAEDER, M. L., REYON, D., JOUNG, J. K. & SANDER, J. D. 2013. High-frequency off-target mutagenesis induced by CRISPR-Cas nucleases in human cells. *Nat Biotechnol*, 31, 822-6.
- FUJIGAKI, S., SAITO, K., SEKIKAWA, K., TONE, S., TAKIKAWA, O., FUJII, H., WADA, H., NOMA, A. & SEISHIMA, M. 2001. Lipopolysaccharide induction of indoleamine 2,3-dioxygenase is mediated dominantly by an IFN- γ -independent mechanism. *Eur J Immunol*, 31, 2313-8.
- FUJITANI, M., YAMAGISHI, S., CHE, Y. H., HATA, K., KUBO, T., INO, H., TOHYAMA, M. & YAMASHITA, T. 2004. P311 accelerates nerve regeneration of the axotomized facial nerve. *J Neurochem*, 91, 737-44.
- FUKUNAGA, M., YAMAMOTO, Y., KAWASOE, M., ARIOKA, Y., MURAKAMI, Y., HOSHI, M. & SAITO, K. 2012. Studies on tissue and cellular distribution of indoleamine 2,3-dioxygenase 2: the

- absence of IDO1 upregulates IDO2 expression in the epididymis. *J Histochem Cytochem*, 60, 854-60.
- GAL, E. M. 1974. Cerebral tryptophan-2,3-dioxygenase (pyrrolase) and its induction in rat brain. *J Neurochem*, 22, 861-3.
- GALPERIN, E., BENJAMIN, S., RAPAPORT, D., ROTEM-YEHUDAR, R., TOLCHINSKY, S. & HOROWITZ, M. 2002. EHD3: a protein that resides in recycling tubular and vesicular membrane structures and interacts with EHD1. *Traffic*, 3, 575-89.
- GAO, X., ZHANG, Y., ARRAZOLA, P., HINO, O., KOBAYASHI, T., YEUNG, R. S., RU, B. & PAN, D. 2002. Tsc tumour suppressor proteins antagonize amino-acid-TOR signalling. *Nat Cell Biol*, 4, 699-704.
- GEORGE, M., AYUSO, E., CASELLAS, A., COSTA, C., DEVEDJIAN, J. C. & BOSCH, F. 2002. Beta cell expression of IGF-I leads to recovery from type 1 diabetes. *J Clin Invest*, 109, 1153-63.
- GESSANI, S. & BELARDELLI, F. 1998. IFN-gamma expression in macrophages and its possible biological significance. *Cytokine Growth Factor Rev*, 9, 117-23.
- GHEZZI, P., BIANCHI, M., MANTOVANI, A., SPREAFICO, F. & SALMONA, M. 1984. Enhanced xanthine oxidase activity in mice treated with interferon and interferon inducers. *Biochem Biophys Res Commun*, 119, 144-9.
- GHEZZI, P., SACCARDO, B. & BIANCHI, M. 1986. Induction of xanthine oxidase and heme oxygenase and depression of liver drug metabolism by interferon: a study with different recombinant interferons. *J Interferon Res*, 6, 251-6.
- GIBSON, U. E. & KRAMER, S. M. 1989. Enzyme-linked bio-immunoassay for IFN-gamma by HLA-DR induction. *J Immunol Methods*, 125, 105-13.
- GINGRAS, A. C., RAUGHT, B. & SONENBERG, N. 2001. Regulation of translation initiation by FRAP/mTOR. *Genes Dev*, 15, 807-26.
- GLEESON, M., CONNAUGHTON, V. & ARNESON, L. S. 2007. Induction of hyperglycaemia in zebrafish (*Danio rerio*) leads to morphological changes in the retina. *Acta Diabetol*, 44, 157-63.
- GODIN-ETHIER, J., HANAFI, L. A., PICCIRILLO, C. A. & LAPOINTE, R. 2011. Indoleamine 2,3-dioxygenase expression in human cancers: clinical and immunologic perspectives. *Clin Cancer Res*, 17, 6985-91.
- GOLDSMITH, J. R. & JOBIN, C. 2012. Think small: zebrafish as a model system of human pathology. *J Biomed Biotechnol*, 2012, 817341.
- GRAHAME-SMITH, D. G. 1964. Tryptophan hydroxylation in brain. *Biochem Biophys Res Commun*, 16, 586-92.
- GRAHAME-SMITH, D. G. 1971. Studies in vivo on the relationship between brain tryptophan, brain 5-HT synthesis and hyperactivity in rats treated with a monoamine oxidase inhibitor and L-tryptophan. *J Neurochem*, 18, 1053-66.
- GREEN, J. A., YEH, T. J. & OVERALL, J. C., JR. 1981. Sequential production of IFN-alpha and immune-specific IFN-gamma by human mononuclear leukocytes exposed to herpes simplex virus. *J Immunol*, 127, 1192-6.
- GRESSER, I. 1990. Biologic effects of interferons. *J Invest Dermatol*, 95, 66S-71S.
- GUIMARAES, E. L., STRADIOT, L., MANNAERTS, I., SCHROYEN, B. & VAN GRUNSVEN, L. A. 2015. P311 modulates hepatic stellate cells migration. *Liver Int*, 35, 1253-64.
- GULER, H. P., SCHMID, C., ZAPF, J. & FROESCH, E. R. 1989. Effects of recombinant insulin-like growth factor I on insulin secretion and renal function in normal human subjects. *Proc Natl Acad Sci U S A*, 86, 2868-72.
- GUO, H., JIN, D., ZHANG, Y., WRIGHT, W., BAZUINE, M., BROCKMAN, D. A., BERNLOHR, D. A. & CHEN, X. 2010. Lipocalin-2 deficiency impairs thermogenesis and potentiates diet-induced insulin resistance in mice. *Diabetes*, 59, 1376-85.
- GUPTA, R. M. & MUSUNURU, K. 2014. Expanding the genetic editing tool kit: ZFNs, TALENs, and CRISPR-Cas9. *J Clin Invest*, 124, 4154-61.

- GUPTA, S. L., CARLIN, J. M., PYATI, P., DAI, W., PFEFFERKORN, E. R. & MURPHY, M. J., JR. 1994. Antiparasitic and antiproliferative effects of indoleamine 2,3-dioxygenase enzyme expression in human fibroblasts. *Infect Immun*, 62, 2277-84.
- GURTNER, G. J., NEWBERRY, R. D., SCHLOEMANN, S. R., MCDONALD, K. G. & STENSON, W. F. 2003. Inhibition of indoleamine 2,3-dioxygenase augments trinitrobenzene sulfonic acid colitis in mice. *Gastroenterology*, 125, 1762-73.
- HAFFTER, P., GRANATO, M., BRAND, M., MULLINS, M. C., HAMMERSCHMIDT, M., KANE, D. A., ODENTHAL, J., VAN EEDEN, F. J., JIANG, Y. J., HEISENBERG, C. P., KELSH, R. N., FURUTANI-SEIKI, M., VOGELSANG, E., BEUCHLE, D., SCHACH, U., FABIAN, C. & NUSSLEIN-VOLHARD, C. 1996. The identification of genes with unique and essential functions in the development of the zebrafish, *Danio rerio*. *Development*, 123, 1-36.
- HAGIHARA, K., NISHIKAWA, T., ISOBE, T., SONG, J., SUGAMATA, Y. & YOSHIZAKI, K. 2004. IL-6 plays a critical role in the synergistic induction of human serum amyloid A (SAA) gene when stimulated with proinflammatory cytokines as analyzed with an SAA isoform real-time quantitative RT-PCR assay system. *Biochem Biophys Res Commun*, 314, 363-9.
- HANNAN, K. M., BRANDENBURGER, Y., JENKINS, A., SHARKEY, K., CAVANAUGH, A., ROTHBLUM, L., MOSS, T., POORTINGA, G., MCARTHUR, G. A., PEARSON, R. B. & HANNAN, R. D. 2003. mTOR-dependent regulation of ribosomal gene transcription requires S6K1 and is mediated by phosphorylation of the carboxy-terminal activation domain of the nucleolar transcription factor UBF. *Mol Cell Biol*, 23, 8862-77.
- HARDWICK, J. P. 2008. Cytochrome P450 omega hydroxylase (CYP4) function in fatty acid metabolism and metabolic diseases. *Biochem Pharmacol*, 75, 2263-75.
- HARRIS, C. M. & MASSEY, V. 1997. The reaction of reduced xanthine dehydrogenase with molecular oxygen. Reaction kinetics and measurement of superoxide radical. *J Biol Chem*, 272, 8370-9.
- HARRIS, D. P., HAYNES, L., SAYLES, P. C., DUSO, D. K., EATON, S. M., LEPAK, N. M., JOHNSON, L. L., SWAIN, S. L. & LUND, F. E. 2000. Reciprocal regulation of polarized cytokine production by effector B and T cells. *Nat Immunol*, 1, 475-82.
- HARRIS, J. F., ADEN, J., LYONS, C. R. & TESFAIGZI, Y. 2007. Resolution of LPS-induced airway inflammation and goblet cell hyperplasia is independent of IL-18. *Respir Res*, 8, 24.
- HASEGAWA, H., YANAGISAWA, M., INOUE, F., YANAIHARA, N. & ICHIYAMA, A. 1987. Demonstration of non-neural tryptophan 5-mono-oxygenase in mouse intestinal mucosa. *Biochem J*, 248, 501-9.
- HASSANAIN, H. H., CHON, S. Y. & GUPTA, S. L. 1993. Differential regulation of human indoleamine 2,3-dioxygenase gene expression by interferons-gamma and -alpha. Analysis of the regulatory region of the gene and identification of an interferon-gamma-inducible DNA-binding factor. *J Biol Chem*, 268, 5077-84.
- HAYAISHI, O. 1976. Properties and function of indoleamine 2,3-dioxygenase. *J Biochem*, 79, 13P-21P.
- HAYAISHI, O. 1996. Utilization of superoxide anion by indoleamine oxygenase-catalyzed tryptophan and indoleamine oxidation. *Adv Exp Med Biol*, 398, 285-9.
- HAYASHI, T., BECK, L., ROSSETTO, C., GONG, X., TAKIKAWA, O., TAKABAYASHI, K., BROIDE, D. H., CARSON, D. A. & RAZ, E. 2004. Inhibition of experimental asthma by indoleamine 2,3-dioxygenase. *J Clin Invest*, 114, 270-9.
- HAYASHI, T., RAO, S. P., TAKABAYASHI, K., VAN UDEN, J. H., KORNBLUTH, R. S., BAIRD, S. M., TAYLOR, M. W., CARSON, D. A., CATANZARO, A. & RAZ, E. 2001. Enhancement of innate immunity against *Mycobacterium avium* infection by immunostimulatory DNA is mediated by indoleamine 2,3-dioxygenase. *Infect Immun*, 69, 6156-64.
- HEDMAN, C. A., FRYSTYK, J., LINDSTROM, T., CHEN, J. W., FLYVBJERG, A., ORSKOV, H. & ARNQVIST, H. J. 2004. Residual beta-cell function more than glycemic control determines

- abnormalities of the insulin-like growth factor system in type 1 diabetes. *J Clin Endocrinol Metab*, 89, 6305-9.
- HEWITT, N. J., LECLUYSE, E. L. & FERGUSON, S. S. 2007. Induction of hepatic cytochrome P450 enzymes: methods, mechanisms, recommendations, and in vitro-in vivo correlations. *Xenobiotica*, 37, 1196-224.
- HEYES, M. P., ACHIM, C. L., WILEY, C. A., MAJOR, E. O., SAITO, K. & MARKEY, S. P. 1996. Human microglia convert l-tryptophan into the neurotoxin quinolinic acid. *Biochem J*, 320 (Pt 2), 595-7.
- HEYES, M. P., BREW, B. J., MARTIN, A., PRICE, R. W., SALAZAR, A. M., SIDTIS, J. J., YERGEY, J. A., MOURADIAN, M. M., SADLER, A. E., KEILP, J. & ET AL. 1991. Quinolinic acid in cerebrospinal fluid and serum in HIV-1 infection: relationship to clinical and neurological status. *Ann Neurol*, 29, 202-9.
- HEYES, M. P., CHEN, C. Y., MAJOR, E. O. & SAITO, K. 1997. Different kynurenine pathway enzymes limit quinolinic acid formation by various human cell types. *Biochem J*, 326 (Pt 2), 351-6.
- HEYES, M. P., SAITO, K. & MARKEY, S. P. 1992. Human macrophages convert L-tryptophan into the neurotoxin quinolinic acid. *Biochem J*, 283 (Pt 3), 633-5.
- HIGUCHI, K. & HAYAISHI, O. 1967. Enzymic formation of D-kynurenine from D-tryptophan. *Arch Biochem Biophys*, 120, 397-403.
- HILL, D. J., SEDRAN, R. J., BRENNER, S. L. & MCDONALD, T. J. 1997. IGF-I has a dual effect on insulin release from isolated, perfused adult rat islets of Langerhans. *J Endocrinol*, 153, 15-25.
- HILLE, R. 2006. Structure and Function of Xanthine Oxidoreductase. *European Journal of Inorganic Chemistry*, 2006, 1913-1926.
- HILLE, R. & NISHINO, T. 1995. Flavoprotein structure and mechanism. 4. Xanthine oxidase and xanthine dehydrogenase. *FASEB J*, 9, 995-1003.
- HOLDEN, B. J., BRATT, D. G. & CHICO, T. J. 2011. Molecular control of vascular development in the zebrafish. *Birth Defects Res C Embryo Today*, 93, 134-40.
- HONG, J. H., CHUNG, H. K., PARK, H. Y., JOUNG, K. H., LEE, J. H., JUNG, J. G., KIM, K. S., KIM, H. J., KU, B. J. & SHONG, M. 2014. GDF15 Is a Novel Biomarker for Impaired Fasting Glucose. *Diabetes Metab J*, 38, 472-9.
- HONIG, A., RIEGER, L., KAPP, M., SUTTERLIN, M., DIETL, J. & KAMMERER, U. 2004. Indoleamine 2,3-dioxygenase (IDO) expression in invasive extravillous trophoblast supports role of the enzyme for materno-fetal tolerance. *J Reprod Immunol*, 61, 79-86.
- HOU, D. Y., MULLER, A. J., SHARMA, M. D., DUHADAWAY, J., BANERJEE, T., JOHNSON, M., MELLOR, A. L., PRENDERGAST, G. C. & MUNN, D. H. 2007. Inhibition of indoleamine 2,3-dioxygenase in dendritic cells by stereoisomers of 1-methyl-tryptophan correlates with antitumor responses. *Cancer Res*, 67, 792-801.
- HOUSTON, M., ESTEVEZ, A., CHUMLEY, P., ASLAN, M., MARKLUND, S., PARKS, D. A. & FREEMAN, B. A. 1999. Binding of xanthine oxidase to vascular endothelium. Kinetic characterization and oxidative impairment of nitric oxide-dependent signaling. *J Biol Chem*, 274, 4985-94.
- HSU, P. D., SCOTT, D. A., WEINSTEIN, J. A., RAN, F. A., KONERMANN, S., AGARWALA, V., LI, Y., FINE, E. J., WU, X., SHALEM, O., CRADICK, T. J., MARRAFFINI, L. A., BAO, G. & ZHANG, F. 2013. DNA targeting specificity of RNA-guided Cas9 nucleases. *Nat Biotechnol*, 31, 827-32.
- HU, D. & CROSS, J. C. 2010. Development and function of trophoblast giant cells in the rodent placenta. *Int J Dev Biol*, 54, 341-54.
- HUNT, M. C. & ALEXSON, S. E. 2002. The role Acyl-CoA thioesterases play in mediating intracellular lipid metabolism. *Prog Lipid Res*, 41, 99-130.
- HUNT, M. C., NOUSIAINEN, S. E., HUTTUNEN, M. K., ORII, K. E., SVENSSON, L. T. & ALEXSON, S. E. 1999. Peroxisome proliferator-induced long chain acyl-CoA thioesterases comprise a highly conserved novel multi-gene family involved in lipid metabolism. *J Biol Chem*, 274, 34317-26.

- HUNT, M. C., SIPONEN, M. I. & ALEXSON, S. E. 2012. The emerging role of acyl-CoA thioesterases and acyltransferases in regulating peroxisomal lipid metabolism. *Biochim Biophys Acta*, 1822, 1397-410.
- HUR, K. Y. 2014. Is GDF15 a Novel Biomarker to Predict the Development of Prediabetes or Diabetes? *Diabetes Metab J*, 38, 437-8.
- HWANG, W. Y., FU, Y., REYON, D., MAEDER, M. L., KAINI, P., SANDER, J. D., JOUNG, J. K., PETERSON, R. T. & YEH, J. R. 2013a. Heritable and precise zebrafish genome editing using a CRISPR-Cas system. *PLoS One*, 8, e68708.
- HWANG, W. Y., FU, Y., REYON, D., MAEDER, M. L., TSAI, S. Q., SANDER, J. D., PETERSON, R. T., YEH, J. R. & JOUNG, J. K. 2013b. Efficient genome editing in zebrafish using a CRISPR-Cas system. *Nat Biotechnol*, 31, 227-9.
- HWU, P., DU, M. X., LAPOINTE, R., DO, M., TAYLOR, M. W. & YOUNG, H. A. 2000. Indoleamine 2,3-dioxygenase production by human dendritic cells results in the inhibition of T cell proliferation. *J Immunol*, 164, 3596-9.
- INABA, T., INO, K., KAJIYAMA, H., YAMAMOTO, E., SHIBATA, K., NAWA, A., NAGASAKA, T., AKIMOTO, H., TAKIKAWA, O. & KIKKAWA, F. 2009. Role of the immunosuppressive enzyme indoleamine 2,3-dioxygenase in the progression of ovarian carcinoma. *Gynecol Oncol*, 115, 185-92.
- INO, K., YOSHIDA, N., KAJIYAMA, H., SHIBATA, K., YAMAMOTO, E., KIDOKORO, K., TAKAHASHI, N., TERAUCHI, M., NAWA, A., NOMURA, S., NAGASAKA, T., TAKIKAWA, O. & KIKKAWA, F. 2006. Indoleamine 2,3-dioxygenase is a novel prognostic indicator for endometrial cancer. *Br J Cancer*, 95, 1555-61.
- IP, E., FARRELL, G. C., ROBERTSON, G., HALL, P., KIRSCH, R. & LECLERCQ, I. 2003. Central role of PPARalpha-dependent hepatic lipid turnover in dietary steatohepatitis in mice. *Hepatology*, 38, 123-32.
- ISAACS, A. & LINDENMANN, J. 1957. Virus interference. I. The interferon. *Proc R Soc Lond B Biol Sci*, 147, 258-67.
- ISAACS, A., LINDENMANN, J. & VALENTINE, R. C. 1957. Virus interference. II. Some properties of interferon. *Proc R Soc Lond B Biol Sci*, 147, 268-73.
- ISSEMANN, I. & GREEN, S. 1990. Activation of a member of the steroid hormone receptor superfamily by peroxisome proliferators. *Nature*, 347, 645-50.
- JAGASIA, D. & MCNULTY, P. H. 2003. Diabetes mellitus and heart failure. *Congest Heart Fail*, 9, 133-9; quiz 140-1.
- JAUNIAUX, E., CINDROVA-DAVIES, T., JOHNS, J., DUNSTER, C., HEMPSTOCK, J., KELLY, F. J. & BURTON, G. J. 2004. Distribution and transfer pathways of antioxidant molecules inside the first trimester human gestational sac. *J Clin Endocrinol Metab*, 89, 1452-8.
- JEE, S., HWANG, D., SEO, S., KIM, Y., KIM, C., KIM, B., SHIM, S., LEE, S., SIN, J., BAE, C., LEE, B., JANG, M., KIM, M., YIM, S., JANG, I., CHO, J. & CHAE, K. 2007. Microarray analysis of insulin-regulated gene expression in the liver: the use of transgenic mice co-expressing insulin-siRNA and human IDE as an animal model. *Int J Mol Med*, 20, 829-35.
- JOLLIE, W. P. 1986. Ultrastructural studies of protein transfer across rodent yolk sac. *Placenta*, 7, 263-81.
- JOLLIE, W. P. 1990. Development, morphology, and function of the yolk-sac placenta of laboratory rodents. *Teratology*, 41, 361-81.
- JONASCH, E. & HALUSKA, F. G. 2001. Interferon in oncological practice: review of interferon biology, clinical applications, and toxicities. *Oncologist*, 6, 34-55.
- JUNG, U. J. & CHOI, M. S. 2014. Obesity and its metabolic complications: the role of adipokines and the relationship between obesity, inflammation, insulin resistance, dyslipidemia and nonalcoholic fatty liver disease. *Int J Mol Sci*, 15, 6184-223.
- JUSOF, F. F., KHAW, L. T., BALL, H. J. & HUNT, N. H. 2013. Improved spectrophotometric human interferon-gamma bioassay. *J Immunol Methods*, 394, 115-20.

- KAMODA, T., SAITOH, H., INUDOH, M., MIYAZAKI, K. & MATSUI, A. 2006. The serum levels of proinsulin and their relationship with IGFBP-1 in obese children. *Diabetes Obes Metab*, 8, 192-6.
- KANAI, M., FUNAKOSHI, H., TAKAHASHI, H., HAYAKAWA, T., MIZUNO, S., MATSUMOTO, K. & NAKAMURA, T. 2009. Tryptophan 2,3-dioxygenase is a key modulator of physiological neurogenesis and anxiety-related behavior in mice. *Mol Brain*, 2, 8.
- KAWASAKI, H., CHANG, H. W., TSENG, H. C., HSU, S. C., YANG, S. J., HUNG, C. H., ZHOU, Y. & HUANG, S. K. 2014. A tryptophan metabolite, kynurenine, promotes mast cell activation through aryl hydrocarbon receptor. *Allergy*, 69, 445-52.
- KEMPF, T., GUBA-QUINT, A., TORGERSON, J., MAGNONE, M. C., HAEFLIGER, C., BOBADILLA, M. & WOLLERT, K. C. 2012. Growth differentiation factor 15 predicts future insulin resistance and impaired glucose control in obese nondiabetic individuals: results from the XENDOS trial. *Eur J Endocrinol*, 167, 671-8.
- KETOLA, H. G. 1982. Amino-Acid Nutrition of Fishes - Requirements and Supplementation of Diets. *Comparative Biochemistry and Physiology B-Biochemistry & Molecular Biology*, 73, 17-24.
- KETTLEBOROUGH, R. N., BUSCH-NENTWICH, E. M., HARVEY, S. A., DOOLEY, C. M., DE BRUIJN, E., VAN EEDEN, F., SEALY, I., WHITE, R. J., HERD, C., NIJMAN, I. J., FENYES, F., MEHROKE, S., SCAHILL, C., GIBBONS, R., WALI, N., CARRUTHERS, S., HALL, A., YEN, J., CUPPEN, E. & STEMPLE, D. L. 2013. A systematic genome-wide analysis of zebrafish protein-coding gene function. *Nature*, 496, 494-7.
- KIMMEL, C. B., BALLARD, W. W., KIMMEL, S. R., ULLMANN, B. & SCHILLING, T. F. 1995. Stages of embryonic development of the zebrafish. *Dev Dyn*, 203, 253-310.
- KINTH, P., MAHESH, G. & PANWAR, Y. 2013. Mapping of zebrafish research: a global outlook. *Zebrafish*, 10, 510-7.
- KLOOSTERMAN, W. P., LAGENDIJK, A. K., KETTING, R. F., MOULTON, J. D. & PLASTERK, R. H. 2007. Targeted inhibition of miRNA maturation with morpholinos reveals a role for miR-375 in pancreatic islet development. *PLoS Biol*, 5, e203.
- KNOX, W. E. & AUERBACH, V. H. 1955. The hormonal control of tryptophan peroxidase in the rat. *J Biol Chem*, 214, 307-13.
- KNOX, W. E. & MEHLER, A. H. 1950. The conversion of tryptophan to kynurenine in liver. I. The coupled tryptophan peroxidase-oxidase system forming formylkynurenine. *J Biol Chem*, 187, 419-30.
- KNUBEL, C. P., MARTINEZ, F. F., FRETES, R. E., DIAZ LUJAN, C., THEUMER, M. G., CERVI, L. & MOTRAN, C. C. 2010. Indoleamine 2,3-dioxygenase (IDO) is critical for host resistance against *Trypanosoma cruzi*. *FASEB J*, 24, 2689-701.
- KONEN-WAISMAN, S. & HOWARD, J. C. 2007. Cell-autonomous immunity to *Toxoplasma gondii* in mouse and man. *Microbes Infect*, 9, 1652-61.
- KONSTANDI, M., SHAH, Y. M., MATSUBARA, T. & GONZALEZ, F. J. 2013. Role of PPARalpha and HNF4alpha in stress-mediated alterations in lipid homeostasis. *PLoS One*, 8, e70675.
- KOOPMANN, J., ROSENZWEIG, C. N., ZHANG, Z., CANTO, M. I., BROWN, D. A., HUNTER, M., YEO, C., CHAN, D. W., BREIT, S. N. & GOGGINS, M. 2006. Serum markers in patients with resectable pancreatic adenocarcinoma: macrophage inhibitory cytokine 1 versus CA19-9. *Clin Cancer Res*, 12, 442-6.
- KOZYRAKI, R. & GOFFLOT, F. 2007. Multiligand endocytosis and congenital defects: roles of cubilin, megalin and amnionless. *Curr Pharm Des*, 13, 3038-46.
- KUDO, Y., BOYD, C. A., SPYROPOULOU, I., REDMAN, C. W., TAKIKAWA, O., KATSUKI, T., HARA, T., OHAMA, K. & SARGENT, I. L. 2004. Indoleamine 2,3-dioxygenase: distribution and function in the developing human placenta. *J Reprod Immunol*, 61, 87-98.
- KUROOKA, S., HOSOKI, K. & YOSHIMURA, Y. 1971. Increase in long fatty acyl-CoA hydrolase activity in the liver and kidney of alloxan diabetic rat. *J Biochem*, 69, 247-9.

- KUSHNER, I. 1982. The phenomenon of the acute phase response. *Ann N Y Acad Sci*, 389, 39-48.
- LAGER, S. & POWELL, T. L. 2012. Regulation of nutrient transport across the placenta. *J Pregnancy*, 2012, 179827.
- LANGENAU, D. M. & ZON, L. I. 2005. The zebrafish: a new model of T-cell and thymic development. *Nat Rev Immunol*, 5, 307-17.
- LEE, G. K., PARK, H. J., MACLEOD, M., CHANDLER, P., MUNN, D. H. & MELLOR, A. L. 2002. Tryptophan deprivation sensitizes activated T cells to apoptosis prior to cell division. *Immunology*, 107, 452-60.
- LEHRKE, M. & LAZAR, M. A. 2004. Inflamed about obesity. *Nat Med*, 10, 126-7.
- LENARD, N. R. & DUNN, A. J. 2005. Potential role for nonesterified fatty acids in beta-adrenoceptor-induced increases in brain tryptophan. *Neurochem Int*, 46, 179-87.
- LEUNG, J. K., CASES, S. & VU, T. H. 2008. P311 functions in an alternative pathway of lipid accumulation that is induced by retinoic acid. *J Cell Sci*, 121, 2751-8.
- LIGAM, P., MANUELPIILLAI, U., WALLACE, E. M. & WALKER, D. 2005. Localisation of indoleamine 2,3-dioxygenase and kynurenine hydroxylase in the human placenta and decidua: implications for role of the kynurenine pathway in pregnancy. *Placenta*, 26, 498-504.
- LIN, Q., WEIS, S., YANG, G., WENG, Y. H., HELSTON, R., RISH, K., SMITH, A., BORDNER, J., POLTE, T., GAUNITZ, F. & DENNERY, P. A. 2007. Heme oxygenase-1 protein localizes to the nucleus and activates transcription factors important in oxidative stress. *J Biol Chem*, 282, 20621-33.
- LINDERHOLM, K. R., SKOGH, E., OLSSON, S. K., DAHL, M. L., HOLTZE, M., ENGBERG, G., SAMUELSSON, M. & ERHARDT, S. 2012. Increased levels of kynurenine and kynurenic acid in the CSF of patients with schizophrenia. *Schizophr Bull*, 38, 426-32.
- LINDQUIST, P. J., SVENSSON, L. T. & ALEXSON, S. E. 1998. Molecular cloning of the peroxisome proliferator-induced 46-kDa cytosolic acyl-CoA thioesterase from mouse and rat liver--recombinant expression in Escherichia coli, tissue expression, and nutritional regulation. *Eur J Biochem*, 251, 631-40.
- LINK, B. A. & MEGASON, S. G. 2008. Zebrafish as a Model for Development. In: CONN, M. P. (ed.) *Sourcebook of Models for Biomedical Research*. Humana Press.
- LIU, X., SHIN, N., KOBLISH, H. K., YANG, G., WANG, Q., WANG, K., LEFFET, L., HANSBURY, M. J., THOMAS, B., RUPAR, M., WAELTZ, P., BOWMAN, K. J., POLAM, P., SPARKS, R. B., YUE, E. W., LI, Y., WYNN, R., FRIDMAN, J. S., BURN, T. C., COMBS, A. P., NEWTON, R. C. & SCHERLE, P. A. 2010. Selective inhibition of IDO1 effectively regulates mediators of antitumor immunity. *Blood*, 115, 3520-30.
- LIVAK, K. J. & SCHMITTGEN, T. D. 2001. Analysis of relative gene expression data using real-time quantitative PCR and the 2^{-Delta Delta C(T)} Method. *Methods*, 25, 402-8.
- LLOYD, J. B., BRENT, R. L. & BECKMAN, D. A. 1996. Sources of amino acids for protein synthesis during early organogenesis in the rat. 3. Methionine incorporation. *Placenta*, 17, 629-34.
- LOB, S., KONIGSRAINER, A., SCHAFER, R., RAMMENSEE, H. G., OPELZ, G. & TERNESS, P. 2008. Levo- but not dextro-1-methyl tryptophan abrogates the IDO activity of human dendritic cells. *Blood*, 111, 2152-4.
- LOB, S., KONIGSRAINER, A., ZIEKER, D., BRUCHER, B. L., RAMMENSEE, H. G., OPELZ, G. & TERNESS, P. 2009. IDO1 and IDO2 are expressed in human tumors: levo- but not dextro-1-methyl tryptophan inhibits tryptophan catabolism. *Cancer Immunol Immunother*, 58, 153-7.
- LUSTER, A. D., UNKELESS, J. C. & RAVETCH, J. V. 1985. Gamma-interferon transcriptionally regulates an early-response gene containing homology to platelet proteins. *Nature*, 315, 672-6.
- MACKENZIE, C. R., HADDING, U. & DAUBENER, W. 1998. Interferon-gamma-induced activation of indoleamine 2,3-dioxygenase in cord blood monocyte-derived macrophages inhibits the growth of group B streptococci. *J Infect Dis*, 178, 875-8.

- MADRAS, B. K., COHEN, E. L., MESSING, R., MUNRO, H. N. & WURTMAN, R. J. 1974. Relevance of free tryptophan in serum to tissue tryptophan concentrations. *Metabolism*, 23, 1107-16.
- MAGHZAL, G. J., THOMAS, S. R., HUNT, N. H. & STOCKER, R. 2008. Cytochrome b5, not superoxide anion radical, is a major reductant of indoleamine 2,3-dioxygenase in human cells. *J Biol Chem*, 283, 12014-25.
- MAGLOTT, D., OSTELL, J., PRUITT, K. D. & TATUSOVA, T. 2005. Entrez Gene: gene-centered information at NCBI. *Nucleic Acids Res*, 33, D54-8.
- MAILANKOT, M. & NAGARAJ, R. H. 2010. Induction of indoleamine 2,3-dioxygenase by interferon-gamma in human lens epithelial cells: apoptosis through the formation of 3-hydroxykynurenine. *Int J Biochem Cell Biol*, 42, 1446-54.
- MARHAUG, G. & DOWTON, S. B. 1994. Serum amyloid A: an acute phase apolipoprotein and precursor of AA amyloid. *Baillieres Clin Rheumatol*, 8, 553-73.
- MARHAUG, G., PERMIN, H. & HUSBY, G. 1983. Amyloid-related serum protein (SAA) as an indicator of lung infection in cystic fibrosis. *Acta Paediatr Scand*, 72, 861-6.
- MARTIN, C. A. & DORF, M. E. 1991. Differential regulation of interleukin-6, macrophage inflammatory protein-1, and JE/MCP-1 cytokine expression in macrophage cell lines. *Cell Immunol*, 135, 245-58.
- MARTINEZ-BEAMONTE, R., NAVARRO, M. A., GUILLEN, N., ACIN, S., ARNAL, C., GUZMAN, M. A. & OSADA, J. 2011. Postprandial transcriptome associated with virgin olive oil intake in rat liver. *Front Biosci (Elite Ed)*, 3, 11-21.
- MARTINEZ, S. M., BRADFORD, B. U., SOLDATOW, V. Y., KOSYK, O., SANDOT, A., WITEK, R., KAISER, R., STEWART, T., AMARAL, K., FREEMAN, K., BLACK, C., LECLUYSE, E. L., FERGUSON, S. S. & RUSYN, I. 2010. Evaluation of an in vitro toxicogenetic mouse model for hepatotoxicity. *Toxicol Appl Pharmacol*, 249, 208-16.
- MAZUREK, G. H., LOBUE, P. A., DALEY, C. L., BERNARDO, J., LARDIZABAL, A. A., BISHAI, W. R., IADEMARCO, M. F. & ROTHEL, J. S. 2001. Comparison of a whole-blood interferon gamma assay with tuberculin skin testing for detecting latent Mycobacterium tuberculosis infection. *JAMA*, 286, 1740-7.
- MCKINNEY, J., KNAPPSKOG, P. M. & HAAVIK, J. 2005. Different properties of the central and peripheral forms of human tryptophan hydroxylase. *J Neurochem*, 92, 311-20.
- MCMENAMY, R. H. 1965. Binding of indole analogues to human serum albumin. Effects of fatty acids. *J Biol Chem*, 240, 4235-43.
- MEEK, R. L. & BENDITT, E. P. 1986. Amyloid A gene family expression in different mouse tissues. *J Exp Med*, 164, 2006-17.
- MEEKER, N. D. & TREDE, N. S. 2008. Immunology and zebrafish: spawning new models of human disease. *Dev Comp Immunol*, 32, 745-57.
- MEHLER, A. H. & KNOX, W. E. 1950. The conversion of tryptophan to kynurenine in liver. II. The enzymatic hydrolysis of formylkynurenine. *J Biol Chem*, 187, 431-8.
- MELLOR, A. L. & MUNN, D. H. 1999. Tryptophan catabolism and T-cell tolerance: immunosuppression by starvation? *Immunol Today*, 20, 469-73.
- MELLOR, A. L. & MUNN, D. H. 2004. IDO expression by dendritic cells: tolerance and tryptophan catabolism. *Nat Rev Immunol*, 4, 762-74.
- MELLOR, A. L. & MUNN, D. H. 2008. Creating immune privilege: active local suppression that benefits friends, but protects foes. *Nat Rev Immunol*, 8, 74-80.
- MELLOR, A. L., SIVAKUMAR, J., CHANDLER, P., SMITH, K., MOLINA, H., MAO, D. & MUNN, D. H. 2001. Prevention of T cell-driven complement activation and inflammation by tryptophan catabolism during pregnancy. *Nat Immunol*, 2, 64-8.
- MERLO, L. M., PIGOTT, E., DUHADAWAY, J. B., GRABLER, S., METZ, R., PRENDERGAST, G. C. & MANDIK-NAYAK, L. 2014. IDO2 is a critical mediator of autoantibody production and inflammatory pathogenesis in a mouse model of autoimmune arthritis. *J Immunol*, 192, 2082-90.

- METZ, R., DUHADAWAY, J. B., KAMASANI, U., LAURY-KLEINTOP, L., MULLER, A. J. & PRENDERGAST, G. C. 2007. Novel tryptophan catabolic enzyme IDO2 is the preferred biochemical target of the antitumor indoleamine 2,3-dioxygenase inhibitory compound D-1-methyl-tryptophan. *Cancer Res*, 67, 7082-7.
- METZ, R., RUST, S., DUHADAWAY, J. B., MAUTINO, M. R., MUNN, D. H., VAHANIAN, N. N., LINK, C. J. & PRENDERGAST, G. C. 2012. IDO inhibits a tryptophan sufficiency signal that stimulates mTOR: A novel IDO effector pathway targeted by D-1-methyl-tryptophan. *Oncoimmunology*, 1, 1460-1468.
- METZ, R., SMITH, C., DUHADAWAY, J. B., CHANDLER, P., BABAN, B., MERLO, L. M., PIGOTT, E., KEOUGH, M. P., RUST, S., MELLOR, A. L., MANDIK-NAYAK, L., MULLER, A. J. & PRENDERGAST, G. C. 2014. IDO2 is critical for IDO1-mediated T-cell regulation and exerts a non-redundant function in inflammation. *Int Immunol*, 26, 357-67.
- MIKKOLA, H. K. & ORKIN, S. H. 2006. The journey of developing hematopoietic stem cells. *Development*, 133, 3733-44.
- MILLER, C. L., LLENOS, I. C., DULAY, J. R., BARILLO, M. M., YOLKEN, R. H. & WEIS, S. 2004. Expression of the kynurenine pathway enzyme tryptophan 2,3-dioxygenase is increased in the frontal cortex of individuals with schizophrenia. *Neurobiol Dis*, 15, 618-29.
- MILLER, C. L., LLENOS, I. C., DULAY, J. R. & WEIS, S. 2006. Upregulation of the initiating step of the kynurenine pathway in postmortem anterior cingulate cortex from individuals with schizophrenia and bipolar disorder. *Brain Res*, 1073-1074, 25-37.
- MOREAU, M., LESTAGE, J., VERRIER, D., MORMEDE, C., KELLEY, K. W., DANTZER, R. & CASTANON, N. 2005. Bacille Calmette-Guerin inoculation induces chronic activation of peripheral and brain indoleamine 2,3-dioxygenase in mice. *J Infect Dis*, 192, 537-44.
- MORRISSETTE, D. A. & STAHL, S. M. 2014. Modulating the serotonin system in the treatment of major depressive disorder. *CNS Spectr*, 19 Suppl 1, 54-68.
- MOSCA, P. J., HOBEIKA, A. C., CLAY, T. M., NAIR, S. K., THOMAS, E. K., MORSE, M. A. & LYERLY, H. K. 2000. A subset of human monocyte-derived dendritic cells expresses high levels of interleukin-12 in response to combined CD40 ligand and interferon-gamma treatment. *Blood*, 96, 3499-504.
- MOSS, J. B., KOUSTUBHAN, P., GREENMAN, M., PARSONS, M. J., WALTER, I. & MOSS, L. G. 2009. Regeneration of the pancreas in adult zebrafish. *Diabetes*, 58, 1844-51.
- MULLER, A. J., SHARMA, M. D., CHANDLER, P. R., DUHADAWAY, J. B., EVERHART, M. E., JOHNSON, B. A., 3RD, KAHLER, D. J., PIHKALA, J., SOLER, A. P., MUNN, D. H., PRENDERGAST, G. C. & MELLOR, A. L. 2008. Chronic inflammation that facilitates tumor progression creates local immune suppression by inducing indoleamine 2,3 dioxygenase. *Proc Natl Acad Sci U S A*, 105, 17073-8.
- MULLER, N. & SCHWARZ, M. J. 2007. The immune-mediated alteration of serotonin and glutamate: towards an integrated view of depression. *Mol Psychiatry*, 12, 988-1000.
- MULLER, W. E. & WOLLERT, U. 1975. Benzodiazepines: specific competitors for the binding of L-tryptophan to human serum albumin. *Naunyn Schmiedebergs Arch Pharmacol*, 288, 17-27.
- MUNDER, M., MALLO, M., EICHMANN, K. & MODOLELL, M. 1998. Murine macrophages secrete interferon gamma upon combined stimulation with interleukin (IL)-12 and IL-18: A novel pathway of autocrine macrophage activation. *J Exp Med*, 187, 2103-8.
- MUNN, D. H. 2006. Indoleamine 2,3-dioxygenase, tumor-induced tolerance and counter-regulation. *Curr Opin Immunol*, 18, 220-5.
- MUNN, D. H. & MELLOR, A. L. 2013. Indoleamine 2,3 dioxygenase and metabolic control of immune responses. *Trends Immunol*, 34, 137-43.
- MUNN, D. H., SHAFIZADEH, E., ATTWOOD, J. T., BONDAREV, I., PASHINE, A. & MELLOR, A. L. 1999. Inhibition of T cell proliferation by macrophage tryptophan catabolism. *J Exp Med*, 189, 1363-72.

- MUNN, D. H., SHARMA, M. D., BABAN, B., HARDING, H. P., ZHANG, Y., RON, D. & MELLOR, A. L. 2005. GCN2 kinase in T cells mediates proliferative arrest and anergy induction in response to indoleamine 2,3-dioxygenase. *Immunity*, 22, 633-42.
- MUNN, D. H., SHARMA, M. D., HOU, D., BABAN, B., LEE, J. R., ANTONIA, S. J., MESSINA, J. L., CHANDLER, P., KONI, P. A. & MELLOR, A. L. 2004. Expression of indoleamine 2,3-dioxygenase by plasmacytoid dendritic cells in tumor-draining lymph nodes. *J Clin Invest*, 114, 280-90.
- MUNN, D. H., ZHOU, M., ATTWOOD, J. T., BONDAREV, I., CONWAY, S. J., MARSHALL, B., BROWN, C. & MELLOR, A. L. 1998. Prevention of allogeneic fetal rejection by tryptophan catabolism. *Science*, 281, 1191-3.
- MURAKAMI, Y. & SAITO, K. 2013. Species and cell types difference in tryptophan metabolism. *Int J Tryptophan Res*, 6, 47-54.
- NAKAMURA, T., NAGAO, M. & ICHIHARA, A. 1987. In vitro induction of terminal differentiation of neonatal rat hepatocytes by direct contact with adult rat hepatocytes [corrected]. *Exp Cell Res*, 169, 1-14.
- NASEVICIUS, A. & EKKER, S. C. 2000. Effective targeted gene 'knockdown' in zebrafish. *Nat Genet*, 26, 216-20.
- NG, A. N., DE JONG-CURTAIN, T. A., MAWDSLEY, D. J., WHITE, S. J., SHIN, J., APPEL, B., DONG, P. D., STAINIER, D. Y. & HEATH, J. K. 2005. Formation of the digestive system in zebrafish: III. Intestinal epithelium morphogenesis. *Dev Biol*, 286, 114-35.
- NISHIMURA, S., MANABE, I., NAGASAKI, M., ETO, K., YAMASHITA, H., OHSUGI, M., OTSU, M., HARA, K., UEKI, K., SUGIURA, S., YOSHIMURA, K., KADOWAKI, T. & NAGAI, R. 2009. CD8+ effector T cells contribute to macrophage recruitment and adipose tissue inflammation in obesity. *Nat Med*, 15, 914-20.
- NISHINO, T. 1994. The conversion of xanthine dehydrogenase to xanthine oxidase and the role of the enzyme in reperfusion injury. *J Biochem*, 116, 1-6.
- NOTREDAME, C., HIGGINS, D. G. & HERINGA, J. 2000. T-Coffee: A novel method for fast and accurate multiple sequence alignment. *J Mol Biol*, 302, 205-17.
- NUTT, S. L., BRONCHAIN, O. J., HARTLEY, K. O. & AMAYA, E. 2001. Comparison of morpholino based translational inhibition during the development of *Xenopus laevis* and *Xenopus tropicalis*. *Genesis*, 30, 110-3.
- NYAGODE, B. A., WATKINS, W. J., KINLOCH, R. D. & MORGAN, E. T. 2012. Selective modulation of hepatic cytochrome P450 and flavin monooxygenase 3 expression during *Citrobacter rodentium* infection in severe combined immune-deficient mice. *Drug Metab Dispos*, 40, 1894-9.
- O'CONNOR, J. C., LAWSON, M. A., ANDRE, C., MOREAU, M., LESTAGE, J., CASTANON, N., KELLEY, K. W. & DANTZER, R. 2009. Lipopolysaccharide-induced depressive-like behavior is mediated by indoleamine 2,3-dioxygenase activation in mice. *Mol Psychiatry*, 14, 511-22.
- O'ROURKE, R. W., METCALF, M. D., WHITE, A. E., MADALA, A., WINTERS, B. R., MAIZLIN, II, JOBE, B. A., ROBERTS, C. T., JR., SLIFKA, M. K. & MARKS, D. L. 2009. Depot-specific differences in inflammatory mediators and a role for NK cells and IFN-gamma in inflammation in human adipose tissue. *Int J Obes (Lond)*, 33, 978-90.
- O'ROURKE, R. W., WHITE, A. E., METCALF, M. D., WINTERS, B. R., DIGGS, B. S., ZHU, X. & MARKS, D. L. 2012. Systemic inflammation and insulin sensitivity in obese IFN-gamma knockout mice. *Metabolism*, 61, 1152-61.
- OHYAMA, F., TONE, S., OKAMOTO, T., SHIMODA, K. & MINATOGAWA, Y. 2007. Induction of indoleamine 2,3-dioxygenase in small intestine of mouse infected with parasitic helminth, *Hymenolepis nana*. *International Congress Series*, 1304, 286-289.
- OKAMOTO, A., NIKAIDO, T., OCHIAI, K., TAKAKURA, S., SAITO, M., AOKI, Y., ISHII, N., YANAIHARA, N., YAMADA, K., TAKIKAWA, O., KAWAGUCHI, R., ISONISHI, S., TANAKA, T. & URASHIMA,

- M. 2005. Indoleamine 2,3-dioxygenase serves as a marker of poor prognosis in gene expression profiles of serous ovarian cancer cells. *Clin Cancer Res*, 11, 6030-9.
- OPITZ, C. A., LITZENBURGER, U. M., SAHM, F., OTT, M., TRITSCHLER, I., TRUMP, S., SCHUMACHER, T., JESTAEDT, L., SCHRENK, D., WELLER, M., JUGOLD, M., GUILLEMIN, G. J., MILLER, C. L., LUTZ, C., RADLWIMMER, B., LEHMANN, I., VON DEIMLING, A., WICK, W. & PLATTEN, M. 2011. An endogenous tumour-promoting ligand of the human aryl hydrocarbon receptor. *Nature*, 478, 197-203.
- OPITZ, C. A., WICK, W., STEINMAN, L. & PLATTEN, M. 2007. Tryptophan degradation in autoimmune diseases. *Cell Mol Life Sci*, 64, 2542-63.
- OUCHI, N., PARKER, J. L., LUGUS, J. J. & WALSH, K. 2011. Adipokines in inflammation and metabolic disease. *Nat Rev Immunol*, 11, 85-97.
- OWE-YOUNG, R., WEBSTER, N. L., MUKHTAR, M., POMERANTZ, R. J., SMYTHE, G., WALKER, D., ARMATI, P. J., CROWE, S. M. & BREW, B. J. 2008. Kynurenine pathway metabolism in human blood-brain-barrier cells: implications for immune tolerance and neurotoxicity. *J Neurochem*, 105, 1346-57.
- OZAKI, Y., EDELSTEIN, M. P. & DUCH, D. S. 1988. Induction of indoleamine 2,3-dioxygenase: a mechanism of the antitumor activity of interferon gamma. *Proc Natl Acad Sci U S A*, 85, 1242-6.
- PACHER, P., NIVOROZHKIN, A. & SZABO, C. 2006. Therapeutic effects of xanthine oxidase inhibitors: renaissance half a century after the discovery of allopurinol. *Pharmacol Rev*, 58, 87-114.
- PASHAJ, A., YI, X., XIA, M., CANNY, S., RIETHOVEN, J. J. & MOREAU, R. 2013. Characterization of genome-wide transcriptional changes in liver and adipose tissues of ZDF (fa/fa) rats fed R-alpha-lipoic acid by next-generation sequencing. *Physiol Genomics*, 45, 1136-43.
- PATSOURIS, D., REDDY, J. K., MULLER, M. & KERSTEN, S. 2006. Peroxisome proliferator-activated receptor alpha mediates the effects of high-fat diet on hepatic gene expression. *Endocrinology*, 147, 1508-16.
- PERUSSIA, B., DAYTON, E. T., FANNING, V., THIAGARAJAN, P., HOXIE, J. & TRINCHIERI, G. 1983. Immune interferon and leukocyte-conditioned medium induce normal and leukemic myeloid cells to differentiate along the monocytic pathway. *J Exp Med*, 158, 2058-80.
- PFEFFER, K. D., HUECKSTEADT, T. P. & HOIDAL, J. R. 1994. Xanthine dehydrogenase and xanthine oxidase activity and gene expression in renal epithelial cells. Cytokine and steroid regulation. *J Immunol*, 153, 1789-97.
- PFEFFERKORN, E. R., ECKEL, M. & REBHUN, S. 1986a. Interferon-gamma suppresses the growth of *Toxoplasma gondii* in human fibroblasts through starvation for tryptophan. *Mol Biochem Parasitol*, 20, 215-24.
- PFEFFERKORN, E. R. & GUYRE, P. M. 1984. Inhibition of growth of *Toxoplasma gondii* in cultured fibroblasts by human recombinant gamma interferon. *Infect Immun*, 44, 211-6.
- PFEFFERKORN, E. R., REBHUN, S. & ECKEL, M. 1986b. Characterization of an indoleamine 2,3-dioxygenase induced by gamma-interferon in cultured human fibroblasts. *J Interferon Res*, 6, 267-79.
- PILOTTE, L., LARRIEU, P., STROOBANT, V., COLAU, D., DOLUSIC, E., FREDERICK, R., DE PLAEN, E., UYTENHOVE, C., WOUTERS, J., MASEREEL, B. & VAN DEN EYNDE, B. J. 2012. Reversal of tumoral immune resistance by inhibition of tryptophan 2,3-dioxygenase. *Proc Natl Acad Sci U S A*, 109, 2497-502.
- PLATTEN, M., HO, P. P., YOUSSEF, S., FONTOURA, P., GARREN, H., HUR, E. M., GUPTA, R., LEE, L. Y., KIDD, B. A., ROBINSON, W. H., SOBEL, R. A., SELLEY, M. L. & STEINMAN, L. 2005. Treatment of autoimmune neuroinflammation with a synthetic tryptophan metabolite. *Science*, 310, 850-5.
- PLATTEN, M., WICK, W. & VAN DEN EYNDE, B. J. 2012. Tryptophan catabolism in cancer: beyond IDO and tryptophan depletion. *Cancer Res*, 72, 5435-40.

- POPOV, A., ABDULLAH, Z., WICKENHAUSER, C., SARIC, T., DRIESEN, J., HANISCH, F. G., DOMANN, E., RAVEN, E. L., DEHUS, O., HERMANN, C., EGGLE, D., DEBEY, S., CHAKRABORTY, T., KRONKE, M., UTERMOHLEN, O. & SCHULTZE, J. L. 2006. Indoleamine 2,3-dioxygenase-expressing dendritic cells form suppurative granulomas following *Listeria monocytogenes* infection. *J Clin Invest*, 116, 3160-70.
- PRENDERGAST, G. C., METZ, R. & MULLER, A. J. 2010. Towards a genetic definition of cancer-associated inflammation: role of the IDO pathway. *Am J Pathol*, 176, 2082-7.
- QIAN, F., LIAO, J., VILLELLA, J., EDWARDS, R., KALINSKI, P., LELE, S., SHRIKANT, P. & ODUNSI, K. 2012. Effects of 1-methyltryptophan stereoisomers on IDO2 enzyme activity and IDO2-mediated arrest of human T cell proliferation. *Cancer Immunol Immunother*, 61, 2013-20.
- REINERS, J. J., JR., CANTU, A. R. & RUPP, T. A. 1990. Coordinate modulation of murine hepatic xanthine oxidase activity and the cytochrome P-450 system by interferons. *J Interferon Res*, 10, 109-18.
- RENSHAW, S. A. & TREDE, N. S. 2012. A model 450 million years in the making: zebrafish and vertebrate immunity. *Dis Model Mech*, 5, 38-47.
- RICHARD, D. M., DAWES, M. A., MATHIAS, C. W., ACHESON, A., HILL-KAPTURCZAK, N. & DOUGHERTY, D. M. 2009. L-Tryptophan: Basic Metabolic Functions, Behavioral Research and Therapeutic Indications. *Int J Tryptophan Res*, 2, 45-60.
- RINALDO, J. E., CLARK, M., PARINELLO, J. & SHEPHERD, V. L. 1994. Nitric oxide inactivates xanthine dehydrogenase and xanthine oxidase in interferon-gamma-stimulated macrophages. *Am J Respir Cell Mol Biol*, 11, 625-30.
- ROHDE, J., HEITMAN, J. & CARDENAS, M. E. 2001. The TOR kinases link nutrient sensing to cell growth. *J Biol Chem*, 276, 9583-6.
- ROMANI, L., FALLARINO, F., DE LUCA, A., MONTAGNOLI, C., D'ANGELO, C., ZELANTE, T., VACCA, C., BISTONI, F., FIORETTI, M. C., GROHMANN, U., SEGAL, B. H. & PUCETTI, P. 2008. Defective tryptophan catabolism underlies inflammation in mouse chronic granulomatous disease. *Nature*, 451, 211-5.
- ROTH, B. L., HANIZAVAREH, S. M. & BLUM, A. E. 2004. Serotonin receptors represent highly favorable molecular targets for cognitive enhancement in schizophrenia and other disorders. *Psychopharmacology (Berl)*, 174, 17-24.
- ROWE, P. B. & KALAZIS, A. 1985. Serine metabolism in rat embryos undergoing organogenesis. *J Embryol Exp Morphol*, 87, 137-44.
- RUBINSTEIN, A. L. 2003. Zebrafish: from disease modeling to drug discovery. *Curr Opin Drug Discov Devel*, 6, 218-23.
- RUDDICK, J. P., EVANS, A. K., NUTT, D. J., LIGHTMAN, S. L., ROOK, G. A. & LOWRY, C. A. 2006. Tryptophan metabolism in the central nervous system: medical implications. *Expert Rev Mol Med*, 8, 1-27.
- SABATINI, D. M., ERDJUMENT-BROMAGE, H., LUI, M., TEMPST, P. & SNYDER, S. H. 1994. RAFT1: a mammalian protein that binds to FKBP12 in a rapamycin-dependent fashion and is homologous to yeast TORs. *Cell*, 78, 35-43.
- SABEH, M. K., KEKHIA, H. & MACRAE, C. A. 2012. Optical mapping in the developing zebrafish heart. *Pediatr Cardiol*, 33, 916-22.
- SAIKI, S., SATO, T., KOHZUKI, M., KAMIMOTO, M. & YOSIDA, T. 2001. Changes in serum hypoxanthine levels by exercise in obese subjects. *Metabolism*, 50, 627-30.
- SAITO, K., CROWLEY, J. S., MARKEY, S. P. & HEYES, M. P. 1993. A mechanism for increased quinolinic acid formation following acute systemic immune stimulation. *J Biol Chem*, 268, 15496-503.
- SAKURAI, K., ZOU, J. P., TSCHETTER, J. R., WARD, J. M. & SHEARER, G. M. 2002. Effect of indoleamine 2,3-dioxygenase on induction of experimental autoimmune encephalomyelitis. *J Neuroimmunol*, 129, 186-96.

- SAMSTEIN, B., HOIMES, M. L., FAN, J., FROST, R. A., GELATO, M. C. & LANG, C. H. 1996. IL-6 stimulation of insulin-like growth factor binding protein (IGFBP)-1 production. *Biochem Biophys Res Commun*, 228, 611-5.
- SANNI, L. A., THOMAS, S. R., TATTAM, B. N., MOORE, D. E., CHAUDHRI, G., STOCKER, R. & HUNT, N. H. 1998. Dramatic changes in oxidative tryptophan metabolism along the kynurenine pathway in experimental cerebral and noncerebral malaria. *Am J Pathol*, 152, 611-9.
- SATO, M., YOSHIDA, H., YANAGAWA, T., YURA, Y., URATA, M., ATSUMI, M., FURUMOTO, N., HAYASHI, Y. & TAKEGAWA, Y. 1984. Interferon activity and its characterization in the sera of patients with head and neck cancer. *Cancer*, 54, 1239-51.
- SCHIMKE, R. T., SWEENEY, E. W. & BERLIN, C. M. 1965a. The Roles of Synthesis and Degradation in the Control of Rat Liver Tryptophan Pyrrolase. *J Biol Chem*, 240, 322-31.
- SCHIMKE, R. T., SWEENEY, E. W. & BERLIN, C. M. 1965b. Studies of the stability in vivo and in vitro of rat liver tryptophan pyrrolase. *J Biol Chem*, 240, 4609-20.
- SCHLEGEL, A. & GUT, P. 2015. Metabolic insights from zebrafish genetics, physiology, and chemical biology. *Cell Mol Life Sci*, 72, 2249-60.
- SCHMIDT, S. K., MULLER, A., HESELER, K., WOITE, C., SPEKKER, K., MACKENZIE, C. R. & DAUBENER, W. 2009. Antimicrobial and immunoregulatory properties of human tryptophan 2,3-dioxygenase. *Eur J Immunol*, 39, 2755-64.
- SCHROCKSNADDEL, H., BAIER-BITTERLICH, G., DAPUNT, O., WACHTER, H. & FUCHS, D. 1996. Decreased plasma tryptophan in pregnancy. *Obstet Gynecol*, 88, 47-50.
- SCHRODER, K., HERTZOG, P. J., RAVASI, T. & HUME, D. A. 2004. Interferon-gamma: an overview of signals, mechanisms and functions. *J Leukoc Biol*, 75, 163-89.
- SCHROEDER, A., MUELLER, O., STOCKER, S., SALOWSKY, R., LEIBER, M., GASSMANN, M., LIGHTFOOT, S., MENZEL, W., GRANZOW, M. & RAGG, T. 2006. The RIN: an RNA integrity number for assigning integrity values to RNA measurements. *BMC Mol Biol*, 7, 3.
- SCHROTEN, H., SPORS, B., HUCKE, C., STINS, M., KIM, K. S., ADAM, R. & DAUBENER, W. 2001. Potential role of human brain microvascular endothelial cells in the pathogenesis of brain abscess: inhibition of *Staphylococcus aureus* by activation of indoleamine 2,3-dioxygenase. *Neuropediatrics*, 32, 206-10.
- SCHWARCZ, R., RASSOULPOUR, A., WU, H. Q., MEDOFF, D., TAMMINGA, C. A. & ROBERTS, R. C. 2001. Increased cortical kynurenate content in schizophrenia. *Biol Psychiatry*, 50, 521-30.
- SEDLMAYR, P. & BLASCHITZ, A. 2012. Placental expression of indoleamine 2,3-dioxygenase. *Wien Med Wochenschr*, 162, 214-9.
- SEDLMAYR, P., BLASCHITZ, A. & STOCKER, R. 2014. The role of placental tryptophan catabolism. *Front Immunol*, 5, 230.
- SEDLMAYR, P., BLASCHITZ, A., WINTERSTEIGER, R., SEMLITSCH, M., HAMMER, A., MACKENZIE, C. R., WALCHER, W., REICH, O., TAKIKAWA, O. & DOHR, G. 2002. Localization of indoleamine 2,3-dioxygenase in human female reproductive organs and the placenta. *Mol Hum Reprod*, 8, 385-91.
- SEGURA, M., VADEBONCOEUR, N. & GOTTSCHALK, M. 2002. CD14-dependent and -independent cytokine and chemokine production by human THP-1 monocytes stimulated by *Streptococcus suis* capsular type 2. *Clin Exp Immunol*, 127, 243-54.
- SHARMA, M. D., BABAN, B., CHANDLER, P., HOU, D. Y., SINGH, N., YAGITA, H., AZUMA, M., BLAZAR, B. R., MELLOR, A. L. & MUNN, D. H. 2007. Plasmacytoid dendritic cells from mouse tumor-draining lymph nodes directly activate mature Tregs via indoleamine 2,3-dioxygenase. *J Clin Invest*, 117, 2570-82.
- SHAYDA, H., MAHMOOD, J. T., EBRAHIM, T., JAMILEH, G., GOLNAZ ENSIEH, K. S., PARIVASH, D., LEILA, B. Y., MOHAMMAD MEHDI, A. & AMIR HASSAN, Z. 2009. Indoleamine 2,3-dioxygenase (IDO) is expressed at feto-placental unit throughout mouse gestation: An immunohistochemical study. *J Reprod Infertil*, 10, 177-83.

- SHIMIZU, T., NOMIYAMA, S., HIRATA, F. & HAYAISHI, O. 1978. Indoleamine 2,3-dioxygenase. Purification and some properties. *J Biol Chem*, 253, 4700-6.
- SIMMONS, D. G., RAWN, S., DAVIES, A., HUGHES, M. & CROSS, J. C. 2008. Spatial and temporal expression of the 23 murine Prolactin/Placental Lactogen-related genes is not associated with their position in the locus. *BMC Genomics*, 9, 352.
- SPANO, P. F., SZYSZKA, K., GALLI, C. L. & RICCI, A. 1974. Effect of clofibrate on free and total tryptophan in serum and brain tryptophan metabolism. *Pharmacol Res Commun*, 6, 163-73.
- SPENCE, R., GERLACH, G., LAWRENCE, C. & SMITH, C. 2008. The behaviour and ecology of the zebrafish, *Danio rerio*. *Biol Rev Camb Philos Soc*, 83, 13-34.
- SPITSBERGEN, J. M., TSAI, H. W., REDDY, A., MILLER, T., ARBOGAST, D., HENDRICKS, J. D. & BAILEY, G. S. 2000. Neoplasia in zebrafish (*Danio rerio*) treated with N-methyl-N'-nitro-N-nitrosoguanidine by three exposure routes at different developmental stages. *Toxicol Pathol*, 28, 716-25.
- STANTON, M. F. 1965. Diethylnitrosamine-Induced Hepatic Degeneration and Neoplasia in the Aquarium Fish, *Brachydanio Rerio*. *J Natl Cancer Inst*, 34, 117-30.
- STOLL, J. & GOLDMAN, D. 1991. Isolation and structural characterization of the murine tryptophan hydroxylase gene. *J Neurosci Res*, 28, 457-65.
- STONE, T. W. 1993. Neuropharmacology of quinolinic and kynurenic acids. *Pharmacol Rev*, 45, 309-79.
- STOW, J. L., LOW, P. C., OFFENHAUSER, C. & SANGERMANI, D. 2009. Cytokine secretion in macrophages and other cells: pathways and mediators. *Immunobiology*, 214, 601-12.
- STREISINGER, G., WALKER, C., DOWER, N., KNAUBER, D. & SINGER, F. 1981. Production of clones of homozygous diploid zebra fish (*Brachydanio rerio*). *Nature*, 291, 293-6.
- SUNDRUD, M. S., KORALOV, S. B., FEUERER, M., CALADO, D. P., KOZHAYA, A. E., RHULE-SMITH, A., LEFEBVRE, R. E., UNUTMAZ, D., MAZITSCHK, R., WALDNER, H., WHITMAN, M., KELLER, T. & RAO, A. 2009. Halofuginone inhibits TH17 cell differentiation by activating the amino acid starvation response. *Science*, 324, 1334-8.
- SUZUKI, S., TONE, S., TAKIKAWA, O., KUBO, T., KOHNO, I. & MINATOGAWA, Y. 2001. Expression of indoleamine 2,3-dioxygenase and tryptophan 2,3-dioxygenase in early concepti. *Biochem J*, 355, 425-9.
- SZANTO, S., KORENY, T., MIKECZ, K., GLANT, T. T., SZEKANECZ, Z. & VARGA, J. 2007. Inhibition of indoleamine 2,3-dioxygenase-mediated tryptophan catabolism accelerates collagen-induced arthritis in mice. *Arthritis Res Ther*, 9, R50.
- SZEKERES-BARTHO, J. & WEGMANN, T. G. 1996. A progesterone-dependent immunomodulatory protein alters the Th1/Th2 balance. *J Reprod Immunol*, 31, 81-95.
- TAGLIAMONTE, A., BIGGIO, G., VARGIU, L. & GESSA, G. L. 1973. Increase of brain tryptophan and stimulation of serotonin synthesis by salicylate. *J Neurochem*, 20, 909-12.
- TAKIKAWA, O., YOSHIDA, R., KIDO, R. & HAYAISHI, O. 1986. Tryptophan degradation in mice initiated by indoleamine 2,3-dioxygenase. *J Biol Chem*, 261, 3648-53.
- TAN, S., GELMAN, S., WHEAT, J. K. & PARKS, D. A. 1995. Circulating xanthine oxidase in human ischemia reperfusion. *South Med J*, 88, 479-82.
- TANIGUCHI, T., HIRATA, F. & HAYAISHI, O. 1977. Intracellular utilization of superoxide anion by indoleamine 2,3-dioxygenase of rabbit enterocytes. *J Biol Chem*, 252, 2774-6.
- TASHIRO, M., TSUKADA, K., KOBAYASHI, S. & HAYAISHI, O. 1961. A new pathway of D-tryptophan metabolism: enzymic formation of kynurenic acid via D-kynurenine. *Biochem Biophys Res Commun*, 6, 155-60.
- TAVARES, B. & SANTOS LOPES, S. 2013. The importance of Zebrafish in biomedical research. *Acta Med Port*, 26, 583-92.
- TAYLOR, A. M. & ZON, L. I. 2009. Zebrafish tumor assays: the state of transplantation. *Zebrafish*, 6, 339-46.

- TAYLOR, M. W. & FENG, G. S. 1991. Relationship between interferon-gamma, indoleamine 2,3-dioxygenase, and tryptophan catabolism. *FASEB J*, 5, 2516-22.
- TERADA, N., LUCAS, J. J., SZEPESE, A., FRANKLIN, R. A., DOMENICO, J. & GELFAND, E. W. 1993. Rapamycin blocks cell cycle progression of activated T cells prior to events characteristic of the middle to late G1 phase of the cycle. *J Cell Physiol*, 154, 7-15.
- TERAKATA, M., FUKUWATARI, T., KADOTA, E., SANO, M., KANAI, M., NAKAMURA, T., FUNAKOSHI, H. & SHIBATA, K. 2013. The niacin required for optimum growth can be synthesized from L-tryptophan in growing mice lacking tryptophan-2,3-dioxygenase. *J Nutr*, 143, 1046-51.
- TERAO, M., CAZZANIGA, G., GHEZZI, P., BIANCHI, M., FALCIANI, F., PERANI, P. & GARATTINI, E. 1992. Molecular cloning of a cDNA coding for mouse liver xanthine dehydrogenase. Regulation of its transcript by interferons in vivo. *Biochem J*, 283 (Pt 3), 863-70.
- TERNESSE, P., BAUER, T. M., ROSE, L., DUFTER, C., WATZLIK, A., SIMON, H. & OPELZ, G. 2002. Inhibition of allogeneic T cell proliferation by indoleamine 2,3-dioxygenase-expressing dendritic cells: mediation of suppression by tryptophan metabolites. *J Exp Med*, 196, 447-57.
- THEATE, I., VAN BAREN, N., PILOTTE, L., MOULIN, P., LARRIEU, P., RENAULD, J. C., HERVE, C., GUTIERREZ-ROELEN, I., MARBAIX, E., SEMPOUX, C. & VAN DEN EYNDE, B. J. 2015. Extensive profiling of the expression of the indoleamine 2,3-dioxygenase 1 protein in normal and tumoral human tissues. *Cancer Immunol Res*, 3, 161-72.
- THISSE, B. & THISSE, C. 2004. Fast Release Clones: A High Throughput Expression Analysis. . *ZFIN Direct Data Submission* (<http://zfin.org>).
- THISSE, C. & THISSE, B. 2008. High-resolution in situ hybridization to whole-mount zebrafish embryos. *Nat Protoc*, 3, 59-69.
- THOMAS, S. R. & STOCKER, R. 1999. Redox reactions related to indoleamine 2,3-dioxygenase and tryptophan metabolism along the kynurenine pathway. *Redox Rep*, 4, 199-220.
- THOMPSON, K. L., PINE, P. S., ROSENZWEIG, B. A., TURPAZ, Y. & RETIEF, J. 2007. Characterization of the effect of sample quality on high density oligonucleotide microarray data using progressively degraded rat liver RNA. *BMC Biotechnol*, 7, 57.
- THORN, C. F., LU, Z. Y. & WHITEHEAD, A. S. 2003. Tissue-specific regulation of the human acute-phase serum amyloid A genes, SAA1 and SAA2, by glucocorticoids in hepatic and epithelial cells. *Eur J Immunol*, 33, 2630-9.
- THORN, C. F., LU, Z. Y. & WHITEHEAD, A. S. 2004. Regulation of the human acute phase serum amyloid A genes by tumour necrosis factor-alpha, interleukin-6 and glucocorticoids in hepatic and epithelial cell lines. *Scand J Immunol*, 59, 152-8.
- THORN, C. F. & WHITEHEAD, A. S. 2002. Differential glucocorticoid enhancement of the cytokine-driven transcriptional activation of the human acute phase serum amyloid A genes, SAA1 and SAA2. *J Immunol*, 169, 399-406.
- TORDJMAN, K., BERNAL-MIZRACHI, C., ZEMANY, L., WENG, S., FENG, C., ZHANG, F., LEONE, T. C., COLEMAN, T., KELLY, D. P. & SEMENKOVICH, C. F. 2001. PPARalpha deficiency reduces insulin resistance and atherosclerosis in apoE-null mice. *J Clin Invest*, 107, 1025-34.
- TRABANELLI, S., OCADLIKOVA, D., CICIARELLO, M., SALVESTRINI, V., LECCISO, M., JANDUS, C., METZ, R., EVANGELISTI, C., LAURY-KLEINTOP, L., ROMERO, P., PRENDERGAST, G. C., CURTI, A. & LEMOLI, R. M. 2014. The SOCS3-independent expression of IDO2 supports the homeostatic generation of T regulatory cells by human dendritic cells. *J Immunol*, 192, 1231-40.
- UHLAR, C. M. & WHITEHEAD, A. S. 1999. Serum amyloid A, the major vertebrate acute-phase reactant. *Eur J Biochem*, 265, 501-23.
- UKAIRO, O., KANCHAGAR, C., MOORE, A., SHI, J., GAFFNEY, J., AOYAMA, S., ROSE, K., KRZYZEWSKI, S., MCGEEHAN, J., ANDERSEN, M. E., KHETANI, S. R. & LECLUYSE, E. L. 2013. Long-term stability of primary rat hepatocytes in micropatterned cocultures. *J Biochem Mol Toxicol*, 27, 204-12.

- UYTTENHOVE, C., PILOTTE, L., THEATE, I., STROOBANT, V., COLAU, D., PARMENTIER, N., BOON, T. & VAN DEN EYNDE, B. J. 2003. Evidence for a tumoral immune resistance mechanism based on tryptophan degradation by indoleamine 2,3-dioxygenase. *Nat Med*, 9, 1269-74.
- WALTHER, D. J., PETER, J. U., BASHAMMAKH, S., HORTNAGL, H., VOITS, M., FINK, H. & BADER, M. 2003. Synthesis of serotonin by a second tryptophan hydroxylase isoform. *Science*, 299, 76.
- WANG, B., KOGA, K., OSUGA, Y., CARDENAS, I., IZUMI, G., TAKAMURA, M., HIRATA, T., YOSHINO, O., HIROTA, Y., HARADA, M., MOR, G. & TAKETANI, Y. 2011. Toll-like receptor-3 ligation-induced indoleamine 2, 3-dioxygenase expression in human trophoblasts. *Endocrinology*, 152, 4984-92.
- WANG, J. & DUNN, A. J. 1998. Mouse interleukin-6 stimulates the HPA axis and increases brain tryptophan and serotonin metabolism. *Neurochem Int*, 33, 143-54.
- WANG, Y., LIU, H., MCKENZIE, G., WITTING, P. K., STASCH, J. P., HAHN, M., CHANGSIRIVATHANATHAMRONG, D., WU, B. J., BALL, H. J., THOMAS, S. R., KAPOOR, V., CELERMAJER, D. S., MELLOR, A. L., KEANEY, J. F., JR., HUNT, N. H. & STOCKER, R. 2010. Kynurenine is an endothelium-derived relaxing factor produced during inflammation. *Nat Med*, 16, 279-85.
- WATSON, E. D. & CROSS, J. C. 2005. Development of structures and transport functions in the mouse placenta. *Physiology (Bethesda)*, 20, 180-93.
- WELSH, J. B., SAPINOSO, L. M., KERN, S. G., BROWN, D. A., LIU, T., BAUSKIN, A. R., WARD, R. L., HAWKINS, N. J., QUINN, D. I., RUSSELL, P. J., SUTHERLAND, R. L., BREIT, S. N., MOSKALUK, C. A., FRIERSON, H. F., JR. & HAMPTON, G. M. 2003. Large-scale delineation of secreted protein biomarkers overexpressed in cancer tissue and serum. *Proc Natl Acad Sci U S A*, 100, 3410-5.
- WERNER-FELMAYER, G., WERNER, E. R., FUCHS, D., HAUSEN, A., REIBNEGGER, G. & WACHTER, H. 1990. Neopterin formation and tryptophan degradation by a human myelomonocytic cell line (THP-1) upon cytokine treatment. *Cancer Res*, 50, 2863-7.
- WESTERFIELD, M. 2000. *The Zebrafish Book. A Guide for the Laboratory Use of Zebrafish (Danio rerio)*, University of Oregon Press, Eugene.
- WESTIN, M. A., HUNT, M. C. & ALEXSON, S. E. 2005. The identification of a succinyl-CoA thioesterase suggests a novel pathway for succinate production in peroxisomes. *J Biol Chem*, 280, 38125-32.
- WHITE, C. R., DARLEY-USMAR, V., BERRINGTON, W. R., MCADAMS, M., GORE, J. Z., THOMPSON, J. A., PARKS, D. A., TARPEY, M. M. & FREEMAN, B. A. 1996. Circulating plasma xanthine oxidase contributes to vascular dysfunction in hypercholesterolemic rabbits. *Proc Natl Acad Sci U S A*, 93, 8745-9.
- WITKIEWICZ, A. K., COSTANTINO, C. L., METZ, R., MULLER, A. J., PRENDERGAST, G. C., YEO, C. J. & BRODY, J. R. 2009. Genotyping and expression analysis of IDO2 in human pancreatic cancer: a novel, active target. *J Am Coll Surg*, 208, 781-7; discussion 787-9.
- WOLF, H. 1974. Studies on Tryptophan-Metabolism in Man - Effect of Hormones and Vitamin-B6 on Urinary-Excretion of Metabolites of Kynurenine Pathway. *Scandinavian Journal of Clinical & Laboratory Investigation*, 33, 1-&.
- WOOD, K. J. & SAKAGUCHI, S. 2003. Regulatory T cells in transplantation tolerance. *Nat Rev Immunol*, 3, 199-210.
- WU, W., NICOLAZZO, J. A., WEN, L., CHUNG, R., STANKOVIC, R., BAO, S. S., LIM, C. K., BREW, B. J., CULLEN, K. M. & GUILLEMIN, G. J. 2013. Expression of tryptophan 2,3-dioxygenase and production of kynurenine pathway metabolites in triple transgenic mice and human Alzheimer's disease brain. *PLoS One*, 8, e59749.
- XI, Y., NOBLE, S. & EKKER, M. 2011. Modeling neurodegeneration in zebrafish. *Curr Neurol Neurosci Rep*, 11, 274-82.

- XU, J., KIMBALL, T. R., LORENZ, J. N., BROWN, D. A., BAUSKIN, A. R., KLEVITSKY, R., HEWETT, T. E., BREIT, S. N. & MOLKENTIN, J. D. 2006. GDF15/MIC-1 functions as a protective and antihypertrophic factor released from the myocardium in association with SMAD protein activation. *Circ Res*, 98, 342-50.
- YAMADA, A., AKIMOTO, H., KAGAWA, S., GUILLEMIN, G. J. & TAKIKAWA, O. 2009. Proinflammatory cytokine interferon-gamma increases induction of indoleamine 2,3-dioxygenase in monocytic cells primed with amyloid beta peptide 1-42: implications for the pathogenesis of Alzheimer's disease. *J Neurochem*, 110, 791-800.
- YAMADA, J., MATSUMOTO, I., FURIHATA, T., SAKUMA, M. & SUGA, T. 1994. Purification and properties of long-chain acyl-CoA hydrolases from the liver cytosol of rats treated with peroxisome proliferator. *Arch Biochem Biophys*, 308, 118-25.
- YAMAZAKI, F., KUROIWA, T., TAKIKAWA, O. & KIDO, R. 1985. Human indolylamine 2,3-dioxygenase. Its tissue distribution, and characterization of the placental enzyme. *Biochem J*, 230, 635-8.
- YANG, H., YOUM, Y. H., VANDANMAGSAR, B., RAVUSSIN, A., GIMBLE, J. M., GREENWAY, F., STEPHENS, J. M., MYNATT, R. L. & DIXIT, V. D. 2010. Obesity increases the production of proinflammatory mediators from adipose tissue T cells and compromises TCR repertoire diversity: implications for systemic inflammation and insulin resistance. *J Immunol*, 185, 1836-45.
- YANG, R. Z., LEE, M. J., HU, H., POLLIN, T. I., RYAN, A. S., NICKLAS, B. J., SNITKER, S., HORENSTEIN, R. B., HULL, K., GOLDBERG, N. H., GOLDBERG, A. P., SHULDINER, A. R., FRIED, S. K. & GONG, D. W. 2006. Acute-phase serum amyloid A: an inflammatory adipokine and potential link between obesity and its metabolic complications. *PLoS Med*, 3, e287.
- YANG, S., CHEN, C., WANG, H., RAO, X., WANG, F., DUAN, Q., CHEN, F., LONG, G., GONG, W., ZOU, M. H. & WANG, D. W. 2012. Protective effects of Acyl-coA thioesterase 1 on diabetic heart via PPARalpha/PGC1alpha signaling. *PLoS One*, 7, e50376.
- YI, X., PASHAJ, A., XIA, M. & MOREAU, R. 2013. Reversal of obesity-induced hypertriglyceridemia by (R)-alpha-lipoic acid in ZDF (fa/fa) rats. *Biochem Biophys Res Commun*, 439, 390-5.
- YOSHIDA, N., INO, K., ISHIDA, Y., KAJIYAMA, H., YAMAMOTO, E., SHIBATA, K., TERAUCHI, M., NAWA, A., AKIMOTO, H., TAKIKAWA, O., ISOBE, K. & KIKKAWA, F. 2008. Overexpression of indoleamine 2,3-dioxygenase in human endometrial carcinoma cells induces rapid tumor growth in a mouse xenograft model. *Clin Cancer Res*, 14, 7251-9.
- YOSHIDA, R. & HAYAISHI, O. 1978. Induction of pulmonary indoleamine 2,3-dioxygenase by intraperitoneal injection of bacterial lipopolysaccharide. *Proc Natl Acad Sci U S A*, 75, 3998-4000.
- YOSHIDA, R., IMANISHI, J., OKU, T., KISHIDA, T. & HAYAISHI, O. 1981. Induction of pulmonary indoleamine 2,3-dioxygenase by interferon. *Proc Natl Acad Sci U S A*, 78, 129-32.
- YOSHIDA, R., NUKIWA, T., WATANABE, Y., FUJIWARA, M., HIRATA, F. & HAYAISHI, O. 1980. Regulation of indoleamine 2,3-dioxygenase activity in the small intestine and the epididymis of mice. *Arch Biochem Biophys*, 203, 343-51.
- YOSHIDA, R., PARK, S. W., YASUI, H. & TAKIKAWA, O. 1988. Tryptophan degradation in transplanted tumor cells undergoing rejection. *J Immunol*, 141, 2819-23.
- YOSHIDA, R., URADE, Y., TOKUDA, M. & HAYAISHI, O. 1979. Induction of indoleamine 2,3-dioxygenase in mouse lung during virus infection. *Proc Natl Acad Sci U S A*, 76, 4084-6.
- YOSHIMOTO, T., TAKEDA, K., TANAKA, T., OHKUSU, K., KASHIWAMURA, S., OKAMURA, H., AKIRA, S. & NAKANISHI, K. 1998. IL-12 up-regulates IL-18 receptor expression on T cells, Th1 cells, and B cells: synergism with IL-18 for IFN-gamma production. *J Immunol*, 161, 3400-7.
- YOUNG, H. A. & HARDY, K. J. 1995. Role of interferon-gamma in immune cell regulation. *J Leukoc Biol*, 58, 373-81.
- YUASA, H. J. & BALL, H. J. 2011. Molecular evolution and characterization of fungal indoleamine 2,3-dioxygenases. *J Mol Evol*, 72, 160-8.

- YUASA, H. J. & BALL, H. J. 2013. Indoleamine 2,3-dioxygenases with very low catalytic activity are well conserved across kingdoms: IDOs of Basidiomycota. *Fungal Genet Biol*, 56, 98-106.
- YUASA, H. J., BALL, H. J., AUSTIN, C. J. & HUNT, N. H. 2010. 1-L-methyltryptophan is a more effective inhibitor of vertebrate IDO2 enzymes than 1-D-methyltryptophan. *Comp Biochem Physiol B Biochem Mol Biol*, 157, 10-5.
- YUASA, H. J., BALL, H. J., HO, Y. F., AUSTIN, C. J., WHITTINGTON, C. M., BELOV, K., MAGHZAL, G. J., JERMIIN, L. S. & HUNT, N. H. 2009. Characterization and evolution of vertebrate indoleamine 2, 3-dioxygenases IDOs from monotremes and marsupials. *Comp Biochem Physiol B Biochem Mol Biol*, 153, 137-144.
- YUASA, H. J., TAKUBO, M., TAKAHASHI, A., HASEGAWA, T., NOMA, H. & SUZUKI, T. 2007. Evolution of vertebrate indoleamine 2,3-dioxygenases. *J Mol Evol*, 65, 705-14.
- ZAVARONI, I., MAZZA, S., FANTUZZI, M., DALL'AGLIO, E., BONORA, E., DELSIGNORE, R., PASSERI, M. & REAVEN, G. M. 1993. Changes in insulin and lipid metabolism in males with asymptomatic hyperuricaemia. *J Intern Med*, 234, 25-30.
- ZHANG, F., SJOHOLM, A. & ZHANG, Q. 2007a. Attenuation of insulin secretion by insulin-like growth factor binding protein-1 in pancreatic beta-cells. *Biochem Biophys Res Commun*, 362, 152-7.
- ZHANG, J., WU, Y., ZHANG, Y., LEROITH, D., BERNLOHR, D. A. & CHEN, X. 2008. The role of lipocalin 2 in the regulation of inflammation in adipocytes and macrophages. *Mol Endocrinol*, 22, 1416-26.
- ZHANG, P., MCGRATH, B. C., REINERT, J., OLSEN, D. S., LEI, L., GILL, S., WEK, S. A., VATTEM, K. M., WEK, R. C., KIMBALL, S. R., JEFFERSON, L. S. & CAVENER, D. R. 2002. The GCN2 eIF2alpha kinase is required for adaptation to amino acid deprivation in mice. *Mol Cell Biol*, 22, 6681-8.
- ZHANG, Y., KANG, S. A., MUKHERJEE, T., BALE, S., CRANE, B. R., BEGLEY, T. P. & EALICK, S. E. 2007b. Crystal structure and mechanism of tryptophan 2,3-dioxygenase, a heme enzyme involved in tryptophan catabolism and in quinolinate biosynthesis. *Biochemistry*, 46, 145-55.
- ZHANG, Z., BLAKE, D. R., STEVENS, C. R., KANCZLER, J. M., WINYARD, P. G., SYMONS, M. C., BENBOUBETRA, M. & HARRISON, R. 1998. A reappraisal of xanthine dehydrogenase and oxidase in hypoxic reperfusion injury: the role of NADH as an electron donor. *Free Radic Res*, 28, 151-64.
- ZHAO, L., LEUNG, J. K., YAMAMOTO, H., GOSWAMI, S., KHERADMAND, F. & VU, T. H. 2006. Identification of P311 as a potential gene regulating alveolar generation. *Am J Respir Cell Mol Biol*, 35, 48-54.
- ZIMMERS, T. A., JIN, X., HSIAO, E. C., PEREZ, E. A., PIERCE, R. H., CHAVIN, K. D. & KONIARIS, L. G. 2006. Growth differentiation factor-15: induction in liver injury through p53 and tumor necrosis factor-independent mechanisms. *J Surg Res*, 130, 45-51.
- ZOHN, I. E. & SARKAR, A. A. 2010. The visceral yolk sac endoderm provides for absorption of nutrients to the embryo during neurulation. *Birth Defects Res A Clin Mol Teratol*, 88, 593-600.